Joint research thesis for the degree of
Doctor of Philosophy

Sapienza, University of Rome
Department of Chemical Engineering Materials Environment

Electrical, Materials and Nanotechnology Engineering (EMNE) (XXXII cycle)

ISAE-ENSMA, Ecole Nationale Supérieure De Mécanique et D'Aérotechnique
Département Physique et Mécanique des Matériaux

Sciences et Ingénierie en Matériaux, Mécanique, Energétique

Maria Carolina Seghini

Investigation into the mechanical properties and fibre/matrix interface optimization for next generation of basalt-plant fibre hybrid composites

---

PhD supervisors: SARASINI Fabrizio, TOUCHARD Fabienne

Rome, 10th January 2020

JURY

Prof. DHAKAL, Hom Nath - University of Portsmouth, United Kingdom	Reviewer
Prof. GONZALEZ, Carlos - Universidad Politécnica de Madrid (UPM), Spain	Reviewer
Prof. CICALA, Gianluca - University of Catania, Italy	
Prof. REMOND, Yves - University of Strasbourg, France	
Dr. CHOCINSKI, Laurence - ISAE-ENSMA, France	
Prof. SARASINI, Fabrizio - Sapienza University of Rome, Italy	
Prof. TOUCHARD, Fabienne - ISAE-ENSMA, France	

Acknowledgements

After three years, it is difficult to thank all the people who supported me to complete this study. The complexity isn't about remembering each one of them, but rather realising that a phase of my life has come to an end. A "traditional" PhD thesis allows to meet a lot of people, to whom it is hard to express all your gratitude. This task becomes even more difficult in a joint PhD program. These last three years have been unforgettable, and I want to thank and show my recognition to everyone who contributed to the success of this thesis. Taking cues from the composite materials studied in the present work, also my thanks will be a hybrid between English, French and Italian.

First and foremost, I would like to express my sincere gratitude to my supervisors, Fabrizio Sarasini and Fabienne Touchard for their continuous support, motivation and immense (really immense) patience! I would like to thank you, not only for sharing your knowledge with me, but for giving me the opportunity to carry out a joint PhD between the Sapienza and ENSMA. This experience provided me with a broad range of professional and personal opportunities. I will always be grateful to you for this.

Special acknowledgment goes to Prof. V. Cech and his research group, which has contributed actively to this work by the realization of plasma modification treatments on flax yarns and basalt fibres. A big thank to Dr. M. Pucci, for her helpfulness and support in the analysis of the wetting properties of both flax yarns and basalt filaments. A heartfelt thanks to Dr. V. Placet and his research team to the development of supercritical CO_2 process.

Un remerciement spécial à Fabienne Touchard et Laurence Chocinski. Je m'estime très chanceuse d'avoir travaillé avec vous. Au cours de la thèse, on a rencontré divers problèmes, mais avec votre patience, vous avez réussi à me guider dans la bonne direction sans jamais me décourager. En outre, d'un point de vue personnel, vous m'avez très bien accueillie, j'ai eu l'impression d'être chez moi ! Je vous remercie infiniment pour ça.

Ce travail de thèse n'aurait sans doute pas abouti sans l'aide et la collaboration de toute l'équipe technique de l'ENSMA. J'aimerais remercier en particulier David pour toutes les images tomographiques et pour sa patience. Merci à Guillaume, Médéric et bien sûr à tout le personnel de l'atelier.

Je remercie ensuite les sourires du secrétariat, de Karine ainsi que ceux de Francine (et ses chats), toujours présents pour m'accueillir et m'aider.

Merci à tous les (nombreux!) doctorants de L'ENSMA, et à l'ATEM pour l'ambiance sympathique maintenue chaque année. En particulier, j'aimerais remercier: Francois, Maxime, Niko, Caroline, Cyril, Coline, Mahak, Sathoshi…merci pour vos sourires!

Merci aux membres du bureau Multimat, à Romain, Vincent, Emeline et Aurélien. En particulier, je voudrais remercier Romain et Vincent qui ont été de parfaits collègues de bureau mais aussi de fantastiques compagnons de voyage en Corse.

Un grazie di cuore va a tutta la grande famiglia degli "Italiani a Poitiers"! Ringrazio Antonio, Marina, Flavio, Vincenzo per le risate a piloffio e soprattutto per le scorpacciate Italo-Calabresi in terra francese. Giovanna, Eleonora, Margherita e Jessica per i pomeriggi Poitevins. Per i tre corvi di Canolle: Federico, Giuseppe, Marco…che dire?? Ringraziarvi del tempo passato insieme non basta. Voi siete stati e sarete per sempre la mia seconda famiglia.

Un ringraziamento speciale va a tutto il laboratorio dell'LIMS della Sapienza di Roma per avermi supportato e sopportato per i tre anni di dottorato passati insieme.

E i dottorandi, post-doc (alcuni quasi Prof.) della Sapienza? Come potrei non ringraziarvi? Alessia, Danilo, Matteo, Francesca, Giulia, Virgilio, Lidia, Laura, Claudia, Matteo (II), con tutti voi ho passato dei momenti splendidi. Da una notte da Lyoni con Alina e Vesna, ai tuffi "proibiti" (ma con cuffia) ad Ischia, passando rapidamente per la "vicina" Australia. Grazie per aver reso ancor più indimenticabile questa avventura.

Infine, il ringraziamento più grande va a mio padre e mia madre, ai quali dedico questo lavoro. I miei traguardi sono il frutto dei vostri sacrifici. Per questo ve ne sarò per sempre grata.

Table of Contents

PART II – MATERIALS AND TECHNIQUES

PART III – MECHANICAL BEHAVIOUR OF HYBRID COMPOSITES

PART IV – SURFACE MODIFICATION TREATMENTS AND THEIR EFFECTS ON FILAMENTS

Introduction

▪ Motivation

In the last two decades, the development of natural fibre reinforced polymer matrix composites has attracted great interest due to their properties and environmentally friendly character. Their global market is forecast to grow at a CAGR (Compound Annual Growth Rate) of 8.2% from 2015 to 2020 [Lucintel, 2015]. In particular, lignocellulosic fibres such as flax, hemp, jute, sisal and abaca have been proposed as substitutes of traditional glass fibres [Kiruthika, 2017]. These fibres offer several advantages over conventional synthetic ones, such as low density, low cost, good specific mechanical properties, wide availability and biodegradability. The automotive and the construction industries represent the two major application areas of natural fibre composites. For example, concerning the automotive sector, natural fibres are employed to produce lightweight parts in order to improve fuel efficiency and reduce CO_2 emissions. At present, the 12% of total carbon dioxide emissions in the European Union (EU) are produced by cars. On 17 April 2019, the European Parliament and Council have adopted the "*Regulation (EU) 2019/631"*, setting new CO_2 emission standards for new passenger cars and for new light commercial vehicles [European Commission, 2019]. In particular, a new average emission target of 95 g CO_2/km was set, quite lower than the value of 120.4 g CO_2/km obtained in 2018. In addition to this, it is important to take into account that in the last few years, the European legislation is becoming more and more restrictive regarding landfilling waste. In particular, the emanation of the "*Directive on Landfill of Waste (Directive 99/31/EC)"* and the "*End-of-life Vehicle Directive (Directive 2000/53/EC)"* severely limits the landfill disposal of materials, such as glass reinforced polymer material (GRP), traditionally used in the automotive sector [Council of the European Union, 1999; European Parliament and Council of the European Union, 2000]. For these reasons, it is not surprising that many car manufacturers have focused their efforts on vehicle weight reduction. An increasing interest has been directed at the use of natural fibre composites in order to reduce not only the cars weight but also their environmental impact [Koronis *et al.*, 2018]. The use of natural fibre composites contributes to weight

reduction by 30% and cost reduction by 20% during manufacturing of a vehicle [Grand View Research, 2018]. However, despite their benefits, the natural fibres drawbacks, such as high moisture sensitivity, low thermal stability, poor compatibility with polymeric matrices and low microbial resistance, make inconvenient the use of these materials in semi- or structural applications. Among the different solutions proposed over the years, the development of hybrid composite materials, by introducing different types of fibres aiming at overcoming the drawbacks of composites reinforced with only one type of fibres, can represent a very attractive way of solving this problem. In this regard, hybridization of plies of natural and synthetic fibres represents a significant strategy to reduce weight and carbon footprint of traditional composite materials, while retaining a sufficient mechanical performance to permit not only cosmetic (i.e. non-structural) applications. Recently a carbon/flax hybrid composite has been developed for the roof of the hybrid electric Range Rover Evoque [Caliendo, 2016]. This hybrid structure, designed by Delta Motorsport and manufactured by KS Composites for Jaguar Land Rover, allows to combine the high strength and stiffness of carbon fibre with the low cost and vibration damping performance of flax.

Figure 1 The carbon/flax hybrid composite roof produced for the Range Rover Evoque. This hybrid structure has been developed within the CARBIO project which involves Jaguar Land Rover, Composites Evolution, SHD Composite Materials, KS Composites, Delta Motorsport and Cranfield University [Vijayenthiran, 2015; Caliendo, 2016].

A wide variety of plant fibres can be employed as reinforcements in composite materials. Among these, flax and hemp are the most widely used because of their good mechanical properties and availability [George *et al.*, 1999; Mohanty *et al.*, 2000]. In recent years, there has been a substantial interest on the possibility to produce hybrids including plant fibre and basalt fibre laminates [Dhakal *et al.*, 2015; Fiore *et al.*, 2016]. Thanks to their natural origin and mechanical properties at least comparable with those of traditional E-glass fibres, basalt

fibres may at the same time overcome the environmental issues of synthetic fibres and the typical limitations of plant natural fibres. In this framework, a basalt-flax hybrid composite material will be developed in this research project in order to obtain a more natural and environmentally friendly composite for semi-structural applications. A detailed quasi-static and dynamic mechanical characterization will be performed in order to highlight the interest of hybridization. The poor fibre/matrix interface adhesion represents the Achilles' heel of these composites. It is very well-known that the mechanical properties of a composite material are strongly dependent on the adhesion quality of fibre/matrix interface and this is even more stringent for natural fibre composites due to the inherent hydrophilic nature of plant fibres [Karger-Kocsis *et al.*, 2015; Pickering *et al.*, 2016]. The poor surface wetting of hydrophilic natural fibres by the more hydrophobic polymer matrices represents the major problem in the interfacial strength of a composite material. The presence of hydroxyl (OH) and carboxylic (COOH) groups in constituents such as hemicellulose, pectin and cellulose makes natural fibres highly susceptible to absorb a significant amount of water. A poor fibre/matrix adhesion results not only in an impaired stress transfer ability from the matrix to the reinforcing fibres, but also it can promote the production of voids within the composites, which can constitute a preferential path for the capillary absorption of water.
Because of the incomplete impregnation and the low wetting of natural fibres with polymer resin, the moisture absorption is localized generally at the fibre/matrix interface zone. The swelling process resulting by the water absorption of natural fibres, can lead to the formation of matrix cracks and debonding at the fibre/matrix interface [Mochane *et al.*, 2019]. As a result, the good specific mechanical properties of the fibres are far from being efficiently exploited, thus leading to an unsatisfactory mechanical performance of the resulting composites that cannot be reliably used in semi-structural applications. A great deal of research efforts has been directed towards the improvement of natural fibre/polymer matrix interface compatibility. To this purpose, various surface treatments have been proposed over the years in order to modify the surface properties of natural fibres and enhance their adhesion with polymer matrices [Kalia *et al.*, 2013]. These treatments are efficient to increase the wetting properties of natural fibres with the polymer matrix. However, the use of polluting modification treatments in order to enhance the mechanical properties of an hybrid composite represents a loss of the environmental sustainability gain achieved by using natural reinforcements. In this regard, in this work, attention will be focused on the research and optimization of more environmentally friendly surface treatments. The plasma

technology is considered as a less aggressive alternative to the environment than the chemical modification treatments. More specifically, plasma treatment does not employ harmful chemicals or gases, it leaves limited or no waste and it is able to modify only the surface of the fibre without affecting its internal properties. Flax yarns and basalt fibres will be treated by two different plasma processes: the oxygen plasma treatment and the plasma polymerization process. Several studies have investigated the use of oxygen plasma treatment on natural fibres to improve their adhesion with polymer matrices [Kim *et al.*, 2011; Bozaci *et al.*, 2013; De Farias *et al.*, 2017]. All these researches have highlighted as the plasma treatment is able to enhance the fibre/matrix interface strength. In literature, several studies have been focused on the use of plasma polymerization process on synthetic glass fibres, but no studies are available on natural fibres. In this work, the plasma polymerization process will be used for the first time on flax yarns and basalt fibres in order to enhance their interfacial adhesion with polymer matrices. The flax yarns will also be subjected to chemical treatments, using enzymatic species and supercritical CO_2. The enzymatic treatment represents a green way to modify natural fibres. It is well-known that enzymes are able to catalyse the removal of undesirable substances like pectin, hemicelluloses, lignin, fat, and waxes from the surface of the fibres improving fibre/matrix adhesion [George *et al.*, 2016; Liu *et al.*, 2017]. Unlike the enzymatic treatments, only a few experimental works have investigated the effect of the supercritical CO_2 process on the fibre/matrix interfacial strength [Gutiérrez *et al.*, 2012; Francois *et al.*, 2017]. In this sense, this work aims to broaden the knowledge of the effect produced by the supercritical CO_2 fluid on the properties of flax. An in-depth analysis of the effects of the different surface modifications treatments on the adhesion properties of flax yarns and basalt fibres with polymers will be performed. In order to investigate the interfacial strength of natural fibres in thermoset systems, two different thermoset matrices will be used in this work: an epoxy and a vinylester resin. The Single Fibre Fragmentation Test (SFFT) will be applied to assess the filament/matrix adhesion in terms of critical fragment length, debonding length and interfacial shear strength. This experimental characterization will be supplemented with high-resolution microcomputed tomography. The use of this non-destructive technique represents another novelty in the field of the fibre/matrix interfacial investigation.

▪ The joint PhD programme

The present research project comes within the framework of a joint PhD programme between the Department of Chemical Engineering Materials Environment, in Sapienza-University of Rome (Italy) and the Department of Physics and Mechanics of Materials, in PPRIME Institute, CNRS-ENSMA-University of Poitiers (France). This collaboration has allowed to take advantage of the skills and knowledges gained by the two research groups, who have long been working at international level in the field of natural fibre reinforced composite materials. The two teams have been working and publishing together since 2012. This joint PhD project, financed by La Sapienza, has been conceived in order to give a new and deeper dimension to this collaborative partnership. The research, lasting a total of 3 years, was carried out for 50% of its duration at Sapienza University of Rome and for 50% at ISAE-ENSMA. The joint programme made possible to perform various tests in order to study the woven composites and the fibre/matrix interfacial properties.
In addition, the results of this project have been possible thanks to the collaboration with other international research groups. These partnerships were crucial in order to carry out different treatments and tests, requiring a specific knowledge and technologies. In particular:

- Plasma modification treatments were performed on flax yarns and basalt fibres. They were carried out in collaboration with the "Brno University of Technology", Czech Republic. Precisely, the experimental work was performed by the research group supervised by Prof. V. Cech and Dr. M. Zvoneck;

- Flax yarns were chemically treated by supercritical CO_2 process carried out in collaboration with the "Institute Franche-Comté Electronics Mechanics Thermal Science and Optics – Sciences and Technologies (FEMTO-ST)" and the "Institute de Chimie Moléculaire", Bourgogne University, France. The experimental work was supervised by Dr. V. Placet;

- An in-depth analysis of the wetting properties of both flax yarns and basalt filaments has been possible thanks to the collaboration with the "IMT Mines Alès", Alès, France. In particular, tensiometric tests were carried out under the supervision of Dr.

M. Pucci, through a stay at the laboratory of the “Centre des Matériaux des Mines d’Alès (C2MA)”.

It is noteworthy that this doctoral project has received a mobility grant, namely "Bando Vinci - Cap.II 2018", financed by Università Italo Francese/Université Franco Italienne (UIF/UFI). The aim of this funding is to support the mobility of joint PhD students and to promote the scientific exchange between Italy and France. Specifically, the project has received a budget of € 5,500, intended to cover the Italy-France and France-Italy mobility costs, as well as the expenses related to participation in activities closely linked to the doctoral programme.

▪ Manuscript organization

Two essential topics are addressed in this manuscript: (i) the mechanical characterization of the flax-basalt hybrid composite materials and (ii) the optimization of the filament/matrix interfacial adhesion through the development and optimization of surface modification treatments. In order to present these subjects in a comprehensive manner, the manuscript is organized into five key-parts:

Part I: State of the art

In the Part I, elements are given on the scientific framework of this study. A state of the art on the natural fibre hybrid composites developed so far is given before focusing on the issue of the interfacial adhesion of natural fibres with polymeric matrices. Particular attention is focused on the description of the main characterization techniques used to assess the fibre/matrix interface. Finally, an overview of the different modification treatments used so far, in order to optimize the fibre/matrix compatibility, is provided.

Part II: Materials and Techniques

The objective of the Part II is to present the whole set of materials and techniques used during the experimental work. First, a description of the single constituents and the manufacture techniques used to produce both woven and monofilament composite materials is presented. The second part focuses on the introduction of the different characterization techniques used.

Part III: Mechanical behaviour of hybrid composites

The Part III of the manuscript presents the experimental results from the mechanical characterization of the different composite materials manufactured: flax fibre composites, basalt fibre composites and flax-basalt hybrid composites. In particular, the outcomes of the quasi-static (tensile, flexural) and dynamic (fatigue, low-velocity impact) mechanical characterizations are reported. The aim of this part of the manuscript is to provide a careful comparison between the mechanical behaviour of flax and basalt composites with that of hybrid composite materials.

Part IV: Surface modification treatments and their effects on flax yarns and basalt fibres

The Part IV of the manuscript is focused on the different surface modification treatments performed on both flax and basalt filaments in order to enhance their adhesion with thermoset resins. An in-depth analysis of the effects of the different treatments on the properties of flax yarns and basalt fibres is provided. At first, the chemical and physical treatments performed on flax yarns are described. In particular, the effects of enzymatic, supercritical CO_2 treatment, oxygen and tetravinylsilane plasma treatments on the wetting, morphological, compositional, and mechanical properties of flax yarns are described. Subsequentially, the changes produced by a thermal de-sizing treatment and a tetravinylsilane plasma deposition process on the properties of basalt fibres are investigated.

Part V: Filament/matrix interfacial properties

The last part of the manuscript presents the experimental results obtained by the Single Fibre Fragmentation Tests performed onto monofilament composite samples. The adhesion quality of untreated and treated flax yarns and basalt fibres with both epoxy and vinylester matrices is discussed in terms of critical fragment length, debonding length and interfacial shear strength (IFSS). The main focus of this section is to analyse in detail the effects of the different surface modification treatments on the adhesion of basalt and flax filaments with polymeric matrices.

The final conclusions as well as the perspectives are presented at the end of the manuscript.

Introduction

(en français)

En 2018, les composites à fibres de verre représentaient environ 95% du marché européen. Mais ces matériaux engendrent de graves problèmes environnementaux liés à leur mode de production et à leur cycle de vie. La prise de conscience mondiale des enjeux environnementaux a conduit à l'émergence de composites «verts», dans lesquels les fibres naturelles sont amenées à remplacer les fibres synthétiques. Ces nouveaux matériaux offrent des alternatives écologiques aux composites synthétiques traditionnels mais sont difficilement utilisables pour des applications semi-structurelles ou structurelles. Une solution possible à ce problème est le développement des composites hybrides. En effet, un composite hybride combinant fibres naturelles et synthétiques offre non seulement une bonne compatibilité environnementale, mais également de bonnes propriétés mécaniques. Dans ce cadre, l'objectif de cette étude est de développer et de caractériser des composites hybrides à base de fibres de basalte et de lin, ainsi que d'optimiser la qualité d'adhésion de l'interface fibre/matrice afin d'accroître les performances mécaniques de ces composites. Une caractérisation mécanique à la fois quasi-statique (traction, flexion) et dynamique (fatigue, impact à basse vitesse) sera réalisée. Différents traitements de modification de surface seront réalisés et étudiés pour les fibres de lin et de basalte dans le but d'accroître leur adhésion à deux matrices thermodures : époxy et vinylester. Un traitement physique par plasma (Plasma Enhanced Chemical Vapor Deposition) sera appliqué aux fibres de lin et de basalte. Les fibres de lin seront également soumises à deux traitements chimiques utilisant des espèces enzymatiques et du CO_2 supercritique. Des tests seront effectués après chaque traitement pour évaluer l'augmentation de l'hydrophobicité des fibres. Les effets des traitements sur la stabilité thermique, la morphologie et les propriétés mécaniques des fibres de lin et de basalte seront évalués par analyse thermogravimétrique, microscopie électronique à balayage et essais de traction sur fibres. Enfin, l'adhésion fibre/matrice sera étudiée en réalisant des tests de fragmentation sur des composites monofilamentaires. La qualité de l'adhésion entre les fibres et les matrices époxy et vinylester sera évaluée en termes de longueur critique de fragment, de longueur de décohésion interfaciale et de résistance au cisaillement interfacial. La microtomographie à rayons X haute résolution sera utilisée pour faciliter l'analyse des mécanismes d'endommagement lors des tests de fragmentation.

▪ ***Organisation du manuscrit***

Deux sujets essentiels sont abordés dans ce manuscrit: (i) la caractérisation mécanique des matériaux composites hybrides lin-basalte et (ii) l'optimisation de l'adhésion interfaciale fibre/matrice par le développement et l'optimisation de traitements de modification de surface. Le manuscrit est organisé en cinq parties :

***Partie I : état de l'art**. Dans la partie I, des éléments sont donnés sur le contexte de cette étude. Un état de l'art sur les composites hybrides à fibres naturelles développés jusqu'à présent est*

présenté avant de se concentrer sur la question de l'adhésion interfaciale des fibres naturelles avec les matrices polymères. Une attention particulière est portée à la description des principales techniques de caractérisation utilisées pour évaluer l'interface fibre/matrice. Enfin, un aperçu des différents traitements de modification utilisés jusqu'à présent pour optimiser la compatibilité fibre/matrice est présenté.

***Partie II : Matériaux et Techniques**. L'objectif de la Partie II est de présenter l'ensemble des matériaux et techniques utilisés lors des travaux expérimentaux. Tout d'abord, une description des constituants de base et des techniques de fabrication utilisées pour produire les matériaux composites tissés et les composites monofilamentaires est présentée. La deuxième partie se concentre sur l'introduction des différentes techniques de caractérisation utilisées.*

***Partie III: Comportement mécanique des composites hybrides.** La partie III du manuscrit présente les résultats expérimentaux de la caractérisation mécanique des différents matériaux composites fabriqués : composites à fibres de lin, composites à fibres de basalte et composites hybrides lin-basalte. En particulier, les résultats des caractérisations mécaniques quasi-statiques (traction, flexion) et dynamiques (fatigue, impact à basse vitesse) sont détaillés. Le but de cette partie du manuscrit est de fournir une comparaison entre le comportement mécanique des composites de lin et de basalte avec celui des matériaux composites hybrides.*

***Partie IV : Les traitements de modification de surface et leurs effets sur les fils de lin et les fibres de basalte**. La partie IV du manuscrit se concentre sur les différents traitements de modification de surface effectués sur les renforts de lin et de basalte afin d'améliorer leur adhésion avec les résines thermodurcissables. Une analyse approfondie des effets des différents traitements sur les propriétés des fils de lin et des fibres de basalte est fournie. Dans un premier temps, les traitements chimiques et physiques effectués sur les fils de lin sont décrits. En particulier, les effets des traitements enzymatiques et du traitement au CO_2 supercritique sont décrits, ainsi que les traitements au plasma d'oxygène et les traitements de polymérisation par plasma. La mouillabilité, la composition chimique et les propriétés morphologiques et mécaniques des fils de lin sont présentées. Par la suite, les changements produits par un traitement thermique et par un dépôt de tétravinylsilane par plasma sur les propriétés des fibres de basalte sont étudiés.*

***Partie V : Propriétés interfaciales fibre/matrice**. La dernière partie du manuscrit présente les résultats expérimentaux obtenus par tests de fragmentation sur composites monofilamentaires. La qualité d'adhésion des fils de lin et des fibres de basalte non traités et traités avec les matrices époxy et vinylester est discutée en termes de longueur critique de fragment, de longueur de décohésion et de résistance au cisaillement interfacial (IFSS). L'objectif principal de cette section est d'analyser en détail les effets des différents traitements de modification de surface sur l'adhésion des renforts de basalte et de lin avec les matrices polymères.*

Chaque partie se finit par une conclusion en anglais et en français.

*Les **conclusions finales ainsi que les perspectives** sont présentées à la fin du manuscrit, en anglais et en français.*

PART I

STATE OF THE ART

The objective of the Part I is to provide an overview of natural fibre hybrid composites materials developed up to the present. The microstructural and mechanical properties, as well as the main factors able to affect the performances of hybrid composites will be described in Chapter I.1. Particular attention will be given to the issue of the interfacial adhesion of natural fibres with polymeric matrices. In Chapter I.2, the main characterization techniques used to assess the fibre/matrix interface will be described. Finally, a short review of the different modification treatments used so far, in order to optimize the fibre/matrix compatibility, will be provided in Chapter I.3.

PART I - STATE OF THE ART

CHAPTER I.1

NATURAL FIBRE HYBRID COMPOSITE MATERIALS

The use of natural fibres as reinforcement in polymer matrix composite materials is hardly a novelty. It was in 1909 that, for the first time, cellulose fibres were employed to reinforce a phenolic matrix [Silva *et al.*, 2011]. This year may be considered as the date of birth of the ecocomposite materials. It took around 40 years to reach the first industrial application of this class of materials. Only in 1941, Henry Ford introduced for the first time in his cars fenders and deck lids produced from soy protein-based ecoplastics. If in the past the research and the development of composite materials produced from renewable and more sustainable sources was considered as of marginal importance compared to the synthetic composites sector, nowadays the use of ecocomposites has become one of the vital components for the next generation of industrial practice. The increasing need for a more sustainable growth is the key factor of the growing importance of ecocomposite materials. Glass fibre represents the dominant material used as reinforcement of fibre-reinforced plastics. Despite the advances and the innovations in other segments of the fibre reinforced plastics/composites market, glass reinforced polymer material (GRP) is still characterised by a market share of over 95%. As reported by the AVK Federation of Reinforced Plastic in the last composites market report, in 2018 the GRP market grew in the European countries for the sixth consecutive year [Witten *et al.*, 2018]. These materials display significant environmental problems related to both their production process and their life cycle. The glass fibre production is a high-temperature, energy-intensive process. This results in an environmental issue because of the emissions of combustion products, and the oxidation of atmospheric nitrogen, i.e. sulphur dioxide, carbon dioxide, and nitrogen oxides. Dust, traces of chlorides and metals, present as impurities in the raw materials, are contained in the furnace emissions. In particular, dust turns out to be very polluter and in most cases is not recycled back to the furnace, due to the presence of aggressive/corrosive components such as sodium chloride

(NaCl) [Scalet *et al.*, 2012]. Technical solutions are possible for minimising all these emissions, but each technique has associated financial and environmental implications unattractive from an industrial point of view. In addition, GRPs are traditionally directed to landfill at their end of life, mainly because recycling operations are often difficult and expensive. In the last few years, because of the increasing global interest in environmental issues, features like recyclability and environmental safety have been gaining greater attention. The European Commission recently made legislative proposals introducing new waste-management targets regarding:

- reuse, recycling and landfilling;
- strengthening provisions on waste prevention and extended producer responsibility;
- streamlining definitions, reporting obligations and calculation methods for targets.

The European environmental legislation is becoming more and more restrictive. The emanation of directives, such as the EU Directive on Landfill of Waste (Directive 99/31/EC) and the End-of-life Vehicle Directive (Directive 2000/53/EC), severely limit the landfill disposal of GRPs and are seen as barriers to the development or continued use of fibre reinforced plastics. These environmental issues represent the driving force of the rising interest towards the use of natural fibres to replace synthetic fibres, in particular glass fibres, as reinforcements in polymer composites. Features such low cost, low density, non-toxicity, high specific properties, no abrasion during processing, and recyclability, contribute to draw the manufacturing industry to green composites. Many studies have been performed on composites made from one kind of reinforcement, i.e. 100% plant fibres (jute, hemp, flax, sisal…) or 100% mineral fibres (as basalt). The results have shown that natural fibre reinforced composites do not provide mechanical properties comparable with those of synthetic fibre composites. Despite their favourable attributes, disadvantages like high susceptibility to moisture absorption, thermal and mechanical degradation during manufacturing, poor compatibility with several polymeric matrices and low microbial resistance make inconvenient the use of natural fibres in composites intended for semi- or structural applications [Koronis *et al.*, 2013]. A possible solution to this problem is the development of natural fibre hybrid composite materials. In fact, hybrid composites made of combination of natural and synthetic fibres may represent a key strategy in engineering new classes of ecocomposite materials. The rationale is to introduce different types of fibres

aiming at overcoming the drawbacks of composites reinforced with only one type of fibres. Hybridization of synthetic fibres with plant fibres represents a significant strategy to reduce on one side weight and carbon footprint of traditional composite materials, whilst retaining a sufficient mechanical performance to permit not only cosmetic applications. The present chapter is split up into two sections. The basics on fibre hybrid composites and on the different hybridization techniques will be discussed in the first section of the chapter. Successively, the second section intends to cover the recent developments on hybrid composites based on natural fibres.

I.1.1 Fibre hybrid composites

Hybrid composites may be defined as laminated composites containing more than one type of fibre. In the case of polymer matrix composites, hybridization may be also considered as a blend of two or more polymers reinforced with one or more fibres, the so called "matrix hybrid composites". The present work is restricted to hybrid composites characterized by only one kind of polymer matrix containing at least two types of reinforcing fibres. Such type of composites may be called "fibre hybrids" or "fibre hybrid composites". Combining two or more fibre types in a single composite has the objective to maintain the good properties of the different fibres and, at the same time, alleviate some disadvantages. Another important purpose, not to be underestimated, is the cost reduction that may be achieved using one of the two components cheaper than the other one. A typical example is offered by carbon/glass hybrid composite. In fact, replacing carbon fibres in the middle of a laminate by glass fibres allows to obtain a cheaper composite characterized by unaffected flexural properties. Depending on the way the constituents are mixed, different types of fibre hybrid composites are possible. Swolfs et al. [Swolfs *et al.*, 2014] report three different configurations: interlayer or layer by layer configuration, in which two or more homogeneous reinforcements are staked in the composite laminate; intralayer or yarn by yarn hybrid configuration, in which the two fibre types are mixed within the same layer; intrayarn or fibre by fibre hybrid, where the two different fibres are mixed or commingled on the fibre level. Figure I.1 shows a schematic description of the three main hybrid configurations. Through the combination of these, other configurations characterized by greater complexity can be obtained. For example, a fibre by fibre hybrid and a homogeneous yarn may be woven together in the same layer. In general, the most diffuse hybrid composites

produced are the interlayer hybrids, because the simplicity of the manufacturing process. According to Pegoretti et al., other fabrication procedures are possible: “selective placement hybrids”, in which specific fibres are placed where additional strength is needed; “superhybrids”, characterised by the presence of metal plies stacked in a specific orientation and sequence [Pegoretti *et al.*, 2004] .

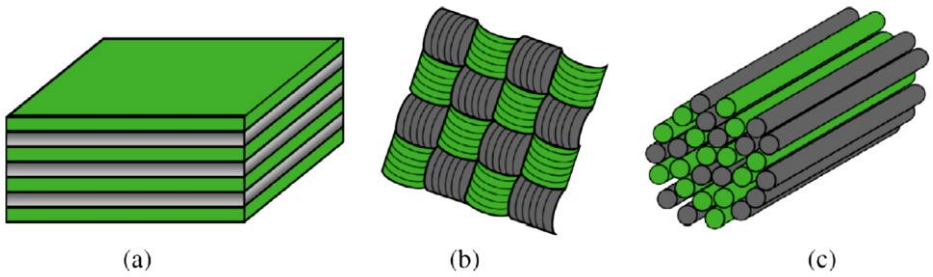

Figure I. 1 Illustration of the three different hybrid configurations: (a) interlayer, (b) intralayer, and (c) intrayarn [Swolfs *et al.*, 2014].

Hybrids can be differentiated according to the degree of dispersion of the different reinforcing fibres used. The fibres dispersion is an important aspect and represents a measure of how well the fibres are mixed. The degree of dispersion can be measured as the reciprocal of the smallest repeat fibre length. The different degrees of fibres dispersion are reported in Figure I.2. The lowest degree of dispersion is obtained when the two fibre types are in two distinct layers, Fig. I.2-a.

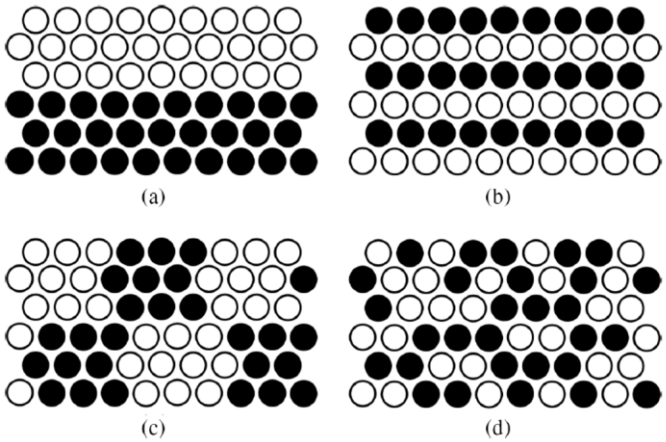

Figure I. 2 Different degrees of fibres dispersion in a hybrid composite material: a) two layers (lowest degree of dispersion), b) alternating layers, c) bundles by bundles and d) completely random dispersion (highest degree of dispersion) [Swolfs *et al.*, 2014].

The dispersion can be improved by increasing the number of layers or decreasing the layer thickness. An enhancement of the dispersion degree may be also achieved by hybridising on the fibre bundle level, Fig. I.2-c. The maximum degree of dispersion is achieved when the two fibre types are completely randomly distributed. According to Santulli [Santulli, 2019], a crucial aspect for the mechanical properties of the hybrid composites is the sequence in which the different layers are arranged. Different studies investigated the effect of the stacking sequence on properties like the damping of the composite and the falling weight impact resistance [Sarasini *et al.*, 2014; Assarar *et al.*, 2015; Andrew *et al.*, 2019]. Two different stacking sequences are possible: the "sandwich hybrid composite", in which the layers reinforced with one of the two different fibres are arranged in the central section of the composite and the layers with the other fibre in the outer zones; the "intercalated hybrid composite", where the two different layers may be placed in more complex ways. The mechanical properties of an hybrid composite material are influenced by several parameters, such as: the reinforcements mechanical properties, matrix mechanical properties, distribution and dispersion of reinforcements, volume fractions of the reinforcements, interfacial adhesion between the matrix and the reinforcement etc.. The different types of fibres used as reinforcement in a hybrid composite can be distinguished by their different failure strain value. In general, the fibres characterized by the lowest failure strain value will be referred to as low elongation fibres (LE). On the contrary, the high elongation (HE) fibres will be the fibres characterized by the highest strain value. It is important to highlight that, the HE fibre does not necessarily have a large failure strain, but just larger than the value of the LE fibre. The most important effect to combining HE and LE fibres together is the apparent failure strain enhancement of the LE fibre, compared to that obtained in a non-hybrid composite. This important phenomenon is known as "Hybrid effect" and it was reported for the first time by Hayashi in 1972 [Hayashi, 1972]. He showed an increase of 40% of the failure strain of the carbon fibre layers in a carbon/glass hybrid composite. Figure I.3 shows a schematic representation of the hybrid effect. Hayashi observed this effect under the assumption that relative volume fraction between the LE and HE fibres is 50/50 and that the hybrid composite is twice as thick as the reference composites. Three different explanations have been hypothesized to explain the hybrid effect: (1) residual stresses, (2) changes in the failure damage development, and (3) dynamic stress concentrations. The first hypothesis is the thermal effect. This explanation is based on the differences in the thermal

contraction of the two fibre types. During the cure process, both LE and HE fibres will have the tendency to change their length due to the rising temperature.

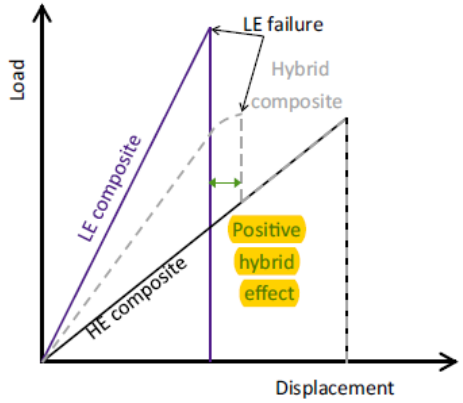

Figure I. 3 Image illustrating the apparent failure strain enhancement of the LE fibres [Swolfs *et al.*, 2014].

The fibre characterized by the higher coefficient of thermal expansion (CTE) will show the tendency to modify its dimension more than the fibre characterized by the lower CTE. When the polymer resin is cured, the composite temperature decreases and both fibres will shrink. The cured resin will oppose to the dimension changes producing a system of compressive residual shrinkage stresses. These compressive stresses counteract the applied stress and increase the failure strain of the HE. In contrast, the apparent failure strain of the LE fibres is reduced. Different studies reported that, despite it is easy to understand, the thermal effect is insufficient to explain the full hybrid effect [Zweben, 1977; Manders *et al.*, 1981].

The second explanation of the hybrid effect is related to changes in the damage development of the hybrid composite. In general, when a unidirectional composite material is loaded and the strain is increased, the first fibre will break, losing its load carrying capacity. The surrounding matrix is loaded in shear and transfers stress back onto the broken fibre. At the same time, the neighbouring fibres will be subjected to stress concentrations and to an additional load caused by the broken fibre. This stress concentration increases the failure probability in the neighbouring fibres. When the strain is further increased, this increased probability will lead to the development of clusters of broken fibres. When the cluster reaches a certain critical size, it becomes unstable and leads to the final failure of the composite. A possible explanation of the apparent increase of the LE fibre failure strain in a hybrid composite may be found in the presence of LE and HE fibres characterized by different stiffness and/or diameter. These differences may interfere with the cluster

development. In particular, the broken LE fibres can be bridged by the HE fibres, obstructing the clusters development and also increasing the critical cluster size.

The last possible explanation of the hybrid effect is based on the dynamic stress concentrations during the failure of unidirectional composites. According to several studies [Hedgepeth, 1961; Ji *et al.*, 1985; Xia *et al.*, 1991], the dynamic stress concentrations have an important contribution to the hybrid effect. Xing et al. [Xing, 1981] proposed a theoretical model that demonstrated the production of two independent stress waves when a LE fibre breaks in a hybrid composite. The first wave propagated in the LE layer, while the second one propagated in the HE layer. Contrary to a unidirectional composite, in a hybrid material these two waves are always out-of-phase, which led to lower stress concentrations in LE/HE and produced a positive hybrid effect.

I.1.2 Natural fibre hybrids

Hybridization may be performed in two ways: by combining synthetic and natural fibres, producing a synthetic-natural hybrid composite, or by combining different natural fibres together, producing a natural-natural fibre hybrid composite.

I.1.2.1 Natural-Synthetic fibre hybrids

The partial replacement of the artificial fibres with the natural ones may lead to the production of synthetic/natural based hybrid composites with intermediate properties between pure natural and pure synthetic fibre composites. In particular, the hybridization of synthetic and natural fibres can allow the production of a hybrid composite material that will be characterized by reasonable costs compared with those of single synthetic fibre material. There is a wide variety of plant fibres that can be used as reinforcements in composite materials, such as flax, hemp, kenaf, sisal and so on. Several works have given an overview on the different properties of synthetic/natural hybrid composites [Ashik *et al.*, 2015; Saba *et al.*, 2016; Mochane *et al.*, 2019]. According to Dong [Dong, 2018], hybrid composites including plant fibres were fabricated most frequently with glass fibres, which are typically reported to improve most mechanical properties. One of the most important positive hybridization effects reported is the reduction in the moisture sensitivity and the mechanical property variability of the natural fibre reinforced composites. Natural fibres are hydrophilic due to their chemical composition. In general, the moisture content of the fibres is between

5 and 15% [Safri *et al.*, 2018]. The moisture uptake causes a swelling of fibre and a dimensional variation of the composite material. In addition, during the manufacturing process, the moisture produces an increase in the void content, affecting fibre/matrix bonding and leading to a decrease in mechanical properties. In this context, the hybridization of natural fibres with hydrophobic synthetic ones offers a possible method to enhance the moisture resistance of the composite material and, at the same time, reduce the degradation of mechanical properties. Panthapulakkal and Sain [Panthapulakkal *et al.*, 2007] observed a strong decrease in the water absorption tendency after the hybridization of short hemp fibres with glass fibres. If compared with those of a traditional short hemp/PP composite, the hybrid is characterized by higher tensile, flexural and impact properties. The thermal properties were also investigated, and the thermogravimetric studies showed an increase in thermal stability of the composite. Hybridization with synthetic fibres can represent a possible way to enhance the durability of natural fibre composites. Akil et al. [Akil *et al.*, 2014] analysed the effect of water absorption on the mechanical properties of jute/glass hybrid reinforced unsaturated polyester composites. The authors demonstrated the positive role played by the addition of glass fibres in terms of moisture resistance. The work reported also that hybrid composites showed superior tensile and flexural properties compared to jute composites, producing an increase in the environmental degradation resistance. Several experimental works described how the glass fibres incorporation allowed an increase in mechanical performances of natural fibre reinforced composites. For example, the hybridization of flax fibres with 30 wt% of glass fibre in a polypropylene matrix allowed to obtain higher mechanical properties than those of a flax fibre bundle/PP composite [Arberlaiz *et al.*, 2007]. Several studies investigated the effect of hybridization on impact performances [Mishra *et al.*, 2003; Santulli *et al.*, 2005; Atiqah *et al.*, 2014; Barouni *et al.*, 2019]. These studies highlighted that the hybridization of low strain to failure fibres, like glass fibres, with high strain to failure fibres, like plant fibres, results in an increase in energy absorption capacity and hence improved impact resistance of the hybrid composite. As reported in section I.1.1, the mechanical properties of hybrid composites are strongly dependent on the stacking sequence of the different fibrous laminates. Shahzad [Shahzad, 2011] investigated the effect of two different kinds of fibre configurations on both impact and fatigue strength of glass/hemp hybrid composites. The hemp skin - glass core, and glass skin - hemp core configurations were used. The authors showed that hybridization of hemp fibres with glass fibres results in considerable improvement in their impact properties. In

particular, the stronger and tougher glass fibres enhance the impact damage tolerance of the composites and this effect is more pronounced when glass fibres are used as skin. Following impact at 4 J energy, hybrid composites with 11% glass fibres, lost only about 30% of their intrinsic strength and stiffness, compared to 70% loss in properties for hemp fibre composites at same impact energy level. Shahzad pointed out how the high strain to failure hemp fibres affected the fatigue properties of hybrid composite. The replacement of 11% of hemp fibres with glass fibres produced an improvement in fatigue strength but no improvement in fatigue sensitivity was observed compared to hemp fibre composites. Zhang et al. [Zhang *et al.*, 2013] investigated the mechanical behaviours of unidirectional flax and glass fibre reinforced phenolic hybrid composites. This study pointed out as stacking sequence can influence the tensile strength and tensile failure strain of the hybrid composite. On the contrary, no influence was found for the elastic modulus.

In recent years, there has been substantial interest on the application of basalt fibres as reinforcement of polymer matrices. These can be proposed as a replacement for glass fibres in view of their advantages in terms of environmental cost relative to their chemical and physical properties. A very interesting solution is the possibility to produce hybrids including plant fibres and basalt fibres [Dhakal *et al.*, 2015; Fiore *et al.*, 2016]. Recent studies concentrated on the manufacturing of hybrids made using basalt fibre composites as the core laminates, in particular introducing, as skins, glass/flax, glass/hemp and hemp/flax laminates [Petrucci *et al.*, 2015]. These studies indicated the suitability of using basalt fibre laminates as the core of more complex laminates, including different fibres, in which impact performance is reduced to a lower extent in comparison with the weight gain obtained. Petrucci et al. [Petrucci *et al.*, 2013] highlighted that adding glass and flax to basalt fibre allows the production of reinforced laminates characterized by very interesting mechanical properties. In their work, the tensile, flexural and interlaminar shear strength of different basalt, glass, flax and hemp fibre epoxy hybrid composite laminates were studied. The results showed that all the hybrid laminates were characterized by higher mechanical properties than the pure hemp and flax fibre reinforced laminates. Only for the basalt fibres a negative hybrid effect was reported, showing mechanical properties lower than the pure basalt composite laminate. Among the different hybrids, the best properties were offered by glass/basalt and flax/basalt laminates. A comparison between different types of hybrid materials was conducted also by Alexander and Elphej Churchill [Alexander *et al.*, 2017]. They explored the properties of hybrid composites composed of sisal/glass, sisal/basalt and

sisal/glass/basalt. Results pointed out that sisal/basalt/epoxy hybrid composites offered the best properties due to the bond strength between sisal and basalt fibres. In addition to glass fibres, natural fibres were also hybridised with carbon fibres to make hybrid composites. Recently, Santulli [Santulli, 2019] presented a review on the mechanical and the impact damage analysis on carbon/natural fibres hybrid composites.

I.1.2.2 Natural-Natural fibre hybrids

Combining two different types of natural fibres into a polymer matrix represents a very attractive solution that is gaining increasing interest. Natural-natural fibre hybrids are characterized by low costs, good mechanical performance and a lower environmental impact than traditional composites based on synthetic fibres, such as carbon and glass fibres. Many researchers have investigated the mechanical properties of natural-natural fibre reinforced hybrid composites [Das, 2017; Maslinda *et al.*, 2017; Akash. *et al.*, 2018; Fragassa *et al.*, 2018; Naidu *et al.*, 2018]. The hybridization of banana/kenaf fibres was able to produce an increase in the mechanical strength of woven hybrid composites, in comparison with the individual fibre-based composites [Alavudeen *et al.*, 2015]. Senthil Kumar et al. [Senthil Kumar *et al.*, 2016] compared the properties of a banana/coconut hybrid composite with those of pure coconut sheath and pure banana composites. The authors found only a slight difference in the mechanical properties between the composites. Jawaid et al. [Jawaid *et al.*, 2014] investigated the effect of different stacking sequences on the mechanical properties of a jute/oil palm hybrid. The results highlighted that the jute/oil palm/jute configuration exhibited superior flexural properties over the oil palm/jute/oil palm sequence, due to the fact that jute fibre has higher flexural strength as an outer layer. Venkatesh [Venkatesh, 2015] found a positive hybrid effect by adding bamboo fibre in sisal/unsaturated polyester composites. Maslinda et al. [Maslinda *et al.*, 2017] reported that kenaf-jute fibre and kenaf-hemp fibre reinforced hybrids exhibited high flexural and tensile properties in comparison to the individual composites. Das [Das, 2017] carried out an interesting study on the possibility to use short fibres derived by waste paper in hybrid composites. In particular, the experimental work investigated the mechanical properties of polyester hybrid composites reinforced with woven jute fabric and waste paper. The results showed that the hybrid polyester composite was characterized by intermediate properties between those of a woven jute fabric and those of a polyester composite reinforced only with waste paper. Similar

results were found for basalt/flax vinylester hybrid composites [Fragassa *et al.*, 2018]. In fact, also in this case, the hybrid composites showed tensile strength, flexural properties and energy absorbed values intermediate between those of a vinylester composite reinforced with flax fibres and of a vinylester composite reinforced with basalt fibres. The combination of natural fibres extracted from plants, like flax, with natural fibres of mineral origin, basalt, turns out to be very interesting. Fiore et al. [Fiore *et al.*, 2016], investigated the use of basalt layers as outer laminate to improve the aging resistance of flax reinforced epoxy composites. The behaviour of a flax/epoxy composite was compared with that of a basalt/flax hybrid, for dry and salt water conditions. The water saturation was reached after one month for both single and hybrid composites. The results showed that the percentage of absorbed moisture was higher for composites reinforced using only flax fibres. A similar study was performed by Zivkovic et al. [Zivkovic *et al.*, 2017]. They investigated the influence of basalt/flax hybridization on the impact properties of dry and salt-water conditioned composite samples. The hybrid composite was made of flax fibre reinforcement (FFR) in the central zone and basalt fibre reinforcement (BFR) in the outer layers. The hybrid composites showed higher impact behaviour than single composites, especially in the case of conditioned samples. Another important result concerns the moisture uptake of the hybrid composite. In fact, due to basalt layer protection, flax fibres in the vinyl ester matrix showed lower moisture uptake and a better fibre/matrix adhesion. This led to more stable behaviour of the hybrid composite and a more uniform response to impact loading. Sarasini et al. [Sarasini *et al.*, 2018] explored the possibility to combine short basalt and hemp fibres to develop hybrids based on a high density polyethylene (HDPE) matrix. Different basalt/hemp combinations were investigated. All the different hybrids were manufactured through extrusion and subsequently injection moulding process. The effects of a maleated coupling agent on the interfacial properties of the resulting composites were evaluated performing single fibre fragmentation tests (SFFT). Results revealed a non-optimal level of adhesion for both basalt and hemp fibres with HDPE matrix. The fibre/matrix adhesion was significantly enhanced by incorporation of a maleated coupling agent. A positive hybridization effect was produced for the tensile properties, crystallinity and the Vicat softening temperature of hemp fibre composites.

Recently, the development of biodegradable hybrids, consisting of biodegradable polymer matrix and natural fibres, received considerable attention. The different studies include those by Jumaidin et al. [Jumaidin *et al.*, 2017] and Edhirej et al. [Edhirej *et al.*, 2017]. They developed hybrid composites by using starch as a matrix and seaweed, sugar palm fibres

(SPF) and cassava as reinforcement. Jumaidin et al. demonstrated that hybrid showed higher tensile and flexural strength in comparison to the individual composites. The highest tensile (17.74 MPa) and flexural strength (31.24 MPa) were achieved for hybrid composites with 50:50 ratio of seaweed/SPF. Ramie and borassus fibres were included in a biodegradable polycaprolactone (PCL) matrix [Sarasini *et al.*, 2017]. The inclusion of ramie fibres in PCL matrix resulted in increases in both the tensile strength and modulus. Further increases in both the tensile strength and modulus were observed when the content of ramie fibres was enhanced. However, the addition of borassus fibres in that system did not improve both the tensile strength and modulus, irrespective of the fibre content.

I.1.2.3 Factors affecting natural fibre hybrid composites

Different factors can influence the final mechanical performance of natural fibre-based hybrid composites. Several studies reported that the volume or weight proportion of fibres in a hybrid composite can affect in a positive or negative way the mechanical properties of the composite. For example, Padma Priya and Rai [Padma Priya *et al.*, 2006] demonstrated that an increase in weight fraction of glass fibre in a silk/glass hybrid composite produced a strong enhancement of the mechanical properties. In particular, the modulus of hybridized composite is found to be higher than the un-hybridized one due to the presence of higher modulus glass fibres. The best performances were obtained with a 50% glass and 50% silk combination. The presence of 50% glass fibre in the hybrid composite leads to efficient load transfer from glass to silk fabric. On the other hand, it is also possible that an increase in weight proportion of fibres in a hybrid composite will produce a negative effect on its mechanical properties. Abdullah-Al-Kafi et al. [Abdullah-Al-Kafi *et al.*, 2006] studied the effect produced by varying the wt% of the fibres on the mechanical properties of a jute polyester, and jute-glass fibres mat-reinforced polyester hybrid composites. The study highlighted as the tensile and flexural properties increased till 25 wt% of the jute fibre content, further increment of the fibre content resulted in a decline in the properties because of formation of agglomerates which hinder stress transfer.

As mentioned above, the stacking sequence represents a crucial aspect for the mechanical properties of the hybrid composites. The effects produced by varying the pattern of arrangement of the different fibre layers in the hybrid composites have been studied by the researchers. In general, optimum mechanical properties were found by placing high strength

fibres as the skin layers [Nunna *et al.*, 2016]. This result was attained by Gupta [Gupta, 2009], for instance. In this study a comparison between the mechanical properties of flax fibre reinforced composite (FFRC) lamina, glass fibre reinforced composite (GRP) lamina, glass-flax-glass-hybrid (GFGH) and flax-glass-flax-hybrid (FGFH) was carried out. The study reported that the stacking arrangement GFGH was superior to FGFH in terms of tensile, compressive, flexural, impact and specific tensile strengths.

In addition, also the conditions under which the hybrid material is exposed during its service may represent a factor affecting the mechanical behaviour. Despite the use of more hydrophobic synthetic fibres allows to enhance the moisture resistance, the exposure to aqueous environmental conditions still remains a critical point in natural fibre hybrid composites. Different studies pointed out that various degradation mechanisms can be obtained depending on the time of exposure and temperature related to various environmental conditions [Phani *et al.*, 1987; Thwe *et al.*, 2003; John *et al.*, 2007; Zamri *et al.*, 2012; Sergi *et al.*, 2019].

A last but not least factor able to influence the mechanical performance of natural fibre-based hybrid composites can be found in the poor compatibility of natural fibres with polymer matrices. The weak fibre/matrix adhesion still represents a major limitation for the industrial exploitation of natural fibres. It is well known that the peculiar chemical composition, hydrophilic properties and surface characteristics of natural fibres prevent them from achieving a proper interfacial adhesion with hydrophobic polymer matrices. The natural fibre/matrix interfacial adhesion can represent a preferential path for water ingress, exposing the hydrophilic groups of the fibre to the attack of water molecules and so producing a composite with poor mechanical properties [Akil *et al.*, 2014; Sergi *et al.*, 2019]. The analysis and optimization of the fibre/matrix interface quality therefore represent crucial issues in the development of hybrid composites. The best mechanical performance of a composite material is achieved when the ability to transfer stress across the fibre-matrix interface is high, i.e. when adhesion is maximized. Adhesion can be seen as the sum of different contributions: interaction forces (like Van der Waals), chemical bonds, residual stresses. There are two types of interfaces in hybrid composites: intraply fibre/matrix interface, between the fibres and the polymer resin, and interply interface, between plies of composite made with different fibres. The adhesion quality of these two types of interfaces will determine the mechanical properties of the hybrid composite. The interply interface has been recognized to play a fundamental role in hybrid composites, such as in basalt-carbon

ones [Ferrante *et al.*, 2015]. A positive hybrid effect on the interplay interface has been also reported. Zhang et al. [Zhang *et al.*, 2013] investigated the effect of the interfacial properties between flax fibre plies and glass fibre plies on the mechanical behaviours of unidirectional flax and glass fibre reinforced hybrid composite. The study reported as the interlaminar shear strength of the flax/glass hybrid was higher than that of a glass fibre reinforced composite. This improvement was mainly due to a "fibre bridging" effect between glass and flax fibres. In fact, observing the different delaminated surfaces produced, it was seen that the twisted flax yarn structures and rough surface of flax fibres led to the production of fibres bridging between flax yarns, flax fibres and glass fibres, which contributed to the improved fracture toughness of the hybrid composite.

CHAPTER I.2

FIBRE/MATRIX INTERFACIAL ISSUES

Interface is a critical zone that plays a key-role for the mechanical performance of the composite material. It has the purpose to guarantee the load transmission from the matrix to the reinforcement during load application. The quality of the fibre/matrix interface is a crucial issue in composite materials. As reported in section I.1.2.3, in natural fibre composites the compatibility of the fibres with the polymer matrices is not as good as in synthetic fibre composites. The adhesion quality between the reinforcement and the matrix determines the mechanical behaviour of the composite. Only a good adhesion is able to assure a good transfer of stress between the constituents. The interface in fibre composites can be defined as an infinitely thin surface formed by the contact between the reinforcing fibre and the matrix, able to maintain the bond between the two constituents for the transfer of loads. It has physical and mechanical properties different from those of the fibre or the matrix. The interface must be distinguished from a second important region: the interphase. A schematic representation of the concept of interphase is illustrated in Figure I.4.

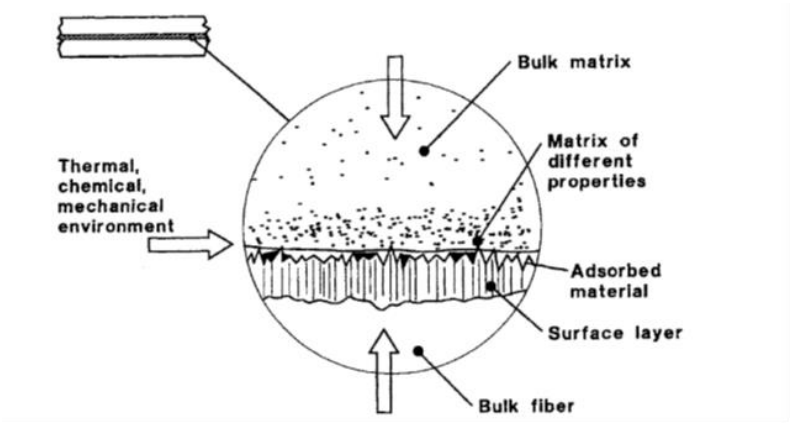

Figure I. 4 A schematic illustration of the interphase between fibre and matrix proposed by Drzal et al. [Drzal *et al.*, 1983].

Unlike interface, the interphase is a contact geometrical surface between the reinforcement and the matrix, characterized by a finite thickness and by mechanical and physical properties that vary continuously between those of the fibre and those of the matrix. According to Drzal et al. [Drzal *et al.*, 1983], the interphase contains all the volume altered during the composite consolidation process, from the original fibre and matrix materials. The combination of interface and interphase constitutes a particular area that ensures the bond between the reinforcement and the matrix and plays a key-role in optimizing the mechanical properties of the composite material.

I.2.1 Theories of adhesion and types of bonding

I.2.1.1 Mechanical bonding

According to the mechanical adhesion theory, the adhesion between the fibre and the polymer matrix can be generated by the presence of cavities, porosity and surface roughness present on the surface of the reinforcing fibres, Figure I.5. These asperities can act as mechanical anchor points between the fibre and the matrix. In the case of natural fibres, the surface roughness plays a very important role on interfacial adhesion. In particular for plant fibres, the surface of fibres is generally characterized by defects and irregularities. During the manufacture of the composite material, the polymeric matrix is in a state of viscous liquid able to infiltrate inside the cavities present on the fibre surface.

Figure I. 5 Interface bonds formed by mechanical interlocking.

I.2.1.2 Electrostatic attraction

According to the theory of electrostatic attraction, the fibre /matrix adhesion is linked to the production of electrostatic bonds between the two surfaces. The charges owned by the two

constituents must be of opposed polarity in order to generate attraction, Figure I.6. The interface strength will depend on the charge density produced.

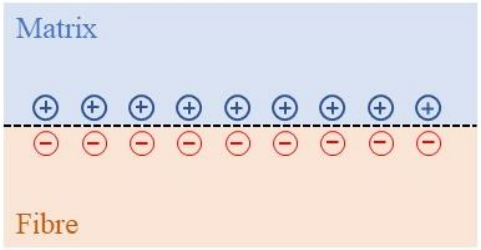

Figure I. 6 Interface bonds formed by fibre/matrix electrostatic attraction.

I.2.1.3 Thermodynamic adhesion: adsorption and wetting

Good wetting of natural fibres with polymer resins during the impregnation stages of fabrication is a basic condition to a proper consolidation of the resulting composites. According to the thermodynamic theory of adhesion, the thermodynamic compatibility, so the fibre/matrix wettability, is related to the surface free energy values characteristic of each component. This free energy is the product of interatomic or/and intermolecular forces (e.g. long-range interaction of Van der Waals type or short-range interaction of acid-base type). In general, the wetting of a liquid to a solid can be expressed in terms of the thermodynamic work that is needed to separate the interface from the equilibrium state of two phases to a separation distance of infinity [Kim *et al.*, 1998]. This reversible work is defined as work of adhesion W_a and can be measured using the Dupre equation, Eq. I.10:

$$W_a = \gamma_l + \gamma_s - \gamma_{sl} \quad \text{(I.10)}$$

where γ_l is the surface free energy of the liquid, γ_s is of the solid and γ_{sl} the solid-liquid interfacial free energy. In general, when a liquid wets a solid surface it exhibits a contact angle. A contact angle in a static system can be measured at equilibrium using the Young equation, Eq. I.11. If we consider the presence of a liquid drop on a solid surface, Figure I.7, the resolution of forces in the horizontal direction at the point where the liquid, solid and vapour phases are in contact can be expressed as:

$$\gamma_{sv} = \gamma_{sl} + \gamma_{lv}cos\theta \quad \text{(I.11)}$$

where γ_{sv} is the surface free energy of the solid-vapor interface, γ_{lv} is the surface free energy of the liquid-vapor interface, γ_{sl} is the surface free energy of the solid-liquid interface and θ is the contact angle. Liquids that form contact angles greater than 90° are called "non-wetting", differently from those that form contact angles less than 90° that are called "wetting" liquids. In an oversimplified way it can be said that, in order to wet a solid surface, the surface energy of the liquid must be lower than that of the solid.

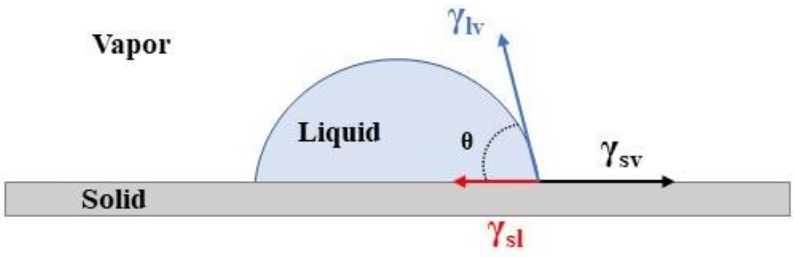

Figure I. 7 Schematic representation of contact angle and surface free energies of the solid-vapor, liquid-vapor and solid-liquid interfaces.

However, it is important to highlight that the total free surface energies of the separated phases can be considered as the sum of two components: a polar component γ^p, linked to the presence of dipole-dipole bonds and hydrogen bonds, and of a dispersive component γ^d, related to the presence of London dispersion forces. The surface energy of the solid and liquid phases can be expressed as follows (Eq. I.12 and Eq. I.13):

$$\gamma_s = \gamma_s^d + \gamma_s^p \quad \text{(I.12)}$$

$$\gamma_l = \gamma_l^d + \gamma_l^p \quad \text{(I.13)}$$

where γ_s^d and γ_s^p are the dispersive and polar components of the solid surface energy, γ_l^d and γ_l^p are the dispersive and polar components of the liquid surface energy, respectively. The surface tension at the solid-liquid interface can be measured by the Owens and Wendt equation (Eq. I.14):

$$\gamma_{sl} = \gamma_s + \gamma_{lv} - 2\left(\gamma_s^d \gamma_l^d\right)^{0.5} + 2\left(\gamma_s^p \gamma_l^p\right)^{0.5} \quad \text{(I.14)}$$

From Eq. I.14 it is evident that the interfacial tension depends on whether the polar and dispersive components of the free surface energy of a phase can form interactions with the corresponding components of an adjacent phase. The solid-liquid interfacial tension will be high for a system in which a solid characterized by a high polar component is placed in contact with a dispersive liquid. In this case a poor wettability of the liquid towards the solid will be produced, with a low value of the adhesion work W_a and a high value of the contact angle. A simplified scheme of this mechanism is shown in Figure I.8.

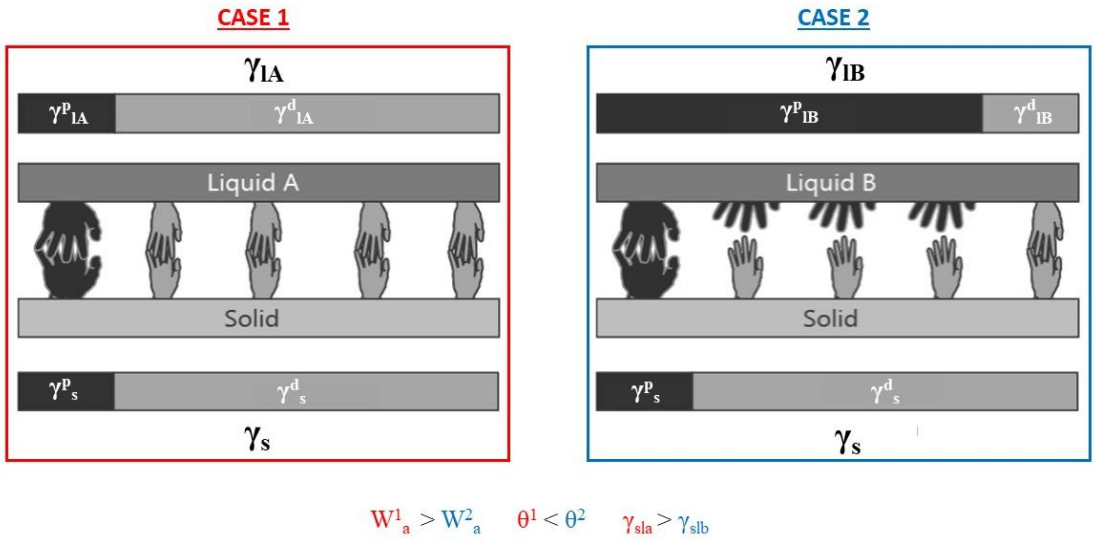

Figure I. 8 Schematic representation of the interaction between polar and dispersive components of a solid with the corresponding components of a liquid A and B, where: γ_s, γ_s^p and γ_s^d are the total surface energy, the dispersive and the polar components of the solid surface energy, respectively; γ_{la}, γ_{la}^p and γ_{la}^d are the total surface energy, the dispersive and the polar components of the liquid A surface energy, respectively; γ_{lb}, γ_{lb}^p and γ_{lb}^d are the total surface energy, the dispersive and the polar components of the liquid B surface energy, respectively; $W_a^{1,2}$ and $\theta^{1,2}$ are the work of adhesion and the contact angle values obtain in case 1 and case 2, respectively. The interface energy for the solid-liquid A and for the solid-liquid B systems are indicated as γ_{la} and γ_{lb}, respectively.

In Figure I.8, the different polar and dispersive components of the free surface energy are symbolized as hands. Only the corresponding hands can connect with each other. It can be seen how in the case 1 the liquid A and the solid tend to interact with each other thanks to the connection between the polar and dispersive components. On the contrary, in case 2, the polar liquid B is not able to interact with the more dispersive solid. In natural fibre reinforced composite materials, the fibre/matrix compatibility is driven by the surface polarity of the reinforcing fibres and the polymeric matrix. In particular, the presence of free water and hydroxyl groups in the cellulosic fibres, mainly in the amorphous regions, decreases the ability of the plant to develop adhesive characteristics with the matrix. For a polar fibre

(hydrophilic) and a dispersive polymer matrix (hydrophobic), the low compatibility leads to a weak adhesion between the two materials.

I.2.1.4 Interdiffusion

This adhesion theory is based on the molecular dynamics theory, according to which the adhesion between two materials is generated by a mutual diffusion (interdiffusion) of the respective macromolecules. Through the interdiffusion phenomenon, the production of a new specific phase called interphase is realized. A thermodynamic equilibrium between the two constituents must exist to activate the interdiffusion mechanism. The strength of the fibre/matrix adhesion will depend on the amount of molecular entanglement, the number of macromolecules involved and the strength of the bonding between the different macromolecules. The phenomenon of interdiffusion is possible only when the macromolecules of the reinforcing fibres have a mobility sufficient to bind to the macromolecules of the matrix or when part of the macromolecules are soluble in the polymer matrix. Interdiffusion may be promoted by the presence of solvents, by the use of coupling agents inside the polymer matrix or on the fibre surface [Kim *et al.*, 1998].

I.2.1.5 Chemical bonding

It consists in the formation of chemical bonds, ionic and/or covalent, between chemical groups present on the surface of the reinforcement and the matrix. The bonding strength will depend on the type and quantity of chemical bonds. For natural fibres, the spontaneous development of chemical bonds is very difficult because of the different chemical composition with the polymer matrices. A possible way to promote the fibre/matrix interface adhesion is the use of coupling agents. Maleic anhydride represents one of the most widely used coupling agents. The use of maleic anhydride grafted PE or PP, called MAPE (for PE) and MAPP (for PP), can increase the interactions between natural fibres and polymers. Maleic anhydride is able to chemically react with the hydroxyl groups present on the fibre surface. The polymeric chain of the MAPE or MAPP can diffuse in the polyethylene or polypropylene matrix, creating bonds between the fibre and matrix. Different works in literature report the tensile strength evolution of the composites as a function of the MA quantity [Sain *et al.*, 2005; Beg *et al.*, 2008; Lopez *et al.*, 2011].

I.2.2 Analysis and characterization techniques of fibre/matrix interface

The fibre/matrix interface plays a crucial role in the stress transfer mechanism from the matrix to the fibre, influencing the mechanical performance of the final composite material. In this context, it is evident that the characterization of this zone is of fundamental importance. The fibre/matrix compatibility can be determined performing different micromechanical characterization tests, each of which is able to measure the local intrinsic properties of the interface. These tests can be divided into two groups: micromechanical tests where an external load is applied directly to the fibre, i.e. the microbond, the pull-out, the push-out and the push-in tests; and micromechanical tests in which the external load is applied to the matrix, i.e. the Broutman test and the single fibre fragmentation test.
The microbond test (MBT) is one of the most used techniques. A small drop of polymer resin is deposited on a single fibre. After polymerization, the resin droplet is mechanically removed from the fibre and the interfacial shear strength is measured by dividing the force necessary to debond the droplet by the contact area between the resin droplet and the fibre. In a recent work [Réquilé *et al.*, 2019], this test was used to assess the interfacial properties of an hemp fibre/epoxy system. In particular, the influence of moisture sorption on hemp/epoxy interface performance was studied using microdroplet debonding tests under various environment relative humidity. An example of the epoxy drop on the hemp fibre is reported in Figure I.9.

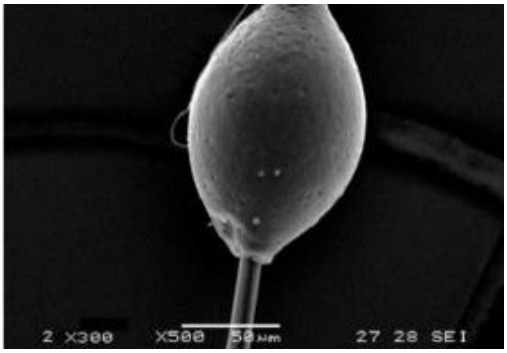

Figure I. 9 Scanning electron micrograph of the epoxy droplet on the hemp fibre surface [Réquilé *et al.*, 2019].

The single fibre pull-out test consists in removing a fibre partially or totally immersed in a resin sample by a tensile force. During test, the applied tensile force is recorded as a function of the displacement of the loaded fibre end. Li et al. used the single fibre pull-out test to assess the effect of a fungal treatment on the adhesion properties of hemp fibres with

polypropylene matrix [Li *et al.*, 2009]. In Figure I.10 is reported a typical force-displacement curve for single fibre pull-out test. Three stages of the pull-out test can be identified. In a first stage, the fibre/matrix interface remains intact and the force-displacement curve is linear. When the external load reaches a critical value of "debond force" (F_d), interfacial cracks are produced, and they propagate along the embedded fibre length. At this second stage the force continues increasing with the fibre end displacement due to the presence of frictional forces in debonded regions that are added to the adhesional forces. Once the maximum load value of F_{max} is reached, the crack propagation becomes unstable, the whole embedded length fully debonds and the measured force drops from F_{max} to F_b. In this last stage of the pull-out test, the force value is due only to fibre/matrix frictional interaction.

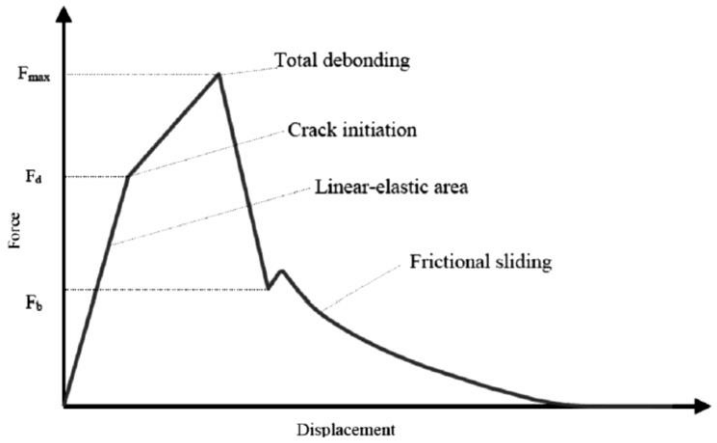

Figure I. 10 A typical force–displacement curve recorded during a pull-out test. [Li *et al.*, 2009]

The fibre push-out and the fibre push-in tests allow the analysis of the fibre/matrix interface directly on composite samples. The local environment in a single fibre composites is very different from the actual environment within a composite. Unlike the characterization tests performed on monofilament samples, in the push-in and push-out tests the influence of parameters such as the local fibre volume fraction, the thermal residual stresses, and the polymer crosslink density can be taken into consideration [Medina *et al.*, 2016]. In the push-out test a top-polished fibre surface is pushed into the matrix through a microindenter. The compression force is applied until there is a complete fracture of the fibre/matrix interface, and the fibre is pushed out of the matrix. The push-in test is performed by loading an individual fibre within the composite until interface fracture occurs. Contrary to the push-out, in the push-in test the fibre s not completely pushed out from the matrix. A schematic

representation of the two tests is reported in Figure I.11. These techniques are well optimized for linear elastic hard or brittle systems without an appreciable elastic mismatch between the fibre and the matrix. That would explain the few studies using these techniques available in literature on plant fibres.

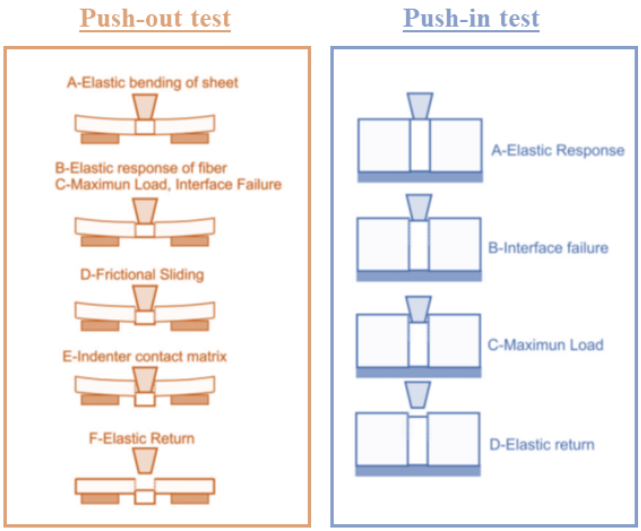

Figure I. 11 Schematic representation of the fibre push-out and push-in tests [Medina *et al.*, 2016].

Concerning the micromechanical tests in which the load is applied to the matrix, the Broutman test and the single fibre fragmentation test (SFFT) can be found. The Broutman test is based on the compression of a necked specimen characterized by the presence of a single fibre longitudinally aligned inside. Due to the load application, compressive stresses will be produced in the smallest cross-section of the sample. These stresses can cause a Poisson's expansion in the transverse direction. If the transverse expansion of the matrix is larger than that of the fibre, a transverse debonding stress at the interface will be produced. The fibre/matrix debonding will be located in the middle of the specimen, where the transverse stress is maximum. This test was used to analyse the adhesion properties of synthetic fibres with polymeric matrices [Ageorges *et al.*, 1999]. At present, the Broutman test is no longer used because of the difficulties involved in the specimens manufacture and in the application of the damage criteria.

The single fibre fragmentation test (SFFT) is one of the most popular methods to evaluate the fibre/matrix interface properties of composites. This is mainly due to the simplicity of sample preparation and the possibility of producing many fragments in a single specimen and then, through statistical analysis, a valid distribution can be obtained from a limited

number of test samples. Basically, the single fibre fragmentation test involves the application of increasing axial stress to a dog-bone specimen containing a single fibre embedded in a polymer matrix. In the case of lignocellulosic fibre-reinforced materials, the MBT and the SFFT tests represent the most widely used techniques for the fibre/matrix interface characterization. Although the MBT test allows an accurate analysis of the interface quality, one cannot ignore the difficulty of this technique to be implemented experimentally because the complications in depositing the resin drop on the fibre surface. In this framework, the fragmentation test was selected to assess the adhesion quality of flax and basalt fibres with polymer matrices. In the following paragraphs an in-depth presentation of the fragmentation technique will be provided.

I.2.2.1 The Single Fibre Fragmentation Test – SFFT

The single fibre fragmentation test is a micromechanical test in which a single fibre is embedded in a dog bone shaped matrix sample and pulled under tension. As the tensile load increases, the fibre inside the resin will break repeatedly into increasingly smaller fragments, at locations where the fibre axial stress reaches its failure tensile strength. In Figure I.12 is reported a schematic representation of the fragmentation phenomenon.

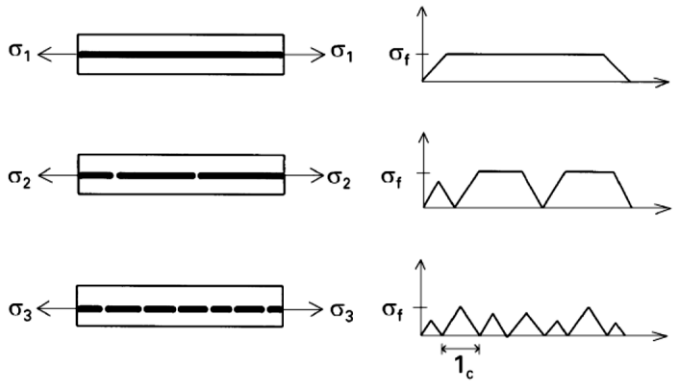

Figure I. 12 Schematic representation of the fibre fragmentation phenomenon. An increase in number of fibre breaks is produced with increasing stress levels in the matrix $\sigma_1 < \sigma_2 < \sigma_3$. The tensile stress in the fibre is a function of position. It increases linearly from the fibre ends to a plateau in longer fragments. When the fibre breaks, the tensile stress at the fracture location reduces to zero [Tripathi *et al.*, 1998].

Due to the constant shear in the matrix, the tensile stress in the fibre is not uniform but it increases roughly linearly from its ends to a plateau in longer fragments. When the fibre breaks, the tensile stress at the fracture location reduces to zero. The higher the tensile stress

transferred, the more fractures will be caused in the fibre. The basic requirements to obtain the fibre fragmentation is that the resin matrix must be characterized by a strain-to-failure higher than the fibre. The fibre fragmentation phenomenon continues until the remaining fibre fragments are shorter than a critical length value l_c. If the fibre fragments have a length equal to or less than the critical value, the stress transferred from the matrix to the fibre is not able to reach the fibre failure strength. As a result, no further fibre breaks are produced with increasing strain of the specimen. This phenomenon is called saturation. The fibre fragmentation phenomenon was analysed for the first time in 1965 by Kelly and Tyson (Kelly and Tyson, 1965), who observed the subsequent breaking of tungsten fibres inside a copper matrix. They proposed a constant shear model to analyse the fibre/matrix adhesion quality. If a long filament is embedded in a resin matrix and the resultant system is elongated, the stress transferable to the filament at a distance *x* from its end may be evaluated by the Equation I.15:

$$\sigma_x = \left(\frac{4 \cdot \tau}{d}\right) \cdot x \qquad \text{(I.15)}$$

where *d* is the diameter of the filament and τ the shear strength at the filament/matrix interface. This equation comes from a simple force balance at filament/matrix interface and it is valid only under the condition of assuming a constant shear stress τ at the interface. When the monofilament composite is elongated further, the tensile stress transferable to the filament increases until it reaches the ultimate tensile strength of the filament, Equation I.16:

$$\sigma_f = \left(\frac{4 \cdot \tau}{d}\right) \cdot x_0 \qquad \text{(I.16)}$$

where x_0 is the value of the distance *x* from the end of the filament at which the tensile stress reaches the ultimate tensile strength of the filament. If a broken piece of filament exceeds $2x_0$ in length, the breakage process repeats itself. On the contrary, if the broken piece is characterized by a length shorter than $2x_0$, the tensile stress transferable to the filament is not able to reach the ultimate tensile strength of the filament and hence no further fragmentation occurs. As reported by Ohsawa et al. [Ohsawa *et al.*, 1978], the length of filament fragments (*l*) follows the uniform distribution characterized by a range $x_0 \leq l \leq 2x_0$, and the average value of the fragment length is given by the equation (I.17):

$$\overline{l} = \frac{1}{2}(x_0 + 2x_0) = \frac{3}{2}x_0 \quad \text{(I.17)}$$

Since x_0 is the length needed for the stress on filament to reach the ultimate tensile strength, the critical fragment length l_c is equal to $2x_0$. By introducing this relationship into Eq. I.17, it is possible to evaluate the critical fragment length from Equation I.18:

$$l_c = \frac{4}{3} \cdot \overline{l} \quad \text{(I.18)}$$

According to the constant shear model proposed by Kelly and Tyson, the filament/matrix interface adhesion quality can be described by determining the interfacial shear strength value (IFSS), using Equation I.19:

$$IFSS = \frac{\sigma_f(l_c) \cdot d}{2 \cdot l_c} \quad \text{(I.19)}$$

where d is the filament diameter, l_c is the critical fragment length and $\sigma_f(l_c)$ is the filament strength at a length equal to the critical fragment length.

The fragmentation test was extensively used to assess the fibre/matrix adhesion quality in synthetic fibre reinforced composites [Tripathi *et al.*, 1998; Asadi *et al.*, 2016; Yao *et al.*, 2017]. In the last few years, the use of this method has been extended to the characterisation of the fibre/matrix interactions in natural fibre reinforced polymers. Joffe et al. [Joffe *et al.*, 2003] investigated the possibility to use the single fibre fragmentation test to evaluate the adhesion of flax fibres with thermoset, vinylester and polyester, resins. In particular, this study supports the use of SFFT as useful technique to assess the effect of two surface treatments of flax fibres, acrylic acid and vinyltrimethoxy silane, on the fibre/matrix interface strength. When applied to natural fibre composites, fragmentation test suffers from several limitations including the need to estimate accurately the fibre strength at the critical fibre fragment length and the significant variation of the fibre diameter not only among fibres but also within the same fibre. The adhesion quality of sisal fibres with polyethylene matrix was investigated by Torres and Cubillas [Torres *et al.*, 2005]. The variability of the results highlighted the necessity to use additional care and caution in assessing the interfacial adhesion through single fibre model composites. The complexity to determine the interfacial shear strength in natural fibre composites was explored by Zafeiropoulos [Zafeiropoulos,

2007]. This study showed that, for a flax fibre/polypropylene system, the most critical parameter for the IFSS value determination is the fibre strength at the critical fibre fragment length. An in-depth investigation of the influence of the testing procedure and the test parameters on the IFSS calculation was carried out by Awal et al. [Awal *et al.*, 2011]. Single fibre fragmentation tests were performed on flax/polypropylene and ramie/polypropylene composites and the effects of different cross-head speeds and gauge lengths were studied. The best test conditions were found to be a gauge length of 15.5 mm and a test speed of 0.2 mm/min. In a recent work, Sun et al. [Sun *et al.*, 2019] investigated the interface bonding between sisal fibres modified by tetraethylorthosilicate sol-gel and γ-aminopropyltriethoxysilane and polypropylene matrix. The fragmentation results indicate that the treated fibre has the highest interfacial shear strength and thus the best interfacial properties. The use of SFFT was extended also to the characterisation of the hemp fibre/polymer matrix interactions [Bouzouita *et al.*, 2010; Sarasini *et al.*, 2018]. Beckermann et al. [Beckermann *et al.*, 2009] performed fragmentation test to determine the critical fibre length and the interfacial shear strength for a composite consisting of 40 wt% $NaOH/Na_2SO_3$ treated hemp fibre, polypropylene and 4 wt% MAPP. An important aspect that it is worth stressing is that, in general, an adequate test configuration should involve a stress distribution similar to that obtain in a real composite. Concerning natural fibre composites, the real stress distribution can be obtained using yarns and not technical fibres. In this framework, for these composites, the interfacial adhesion should be assessed at the yarn scale, where short fibres are twisted with an angle to the yarn axis in order to provide axial strength to the yarn. Some experimental works have extended the SFFT at the yarn scale, thus embedding one single yarn in a polymer resin [Guillebaud-Bonnafous *et al.*, 2012; Perrier *et al.*, 2017]. In these works, detailed experimental, numerical and full-field strain measurements by digital image correlation helped in getting insight into the strong heterogeneity of strain fields that develop with the applied stress and in providing a first step towards the assessment of local behaviour. The complexity to adapt the fragmentation test to yarns stems also from the cross-sectional area of the yarn that typically includes voids between the fibres which are then replaced by matrix during the impregnation of the single yarn.

CHAPTER I.3

NATURAL FIBRE SURFACE MODIFICATION TREATMENTS

The poor compatibility with polymer matrices represents the major limitation for the industrial exploitation of natural fibres. Their peculiar chemical composition and surface characteristics prevent them from achieving a proper interfacial adhesion with the more hydrophobic polymer matrices, which leads to poor mechanical properties of the resulting composites. Cellulose, hemicellulose, wax, lignin and pectin represent the main constituents of a plant fibre. Due to the growing conditions, the percentage composition of each of these components may vary according to prevailing conditions. In general, the components that principally contribute to the physical properties of plant fibres are cellulose, hemicellulose and lignin. Cellulose is the stiffest and the strongest organic constituent in the fibre. In Figure I.13 is reported the chemical structure of cellulose. It is a semicrystalline polysaccharide with a large amount of hydroxyl groups (-OH), able to form hydrogen bonds within the cellulose macromolecules (intramolecular) and with other cellulose molecules (intermolecular).

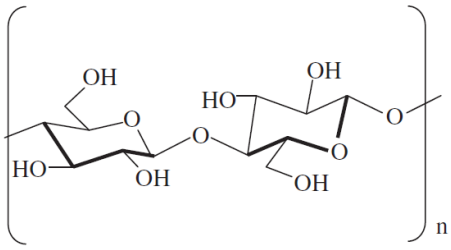

Figure I. 13 Chemical structure of cellulose [Kabir *et al.*, 2012].

The large amount of hydroxyl groups gives the hydrophilic nature to plant fibre when used to reinforce hydrophobic matrices [Kabir *et al.*, 2012]. As reported in section I.2.1.3, in plant

fibre reinforced composites, the fibre/matrix compatibility is driven by the surface polarity of the reinforcing fibres and the polymeric matrix. The presence of hydroxyl groups makes cellulosic fibres strongly polar decreasing the ability of the plant to develop adhesive characteristics with the more dispersive polymer matrix (hydrophobic). Another problem associated with the strongly hydrophilic behaviour of natural fibre is the moisture retention [Pickering *et al.,* 2016]. If not eliminated before the manufacturing process of the composite, moisture can form a barrier between fibre and matrix, preventing their effective adhesion.
In addition, voids and porosities can be produced by the absorbed water droplets, thus weakening the resulting material. In order to alleviate these drawbacks, research has been targeted at altering the chemical and surface properties of natural fibres via modification treatments of the material. Various surface treatments have been proposed over the years, which have been the subject of extensive and detailed reviews [George *et al.*, 2001; Li *et al.*, 2007; John *et al.*, 2008; Kalia *et al.*, 2009; Pickering *et al.*, 2016]. These treatments can be separated into two broad categories: physical methods (e.g. ultrasound, thermal and nonthermal plasma, electric discharge method, etc.) and chemical methods (e.g. alkalisation, acetylation, benzoylation, acrylation, coupling agents etc.). Despite many of these techniques can successfully increase the wettability properties of natural fibres in respect of the polymer matrix, the management and the search for a proper disposal of the large amounts of chemicals used makes these types of treatments expensive and unattractive from an industrial point of view. In this framework, the effects of more environmentally friendly surface treatments on the adhesion quality of flax and basalt filaments to different thermoset resins were investigated in this experimental work. This chapter aims to provide a brief description of the most important chemical and physical modification treatments used so far. In particular, more attention will be given to the explanation of greener chemical and physical modification treatments that can represent an effective alternative to the traditional treatments, specifically: the enzymatic biochemicals treatments, the chemical modification via supercritical CO_2 and the plasma modification treatment.

I.3.1 Chemical modification treatments

The alkaline treatment (mercerization) is one of the most common chemical processes used to modify the cellulosic molecular structure of natural fibres. The effect of alkaline on cellulose fibre is a swelling reaction, during which the natural crystalline structure of the

cellulose relaxes. In alkaline solution, pectin and hemicellulose undergo base-mediated hydrolysis and dissolve. The alkali sensitive hydroxyl (OH) groups present in the hemicellulose and pectin molecules become more reactive with water and then able to move out from the fibre structure. Hemicellulose and pectin are strongly hydrophilic, so their removal can reduce the water retention of mercerized fibres. Mercerization was found to change also the fibre surface topography. A result of the alkali modification is the reduction of the fibre diameter, increasing the aspect ratio of the treated fibres (length/diameter) [Joseph *et al.*, 2003]. In addition, the mercerization process leads to the development of a rough surface topography that results in better fibre/matrix interface adhesion. The type of alkali solution used will influence the degree of cellulose swelling. It has been reported that Na^+ has a favourable diameter, able to widen the smallest pores in between the lattice planes and penetrate into them. Consequently, the sodium hydroxide (NaOH) is the most used alkaline solution in mercerization treatments. It is important to highlight that, mercerization parameters such as alkaline solution concentration, temperature and soaking duration can produce different effects on natural fibres. For example, an excess of the alkali concentration can produce an excess of delignification, resulting in weakening or damaging the treated fibres [Li *et al.*, 2007]. The effects of the different mercerization treatment parameters on the mechanical properties enhancement of natural fibre reinforced composite were in depth reviewed by Hashim et al. [Hashim *et al.*, 2012]. The effect of the alkaline treatment on the properties of cellulosic fibres has been the subject of multiple studies [John and Anandjiwala, 2008; Kalia *et al.*, 2009; Kabir *et al.*, 2012; Cruz and Fangueiro, 2016]. Among these, various experimental works have investigated the effect of mercerization on flax fibres [Jähn *et al.*, 2002; Van de Weyenberg *et al.*, 2003; Arbelaiz *et al.*, 2005; Aydın *et al.*, 2011; Zhang *et al.*, 2015]. The mercerization treatment is also used as a pre-treatment of the fibres, subsequently subjected to other surface modification processes. An alkali pre-treatment using NaOH was used to activate the hydroxyl groups of cellulose and lignin of flax fibres before a silane, peroxide and a benzoylation treatment [Wang *et al.*, 2003, , 2008].

Silanes coupling agents have been used to increase the adhesion of natural fibres with polymer resins. They represent a versatile class of coupling agents that can be tuned to suit the characteristics of a wide range of polymer matrices. The most commonly reported silanes used are amino, methacryl, glycidoxy and alkyl silanes [Pickering *et al.*, 2016]. These silanes are able to interact with hydrophilic groups on the fibre and with hydrophobic groups in the matrix. In fact, the silane structure takes the form of R-Si-$(OR')_3$, where R is a functional

group able to react with the matrix and, -OR' is an alkoxy group that can interact with cellulose [Bousfield *et al.*, 2018]. For example, in presence of moisture, the alkoxy group leads to the formation of silanols. The silanol then reacts with the hydroxy groups of the fibre, forming polysiloxane structures able to influence the wettability, thus the compatibility, of fibres with the polymer matrix. Wang et al. reported that the addition of a small amount of silane coupling agent significantly improves the mechanical properties of flax fibre-reinforced plastic composites [Wang *et al.*, 2008]. As reported before, the efficiency of silane treatment can be strongly increased by the NaOH pre-treatment, because the generation of more reactive sites involved in the fibre-silane reaction. Huda et al. [Huda *et al.*, 2008] and Yu et al. [Yu *et al.*, 2010] investigated the effect of a combined alkali/silane treatment on kenaf/PLA and ramie/PLA laminated composites, respectively. These studies highlighted as the combination of the mercerization with the silane treatment allows to obtain the best results in composite mechanical properties.

The peroxide treatment was used to decrease the hydrophilicity of natural fibres [Sreekala *et al.*, 2000, , 2002]. Organic peroxides tend to decompose easily to free radicals (RO) which react with the hydrogen group of the polymer matrix and the cellulose fibres. The decomposition reaction of peroxide and its reaction with the cellulose interface is schematically reported in Figure I.14.

$$RO - OR \rightarrow 2RO.$$

$$RO. + Cellulose - H \rightarrow R - OH + Cellulose.$$

Figure I. 14 The reaction between the cellulose and the peroxide free radical [Sreekala *et al.*, 2000].

Flax fibres were treated using dicumyl peroxide after alkali pre-treatment [Wang *et al.*, 2003]. The treatment was carried out for 30 min at 70°C and then the chemically treated flax fibres were washed with distilled water and dried at 80°C for 24 h. This study reported that the treated flax fibres showed a higher tensile strength than the untreated fibres.

A reduction in the hydrophilic nature of natural fibres can be achieved by grafting the benzoyl group ($C_6H_5C{=}O$) on the fibre. The solution normally used to carry out the benzoylation treatment is a benzoyl chloride (C_6H_5COCl) solution. In general, the first step of benzoylation is an alkali pre-treatment of the fibres, in order to activate the hydroxyl groups of the cellulose and the lignin in the fibre, Figure I.15.

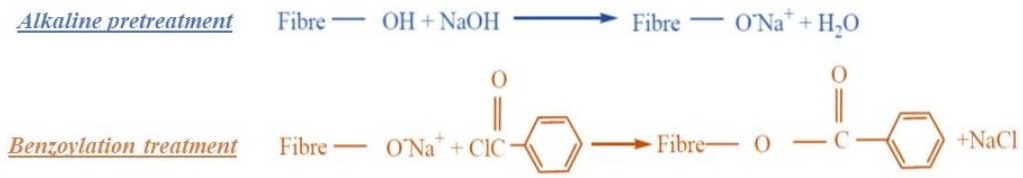

Figure I. 15 Reaction mechanism between the cellulosic hydroxyl groups and the benzoyl chloride [Wang *et al.*, 2003].

Wang et al. investigated the effect of a benzoylation treatment on flax fibres [Wang *et al.*, 2008]. The modified fibres were then extruded with the polymer matrix to form the composite. The study showed that the water absorption and swelling of the treated flax fibre composites was lower than that of composites based on untreated flax fibres.

The esterification treatments represent an attractive chemical method of modifying the surface of natural fibres and making them more hydrophobic. The main principle of the esterification method is the reaction between the esters with the hydroxyl groups of the fibres. In addition, some esters can also react with the polymer matrix, improving the fibre/matrix compatibility. Acetic anhydride and maleic anhydride are the more frequently solutions used for the esterification treatments. The acetylation treatment is based on the reaction of the hydroxyl group of the fibre with the acetyl groups (CH_3CO) at elevated temperatures. The hydroxyl groups that react are those of the lignin, hemicellulose and of the amorphous cellulose. Acetylation has been used in order to reduce the hydrophilic behaviour of natural fibres [Bledzki *et al.*, 1999; Mishra *et al.*, 2003]. An in-depth investigation on the acetylation effects on the tensile strength of flax fibres was performed by Zafeiropoulos et al. [Zafeiropoulos *et al.*, 2003; Zafeiropoulos *et al.*, 2007; Zafeiropoulos *et al.*, 2007].

They found that the acetylation did not affect the fibre strength for treatment times up to 2 h, while the flax strength was affected for a 4htreatment time. A morphological investigation of the fractured fibre surfaces revealed that acetylation changes the bulk properties of flax fibres and not just the surface of flax fibres. Zafeiropoulos and co-workers investigated also the influence of acetylation on the flax fibre/PP interfacial adhesion [Zafeiropoulos *et al.*, 2002]. Single fibre fragmentation tests were performed in order to assess the effect of the treatments on the interface strength. It was found that acetylation treatment led to improvement of the stress transfer efficiency at the interface.

The fundamental difference in using the maleic anhydride (MA), instead of the acetic anhydride, is the possibility to graft the anhydride functionality onto polymers. In fact, MA is not only used to modify the fibre surface, producing chemical bonds with the hydroxyl groups, but also the polymeric matrix, forming a covalent network between the fibre and the matrix. A large number of studies have investigated the effect of MA grafting on the mechanical properties of natural fibre based composite materials [Sanjay *et al.*, 2018]. For example, Park et al. reported an increase in the interfacial shear strength for hemp/PP-g-MA and jute/ PP-g-MA composites compared to those which did not contain the anhydride [Park *et al.*, 2006]. A 50% increase in tensile, 30% in flexural and 58% increase in impact strengths were obtained for sisal fibres/PP-MA composites [Mohanty *et al.*, 2004]. The effects of maleic anhydride grafted high density polyethylene (MAPE) coupling agent on the mechanical properties of basalt, hemp and basalt/hemp fibre reinforced hybrid HDPE composites were investigated by Sarasini et al. [Sarasini *et al.*, 2018]. A commercial grade basalt fibre, with sizing optimised for thermoplastics, were submitted to a combination of soxhlet acetone extraction and thermal exposure in an attempt to remove the sizing. A strong increase in the interfacial adhesion of both hemp and basalt fibres with the HDPE matrix was produced by incorporation of the maleated coupling agent. Comparing the fracture surfaces found for the hemp/HDPE and the acetone + thermal treated basalt/HDPE composites, without and with the MAPE coupling agent, it is possible to highlight that composites with coupling agent showed higher level of interfacial adhesion with the matrix than the respective composites without coupling agent, Figure I.16.

Several experimental works employed isocyanates as coupling agents for different types of natural fibres and polymer matrices [George *et al.*, 2001; Kalia *et al.*, 2009]. Isocyanate has a -N=C=O functional group that is highly reactive with the hydroxyl groups of cellulose and lignin constituents of the fibres and can provide strong covalent bonds between the fibre and matrix. Isocyanate can produce an increase in the moisture resistance properties of the fibre. In fact, it reacts with the moisture present on the fibre surface and forms urea which can further react with the hydroxyl groups of the cellulose. George et al. [George *et al.*, 1999] used isocyanate to treat flax fibres. The treated flax/epoxy composite showed 12.5% and 17.7% higher tensile strength and modulus properties, respectively, compared to the untreated fibre composite.

Among the chemical treatments able to reduce the hydrophilic tendency of natural fibres, some attention has been paid to the permanganate and the sodium chlorite treatments. The

permanganate treatment is performed by potassium permanganate ($KMnO_4$) in acetone solution. During the treatment, highly reactive permanganate (Mn^{3+}) ions are produced and react with the cellulose hydroxyl groups. This treatment can enhance the fibre/matrix chemical interlocking at the interface and provides better adhesion with the matrix [Paul *et al.*, 2010].

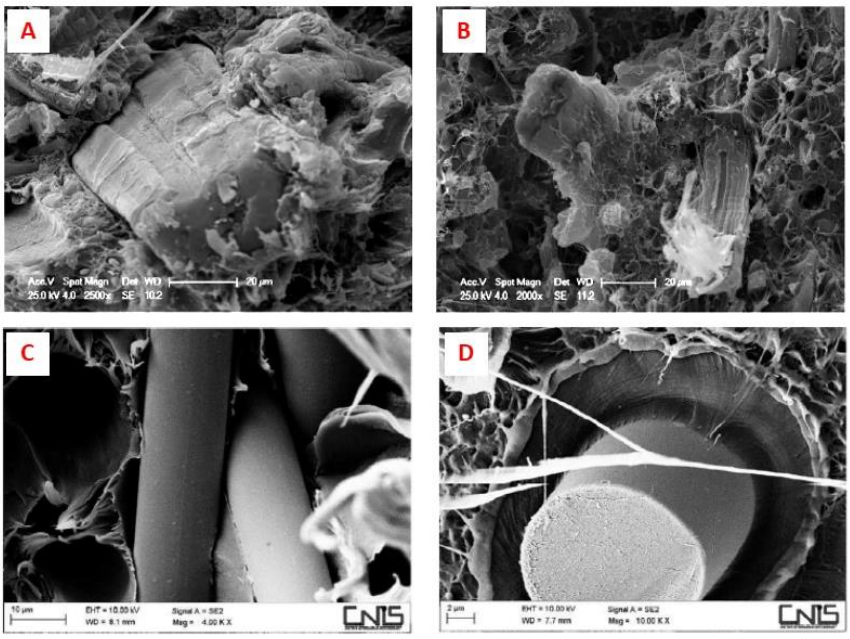

Figure I. 16 SEM micrographs of tensile fracture surfaces of: hemp/HDPE composites without (A) and (B) with coupling agent; acetone + thermal treated (TT) basalt/HDPE composites without (C) and (D) with coupling agent [Sarasini et al., 2018].

The main principle of the sodium chlorite treatment is the reaction between chlorine dioxide (ClO_2), liberated by the acidified $NaClO_2$, and the lignin constituents of the fibre [Zahran *et al.*, 2005]. Sodium chlorite treatment was employed to improve the bonding of flax fibres with the polyethylene matrix [Panigrahi *et al.*, 2009].

Another surface chemical modification of natural fibres is the graft copolymerization. The production of a graft co-polymer takes places through the polymerization of a specific monomer onto an activated backbone polymer. The activation process of the polymeric backbone consists in creation of active sites, such as free radical or chemical groups, which may get involved in a ionic polymerization or condensation process. A number of different methods can be used for the generation of active sites on the polymeric backbone. They can be divided in: chemical methods, physical methods, physical-mechanical methods, radiation methods and enzymatic grafting [Kalia *et al.*, 2009]. Grafting of polymer monomers onto

cellulose is an important tool for the modification of plant fibres. Depending on the monomer grafted onto cellulose, fibres gain new properties such as: water absorption, hydrophilic or hydrophobic character, heat resistance, thermosensitivity, pH sensitivity, antibacterial effect, resistance to microbiological attack, etc. [Gurdag *et al.*, 2013]. Kaith and Kalia studied the effect of the graft copolymerization of flax fibres with vinyl monomers [Kaith *et al.*, 2008]. The grafting of methyl methacrylate onto flax fibre under different conditions (in air, under pressure and under the influence of micro-wave radiations) was investigated. The graft copolymerization performed in air at 55°C has proved to be the best treatment able to produce the maximum percentage grafting (41.7%). Graft copolymerization of acrylonitrile (AN) on sisal fibres was studied by Mishra et al. [Mishra *et al.*, 2001]. It was found that process parameters such as reaction medium, treatment time, initiator, AN concentration influenced the graft effect. A strong reduction in water absorption was found for the AN-grafted sisal fibres, suggesting a reduced affinity of fibres to moisture. The stearic acid treatment and the fatty acid derivate treatments are also reported in literature as chemical process used to modify the fibre surfaces [Kabir *et al.*, 2012].

In addition to the traditional chemical treatments, natural fibre surface has also been modified using bio-chemical methods, such as fungal treatment, the nanocellulose treatment, the enzymatic biochemical process and the supercritical CO_2 treatments [Kalia *et al.*, 2013]. In this experimental work the effects of an enzymatic biochemical treatment and a supercritical CO_2 treatment on the adhesion quality of flax yarns to different thermoset resins were investigated. For this reason, these two treatments will be extensively described in sections I.3.1.1 and I.3.1.2. In the last few years, the fungal treatment has encountered a certain interest. This biological treatment was used to remove non-cellulosic components (such as wax) from the fibre surface by the action of specific enzymes. According with Lee et al. [Lee *et al.*, 2011] fungi can be classified into four categories: basidiomycetes, ascomycetes, zygomycetes and deuteromycetes. Among these only the basidiomycetes (white rot fungus) can degrade lignin, exposing cellulose and hemicellulose. Different studies in literature used white rot fungus to modify natural fibres [Gulati *et al.*, 2006; Schirp *et al.*, 2006]. White rot fungi produce extracellular oxidases enzymes that react with lignin constituents (lignin peroxidase). This causes the removal of lignin from the fibre. It also reduce the presence of non-cellulosic materials, such pectin, waxes and oils, leading to exposure of more reactive hydroxyl sites, increasing hydrophilicity of fibre [Pickering *et al.*, 2007]. In addition, fungi create fine holes on the fibre surface and produces a rough interface

for better interlocking with the matrix. Li et al. studied fungal treatment on hemp fibre [Li *et al.*, 2009]. FTIR and XRD results showed that the fungal modification treatment produces a removal of the non-cellulosic compounds of the fibres. Morphological analysis highlighted an increased surface roughness, able to improve interfacial bonding between the fibre and matrix by exposing more effective contact area. In particular, an increase of 22% in the composite strength was achieved in comparison to the untreated one.

A novel approach of modifying natural fibres with nanocellulose has been investigated. Dai et al. [Dai *et al.*, 2013] used nanocellulose as coupling agent to modify hemp fibres. The authors reported an increase of 50% in the resin adsorption of the fibres, which led to an increase in the fibre/matrix interfacial properties. The surface of natural fibres can be modified also by coating them with a layer of bacterial cellulose nanofibrils. Coating of fibres with bacterial cellulose results in an improved interfacial adhesion between the fibres and the matrix. Acetobacter xylinum is one of the most efficient producers of bacterial cellulose [Kalia *et al.*, 2011]. The deposition of bacterial cellulose (BC) onto natural fibres provides an increase in the effective area of the interface and enhances the fibre/matrix interfacial adhesion through mechanical interlocking. In addition, an enhancement of the wettability of the fibres by the matrix is produced, because of the higher surface tension of BC than natural fibres [Lee *et al.*, 2011]. Pommet et al. proposed a way to modify the surfaces of sisal and hemp fibres by utilizing bacteria acetobacter xylinum bacteria [Pommet *et al.*, 2008]. After 2 days of bacteria culturing, a layer of BC nanofibrils was deposited on the surface of both hemp, Figure I.17, and sisal fibres, Figure I.18.

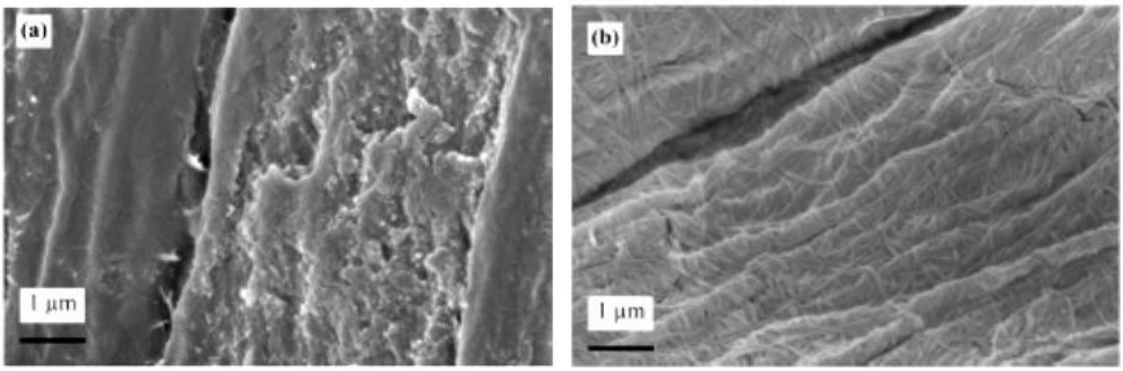

Figure I. 17 SEM images showing (a) neat hemp fibre and (b) hemp fibre coated with bacterial cellulose [Pommet *et al.*, 2008].

Single fibre pull-out tests were performed in order to assess the effect of BC on the interface quality of the modified fibres with the renewable polymers cellulose acetate butyrate and poly(L-lactic acid). The results showed a strong increase in the interfacial adhesion to both polymers.

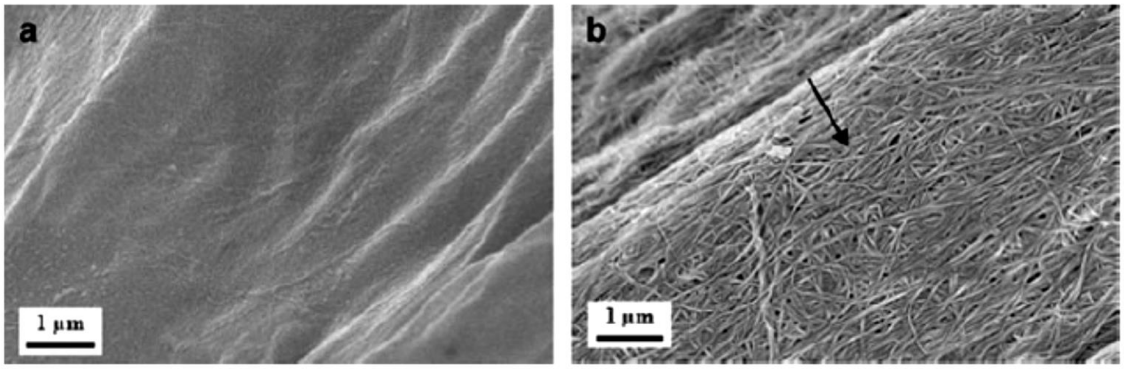

Figure I. 18 SEM images showing (a) neat sisal fibre and (b) sisal fibre coated with bacterial cellulose [Pommet *et al.*, 2008].

I.3.1.1 Enzymatic treatments

The use of enzyme technology in the field of textile and natural fibre modification is rapidly increasing. The enzymatic treatment represents a green way to modify natural fibres. In literature, there are a lot of works about the use of enzymes to separate bast fibres from non-fibre tissues in the stems (retting processes). Traditionally, the processes used for the natural fibre extraction are the water retting and the dew retting. In water retting, micro-organisms present in water will degrade pectin and hemicellulose of plant fibres. In dew retting, natural fibres are spread on the field and subjected to the actions of fungi present in soil and/on plants. However, these treatments are characterized by several drawbacks. Water-retting is expensive and produces vast amounts of fermentation waste, while dew retting has the disadvantage of producing fibres that possess low quality due to the inherent difficulties in controlling the retting parameters. In this context, the enzyme retting is favourable when compared to conventional water-retting and dew-retting methods. Enzymatic processes are characterized by a high selectivity, specificity and mild process conditions, while no chemicals are required. However, the main disadvantage of the enzyme-retting is its high operating and capital cost when compared to water- and dew-retting methods. For this reason, this treatment is still limited to pilot scale. A detailed review on the enzymatic

extraction methods for applying natural fibres in composites was proposed by De Prez et al. [De Prez *et al.*, 2018]. In addition to using enzymes for the extraction of natural fibres, different studies have shown that the enzymatic treatment may be able to catalyse the removal of undesirable substances like pectin, hemicelluloses, lignin, fat, and waxes from the surface of the fibres improving fibre/matrix adhesion. In fact, pectic and hemicellulosic content of natural fibres are the primary components contributing to surface polarity which promotes a hydrophilic behaviour and leads to moisture absorption. A careful selection of enzymes and their dosages is crucial in order to obtain an efficient treatment. The main enzymes used in the fibre modifications are: pectinases, used to hydrolyse pectin; hemicellulases and xylanases, able to break down the hemicellulosic material; laccases, able to degrade the lignin structure in the fibre matrix; cellulases, responsible for degradation of cellulose polymers. Adding chelators to the enzyme formulation can play an essential role in an improved modification of natural fibres. Different chelators, such as ethylenediaminetetraacetic acid (EDTA), oxalic acid, trisodium phosphate, sodium tripolyphosphate and sodium gluconate, were largely used for the retting of natural fibres [Henriksson *et al.*, 1997; Akin *et al.*, 2001; Adamsen *et al.*, 2002, , 2002]. During the retting process, the main action of the chelator agent is to withdraw the calcium from the solution, enhancing the degradation of the plant cell walls and thus the retting efficiency. Stuart et al. used enzymes, chelators and enzyme/chelator systems to improve the quality of flax fibre for composite applications [Stuart *et al.*, 2006]. Flax fibres were treated using a commercial pectinase preparation (Pectinex AR, supplied by Noveo Nordisk), Ethylene Diamine Tetraacetic Acid (EDTA) and a combination of enzyme preparation and EDTA. A morphological investigation of the fibres surface after the different treatments was performed by SEM. This analysis showed that the flax fibres treated only with the enzyme solution present some fibre separation, but a significant amount of debris adhering to the surface of the fibre bundles still remains, Figure I.19-b. On the contrary, a great degradation of pectin and the removal of the extraneous material, leaving the fibre surfaces significantly clean, appears through the use of enzymes in combination with the EDTA, Figure I.19-c and Figure I.19-d. Epoxy matrix composites reinforced with the untreated and chemically treated flax fibres were produced. Fibre modification using EDTA provided the greatest improvements in composite strength, whilst the enzyme/EDTA treatment produced composites with intermediate properties. A possible explanation of this result can be found in the excessive activity of enzyme preparation on the strength of the fibre, particularly in

the zone adjacent to the interface. Different studies in literature investigate the effect of enzymatic treatments on the mechanical performances of composite materials. Bledzki et al. [Bledzki *et al.*, 2010] investigated the effects of a enzymatic treatment (fungamix) on the properties of abaca fibres.

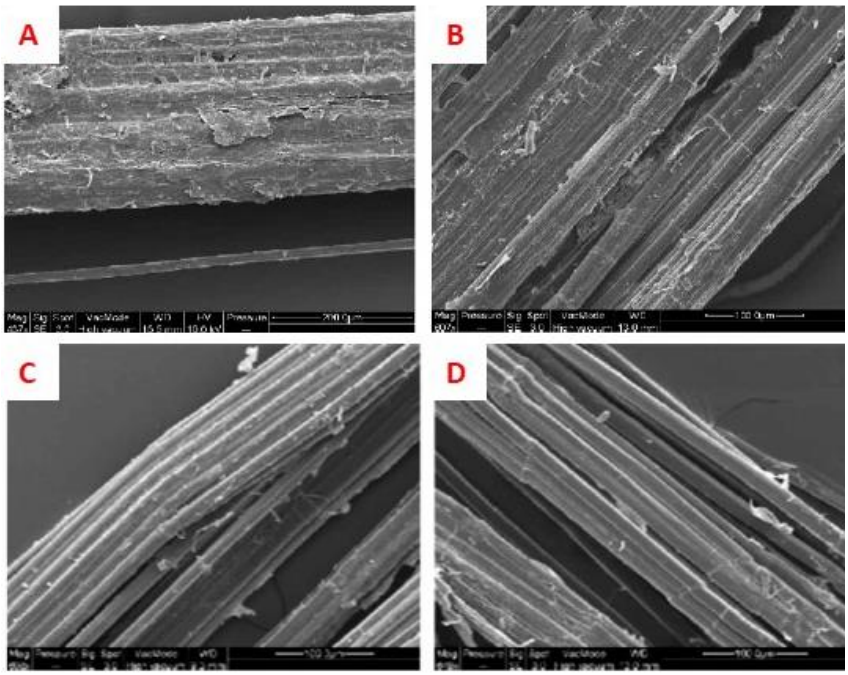

Figure I. 19 SEM micrographs of flax fibres that are (a) untreated or treated with (b) enzyme solution and a combination of enzyme and EDTA solutions (c - d) [Stuart *et al.*, 2006].

Treated abaca fibre reinforced PP composites were prepared by injection moulding with 30 wt% of fibre content. Firstly, it was observed that the enzymatic treatment removes the waxy material and the protruding parts from the fibre surface, producing a decrease in the fibre roughness. Fibrillation also occurred when the binding materials are removed from the surface of the treated fibres. Tensile and flexural tests were performed on the untreated and enzymatically treated abaca fibres/PP composite specimens. The results highlighted an increase of 5–45% for the tensile strength and of 10-35% for the flexural strength after the fibres modification. In addition, the moisture absorption of the composites was found to be reduced of around 20–45%. The tensile strength of enzyme treated abaca composites was found to increase in the range 5–45% due to modification.

A comparison between the effect of NaOH and enzymatic treatments on fibres and fibre/matrix interface was investigated by Karaduman et al. [Karaduman *et al.*, 2013]. Jute fabrics were treated with pectinase, laccase, cellulase and xylanase enzyme solutions with

varying enzyme mixtures and treatment time. From a morphological investigation of the fibre surfaces, it was observed that enzymes reduced the technical fibre diameter and increased the fibre aspect ratio. This effect can be linked to the enzyme ability to produce a fibre fibrillation by removal of adhesive substances like hemicelluloses, lignin, pectin and oils. Enzymes created a rougher fibre surface which facilitates resin bonding onto fibres and improves the fibre/matrix adhesion. An increase in the tensile modulus for both enzyme-treated and NaOH-treated jute fibres composites was found. The composites with the laccase-treated jute fabrics showed higher flexural modulus than the specimens with untreated and other enzyme-treated jute fabrics.

George et al. investigated in detail the effects of enzymatic treatment on the properties of hemp and flax fibres [George *et al.*, 2014; George *et al.*, 2014; George *et al.*, 2016]. The impact of five commercially available enzyme systems (xylanase, pectinmethylesterase, polygalacturonase, laccase and a xylanase with cellulase background) on the surface chemical, morphological and thermal properties was investigated. All the enzymatic treatments on hemp and flax fibres result in an increase of cellulose content, because the purification of the fibre from other components. Only the xylanase + cellulase mixture produced a significant decrease in cellulose content. An increase in the protein and ash content of fibres was reported after the enzymatic treatments. A possible explanation was the presence of enzymes entrapped in the fibre network after treatment. The morphological investigation highlighted the ability of enzymatic solutions to produce a defibrillation of the technical fibres. In particular, xylanase and polygalacturonate can degrade hemicellulose and remove material from the fibre surface, while the lignin removal performed by laccase and polygalacturonase treatments can produce an exposure of fibre surface. George et al. investigated the effect of the previous different enzymatic treatments on the adhesion of flax and hemp fibres in polypropylene matrix composites [George *et al.*, 2016]. For all systems, natural fibre-reinforced polypropylene (NFPP) composites with a fixed mass of 20% of fibre were produced. A morphological investigation of the fracture surfaces of the different systems was performed by SEM after Charpy testing Figure I.20. This analysis showed that the untreated fibre composites were characterized with a larger area of fibre pull out from the matrix. One plausible reason for this may be the poor interfacial bonding or mixing exhibited by the untreated fibres because of the high surface polarity. On the contrary, a better distribution of matrix and fibre, indicating a better mixing and interface, was found for the treated samples. Enzymatic treatment of hemp and flax fibres result in significant

improvements in moisture resistance of composites. In particular, the xylanase+cellulase and polygalacturonase solutions showed the best results. Thermogravimetric analysis (TGA) was used to determine the thermal stability of the different samples. The study reported that enzymes can be used to address the limited thermal stability of natural fibres by selectively removing the least stable pectic and hemicellulosic content.

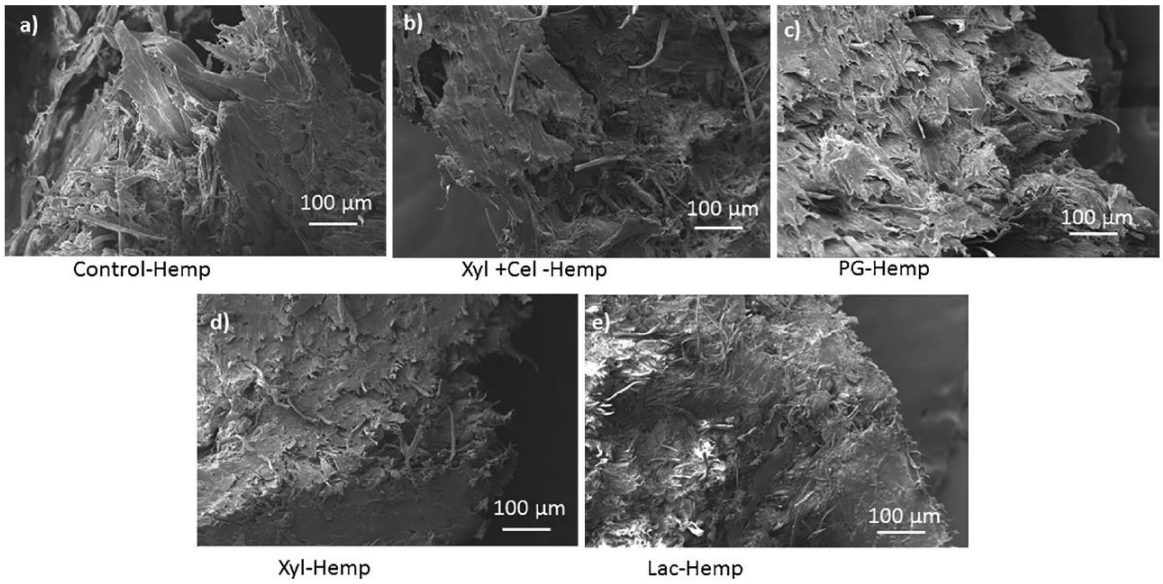

Figure I. 20 SEM micrographs for untreated (a) and enzyme-treated hemp-reinforced composites: (b) xylanase+cellulase, (c) polygalacturonase, (d) xylanase and (e) laccase [George *et al.*, 2016].

A similar result was found also by Liu et al. [Liu *et al.*, 2017]. An increase of maximum degradation temperature of about 5°C was reported for hemp fibres after laccase treatment. Liu et al. investigated the effect of a new natural fibre treatment method using EDTA, endo-polygalacturonase (EPG) and laccase enzymes on the mechanical properties of hemp fibres and hemp fibre/epoxy composites. This treatment consists in two steps: a first step in which a mixture of 0.5% EDTA and 0.2% EPG is used to remove pectin in order to improve the bonding between fibres and matrix polymers; a second step consisting in the polymerization of phenolic compounds onto the natural fibres to further increase mechanical properties of fibres and their composites. A strong increase in the mechanical properties of composite materials was reported after the laccase treatment. Composites with 0.5% EDTA + 0.2% EPG + 0.5% laccase treated fibres showed the highest stiffness of 42 GPa and the highest ultimate tensile strength of 326 MPa at a fibre volume content of 50%.

The authors suggest that this improvement in the mechanical performances of the composites can be related to the polymerization of lignin during the laccase treatment. This phenomenon can form complex products and the cross-linking of aromatic substances able to add mechanical strength to the fibres.

I.3.1.2 Supercritical CO_2

The supercritical carbon dioxide "SC-CO_2" process represents a possible "green-way" to enhance the adhesion of natural fibres with polymer resins. SC-CO_2 is a green attractive alternative to chemical solvents because it is inexpensive, essentially nontoxic, non-flammable, requires relatively gentle critical conditions (critical temperature, T_C = 31.1°C and critical pressure, P_C = 7.38 MPa) and can easily be recovered and recycled after use. Combining a viscosity close to that of gases (10^{-5}–10^{-4} Pas), a density close to that of liquids and a high diffusion coefficient (10^{-8}–10^{-7} m^2s), SC-CO_2 allows to clean surfaces, extract fluids, or encapsulate active substances. Such characteristics make SC-CO_2 a particularly attractive solvent for the extraction of hydrophilic components in cellulosic fibre.

Gutiérrez et al. [Gutiérrez *et al.*, 2012] studied the effect of supercritical carbon dioxide on the properties of Curaua (*Ananas lucidus*) fibres. The treatment with supercritical CO_2 may result in the partial lignin extraction from the fibres. This result was confirmed by a FT-IR and a thermogravimetric analysis. In particular, the untreated Curaua fibres showed the presence of three steps of mass loss: a first stage at a temperature of 100°C, attributed to the presence of moisture in the fibre; a second stage around 300°C associated with the hemicellulose and cellulose decomposition; a final step of mass loss at a temperature of 400°C, linked to the lignin decomposition and the production of volatile substances. The thermogravimetric curves found for the SC-CO_2 treated fibres showed the presence of the first two decomposition steps, confirming the lignin extraction process produced by the supercritical solvent. The morphological analysis carried out by optical microscopy showed a strong reduction in the fibre diameter after the supercritical treatment, passing from 72 ± 5 μm to a value of 10 ± 2 μm. This decrease can be related with both the delignification process and the high pressure able to produce a fibre fibrillation. Two series of biocomposites, one plasticized with dioctyl phtalate (DOP) and another with triethyl citrate (TEC), were prepared by extrusion. Fibrillation and uniform distribution of fibres in the cellulose acetate matrix were observed for both biocomposites. Recently, a supercritical CO_2 treatment has

been developed in order to reduce the hygroscopic capacity and modify the physicochemical properties of hemp fibres [Francois *et al.*, 2017]. The authors reported a decrease in the hygroscopic behaviour of hemp fibres after the supercritical CO_2 treatment. The extraction of polysaccharides from the fibre structure, such us hemicellulose and pectin, rich in hydroxyl groups, could explain this decrease. The study confirmed that the SC-CO_2 treatment represents a very promising solution in order to optimize the adhesion of the hydrophilic natural fibres with the more hydrophobic polymer matrices.

I.3.2 Physical modification treatments

Physical treatments, such as steam explosion, decortication and thermomechanical process, are normally used to separate the fibre bundles into the individual fibres. However, physical treatments have also been used to modify the fibres surface in order to enhance their adhesion with polymer matrices. Contrary to chemical treatments, physical treatments do not extensively change the chemical composition of the fibres but modify the structural and the surface properties of the fibres. The fibre/matrix interface is generally enhanced producing mechanical interlocking between the fibre and the matrix. Several physical modification approaches are possible: plasma treatments, corona discharge treatment, dielectric-barrier discharge method, ultrasounds and ultraviolet treatments.

Corona discharge treatment CDT is one of the most interesting physical treatments for the improvement of the compatibilization between hydrophilic natural fibres and the hydrophobic matrix. This treatment consists of applying a non-uniform high-voltage beam from a thin electrode to the material surface. This process oxidizes the surface by adding functional polar groups such as hydroxyl (OH), carbonyl (C=O), and carboxylic (COOH) groups. Cellulose fibres and polypropylene matrix were modified using a wide range of corona treatment levels and concentrations of oxygen [Belgacem *et al.*, 1994]. The CDT was able to successfully increase mechanical properties of cellulose/PP composites. The best results were obtained for composites with treated cellulose fibres. The yield stress of composites incorporating treated fibres increased by as much as 24%, while conversely when only PP was treated, the yield strength increased by a mere 6%. The yield stress of composites incorporating treated fibres was seen to be a function of corona current.

Ragoubi et al. [Ragoubi *et al.*, 2010] investigated the effect of corona discharge treatment on hemp fibres and polypropylene. Hemp fibre/PP composites, characterized by different

combinations of untreated and corona treated fibres, were manufactured by extrusion–compression moulding process. CDT of fibres and PP matrix leads to a significant increase in tensile strength. The modification of hemp reinforcements rather than PP matrix allows greater improvement of the composite properties with an enhancement of 30% of Young's modulus. This mechanical enhancement was dependent on the etching effect of the corona treatment. In Figure I.21 it is possible to see that an increase of roughness is produced increasing the treatment duration. The CDT produces micro-pits and cavities on the fibre surface favouring the mechanical anchorage of PP matrix and allowing an interlocked structure upon the fibre surface.

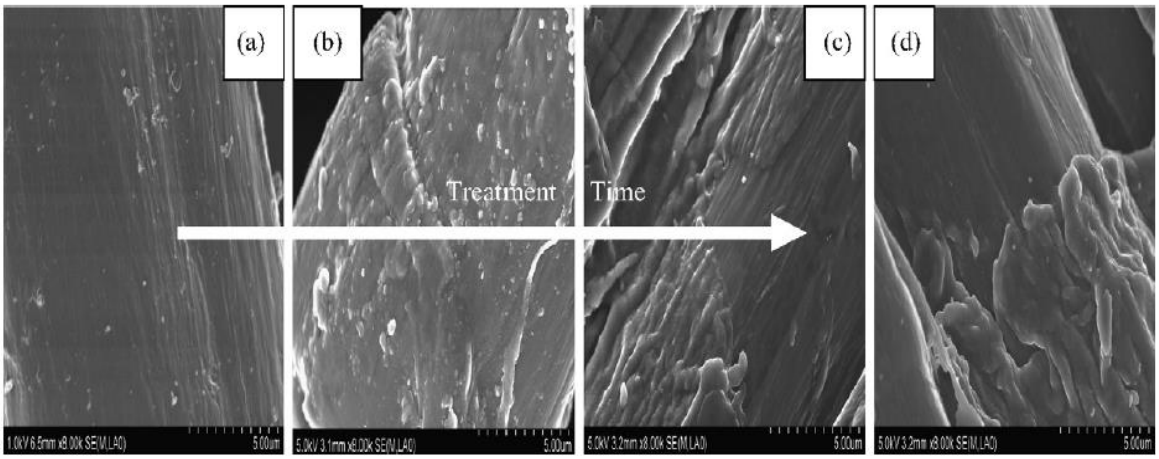

Figure I. 21 SEM micrographs of the hemp fibres surface: raw hemp (a), treated 15 min (b), 30 min (c), 40 min (d) [Ragoubi *et al.*, 2010].

Corona treatment was used also to modify fibre mats. Pizzi et al. [Pizzi *et al.*, 2009] investigated the effect of the duration of the CDT on the mechanical properties of hemp and flax mats reinforced composites. The authors reported that the composite tensile breaking strength reaches a maximum after only 5 min of corona treatment and declines rapidly afterwards. A morphological investigation of the fibre surfaces confirmed that short periods of corona treatment are sufficient to improve the fibre/matrix adhesion. On the contrary, a degradation of the fibres is produced with increasing treatment times.

The dielectric-barrier discharge method (DBD) consists in generating a reactive cold plasma to modify the surface chemistry of synthetic and natural materials. This is a very attractive method, because of advantages such as easy realization, easy sample preparation and low environmental impact. The DBD plasma contains numerous highly reactive oxidative

intermediates, including OH, N, O, O_3, excited states of N_2 and O_2 and atomic oxygen and nitrogen, which provide a surface activation of materials. DBD treatment of material surfaces can result in surface oxidation, increased surface energy, and the generation of free radicals which can readily react with additives to generate new surface grafted material. Vander Wielen and Ragauskas [Vander Wielen *et al.*, 2004] performed the atmospheric DBD to produce the grafting of acrylamide onto the surface of fully bleached kraft pulp (BKP) and thermomechanical pulp (TMP) fibre. Differences in the level of acrylamide incorporation between BKP and TMP can be attributed to the presence of lignin. The phenolic groups in lignin generate less reactive radical species and this diminishes the efficiency of grafting. The morphological analysis confirmed the effective polymerization of acrylamide and its incorporation into the fibre surface. Increased dielectric-barrier discharge treatment allows for increased polymerization and incorporation onto fibres.

The ultraviolet modification treatment (UV) is able to alter the polarity of the natural fibres and subsequently improve their wettability with polymer matrices. Gassan and Gutowski reported a comparison between the effects of corona discharge and ultraviolet on the physical properties of jute fibres and their composites [Gassan *et al.*, 2000]. The UV treatment of jute single fibres and yarns produces higher gains in polarity (up to 200% increase) in comparison with corona treatment. A decrease in the yarn tenacity was observed with increasing corona energy level. This result can be explained in the difficulty to use corona discharge treatment on fibrous materials. The authors found that the UV and corona treatment distance have a strong effect on the polarity and on the mechanical properties of jute yarn. Increasing treatment time at a constant sample distance or alternatively decreasing the distance significantly increased the polarity and decreased yarn tenacity. An increase of 30% in composite strength was achieved after a 10 min of UV treatment at a distance of 150 mm away from the UV lamp.

Another physical modification treatment of fibres is ultrasound. This treatment was traditionally used in medicine and diagnostic but, in the last few years, ultrasound has also been tried for the treatment of cellulosic fibres [Mukhopadhyay *et al.*, 2009].

Among the physical treatments, the plasma technology is one of the more popular surface modification techniques, considered a new alternative less aggressive to the environment, when compared to chemical treatments. In this experimental work the effects of two different plasma treatments on the adhesion quality of flax yarns and basalt filaments with different thermoset resins were investigated. In particular, an oxygen plasma and a plasma

polymerization treatment have been performed. For this reason, an in-depth analysis of plasma treatment will be provided in section I.3.2.1.

I.3.2.1 Plasma treatments

The plasma treatment represents a clean and environmentally friendly superficial modification technique. This treatment has the ability to change the surface properties of the fibres through the formation of reactive species in the plasma stream, without the need of any solvents or hazardous chemicals. Plasma can be considered as a “mixture” of electrons, ions, radicals, molecules, atoms and excited particles depending on the gas plasma used. The free electrons present in the gas plasma gain energy thanks to an imposed radiofrequency electric field. Once excited, electrons collide with the neutral gas molecules, dissociating them into reactive species. This phenomenon can occur according to two reactions: a first reaction of "electron impact", which involves the impact between electrons and plasma gas molecules; a second reaction of "photoionization", which consists in the collision between a plasma gas molecule and a photon, produced by the transition of an excited electron to a lower energy content state. These two reactions mechanisms are reported in Equation I.20 and I.21 [Sun, 2016]:

$$e + M \rightarrow M^{+} + 2e^{-} \quad \text{(I.20)}$$

$$h\gamma + M \rightarrow M^{+} + e^{-} \quad \text{(I.21)}$$

where e is the electron, M is the gas molecule and $h\gamma$ is the energy of the photons. The produced energy particles, travelling in the stream of plasma, can impinge on the solid surface of a substrate placed in the plasma reactor, producing a modification of its surface properties, such as the wettability and the surface roughness. A schematic representation of the plasma surface treatment of a substrate is described in Figure I.22.

A variety of surface modifications can be achieved, depending on the nature of the plasma feed gas used. In particular, the interactive mechanisms between plasma and material surfaces can be classified in:

- *Ablation process*: where the substrate is subjected to a weight loss process. The chemical and physical properties of the substrate are unchanged. This process can

occur by physical sputtering (in a chemically non-reactive plasma) and by chemical etching (in a chemically reactive plasma) of the surface;

- *Plasma polymerization process*: in which a polymer coating is deposited on the substrate surface. This process occurs when a polymer monomer is introduced into plasma and excited by inelastic collision. The monomer is subsequentially fragmented into activated small molecules, which are recombined to form larger polymer molecules;

- *Plasma implantation process*: consists in introducing oxygen-containing functional groups, i.e. carbonyl, carboxyl, hydroxyl etc., on the substrate surface;

- *Plasma-aided graft copolymerization*: in which there is the creation of radical species on the substrate surface or the grafting of polymer monomers.

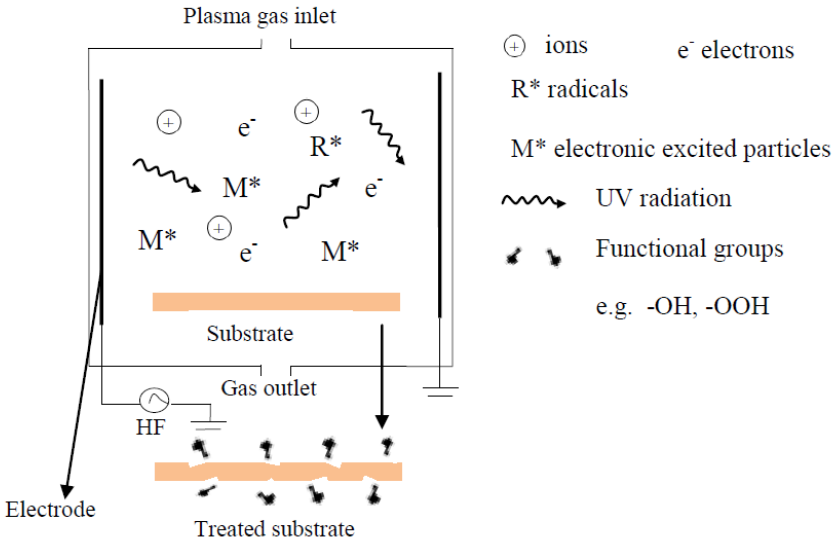

Figure I. 22 Representation of a plasma surface treatment of a substrate [Sun, 2016].

Plasma treatments can be carried out under atmospheric pressure or in vacuum condition. In the first case, the plasma process is known as "Atmospheric Plasma" (AP). The atmospheric plasma technique is highly attractive since the substrate can be treated in an open environment. The vacuum type of plasma process, called "Low-Pressure Vacuum Plasma", requires the parts to be treated under low vacuum pressure in a close chamber.

I.3.2.1.1 Application of plasma treatments on natural fibres

In literature several studies have investigated the use of plasma treatment on natural fibres to improve the fibre/matrix adhesion. Scalici et al. [Scalici *et al.*, 2016] studied the effects of plasma treatment on the properties of Arundo Donax L. leaf fibres. The plasma treatment was performed in air using a pressure of 0.5 mbar. From the remarkable enhancements of mechanical properties of the resulting composites, this study concluded that the plasma treatment is able to enhance the fibre/matrix adhesion. In particular the authors reported a strong increase in the flexural modulus and flexural strength values of the plasma treated composites in comparison to the untreated ones. These results were confirmed also by a morphological investigation of the fractured surfaces of the different composites. Baltazar-y-Jimenez et al. [Baltazar-y-Jimenez *et al.*, 2008] reported as the atmospheric air pressure plasma treatment produced an increase of the interfacial shear strength values for flax, sisal and hemp fibres with cellulose acetate butyrate matrix, despite a decrease in mechanical properties of the fibres with increasing treatment duration. This increase was ascribed to the introduction of functional groups, the cleaning of contaminant substances and the enhanced surface roughness able to promote the mechanical interlocking between the fibre and the matrix. The effects of argon and air atmospheric pressure plasma on woven flax fibres have been explored by Bozaci et al. [Bozaci *et al.*, 2013]. The study showed that argon treatment is effective in increasing the roughness and so the adhesion of flax fibres with high density polyethylene (HDPE) matrix by mechanical interlocking. On the contrary, air plasma was found to strongly affect the oxygen/carbon ratio on the fibre surface and so to promote the adhesion with unsaturated polyester matrices. Most of the available studies in literature on surface modification of natural fibres used plasma treatment for surface etching and/or functionalization. Marais et al. [Marais *et al.*, 2005] investigated the effect of a helium cold plasma treatment on the properties of a flax reinforced polyester composite. This work highlighted that the use of helium introduces some radicals on the surface of the flax fibres that react with the unsaturated polyester chains of the matrix. In addition, a cleaning step occurring during the cold plasma process was able to remove impurities from the fibre surface. At the same time, the He plasma increased the surface roughness by etching the fibre surface. All these effects contribute to create strong interfaces, thus improving the fibre/matrix adhesion. The mechanical characterization of the composites highlighted an enhancement in the stiffness of the composite material. This effect can be explained in the

improved fibre/matrix adhesion after the plasma treatment. On the other hand, at the same time, the mechanical degradation of the flax fibres by plasma treatment produced a decrease in the tensile strength and the failure strain values of the composite. The oxygen plasma treatment increases the surface roughness and introduces functional groups such as -OH, C-O, C=O and O-C=O in the surface of natural fibres, thus resulting in improved wettability. Low pressure plasma has been used by de Farias et al. [De Farias *et al.*, 2017] to modify coir fibres. An increase of the surface roughness of fibres and an exposition of the crystalline cellulose were the main outcomes using air and oxygen gases, which resulted in improved mechanical properties of the composites. The oxygen plasma treatment showed a stronger etching ability compared to air plasma. The inner structure of the coir fibres was more clearly visible after the oxygen treatment. The stronger etching effect of the oxygen plasma can be attributed to the higher reactivity of the excited and ionized oxygen than the nitrogen. De Farias et al. proposed a model to describe the etching process and the evolution of the removal of the amorphous layer covering the coir fibre. A schematic representation of this model is presented in Figure I.23. At first, the outer layer of the coir fibre is thick and covers completely the internal structure (Fig. I.23-a). After plasma treatment the outer layer is etched, becoming thinner and rougher. As time is increased the etching thins the outer layer further, holes start to form (Fig. I.23-b). Increasing the plasma power or using a longer time, only small portions of the outer layer remain, and the internal porous structure of the fibre is almost completely exposed (Fig. I.23-c).

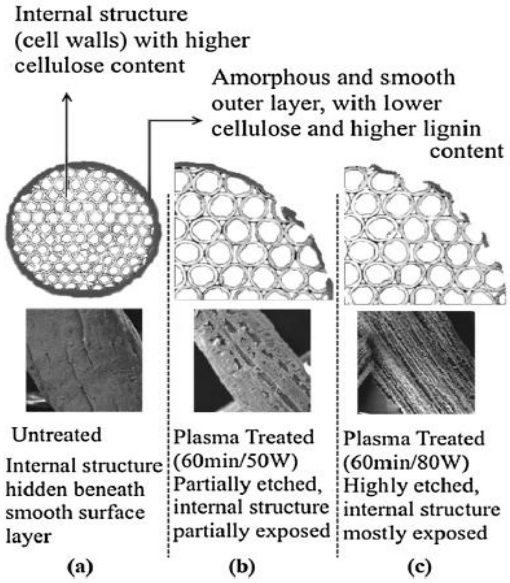

Figure I. 23 Representation of the etching process model proposed by De Farias et al. [De Farias *et al.*, 2017].

The increase in surface roughness achieved by air and oxygen plasma treatments had a strong effect on the load transfer between the matrix and the fibres. In particular, after the oxygen plasma treatment, performed using a power of 80 W and for a duration of 7.2 min, an increase in tensile strength by up to 300% and an enhancement of the elastic modulus by a factor of nearly 20 times were found. A low-temperature atmospheric oxygen plasma was used to increase the adhesion properties of basalt fibres with epoxy matrix [Kim *et al.*, 2011]. A measurement of the advancing and static contact angle was performed in order to determine changes in the wettability behaviour of basalt fibres after the oxygen plasma treatment. The study reported a significant increase in the wettability of basalt fibres, confirmed by a reduction of the advancing angle from 76 ° to 16.23 °, and from 52.95 ° to 25.51 ° for the receding angle. This result can be linked to the formation of chemical functional groups containing oxygen and nitrogen promoted by the oxygen plasma treatment. The surface of basalt fibres was etched by oxygen radicals present in the plasma, producing an increase in roughness. The largest reactive area promotes a mechanical interlocking between the treated fibres and the resin, thus enhancing the fibre/matrix interface strength. The effect of the oxygen plasma treatment on the mechanical properties of the basalt/epoxy woven composites was investigated by performing interlaminar fracture tests (mode I fracture). The authors reported an increase of 16% for the interlaminar fracture toughness of composites after the oxygen plasma treatment. A morphological analysis on the fractured surface confirmed the improvement of fibre/matrix compatibility, Figure I.24. Epoxy resin attached around to the basalt fibres was found in oxygen plasma-treated specimen (Fig. I.24-b), indicating that the adhesive force between the fibre and the resin was improved by oxygen plasma treatment.

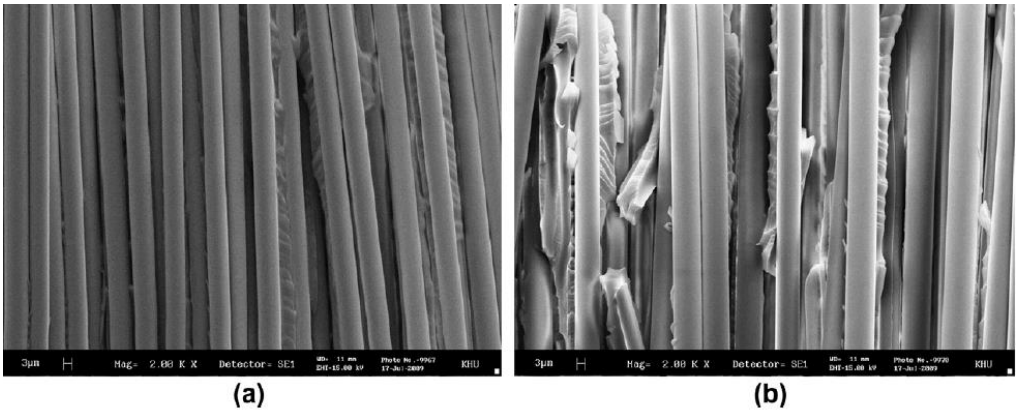

Figure I. 24 SEM micrographs of the fracture surfaces of basalt/epoxy woven composites after interlaminar fracture tests: (a) desized and (b) oxygen plasma treated [Kim *et al.*, 2011].

Jute fibres were treated in radio frequency “RF” and low frequency “LF” plasma reactors using oxygen and different plasma power conditions [Seki *et al.*, 2010]. The oxygen plasma treatment of jute fibres by using RF plasma system showed greater improvement on the mechanical properties of jute/polyester composites compared to using LF plasma system. As previously reported, one of the possible interactive mechanisms between plasma and material surfaces is the plasma polymerization process. This treatment consists in a plasma polymerized film deposition (Plasma Enhanced Chemical Vapour Deposition - PECVD) that can increase the wettability and consequently the fibre/matrix adhesion through an engineered deposition of a compatible interlayer on the fibre surface. Monomer and gas molecules are fragmented and ionized in plasma producing excited species, free radicals and ions. Adsorbed activated fragments recombine forming a thin plasma polymer film onto the fibre surface. Unlike the traditional plasma treatments, which are used to increase the surface roughness and introduce functional groups into the surface layer of fibres, the plasma polymerization process is able to produce homogeneous and pinhole free films on the fibres in a clean environment without use of solvents and at low temperature, thus minimizing the risks of mechanical properties degradation of the substrate. This process was proved to be successful for synthetic glass fibres [Cech *et al.*, 2003, 2014, 2017; Cech, 2007; Zvonek *et al.*, 2019], but no study is available in literature on natural fibres. For this reason, the use of plasma polymerization process on natural fibres represents an innovative way in the field of interfacial issues.

Conclusion of Part I

The development of natural fibre hybrid composite materials represents a key strategy in engineering a new class of ecocomposite materials. In the last few years, global awareness of environmental issues has resulted in the emergence of "green" composites, in which natural fibres, such as jute, flax, hemp or sisal, are used to replace synthetic ones, such as carbon and glass fibres. These new materials offer eco-friendly and sustainable alternatives to traditional synthetic composites. However, natural fibres drawbacks, such as high moisture sensitivity, low thermal stability, poor compatibility with polymeric matrices and low microbial resistance, make inconvenient the use of ecocomposite materials in semi- or structural applications. In this regard, hybridization of different types of natural fibres can be considered as an attractive solution to reduce the environmental impact of traditional composite materials while retaining good mechanical performances. Hybridization may be performed by combining synthetic and natural fibres, producing a synthetic-natural hybrid composite, or by combining different natural fibres together, producing a natural-natural fibre hybrid composite. The latter represents a very interesting strategy to manufacture 100% natural fibre reinforced hybrids, characterized by low costs, good mechanical performance and a lower environmental impact than traditional composites based on synthetic fibres. Section I.1.2.2 provided an overview of the main studies that investigated the mechanical properties of natural-natural fibre reinforced hybrid composites. From the results found, all these studies concluded that the combination of different types of natural fibres allows to obtain a hybrid composite characterized by intermediate properties compared to those obtained using a single type of reinforcement. Among the different natural-natural fibre hybrids proposed, particularly interesting was the development of hybrid composites reinforced with plant and mineral natural fibres, i.e. basalt fibres [Fiore *et al.*, 2016; Zivkovic *et al.*, 2017; Sarasini *et al.*, 2018]. Thanks to natural origin and mechanical properties at least comparable with those of traditional E-glass fibres, basalt fibres may at the same time overcome the environmental issues of synthetic fibres and the typical limitations of plant natural fibres. In this context, the aim of this research project was to develop a basalt-flax fibre hybrid composite material with a view to obtaining more environmentally friendly

composites for semi-structural applications. Hybrid composites were produced through vacuum infusion moulding with epoxy matrix. A detailed quasi-static (tensile, flexural) and dynamic (fatigue, low-velocity impact) mechanical characterization was performed in order to highlight the interest of hybridization. For comparison purposes, two other types of woven composites were manufactured and tested: plant fibre composites (100% flax) and basalt fibre composites (100% basalt). As mentioned in section I.1.2.3, the mechanical performance of natural fibre-based hybrid composites can be affected by different factors, like the volume or weight proportion of fibres, the stacking sequence of the different fibre layers, the service conditions and the fibre/matrix adhesion. In particular, the compatibility between natural fibres and polymer resins represents the key-factor of the composite performance. The quality of the fibre/matrix interface plays a crucial role in conditioning the mechanical performance of the final composite material and its characterization is of fundamental importance. In this experimental work an in-depth characterization of the fibre/matrix adhesion properties was carried out. Among the different techniques reported in section I.2.2, the single fibre fragmentation test (SFFT) was selected to assess the adhesion quality of flax and basalt filaments with polymer (epoxy and vinylester) matrices. The adhesion quality of flax and basalt filament with both epoxy and vinylester matrices has been assessed in terms of critical fragment length, interfacial shear strength (IFSS) and debonding length. Fragmentation tests were supplemented with microcomputed tomography (micro-CT). In particular, high-resolution micro-CT allowed the measurement of the debonding length between the different filaments and the polymer matrices. The use of microcomputed tomography technique to study the quality of the fibre/matrix interface represents an innovative aspect of this research. In literature, no experimental works have used this analysis to verify the quality of fibre/matrix adhesion. In order to enhance the poor compatibility of natural fibres with polymer matrices, research has been targeted at altering the chemical and surface properties of natural fibres via modification treatments. An overview of the different modification treatments used so far was provided in Chapter I.3. They can be divided into two broad categories: physical methods (e.g. ultrasound, thermal and nonthermal plasma, electric discharge method, etc.) and chemical methods (e.g. alkalisation, acetylation, benzoylation, acrylation, coupling agents etc.). Despite the results reported in literature showed that chemical and physical processes have a positive effect on the fibre/matrix adhesion, it is important to stress that these treatments involve a large consumption of chemical substances, require high energy and can cause a significant

decrease in the mechanical properties of the individual fibres. In particular, because of stricter and stricter environmental regulations, the need of a proper disposal way of the used chemical substances represents an important source of cost for industries. For this reason, there is currently a growing interest in research and development of greener surface modification treatments. The present work was focused on the study of "green treatments" able to promote the interfacial strength between natural fibres and polymeric matrix with a concurrent limited impact on the environment. Among the different chemical treatments, an enzymatic biochemical process and a supercritical CO_2 modification treatment have been selected to modify the surface properties of flax. Both treatments consist in extracting all the substances, i.e. hemicellulose, wax, lignin and pectin, that contribute to the surface polarity and the hydrophilic behaviour of natural fibres. Unlike the enzymatic treatments, only a few experimental works have investigated the effect of the supercritical CO_2 process on the fibre/matrix interfacial strength [Gutiérrez *et al.*, 2012; Francois *et al.*, 2017]. The results demonstrated the potential of this treatment in changing the surface properties of natural fibres. Concerning the physical treatments, the plasma technology is considered as a less aggressive alternative to the environment than the chemical modification treatments. Several studies have investigated the use of plasma treatment on natural fibres to improve their adhesion with polymer matrices [Marais *et al.*, 2005; Baltazar-y-Jimenez *et al.*, 2008; Kim *et al.*, 2011; Bozaci *et al.*, 2013; Scalici *et al.*, 2016; De Farias *et al.*, 2017]. All these researches have highlighted as the plasma treatment is able to enhance the fibre/matrix interface strength. In this experimental work an oxygen plasma and a plasma polymerization treatment have been performed in order to enhance the adhesion quality of flax and basalt filament to different thermoset resins. In literature, several studies have been focused on the use of plasma polymerization process on synthetic glass fibres [Cech et al., 2003, 2014, 2017; Cech, 2007; Zvonek et al., 2019], but no studies are available on natural fibres. In this work, the plasma polymerization process was used for the first time on flax and basalt filaments in order to enhance their interfacial adhesion with polymer matrices.

Conclusion de la Partie I

(en français)

Le développement de matériaux composites hybrides à fibres d'origine naturelle représente une stratégie clé dans l'ingénierie d'une nouvelle classe d'éco-composites. Au cours des dernières années, la prise de conscience mondiale des problèmes environnementaux a entraîné l'émergence de composites «verts», dans lesquels des fibres naturelles, comme le jute, le lin, le chanvre ou le sisal, sont utilisées pour remplacer les fibres synthétiques, telles que les fibres de carbone et de verre. Ces nouveaux matériaux offrent des alternatives écologiques et durables aux composites synthétiques traditionnels. Cependant, les inconvénients des fibres naturelles, tels que leur sensibilité élevée à l'humidité, leur faible stabilité thermique, leur mauvaise compatibilité avec les matrices polymères et leur faible résistance microbienne, rendent l'utilisation des éco-composites peu adaptée aux applications semi-structurelles ou structurelles. À cet égard, l'hybridation de différents types de fibres d'origine naturelle peut être considérée comme une solution intéressante pour réduire l'impact environnemental des matériaux composites traditionnels tout en conservant de bonnes performances mécaniques. L'hybridation peut être effectuée en combinant des fibres synthétiques et naturelles, pour produire un composite hybride synthétique-naturel, ou en combinant différentes fibres naturelles ensemble, pour produire un composite hybride de fibres naturelles-naturelles. Ce dernier représente une stratégie très intéressante pour fabriquer des hybrides 100% renforcés de fibres naturelles, caractérisés par des coûts bas, de bonnes performances mécaniques et un impact environnemental moindre que les composites traditionnels à base de fibres synthétiques. La section I.1.2.2 a donné un aperçu des principales études concernant les propriétés mécaniques des composites hybrides renforcés de fibres naturelles. À partir des résultats obtenus, toutes ces études ont conclu que la combinaison de différents types de fibres naturelles permet d'obtenir un composite hybride avec des propriétés intermédiaires par rapport à celles obtenues en utilisant un seul type de renfort. Parmi les différents hybrides de fibres naturelles proposés, le développement de composites hybrides renforcés de fibres naturelles végétales et minérales, à savoir les fibres de basalte, est particulièrement intéressant [Fiore et al., 2016; Zivkovic et al., 2017; Sarasini et al., 2018]. Grâce à leur origine naturelle et à leurs propriétés mécaniques au moins comparables à celles des fibres de verre E traditionnelles, les fibres de basalte peuvent à la fois surmonter les problèmes environnementaux des fibres synthétiques et les limitations typiques des fibres naturelles végétales. Dans ce contexte, l'objectif de ce projet de recherche est de développer un matériau composite hybride à fibres de basalte et de lin pour applications semi-structurelles, plus respectueux de l'environnement.

Dans ce but, des composites hybrides ont été élaborés par moulage par infusion sous vide avec une matrice époxy. Une caractérisation mécanique quasi statique (traction, flexion) et dynamique (fatigue, impact à basse vitesse) a été réalisée afin de mettre en évidence l'intérêt de l'hybridation. À des fins de comparaison, deux autres types de composites tissés ont été fabriqués et testés : des composites à fibres végétales (100% lin) et des composites à fibres de

basalte (100% basalte). Comme mentionné dans la section I.1.2.3, les performances mécaniques des composites hybrides à base de fibres naturelles peuvent être affectées par différents facteurs, tels que la proportion volumique ou massique des fibres, la séquence d'empilement des différentes couches de fibres, les conditions de service et l'adhérence fibre / matrice. En particulier, la compatibilité entre fibres naturelles et résine polymère constitue un facteur clé pour la performance du composite. La qualité de l'interface fibre / matrice joue un rôle crucial dans les performances mécaniques du matériau composite final et sa caractérisation est d'une importance fondamentale. Dans ce travail expérimental, une caractérisation approfondie des propriétés d'adhésion fibre / matrice a été réalisée. Parmi les différentes techniques décrites dans la section I.2.2, le test de fragmentation sur composite monofilamentaire (SFFT) a été sélectionné pour évaluer la qualité d'adhérence des filaments de lin et de basalte avec des matrices polymères (époxy et vinylester). La qualité d'adhérence du lin et du basalte avec les matrices époxy et vinylester a été évaluée en termes de longueur critique de fragment, de résistance au cisaillement interfacial (IFSS) et de longueur de décohésion. Les tests de fragmentation ont été complétés par une analyse microtomographique (micro-CT). En particulier, la micro-CT haute résolution a permis de mesurer la longueur de décohésion entre les renforts et les matrices polymères. L'utilisation de la technique de microtomographie pour étudier la qualité de l'interface fibre / matrice représente un aspect innovant de cette recherche. Dans la littérature, aucun travail expérimental n'a utilisé cette analyse pour vérifier la qualité de l'adhésion fibre / matrice. Afin d'améliorer la compatibilité des fibres naturelles avec les matrices polymères, ce travail a eu pour objectif de modifier les propriétés chimiques et de surface des fibres naturelles via des traitements de modification. Un aperçu des différents traitements de modification utilisés jusqu'à présent a été fourni au chapitre I.3. Ils peuvent être divisés en deux grandes catégories : les méthodes physiques (par exemple ultrasons, plasma thermique et non thermique, méthode de décharge électrique, etc.) et les méthodes chimiques (par exemple alcalinisation, acétylation, benzoylation, acrylation, agents de couplage, etc.). Malgré les résultats rapportés dans la littérature montrant que les processus chimiques et physiques ont un effet positif sur l'adhésion fibre / matrice, il est important de souligner que ces traitements impliquent une grande consommation de substances chimiques, nécessitent une énergie élevée et peuvent provoquer une diminution des propriétés mécaniques des renforts. Cependant, pour suivre les réglementations environnementales de plus en plus strictes, la nécessité d'opter pour un mode d'élimination approprié des substances chimiques utilisées représente une source de coût importante pour les industriels. Pour cette raison, il existe actuellement un intérêt croissant pour la recherche et le développement de traitements de modification de surface plus écologiques. Le présent travail était axé sur l'étude de «traitements verts» capables d'améliorer l'adhésion interfaciale entre les fibres naturelles et la matrice polymère tout en ayant un impact limité sur l'environnement. Parmi les différents traitements chimiques, un processus biochimique enzymatique et un traitement par CO_2 supercritique ont été sélectionnés pour modifier les propriétés de surface du lin. Les deux traitements consistent à extraire toutes les substances, à savoir l'hémicellulose, la cire, la lignine et la pectine, qui contribuent à la polarité de surface et au comportement hydrophile des fibres naturelles. Contrairement aux traitements enzymatiques, seuls quelques travaux expérimentaux ont étudié l'effet du CO_2 supercritique sur l'adhésion interfaciale fibre / matrice [Gutiérrez et al., 2012; François et al., 2017]. Les résultats ont démontré le potentiel de ce

traitement pour modifier les propriétés de surface des fibres naturelles. Concernant les traitements physiques, la technologie plasma est considérée comme une alternative moins agressive à l'environnement que les traitements de modification chimique. Plusieurs études ont étudié l'utilisation du traitement plasma sur les fibres naturelles pour améliorer leur adhérence aux matrices polymères [Marais et al., 2005; Baltazar-y-Jimenez et al., 2008; Kim et al., 2011; Bozaci et al., 2013; Scalici et al., 2016; De Farias et al., 2017]. Toutes ces recherches ont mis en évidence que le traitement au plasma est capable d'améliorer la résistance de l'interface fibre/matrice. Dans ce travail expérimental, un plasma d'oxygène et un traitement de polymérisation au plasma ont été effectués afin d'améliorer la qualité d'adhésion du lin et du basalte avec différentes résines thermodurcissables. Dans la littérature, plusieurs études se sont concentrées sur l'utilisation du procédé de polymérisation plasma sur les fibres de verre synthétiques [Cech et al., 2003, 2014, 2017; Cech, 2007; Zvonek et al., 2019], mais aucune étude n'est disponible sur les fibres naturelles. Dans ce travail, le procédé de polymérisation plasma a été utilisé pour la première fois sur des renforts de lin et de basalte afin d'améliorer leur adhérence interfaciale avec les matrices polymères.

PART II

MATERIALS AND TECHNIQUES

The objective of the Part II is to present the whole set of materials and techniques used during the experimental work. This part is subdivided into two chapters: Chapter II.1, which describes the reinforcements, the matrices and the manufacture techniques used for the production of the woven and the monofilament composite materials; Chapter II.2, in which the different characterization techniques used are introduced.

PART II – MATERIALS AND TECHNIQUES

CHAPTER II.1

MATERIALS

A multiscale study has been performed in order to fully characterize the considered hybrid composite. Tests have been realised on each constituent (reinforcements and resins), on woven composites and on monofilament composites. In the following chapter, all these studied materials will be presented in detail.

II.1.1 Reinforcements

For the manufacture of the different composite materials, a basalt and a flax woven fabric have been selected. Concerning the plant reinforcement, a Biotex flax fabric (*Linum usitatissimum*), supplied by Composites Evolution (UK) was used. This fabric is commercialized without any specific sizing. It is a 2×2 twill fabric (200 g/m^2) in which two warp yarns pass alternately under and over two other weft yarns. The architecture of the flax fabric has been highlighted performing microtomography observations on the composite (Figure II.1).

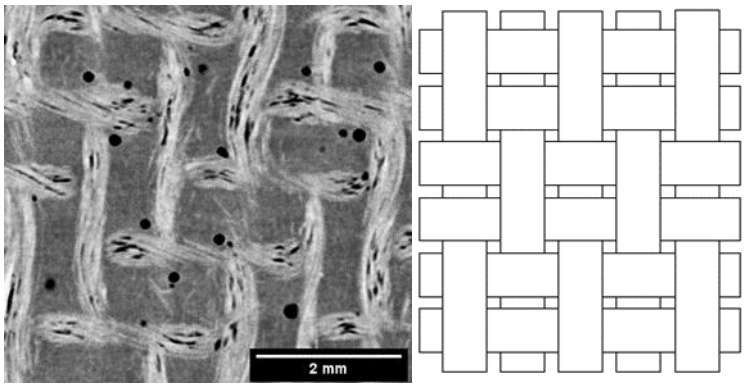

Figure II. 1 Flax fabric architecture observation by micro-CT (14 µm resolution) and scheme of the 2x2 twill elementary motif.

Each flax yarn has a diameter of about 327 μm and is made of several elementary flax fibres twisted together. A typical elementary flax fibre has a diameter of about 25 μm. The different surface modification treatments have been performed on flax yarns that have been extracted from the flax fabric. Then, flax yarns have been used for the manufacture of monofilament composites. Some elementary flax fibres have also been carefully extracted by hand from the flax yarns in order to realise the tensiometric tests. Concerning the mineral reinforcement, a basalt woven fabric, supplied by Basaltex (Belgium), has been selected. It is a plain woven fabric (220 g/m^2), made of 100% BCF (basalt continuous filament) roving, in which each warp strand passes alternately under and over each weft strand. The fabric is symmetrical, with good stability and commercialized with a specific sizing that allows good compatibility with epoxy matrix. An observation of the basalt fabric architecture has also been performed by micro-CT analysis (Figure II.2).

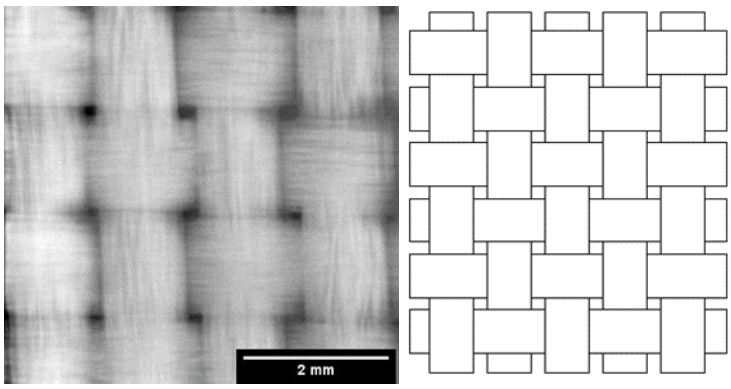

Figure II. 2 Basalt fabric architecture observation by micro-CT (14 μm resolution) and scheme of the plain elementary motif.

Individual basalt fibres have been carefully extracted by hand from the strands in the basalt fabric in order to realise the different surface modification treatments and the different tests. One basalt fibre has a nominal diameter of 13μm.

II.1.2 Resins

Two thermoset resins have been investigated in this work. At first an epoxy resin has been selected, made of PRIME 27 infusion resin and PRIME 20 slow hardener, both delivered by GURIT. The curing process was carried out with a recommended mixing ratio of 100:28 by weight. The main physical properties of the resin provided by the manufacturer are shown

in Table II.1. A vinylester resin has also been used to carry out the fibre/matrix interface study. In order to reduce the risks derived from styrene, an innovative styrene-free vinylester resin was selected. Specifically, the Advalite VH-1207 vinylester infusion resin, supplied by Reichhold, was chosen. In this resin, the styrene monomer used as reactive diluent is replaced by 1,4-butanediol dimethacrylate (BDDMA). This resin is formulated for use in resin vacuum infusion process. The Norpol Peroxide PMEC N24 hardener, supplied by Reichhold, was used as curing agent and the curing process was carried out with a mixing ratio of 1 phr. The resin is pre-accelerated for room temperature cure. The main physical properties of the resin provided by the manufacturer are shown in Table II.2.

Table II. 1 Properties of Epoxy Gurit PRIME 27 resin.

Epoxy Gurit PRIME 27	
Viscosity [cP]	510
Density [g/cm^3]	1.13
Tensile Strength [MPa]	73.3
Tensile Modulus [GPa]	3.4

Values provided by the manufacturer for a resin mixed with the slow PRIME20 hardener, using the ratio 100: 28 by weight.

Table II. 2 Properties of Vinylester Advalite VH-1207 resin.

Vinylester Advalite VH-1207	
Viscosity [cP]	220
Density [g/cm^3]	1.13
Tensile Strength [MPa]	55
Tensile Modulus [GPa]	4

Values provided by the manufacturer for a resin mixed with the NORPOL Peroxide 11 hardener, using the ratio of 1phr.

II.1.3 Woven composites manufacturing

Three kinds of epoxy matrix woven composites, with different ply interface configurations, have been manufactured:

- Flax composites (100% flax) – as reference materials;

- Basalt composites (100% basalt) – as reference materials;
- Hybrid composites (50% of flax plies and 50% of basalt plies) with a symmetrical intercalated sequence: $[(basalt/flax)_2]_s$;

The different composite laminates were produced in collaboration with the Institute of Polymers, Composites and Biomaterials (IPCB) of Portici (Italy). All composite laminates have been produced by Vacuum Infusion process, that involved: layup of a fibre preform, vacuum application and fibre impregnation by a thermoset resin, cure of the resin. The reinforcement is placed between the one-sided rigid mould and a formable vacuum bag material. The resin is injected from an input channel. Vacuum is applied through a single vent to remove the air from the fibre preform and to drive the fibre impregnation by resin. A resin distribution net medium is placed onto the reinforcement to promote the resin flow allowing the complete wet-out of the preform and eliminating voids and dry spots. After infusion, the panels were post-cured for 7h at 90°C to obtain a fully cross-linked epoxy. Table II.3 shows some geometrical and physical characteristics of the different woven composites. The fibre, matrix and void volume fractions were evaluated on composite samples characterised by a length of 150 mm and a width of 25 mm. For each sample the mass and the thickness were measured through an analytical balance (resolution 10^{-4} g) and a caliper, respectively.

Table II. 3 Summary of properties of the different woven epoxy composites produced.

	Laminate thickness [mm]	Fibre volume fraction [%]	Void volume fraction [%]	Number of plies	Ply orientation
Basalt	2.4 ± 0.07	55 ± 1	6 ± 3	16	0º/90º and ±45º
Flax	2.2 ± 0.07	26 ± 0.6	7 ± 6	4	0º/90º and ±45º
Hybrid	2.8 ± 0.08	33 ± 0.7	9.5 ± 5	8	0º/90º and ±45º

The fibre volume fraction V_f, the matrix volume fraction V_m and the void volume fraction V_v were calculated using Equation II.1, II.2 and II.3, respectively:

$$V_f = \frac{A_r n}{s \rho_f} \quad \text{(II.1)}$$

$$V_m = \left(1 - \frac{A_r n A}{M}\right) \frac{\rho_c}{\rho_m} \quad \text{(II.2)}$$

$$V_v = 1 - V_f - V_m \quad \text{(II.3)}$$

Where A_r is the mass of one ply per unit area, s is the specimen thickness, A is the specimen area, M the specimen mass and ρ_c, ρ_f and ρ_m represent the composite, the fibre and the matrix densities, respectively. In order to assess the influence of fibre orientation on the mechanical properties of the composite, specimens have been cut in two different directions from the manufactured plates. Therefore, two stacking sequences have been studied. A first sequence, identified as 0°/90°, is characterized by the warp yarns aligned along the loading direction. The second sequence, identified as ± 45°, corresponds to an orientation of the warp yarns at 45 ° degrees with respect to the loading direction of the composite.

II.1.4 Monofilament composites manufacturing

The Single Filament Fragmentation Test (SFFT) aims to produce a multiple breaking of a single filament incorporated in a sample subjected to a tensile load. As thoroughly described in section I.2.2, thanks to the simplicity of sample preparation and the possibility to obtain a large amount of data from a limited number of tests, SFFT is one of the most popular micromechanical methods to evaluate the fibre/matrix interface properties. In order to replicate the stress distribution conditions present in real natural fibre composites, in this study the interfacial adhesion of flax with polymer resin was assessed at the yarn scale. It is different for the basalt reinforcement, for which individual fibres can be used in fragmentation tests. In this study, a specific metallic mould has been designed to manufacture the monofilament composite specimens. Figures II.3-a and II.3-b show the metallic mould used for the sample manufacture and the specimen geometry, respectively. The dog bone specimens, characterised by a reduced gauge section with a length of 15 mm, a thickness of 2 mm and a width of 3 mm, have been produced. Before casting, both flax yarns and basalt fibres were conditioned at 45°C for 24h for moisture elimination. The whole surface of the mould was prepared by applying three layers of a release agent (Axon 841) and a layer of polyvinyl alcohol (PVA). Each basalt fibre and flax yarn was positioned in the mould and held in place by adhesive tape. Some little slots were designed at each end of the negative samples to facilitate the filament placement in the middle of the specimen. In order to avoid the leakage of the resin from the mould, a plasticine has been applied along the edges to prevent the flow of the resin.

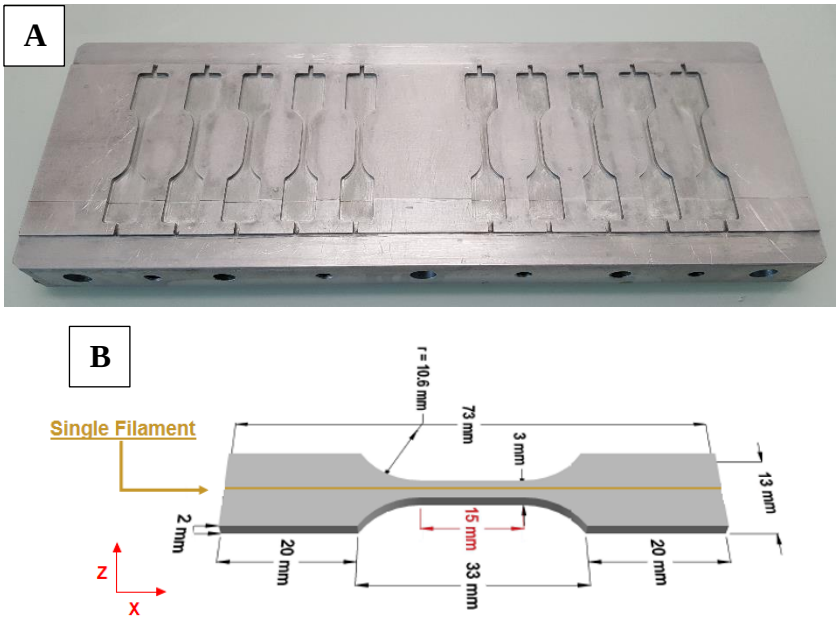

Figure II. 3 (A) Metallic mould used for sample manufacture; (B) Specimen geometry for the single filament fragmentation tests.

In order to ensure the right quantity of resin and to reduce as much as possible the formation of a meniscus due to the shrinkage during the crosslinking process of the resin, the mould has been filled up with resin using a syringe. A curing procedure of 7h at 90°C was optimized to obtain a fully cross-linked epoxy. Regarding the vinylester resin, a curing procedure of 72h at room temperature has been selected.

CHAPTER II.2

CHARACTERIZATION TECHNIQUES

In the following chapter, it will be described the main characterization techniques used during the experimental work performed in the laboratories of Sapienza University of Rome and the ISAE-ENSMA.

II.2.1 Observation Techniques

II.2.1.1 Optical microscopy

Two optical microscopes were used:

- Nikon Eclipse 150L (up to 100x magnification), equipped with the image analysis software Lucia Measurement, at Sapienza University of Rome;
- ZEISS Axio Imager optical microscope (up to 800x magnification), equipped with the image analysis software Axio vision, at ISAE-ENSMA.

Optical microscopy was used to measure the diameter of both flax and basalt filaments. For each filament an average diameter has been measured in at least five points along its length (Figure II.4).

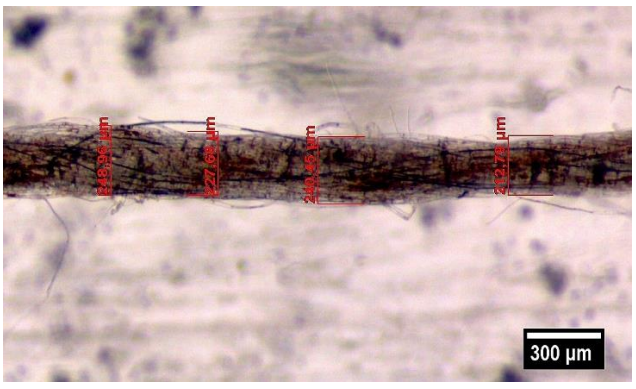

Figure II. 4 An example of optical micrographs of a single flax yarn inside an epoxy resin sample. The image shows the measurement of the diameter of the yarn.

Moreover, for both flax yarn and basalt fibre, optical microscopy was used to measure the fragment and the debonding length values in the gauge length region of the monofilament specimens after fragmentation test.

II.2.1.2 Field Emission Scanning Electron Microscopy

Field-Emission Scanning Electron Microscopy (FE-SEM) has been employed to carry out a careful and high magnification morphological analysis of both the surfaces of the individual filaments and the fracture surfaces of woven and monofilament composites (Figure II.5). In particular, were used:

- Jeol JSM-7000F FE-SEM, at ISAE-ENSMA;
- Zeiss Auriga FE-SEM, at "Interdepartmental research centre on nanotechnologies applied to engineering" (CNIS) of Sapienza University of Rome;
- Tescan MIRA 3 FE-SEM, at Sapienza University of Rome;

All specimens were sputter coated with gold or chromium prior to FE-SEM observation.

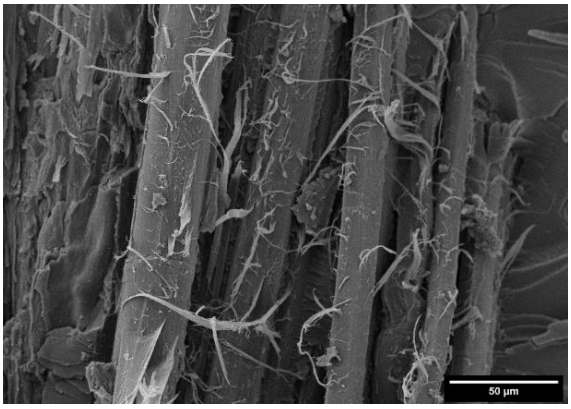

Figure II. 5 Example of FE-SEM micrograph: surface of flax fibres in a flax/epoxy woven composite.

II.2.1.3 Atomic Force Microscopy

The atomic force microscopy has been used in this study in order to perform a topographic analysis of the surface of the fibres. In particular, the roughness of basalt fibres has been measured using a Bruker Dimension Icon AFM, equipped with Nanoscope V controller, at CNIS laboratory of Sapienza University of Rome (Figure II.6). A Bruker Tapping Probe

cantilever (Sb doped n Si) characterized by an elastic constant of 40 N/m and nominal resonance frequency of 300 kHz has been used.

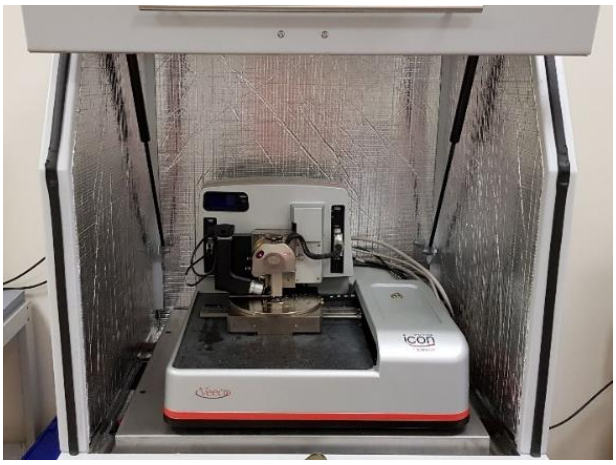

Figure II. 6 The Bruker Dimension Icon atomic force microscopy, CNIS – Sapienza University of Rome.

Topographic imaging has been acquired in tapping mode on a scan area of (3×3) μm^2 and using a scan rate between 0.3 and 0.5 Hz. A minimum of three different areas were scanned for each sample and then measured. All measurements have been performed in an insulating chamber to avoid acoustic excitation. The roughness of each fibre surface has been measured using root mean square (RMS) roughness after removing the fibre curvature by polynomial fitting. AFM data have been processed using Gwyddion software.

II.2.1.4 X-ray microtomography

X-ray microtomography is a non-destructive analysis technique that allows to carry out a three-dimensional reconstruction of an object and to visualize its internal structure. An X-ray beam, generated by an X-ray source, is transmitted through the sample and subsequently recorded by an X-ray detector in the form of a 2D projection image. The sample is placed on a motorized plate and placed in rotation with an angular pitch defined by the user. An X-ray projection image is taken at each rotation and this step is repeated several times up to a total sample rotation of 180° or 360° degrees. The series of X-ray projection images is then computed in cross-sectional images through the reconstruction process. In this work, the image acquisition of samples has been performed using an UltraTom CT scanner manufactured by RX Solutions (France), at ISAE-ENSMA (Figure II.7).

Figure II. 7 The UltraTom CT scanner.

The system consists in a Hamamatsu open type microfocus X-ray tube operating at 20-100 kV / 0-200 µA, within a maximum power of 20 W (configuration with a Lanthanum hexaboride filament). A precision object manipulator with two translations and one rotation facilitates rotating the sample for acquisition of tomographic data, and displacement along the optical axis to adjust the magnification. X-rays generated by the source diverge at an angle providing a cone-beam, thus sample can be imaged at various geometric magnifications by moving it close to the source to provide high resolution mode or close to the detector to provide low resolution measurements. The generator and the detector are also mobile to cover a large range of magnification. The X-ray detector consists in an X-ray CsI scintillator screen which is settled on an amorphous silicon layer. For 3D reconstruction, X-ray images were acquired from 1120 rotation views over 360° (approximately 0.32° rotation step). The reconstruction was performed using an algorithm based on the filtered back-projection procedure for Feldkamp cone beam geometry. In this study, the micro-CT analysis was used both on monofilament composite samples, in order to perform an in-depth investigation of the adhesion level of both flax and basalt filaments with the polymeric matrices, and on woven composites, in order to assess the internal damage level of the samples after mechanical characterization tests (Figure II.8). Resolutions of 1.5 µm and 14 µm were used for monofilament and woven composites samples, respectively. The analysis of the micro-CT pictures has been performed by using the Avizo 9.0 software. The reconstructed 3D image consists of a set of 3D monochrome pixels, named voxels. Each voxel is characterized by a grey level that depends on the local variation of the X-ray absorption rate on the sample. These variations are related to the difference in mass density characteristic of each material. The presence of completely black pixels indicates a null

absorption of X-rays, relative to the zones where the material is absent, such as cracks or voids.

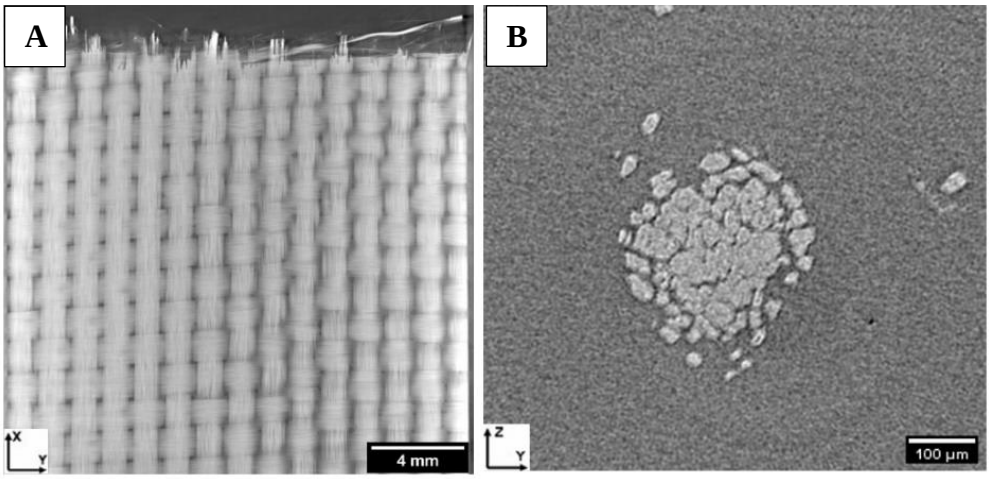

Figure II. 8 Examples of micro-CT images: (A) Basalt 16 - 0°/90° woven composite sample; (B) Flax yarn in the epoxy resin monofilament composite.

The difference in density of the analysed materials has represented a problematic issue in the 3D reconstruction of tomographic images. This was especially true for woven hybrid composites. In fact, basalt fibres are characterized by a much greater density than flax fibres and the epoxy matrix. Such materials are therefore characterized by a large difference in X-rays absorption. In the reconstructed tomographic images, the flax yarns and the epoxy matrix, less absorbing phases, are characterized by a weak contrast with respect to basalt fibres, the most absorbing phase. An example of a tomographic image of a hybrid composite sample is shown in Figure II.9. It is possible to observe how, because of the greater mass density of basalt, flax reinforcement is hardly discernible from epoxy resin.

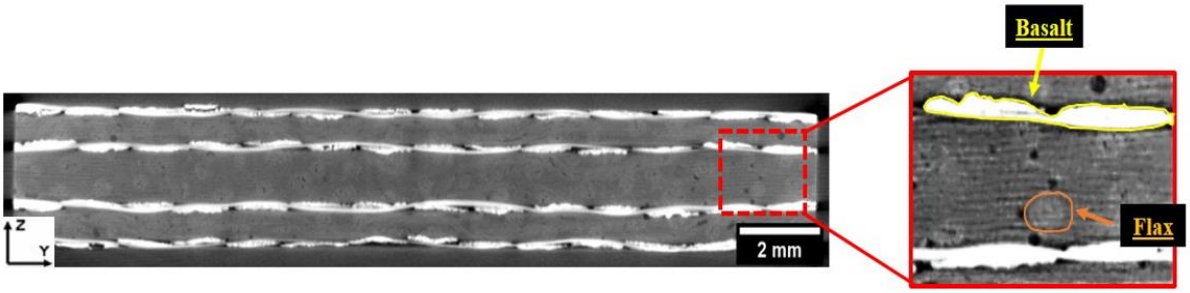

Figure II. 9 Micro-CT image of a woven hybrid composite.

II.2.1.5 Photoelasticity analysis

The photoelasticity is a technique for measuring and visualizing the stress fields inside a material. This technique is based on the birefringence properties of a material subjected to a load. The birefringence in polymer materials is linked to the variation in the refractive indexes due to molecular orientation under loading. In fact, according to the Maxwell's stress-optic law, the refraction of an incident light ray will be linearly proportional to the load applied to a linear elastic material [Bonnafous, 2011]. During the photoelasticity analysis, two different types of optical fringes will occur: isoclinic fringes, dark lines which describe the directions of the principal stress, and isochromatic fringes, lines of a constant colour related to the level of loading. In order to analyse the material stress field, two different types of polariscope are usually used: a linear (plane) polariscope or a circular polariscope. Both isoclinic and isochromatic fringes are observed through the linear polariscope, whereas only the isochromatic fringes are observed using the circular polariscope. In this experimental work, a circular polariscope was used in order to analyse the stress field present inside the different samples. The specimen to be studied was placed between a right-circular polarizer, formed by the combination of a linear polarizer and a quarter wave plate, and a left-circular analyser formed by the association of a linear analyser and a quarter wave plate (Figure II.10). The intensity *I* transmitted from the analyser can be defined according to the equation, Eq. II.4:

$$I = I_0 \sin^2\left(\frac{\varphi}{2}\right) \qquad \text{(II.4)}$$

where I_0 is the incident intensity and φ is the phase displacement. The isochromatic fringes observed through the circular polariscope will be characterized by a phase displacement $\varphi = 2n\pi$, where *n* is an integer number representing the fringe order. The stress level at any point along the isochromatic fringe is related to the fringe order *n* by the stress-optic law, Eq. II.5:

$$\sigma_1 - \sigma_2 = 2\tau_{12} = \frac{n\lambda}{eC} \qquad \text{(II.5)}$$

where τ_{12} is the shear stress, λ is the wavelength value, *n* is the fringe order, *C* the photoelastic constant and *e* is the thickness of the sample.

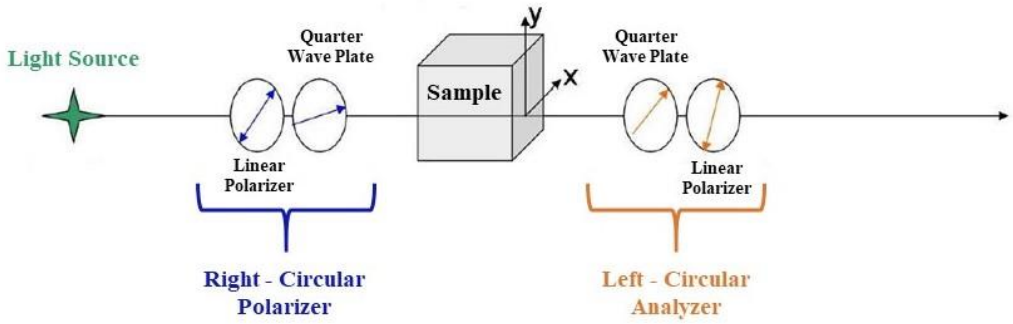

Figure II. 10 A schematic description of the circular polariscope used in this study [Bonnafous, 2011].

In this study the photoelasticity analysis was performed in order to observe the distribution of interfacial stresses in the single flax yarn reinforced composites. During fragmentation tests, specimens were placed into a circular polariscope to reveal the stress state near the yarn breaks and at the yarn/matrix interface. An AVT-Dolphin high resolution camera, focusing on the reduced gauge section of the specimens, has been used during tests (Figure II.11). The light source was a LED lamp positioned behind the sample so as to pass through the circular polariscope and subsequently normally hit the high resolution camera. To ensure a continuous recording, pictures have been taken every 2 s.

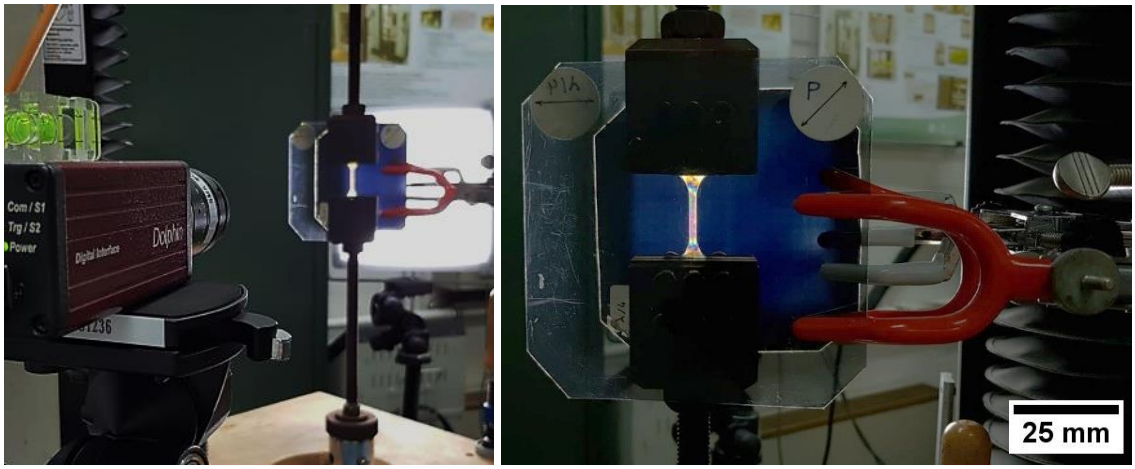

Figure II. 11 Example of fragmentation test instrumented by the high resolution camera and the circular polariscope (ISAE-ENSMA).

The circular polariscope was used also to study in a proper manner the interfacial debonding phenomena between the basalt fibre and the epoxy resin. During optical microscopy observation, the fragmented single filament composite samples were placed into a circular polariscope in order to observe the stress state near the filament breaks and the interface

between the single basalt filament and the matrix. For both flax and basalt filaments, the photoelasticity analysis was performed on monofilament epoxy samples. On the contrary, concerning the vinylester specimens, it was not possible to find any stress pattern around the filament fracture zone because of the no-birefringence character of this resin.

II.2.2 Thermal and Compositional Characterization

II.2.2.1 Thermogravimetric analysis

The thermal stability of untreated and treated basalt and flax filaments has been investigated using a SetSys Evolution (Setaram Instrumentation) thermogravimetric analyser, at Sapienza University of Rome. The different samples were placed in an alumina pan and heated at a rate of 10°C/min to a maximum temperature of 800°C in nitrogen atmosphere. Weight changes versus temperature and the derivative of weight changes versus temperature have been recorded.

II.2.2.2 Fourier-Transform Infrared analysis

In order to analyse the chemical composition of both as-received flax and basalt filaments and to evaluate the effects of the different surface modifications treatments, a compositional analysis was performed through Fourier-Transform Infrared (FTIR) spectroscopy at Sapienza University of Rome. Infrared measurements were carried out with a Bruker Vertex 70 spectrometer (Bruker Optik GmbH) equipped with a single reflection Diamond ATR cell. For all samples, spectra were recorded with a 3 cm^{-1} spectral resolution in the mid infrared range (400–4000 cm^{-1}) using 512 scans.

II.2.3 Characterization of wetting properties

An in-depth analysis of the wetting properties of both basalt and flax reinforcements has been carried out in this research. Two different kinds of tests have been performed depending on whether fabrics or single fibres. In order to investigate the wetting properties of the flax fabric, a drop test has been performed. This analysis has been carried out using a video-based optical contact angle measuring instrument, OCA 15 Pro (DataPhysics GmbH) at Sapienza University of Rome, (Figure II.12). This instrument allows the determination of different

surface and interface parameters through the deposition of a liquid drop that hangs out from a dosing needle on the solid surface.

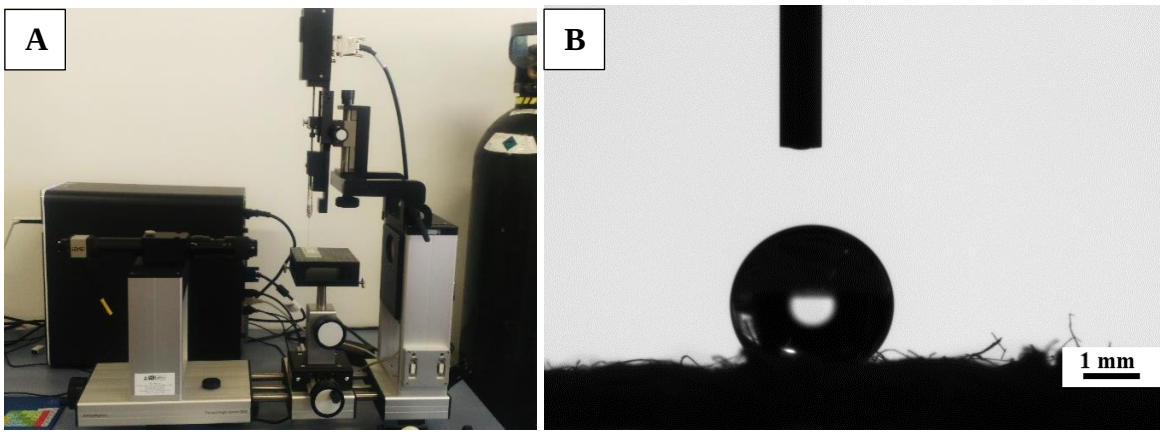

Figure II. 12 The OCA 15 Pro video-based optical contact angle measuring instrument at Sapienza University of Rome (A); example of the water micro drop onto the flax fabric surface (B).

Generally, the video-based optical contact angle measuring instrument is used in order to perform a contact angle measurement using the sessile drop method on homogeneous solid substrates. In this work, instead, due to the non-homogeneous characteristics of flax fabrics, it was not possible to carry out a contact angle measurement and, the wetting behaviour of the fabric was measured in terms of time for complete absorption of the liquid, "water retention time". During the test, degassed water drops with a volume of 4 µl were applied to the flax fabric and the time until the applied drop is absorbed completely was measured. The lesser the time required for the water drop to be completely absorbed, the greater the wettability of the fabric and so its degree of hydrophilicity. However, various problems have arisen during tests. In particular, a strong relationship between the water retention time values and the degree of weaving and/or the mesh size of the different flax fabrics analysed was observed. For this issue, the different time values obtained were considered as qualitative results, useful to give an idea of the wettability properties of flax reinforcements. In order to carry out a more accurate and quantitative analysis of the wettability properties of both single basalt and flax fibres, a tensiometric method was also used to measure contact angles and surface energies. This experimental work was carried out at the laboratory of the Centre des Matériaux des Mines d'Alès (C2MA), IMT Mines Alès. A single fibre Tensiometer – K100SF (Kruss) with a resolution of 0.1 µg was used to perform contact angle measurements (Figure II.13). The tensiometer is able to measure precisely the mass of the

liquid meniscus that occurs when a fibre is immersed and wetted in a specific test liquid. In this study, two test liquids were used for the wetting analysis: water and diiodomethane.

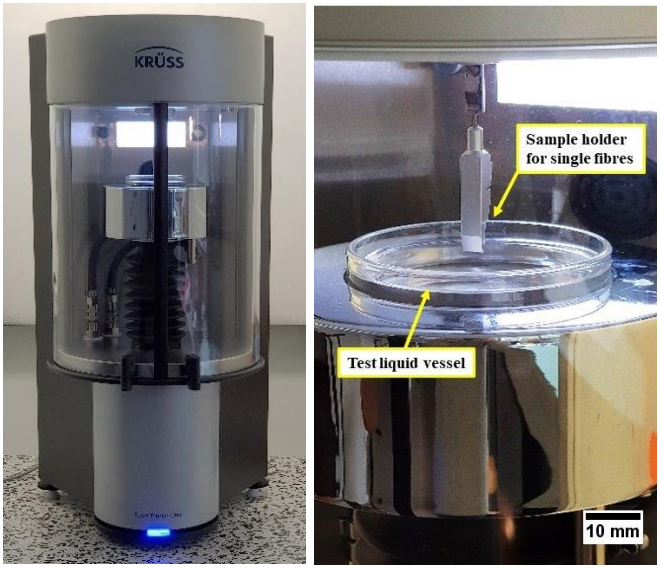

Figure II. 13 The tensiometer K100SF and the sample holder system with the test liquid vessel.

Water is the most common liquid with a high polar component and surface tension. Diiodomethane is a liquid almost totally dispersive with a relatively high surface tension. However, a third liquid was employed during the analysis. The n-Hexane is a totally wetting liquid because of its very low and totally dispersive surface tension, then the contact angle can be theoretically considered as null. For this reason, this liquid was selected in order to measure the wetted length of the immersed fibre. The properties at room temperature of the three different test liquids are reported in Table II. 4. The mass of liquid meniscus *m* formed around a fibre during a complete cycle of advancing, static and receding conditions is recorded.

Table II. 4 Properties of the different test liquids at 20°C. In particular the viscosity η, the density ρ, the dispersive γ_l^d and polar γ_l^p components of the liquid surface tension γ_l are reported [Rulison, 1996; Carré, 2007].

	η [mPas]	ρ [g/cm³]	γ_l^p [mN/m]	γ_l^d [mN/m]	γ_l [mN/m]
Water	1	0.998	51	21.8	72.8
Diiodomethane	2.76	3.325	0	50.8	50.8
n-Hexane	0.32	0.659	0	18.4	18.4

The sample immersion depth was set to 5 mm and the different test liquid vessels were placed manually close to the fibre, in order to make sure that a minimum of 3 mm of immersion depth was always respected. Fibres were immersed in the test liquid that moved with a low speed of 1 mm/min up to the specific immersion depth (advancing phase). Then fibres were maintained in this position for 60 seconds (static phase), allowing the measurement of a representative value of meniscus weight in static conditions. According to different studies [Vega *et al.*, 2007; Pucci *et al.*, 2017], the time of 60 seconds was considered as sufficient for reaching the static conditions of the test liquid. Finally, the liquid moved down and the fibres were withdrawn at the same speed up to the initial position (receding phase). One complete cycle in advancing, static and receding phase was performed for each test (Figure II.14). For each family of fibres, a minimum of five tests were carried out. The diameter of the single basalt and flax fibres was calculated performing tests with n-Hexane liquid. Once the meniscus mass m and the fibre wetted length p are known, advancing θ_a, static θ_s and receding contact angles θ_r were measured using the Wilhelmy equation, (Eq. II.6):

$$F_c = ma = p\gamma_l cos\theta \qquad \text{(II.6)}$$

where F_c is the capillary force, m is the liquid mass, a is the acceleration of gravity and γ_l is the liquid surface tension.

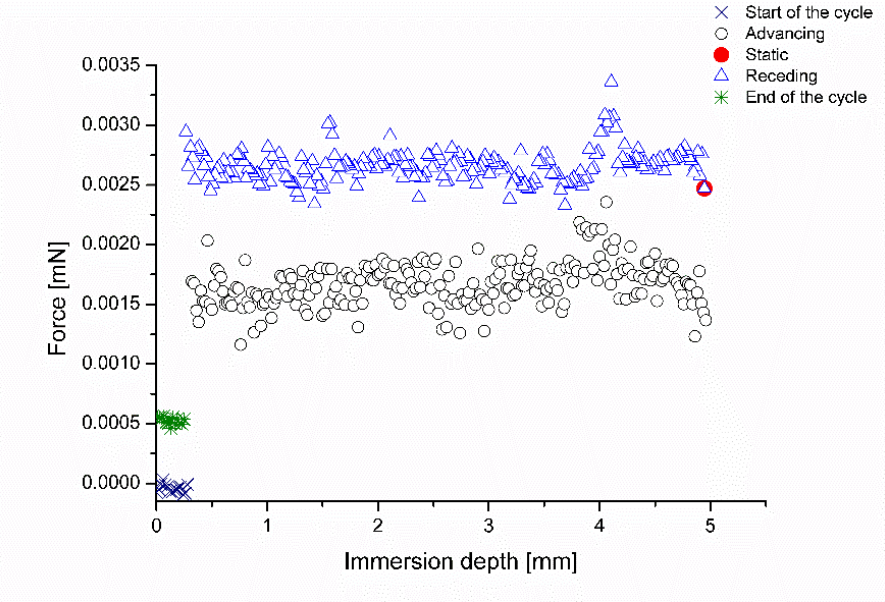

Figure II. 14 Example of the advancing, static and receding phases for a test on basalt fibre in water.

The Owens and Wendt (Eq. II.7) and the Young-Laplace equilibrium (Eq. II.8) equations were used to measure dispersive and polar components of basalt and flax fibres surface energy γ_s:

$$\gamma_s + \gamma_l - \gamma_{sl} = 2\left(\gamma_s^d \gamma_l^d\right)^{0.5} + 2\left(\gamma_s^p \gamma_l^p\right)^{0.5} \quad \text{(II.7)}$$

$$cos\theta_e = \frac{(\gamma_s - \gamma_{sl})}{\gamma_l} \quad \text{(II.8)}$$

where γ_s is the basalt and flax fibres surface energy, γ_l is the liquid surface tension, γ_{sl} is the solid-liquid surface energy, γ_s^d and γ_s^p are the dispersive and polar components of the solid surface energy, γ_l^d and γ_l^p are the dispersive and polar components of the liquid surface energy and θ_e is the equilibrium (static) contact angle. Combining equations II.7 and II.8, the Owens and Wendt equation can then be rewritten as follows, Eq. II.9:

$$\frac{\gamma_l(1+cos\theta_e)}{2\sqrt{\gamma_l^d}} = \sqrt{\gamma_s^p}\left(\frac{\sqrt{\gamma_l^p}}{\sqrt{\gamma_l^d}}\right) + \sqrt{\gamma_s^d} \quad \text{(II.9)}$$

The values of contact angles, θ_e, that are inserted in the Owens and Wendt method (Eq. II.6), are the values of contact angles measured in static conditions. Considering the left hand-side term as the *Y* axis, and the fraction between the square root of polar and dispersive components of the liquid surface tension in the right hand-side term as the *X* axis, the slope and the y-intercept of the linear fit are the square root of fibre polar and dispersive components, respectively.

II.2.4 Interface Characterization: Single Filament Fragmentation Test

The single filament fragmentation test was carried out to assess the interfacial properties of flax yarns and basalt fibres with epoxy and vinylester matrices. The fragmentation testing was performed with an Instron E1000 ElectroPuls test machine equipped with a load cell of 2 kN, using a crosshead speed of 0.005 mm/min (Figure II.15). The test was carried out at a rather low loading rate and the loading phase was stopped if the specimen failed, or when the fragmentation saturation level was achieved. This last case was defined when no new

filament breaks appeared during a subsequent strain increase by 0.5%, as frequently reported in literature [Joffe *et al.*, 2005].

Figure II. 15 The Instron E1000 ElectroPuls test machine and the clamping of a monofilament sample (ISAE-ENSMA).

In order to be sure to reach the saturation level, epoxy- and vinylester-based specimens were loaded up to failure at strains higher than 9% and 11%, respectively. All the different basalt fibres and flax yarns are characterised by a strain at failure at least three and two times smaller than the failure strain of both epoxy and vinylester resins, respectively. This is a crucial aspect for carrying out the fragmentation tests and to reach the saturation level. In fact, only in systems characterized by a brittle filament and a comparatively ductile matrix, it is possible to ensure a full debonding/yielding of the filament fragments, attain a constant shear at the filament/matrix interface and so a full satisfaction of the Kelly-Tyson requirements [Kelly *et al.*, 1965].

II.2.5 Mechanical Characterization

II.2.5.1 Single basalt fibres and flax yarns

A mechanical characterization was carried out on filaments, i.e. individual fibres for basalt and yarns for flax. Tensile properties have been determined by single filament tensile tests in accordance with ASTM C-1557 standard test method. Tensile tests were carried out at

room temperature using a Zwick/Roell Z010 machine (Sapienza University of Rome) equipped with a 100 N load cell. Each test has been performed in displacement control at a cross-head speed of 2 mm/min. Individual basalt fibres and flax yarns were carefully separated by hand from the different fabrics and glued (Loctite™ Gel Superglue) onto a card tab with a central window cut out to match the gauge length of 20, 30 and 40 mm. At least 30 filaments were tested for each type of family and gauge length. In order to avoid damaging the fibre surface, samples were handled with utmost care. Before testing, all fibres and yarns were conditioned at 45°C for 24 h. The card tab was inserted between the machine grips, taking care to align both filament and crosshead axis in order to ensure a uniform stress condition and to avoid sample twisting. Screw grips were used. A sufficient pressure was applied to clamp the samples in order to avoid the slippage of the card tab but, at the same time, not so high to produce local stress or filament fractures. If the fracture occurred outside the gauge length, the test was discarded. Before the start of the tensile test, both sides of the window in the paper support were cut (Figure II.16). Because of the small dimension of filaments, the use of standard extensometers was not been possible. The actual specimen elongation in the gauge length was determined by subtracting the displacement associated with the system compliance from the total cross-head displacement. The system compliance was measured according to ASTM C1557 by obtaining the force versus displacement behaviour of the filaments at the three gauge lengths.

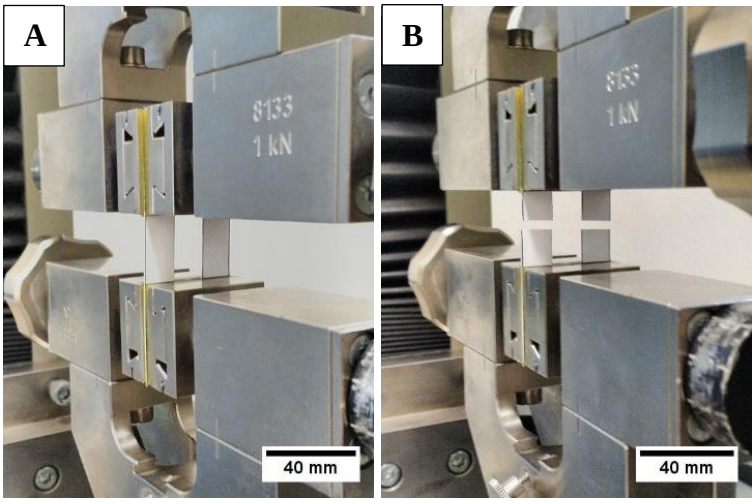

Figure II. 16 Clamping of the card tab between the grips of the tensile machine (A) and the cutting of the two edges of the tab before the start of the tensile test (B).

II.2.5.2 Woven composite materials

II.2.5.2.1 Tensile test

A mechanical characterization of the basalt/epoxy, flax/epoxy and basalt-flax/epoxy composite materials was carried out by tensile test (ASTM D 3039). Tests have been performed at room temperature using an Instron 1195 machine (ISAE-ENSMA) equipped with a 100 kN load cell and characterized by manual wedge action grips. For each test a cross-head speed of 2.5 mm/min has been used and the sample deformation has been evaluated using an axial clip-on extensometer. A minimum of three specimens for each type of composite laminate were tested. Tensile tests were performed on rectangular composite samples, all characterized by an overall length of 150 mm and a width of 25 mm. For all samples a gauge length of 80 mm has been used.

II.2.5.2.2 Bending test

Four-point bending tests were performed on all the different types of composites, according to the ASTM D 6272 standard test method. A minimum of three specimens for each type of composite laminate were tested. All specimens were loaded under four-point bending using a Zwick/Roell Z010 universal testing machine equipped with a 10 kN load cell, (Sapienza University of Rome). Tests were performed using a cross-head speed of 2.5 mm/min. Figure II.17-A reports a description of the bending test configuration used. In particular a support span of 84 mm, a loading span and a shear span equal to one-half (42 mm) and one-fourth (21 mm) of the total span were used, respectively.

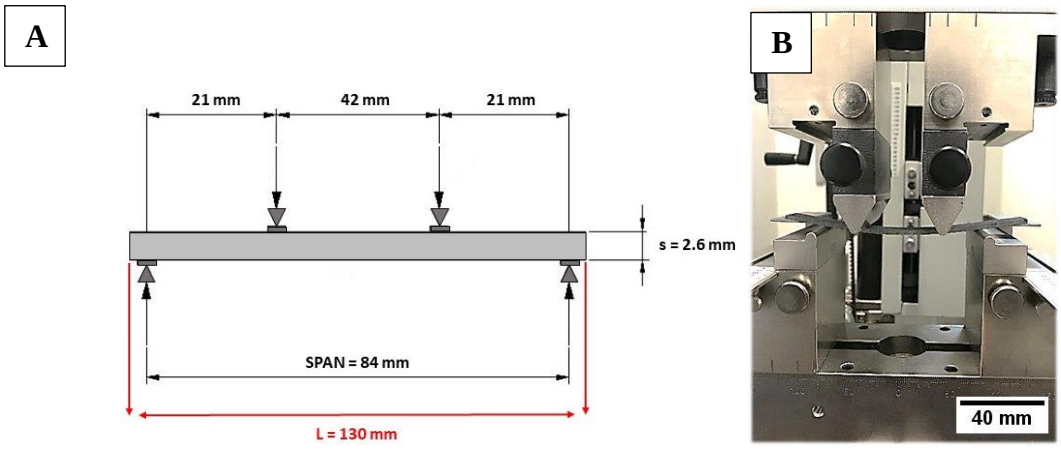

Figure II. 17 The bending test configuration: (A) a schematic representation and (B) the bending system used.

As for the tensile tests, bending tests were performed on rectangular composite specimens, all characterized by an overall length of 150 mm and a width of 25 mm.

II.2.5.2.3 Fatigue test

Fatigue tests were performed using an Instron 8874 servo-hydraulic bi-axial testing machine equipped with a 25 kN load cell (ISAE-ENSMA). Tests were performed according to the ASTM D 3479 standard test method. Constant amplitude loads were applied in a sinusoidal waveform at a frequency of 5 Hz under load-control. Tension-tension mode fatigue tests were carried out with a ratio of the minimum load to the maximum load (R) of 0.1. Fatigue tests were performed on all the three different families of composite samples. For each type of composite laminate, tests were carried out for both 0°/90° and ± 45° orientations. Different levels of maximum stress S_{max} have been used, specifically 85%, 65%, 50%, 45%, 35%, 30% and 25% of the ultimate tensile strength. Fatigue tests were interrupted at specimen failure or when more than 10^6 cycles were reached. Plate grips characterized by the presence of a system of five screws were used (Figure II.18). In order to avoid an excessive force concentration, the sample clamping was performed using a torque wrench.

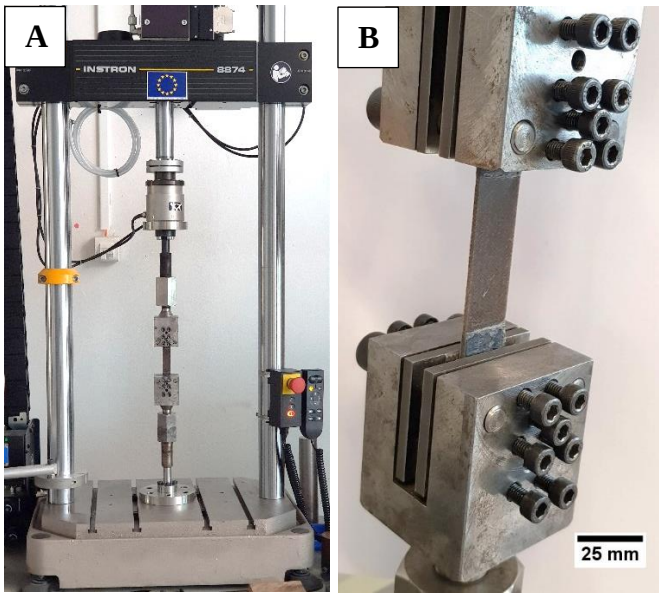

Figure II. 18 The Instron 8874 testing machine (A), and the grips configuration used (B).

In a first phase, fatigue tests were performed on samples not equipped with tabs. Subsequently, in particular for the $[0°/90°]_s$ composites, it was necessary to use tabs in order to produce a valid failure mode within the central gage section of the specimen. Different tab configurations were tested, with various geometries and various materials: aluminium, glass fibre/PP laminate and glass fibre/epoxy laminate. Tabs made of glass fibre/epoxy with a length of 45 mm, a thickness of 1.3 mm and a taper angle of 15° were chosen. The ADEKIT H 9951 structural epoxy adhesive, supplied by Axon, was selected for the tabs bonding. In order to maximize the grip of the adhesive and to promote its mechanical anchoring with the composite surface, both tabs and samples surfaces were sanded (only in the tab region), cleaned by solvent and compressed air. A curing process of 24h at room temperature was carried out to reach the maximum of the mechanical properties of the glue. Figure II.19-A and II.19-B show the flax/epoxy specimens without and with tabs. As for the tensile and bending tests, composite samples were characterized by a rectangular shape, an overall length of 150 mm and a width of 25 mm. For all samples, a gauge length of 60 mm was used.

Figure II. 19 Example of flax/epoxy composite specimens without and with the presence of the glass fibre/epoxy tabs on the y-x plane (A) and on the z-x plane (B).

II.2.5.2.4 Low-velocity impact test

Low-velocity impact tests were performed to compare the dynamic behaviour of the different woven composite materials. An instrumented drop-weight CEAST/Instron 9340 impact testing machine (Sapienza University of Rome) was used, equipped with a hemispherical striker characterized by a diameter of 16 mm. The woven composites panels were cut to create test coupons measuring 8.5 x 8.5 cm^2. A number of impact tests were performed at room temperature under various impact energies ranging from 1 J to 40 J in order to examine damage process in the different composites.

Conclusion of Part II

The different materials and techniques used in the experimental work have been presented. The single filament fragmentation test (SFFT) was used to assess the interfacial properties of flax yarns and basalt fibres with both epoxy and vinylester matrices. A metallic mould was optimized for the manufacture of monofilament composite specimens reinforced with a single filament aligned along the load direction. It is important to highlight that for the first time, the microcomputed tomography was used as supplementary analysis of the SFFT technique. In fact, a high-resolution microtomography (1.5 μm) allowed the measurement of the debonding length of flax yarn and basalt fibres with polymer matrices. To study in a proper manner the interfacial debonding phenomena and the stress field produced during the fragmentation test, a birefringence analysis has been performed on the different monofilament composites. Through a stay at the laboratory of the Centre des Matériaux des Mines d'Alès (C2MA), IMT Mines Alès an in-depth analysis of the wetting properties of the different fibres used was carried out. In particular, a tensiometric method was used to measure the contact angles and the surface tensions of both single basalt and flax fibres. Different composite laminates were manufactured using the vacuum infusion technique in collaboration with the Institute of Composites and Biomaterials (IPCB) of Portici (Italy). Tensile tests were carried out both on composite laminates and on single flax yarns and basalt fibres. An in-depth mechanical characterization of the composite laminates was carried out performing 4-point bending tests, low-velocity impact and fatigue tests. In this last case, a study and optimization of the tabs to be used during the test were necessary in order to produce a valid failure mode within the central gauge section of the specimen. A final configuration of glass fibre/epoxy tabs was chosen. Post-mortem observations were carried out on the different samples both by scanning electron microscopy and by micro-CT, in order to assess the internal damage level.

Conclusion de la Partie II

(en français)

Les différents matériaux et techniques utilisés dans ce travail de thèse ont été présentés dans la Partie II. Le test de fragmentation sur composite monofilamentaire (SFFT) a été utilisé pour évaluer les propriétés interfaciales des fils de lin et des fibres de basalte avec des matrices époxy et vinylester. Un moule métallique a été optimisé pour la fabrication d'échantillons composites monofilamentaires renforcés par un seul filament aligné dans la direction de la sollicitation. Il est important de souligner que pour la première fois, la microtomographie a été utilisée comme analyse complémentaire aux tests de fragmentation. L'utilisation de la microtomographie à haute résolution (1,5 µm) a permis de mesurer la longueur de décohésion du lin et du basalte avec les matrices polymères. Afin d'étudier de manière appropriée les phénomènes de décohésion interfaciale et le champ de contraintes produits lors du test de fragmentation, une analyse par biréfringence a été réalisée sur les différents composites monofilamentaires. Grâce à un séjour au laboratoire du Centre des Matériaux des Mines d'Alès (C2MA), IMT Mines Alès, une analyse approfondie des propriétés de mouillage des différentes fibres a été réalisée. En particulier, une méthode tensiométrique a été utilisée pour mesurer les angles de contact et les tensions de surface des fibres unitaires de basalte et de lin. Différents stratifiés composites ont été fabriqués en utilisant la technique d'infusion sous vide en collaboration avec l'Institut des composites et des biomatériaux (IPCB) de Portici (Italie). Des essais de traction ont été effectués à la fois sur des stratifiés composites et sur des fils de lin et des fibres de basalte. Une caractérisation mécanique approfondie des stratifiés composites a été réalisée en effectuant des tests de flexion 4 points, des tests d'impact à basse vitesse et des tests de fatigue. Dans ce dernier cas, une étude et une optimisation des talons à utiliser lors du test ont été nécessaires afin d'obtenir une rupture dans la longueur utile de l'échantillon. Une configuration finale des talons en fibre de verre/époxy a été choisie. Des observations post mortem ont été effectuées sur les différents échantillons à la fois par microscopie électronique à balayage et par micro-CT, afin d'évaluer le niveau de dommage interne.

PART III

MECHANICAL BEHAVIOUR OF HYBRID COMPOSITES

Part III deals with the mechanical performance of basalt/epoxy, flax/epoxy and basalt-flax/epoxy woven composites. The aim of this section is to assess the effect of basalt-flax hybridisation on the mechanical properties of composites. The results of a quasi-static mechanical characterization will be reported in Chapter III.1. Specifically, quasi-static tensile tests and four-point bending tests will be carried out. In order to analyse the dynamic behaviour of the different types of woven composites, the results of tension-tension fatigue and low-velocity impact tests will be discussed in Chapter III.2.

PART III – MECHANICAL BEHAVIOUR OF HYBRID COMPOSITES

CHAPTER III.1

QUASI-STATIC MECHANICAL CHARACTERIZATION

The aim of the present chapter is to assess the mechanical behaviour of the basalt/epoxy, flax/epoxy and basalt-flax/epoxy composites subjected to quasi-static tensile tests and four-point bending tests. For each composite material, tests were carried out for two different reinforcement orientations with respect to the x-axis of the sample (Figure III.1): 0°/90° and ±45°. Currently, woven fabric reinforced laminates are largely used in applications where they are subjected to off-axis loading conditions. An off-axis loading test is the easiest way to generate a complex stress state, due to the spatially varying fibre orientation in a lamina, a local multiaxial stress state can be achieved even if the loading scheme is uniaxial, which is usually known as internal multiaxiality [Quaresimin *et al.*, 2010]. The objective of the experimental work was to carry out a characterization of the mechanical performance of the different composites, but also, in the case of tensile tests, to select the load levels to be used in the subsequent fatigue tests.

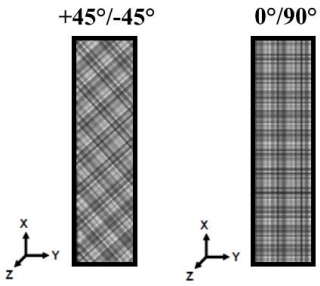

Figure III. 1 Different ply orientations of the composite samples.

III.1.1 Tensile behaviour of woven composites

As reported in section II.2.5.2.1, tensile tests were performed at room temperature using an Instron 1195 machine equipped with a 100 kN load cell. For each test a cross-head speed of 2.5 mm/min was used and the sample deformation was evaluated using an axial clip-on

extensometer. Table III.1 reports the values of tensile strength σ_{max}, tensile modulus E and strain at the maximum tensile stress ε_{max} found for the different composites. From the values shown in Table III.1, it can be observed how, both in the 0°/90° and the +45°/-45° ply orientation, the flax fibre composites are characterized by a significantly lower tensile strength than the basalt composites. Hybrid composites showed an intermediate behaviour.

Table III. 1 Tensile properties of the different composite materials.

Ply orientation		**σ_{max} [MPa]**	**E [GPa]**	**ε_{max} [%]**
0°/90°	Basalt	635 ± 50	28.8 ± 0.2	2.85 ± 0.26
	Flax	106.3 ± 5.2	5.8 ± 0.1	2.07 ± 0.11
	Hybrid	190.9 ± 6.4	13.2 ± 0.03	2.03 ± 0.03
+45°/-45°	Basalt	154.3 ± 5.4	14.6 ± 0.5	15 ± 0.21
	Flax	63.6 ± 0.6	3.7 ± 0.1	2.51 ± 0.28
	Hybrid	118.4 ± 1.7	6.8 ± 0.8	8.65 ± 0.26

Concerning the 0°/90° ply orientation, the basalt fibre composites are characterized by a tensile strength and a tensile modulus higher than those of hybrids. However, these differences are strongly reduced in the +45°/-45 ° orientation. In this case, it is possible to highlight that the results reported in Table III.1 are in accordance with the "hybrid effect" described in section I.1.1. In fact, a positive hybrid effect of failure strain enhancement of flax fibre (low elongation - LE), compared to that obtained in a non-hybrid composite, is produced. It is important to stress that the fibre volume fraction values have an influence on the mechanical performance of the different composites. Several studies investigated the behaviour of the hybrid composites by varying the volume/weight fraction of the fibres [Nunna *et al.*, 2016]. As reported in Section II.1.3, hybrid composites present a total fibre volume percentage of 33% (20% flax and 13% basalt). This is an intermediate value between that of pure basalt (55%) and flax (26%) laminates. The addition of 13% of higher modulus basalt fibres allowed to improve the tensile strength and the tensile modulus of composites based on flax fibres. The good improvement in tensile properties of hybrid composites can be also related to the presence of basalt fibres as extreme plies on both sides of the laminate. In fact, as mentioned in section I.1.2.3, the stacking sequence of the different fibre layers represents a crucial aspect for the mechanical properties of the hybrid composites. Different

studies reported that the optimum mechanical properties were found by placing high strength fibres in the skin layers [Gupta, 2009; Nunna *et al.*, 2016]. The tensile modulus of hybrid composites with basalt fibres at the outer layers can produce higher values than any other layered pattern due to excellent load-carrying capacity of basalt fibres. The enhancement in the tensile strength and modulus of the hybrid composites compared to the 100% flax composites is due to the addition of high modulus basalt fibres compared to the flax fibres. Figure III.2 reports the stress-strain characteristic curves obtained for the different woven composites, with both the 0°/90° (Figure III.2-A) and +45°/-45° (Figure III.2-B) ply orientations.

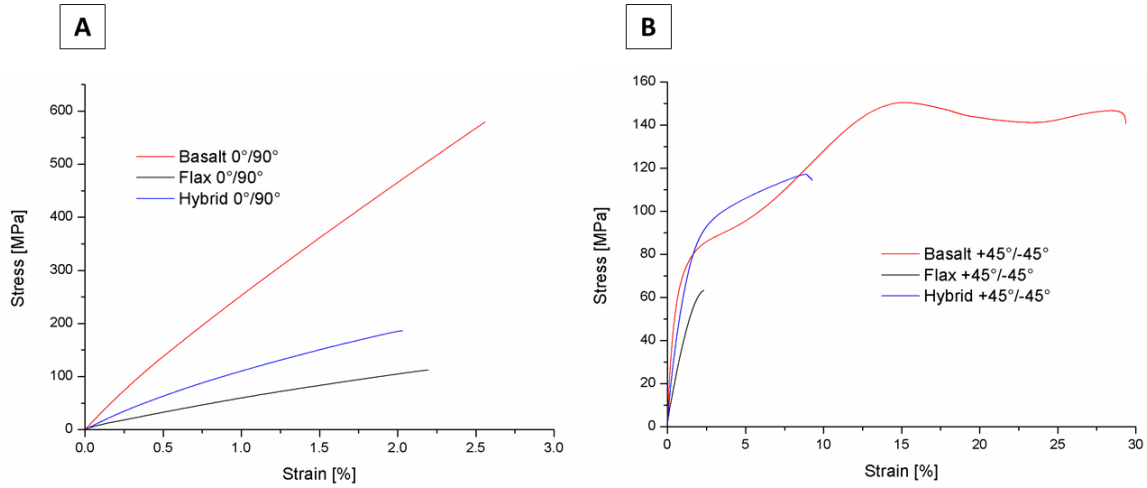

Figure III. 2 Typical tensile stress-strain curves for basalt, flax and flax/basalt hybrid composites for (A) 0°/90° orientation, (B) +45°/-45° orientation.

Concerning the tensile behaviour of 0°/90° samples, an approximately linear trend has been reported for all the different composite laminates with a slight change in slope when a knee point is reached. This behaviour of woven composites under quasi-static tensile loading along warp direction is typical and has been widely reported in literature [John *et al.*, 2001; Pandita *et al.*, 2001; Daggumati *et al.*, 2010]. This knee point is usually associated with matrix crack propagation in the weft yarns due to crack initiation near the weaving points. The waviness in the longitudinal yarns is able to induce bending loads in the transverse yarns where microcracks are first generated and propagate through the strand thickness until a saturation level is reached. These cracks are frequently the source of delaminations at the interface between longitudinal and transverse fibre bundles within the same layer or delaminations between plies. A different behaviour was found for the composite samples

with the +45°/-45° ply orientation. The failure behaviour of woven fabric composites is complex and because of the interlaced nature of warp and weft fibres, their reorientation along the loading direction is possible in off-axis samples. In all cases, the mechanical coupling between warp and weft fibres as a result of the interlaced structure allowed higher failure strains to be reached in the off-axis samples [Lisle *et al.*, 2015]. The tensile strength values of the off-axis specimens were always lower than those of the on-axis ones due to the interaction of tensile and shear stresses. The non-linearity was found to be predominant in the off-axis samples, especially for basalt fibre composites, where intermittent rise and fall of load was clearly detected (Figure III.2-B). This is due to the reorientation of fibres along the loading direction that is triggered by the simultaneous deformation of interlaced fibre bundles. This behaviour is partially inherited by hybrid laminates due to the presence of basalt fibres, while in flax-based laminates this effect was far less evident. During off-axis loading of samples, a significant role is also expected to be played by the shearing deformation of the matrix. In pure flax laminates, the presence of a higher amount of voids allowed their coalescence during the first loading phase thus preventing an extensive deformation and significant fibre reorientation, as the matrix failure precedes the ultimate failure of an off-axis woven fabric composite [Naik *et al.*, 1991]. In addition, in basalt fibre laminates a marked change in geometry during uniaxial tension loading was detected. Different levels of axial elongation and lateral contraction occurred, resulting in the typical contraction phenomenon. The same behaviour was also observed during tension-tension fatigue tests.

III.1.2 Bending behaviour of woven composites

Four-point bending tests were carried out on all the different types of composites. As reported in section II.2.5.2.2, bending tests were carried out using a Zwick/Roell Z010 universal testing machine equipped with a 10 kN load cell. A cross-head speed of 2.5 mm/min was used. In Table III.2 are reported the values of flexural strength σ_{max}, flexural modulus E_f and strain at the maximum flexural stress ε_{max} found for the different samples. A comparison of quasi-static behaviour under tensile and bending loadings for basalt, flax and hybrid composites with 0°/90° and ±45° orientations is reported in Figure III. Considering both the 0°/90° and the +45°/-45° ply orientations, the flax fibre composites are

characterized by a significantly lower flexural strength than the basalt composites. Hybrids showed an intermediate behaviour between that possessed by flax and basalt composites.

Table III. 2 Flexural properties of the different composite materials.

Ply orientation		σ_{max} [MPa]	E_f [GPa]	ε_{max} [%]
0°/90°	Basalt	440.8 ± 13.1	25.4 ± 0.7	2.16 ± 0.03
	Flax	97 ± 9.6	5.7 ± 0.8	2.98 ± 0.06
	Hybrid	229.7 ± 3.5	14 ± 0.1	2.43 ± 0.17
+45°/-45°	Basalt	163.6 ± 8.1	13.5 ± 0.8	2.64 ± 0.04
	Flax	85.7 ± 4.4	4.5 ± 0.4	2.81 ± 0.06
	Hybrid	126.8 ± 2.7	8.6 ± 0.2	2.77 ± 0.03

The flexural strength of the flax/epoxy composites has been increased with the content of basalt fibres due to their higher inherent mechanical properties. The stacking sequence of fibre layers can influence the flexural properties of hybrids. In particular, the good flexural properties shown by basalt-flax/epoxy hybrids can be related to the presence of basalt layers at the outer layers of composites, because the flexural strength and stiffness are mainly controlled by the properties of the extreme plies.

From Figure III.3, it is possible to notice that the bending results are consistent with those found previously by tensile tests. The bending tests confirm, once again, the intermediate mechanical performances obtained for the hybrid basalt-flax composites with respect to the 100% flax and 100% basalt composites.

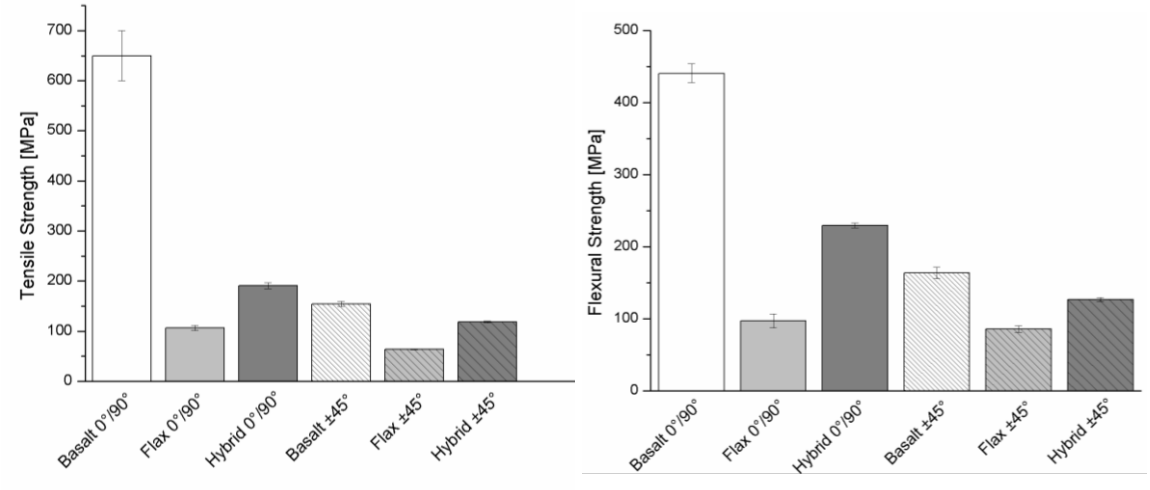

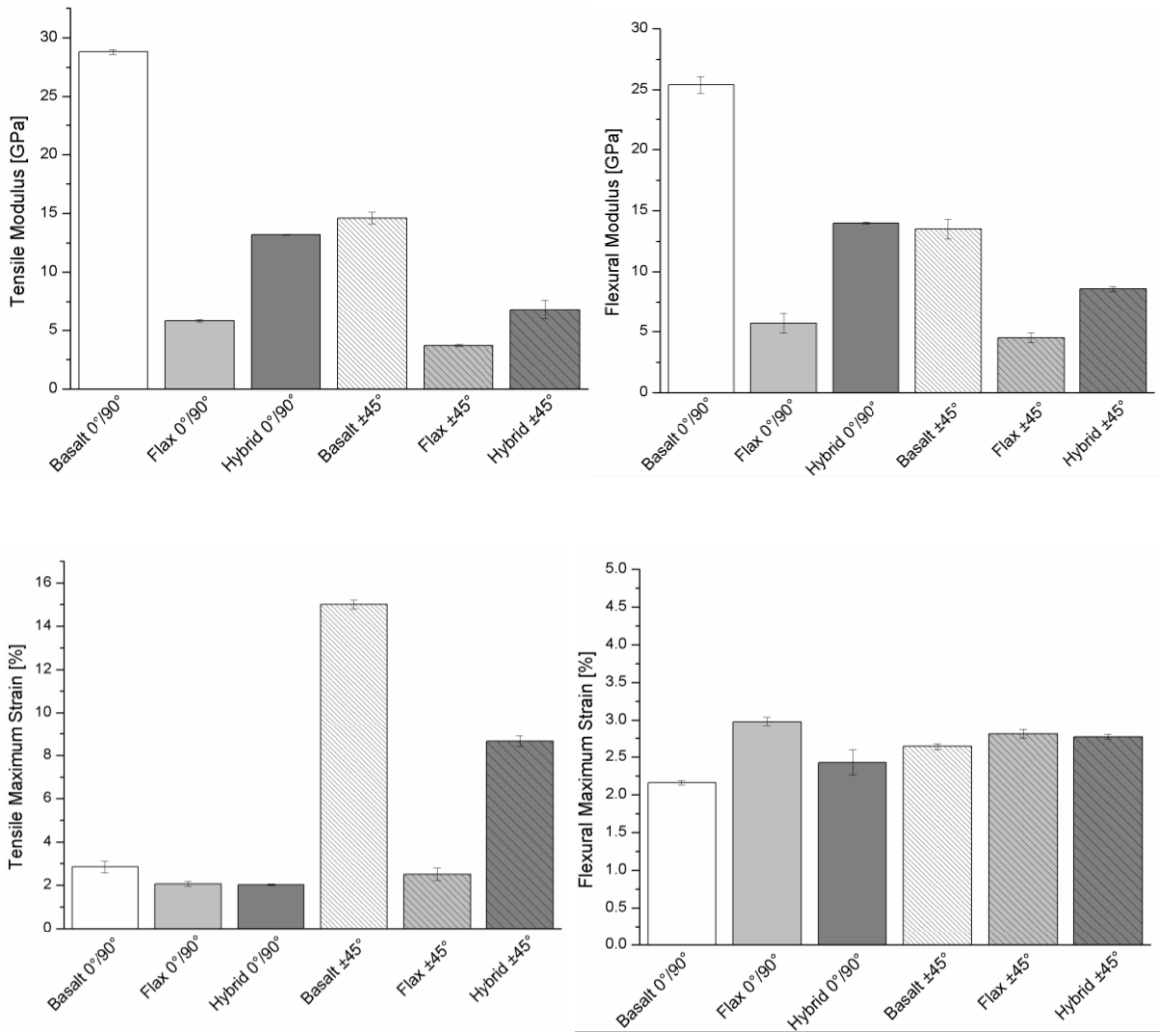

Figure III. 3 Comparison of quasi-static behaviour under tensile and bending loadings for basalt, flax and hybrid composites with 0°/90° and ±45° orientations.

CHAPTER III.2

DYNAMIC MECHANICAL CHARACTERIZATION

The aim of the present chapter is to provide a mechanical characterization of the dynamic behaviour of the basalt/epoxy, flax/epoxy and basalt-flax/epoxy composites. Tension-tension fatigue and low-velocity impact tests were performed on the different types of composites. For each type of composite laminate, tests were carried out for both 0°/90° and ±45° reinforcement orientations.

III.2.1 Fatigue behaviour of woven composites

As reported in detail in Section II.2.5.2.3, fatigue tests were performed on all the three different families of composite samples using an Instron 8874 servo-hydraulic bi-axial testing machine equipped with a 25 kN load cell. Constant amplitude loads were applied in a sinusoidal waveform at a frequency of 5 Hz under load-control. Tension-tension mode fatigue tests were carried out with a ratio R of the minimum stress S_{min} to the maximum stress S_{max} of 0.1. The different levels of maximum stress S_{max} used in this study were defined from the tensile stress-strain curves obtained after the quasi-static tensile tests performed on the different composites (Section III.1.2).

Specifically:

- for samples with 0°/90° ply orientation, the selected levels of maximum stress are 25%, 35%, 45%, 65% and 85% of the tensile strength;

- for the samples with ±45° ply orientation, the selected levels of maximum stress are 35%, 45%, 50%, 65% and 85% of the tensile strength.

III.2.1.1 Wöhler diagrams

The average number of fatigue failure cycles for each type of composite laminate is given in Tables III.3 - III.5.

Table III. 3 The average number of fatigue failure cycles and the corresponding logarithmic value for basalt/epoxy composites tested in fatigue.

Basalt 0°/90°			*Basalt +45°/-45°*		
	N_f	**Log(N_f)**		**N_f**	**Log(N_f)**
85% $S_{u,0°}$	73	1.87	**85% $S_{u,45°}$**	106	2.02
65% $S_{u,0°}$	231	2.36	**65% $S_{u,45°}$**	382	2.58
45% $S_{u,0°}$	804	2.74	**50% $S_{u,45°}$**	1010	3
35% $S_{u,0°}$	8001	3.9	**45% $S_{u,45°}$**	7014	3.69
30% $S_{u,0°}$	69965	4.84	**35% $S_{u,45°}$**	2924442	6.46
25% $S_{u,0°}$	2852941	6.45			

Table III. 4 The average number of fatigue failure cycles and the corresponding logarithmic value for flax/epoxy composites tested in fatigue.

Flax 0°/90°			*Flax +45°/-45°*		
	N_f	**Log(N_f)**		**N_f**	**Log(N_f)**
85% $S_{u,0°}$	17	0.57	**85% $S_{u,45°}$**	2370	3.37
65% $S_{u,0°}$	3165	3.2	**65% $S_{u,45°}$**	21690	4.33
45% $S_{u,0°}$	69480	4.83	**50% $S_{u,45°}$**	813931	5.9
35% $S_{u,0°}$	1097894	6.04	**45% $S_{u,45°}$**	1535002	6.17
25% $S_{u,0°}$	>3145098	>6.5	**35% $S_{u,45°}$**	>3933076	6.59

Table III. 5 The average number of fatigue failure cycles and the corresponding logarithmic value for hybrid composites tested in fatigue.

Hybrid 0°/90°			*Hybrid +45°/-45°*		
	N_f	**Log(N_f)**		**N_f**	**Log(N_f)**
85% $S_{u,0°}$	167	1.65	**85% $S_{u,45°}$**	210	2.31
65% $S_{u,0°}$	3214	3.26	**65% $S_{u,45°}$**	1541	3.18
45% $S_{u,0°}$	16167	4.21	**50% $S_{u,45°}$**	57596	4.76
35% $S_{u,0°}$	330527	5.45	**45% $S_{u,45°}$**	268131	5.42
25% $S_{u,0°}$	>10000000	>7	**35% $S_{u,45°}$**	2832228	6.45

Fatigue tests were interrupted at specimen's failure or when more than 4×10^6 cycles were reached. The corresponding Wöhler diagrams are plotted in Figure III.4. The points related to the non-broken samples are indicated by an arrow. Results demonstrate that, for each type of composite, for a given maximum fatigue stress value, the fatigue life for the ±45° orientation is far lower than for the 0°/90° one. But, at the same time, for each type of composite, there is an increase in the fatigue resistance passing from a 0°/90° to a ±45° ply orientation.

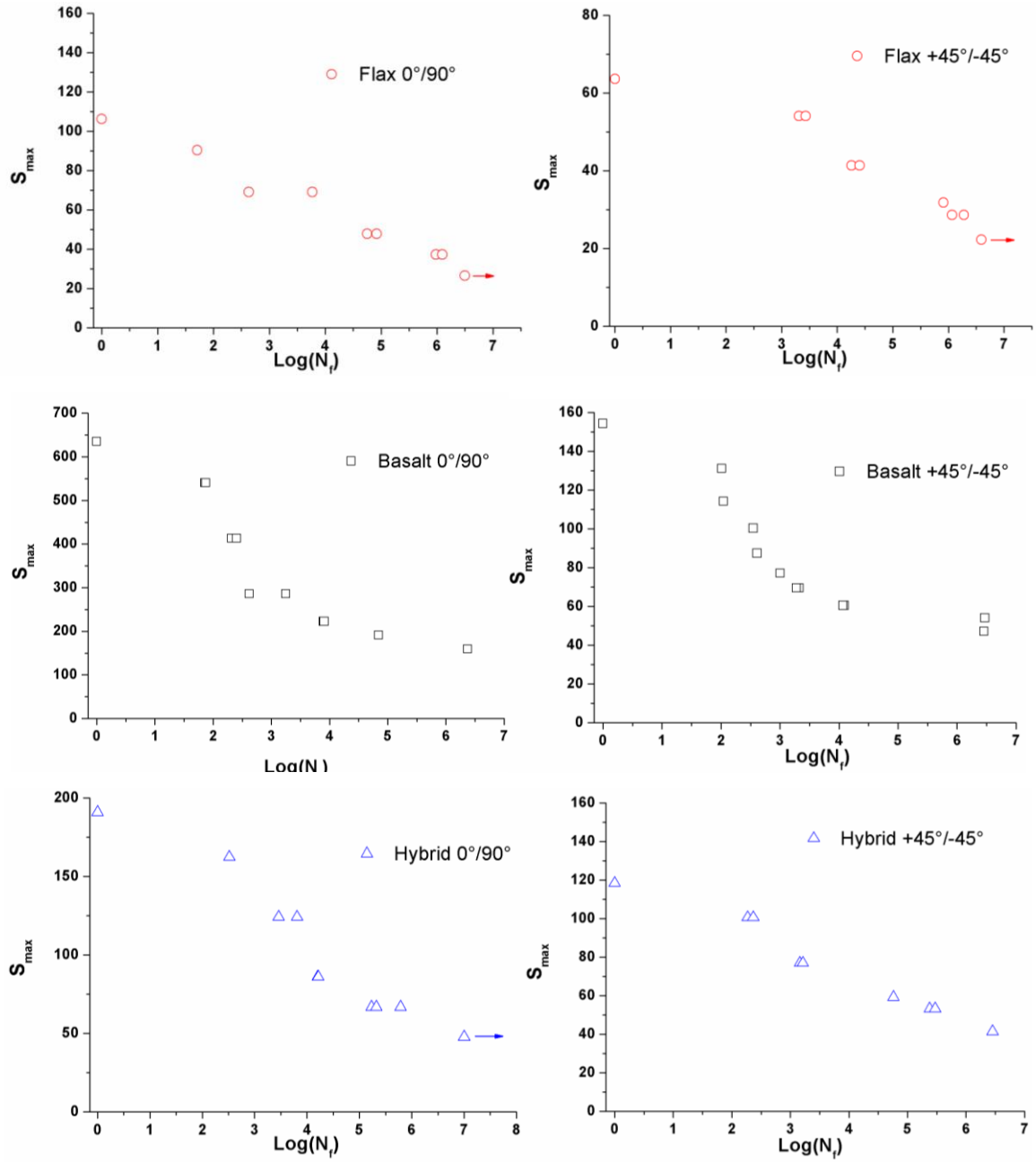

Figure III. 4 Wöhler diagrams for basalt, flax and hybrid composites with 0°/90° and ±45° orientations.

In order to compare the fatigue strength of the different materials, normalized diagrams are reported in Figure III.5 and Figure III.6 for the 0°/90° and ±45° ply orientations, respectively. In these figures, the x-axis shows the logarithm of the number of cycles to failure for each sample, while the y-axis reports the ratio between the maximum applied stress and the ultimate tensile strength. The points related to the non-broken samples are again indicated by an arrow.

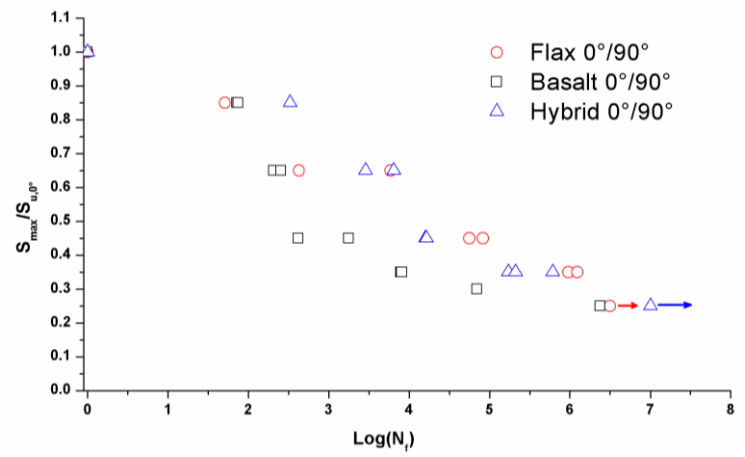

Figure III. 5 Normalized Wöhler diagram for the different composites for a 0°/90° reinforcement orientation.

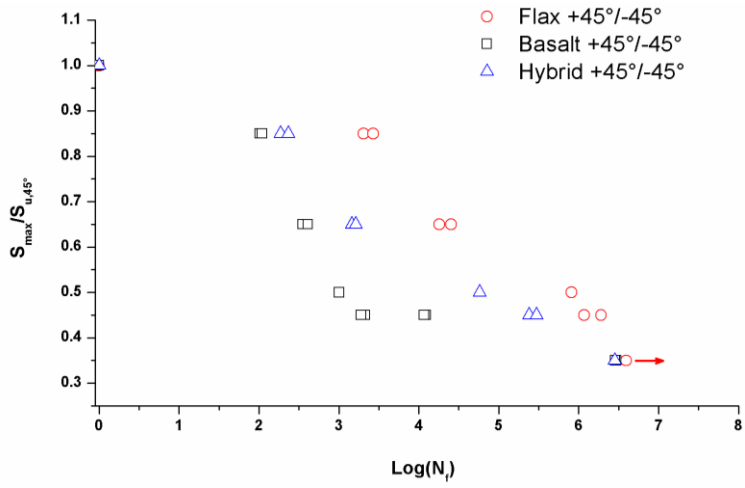

Figure III. 6 Normalized Wöhler diagram for the different composites for a +45°/-45° reinforcement orientation.

The main aspect emerging from Figures III.5,6 is the positive effect of hybridization. For both the 0°/90° and ±45° ply orientations, the hybrid composites exhibit an intermediate fatigue behaviour between those of basalt/epoxy and flax/epoxy composites. The fatigue resistance of basalt/epoxy composites is enhanced by combining flax fibres with basalt

fibres. From Figures III.5,6 it is possible to point out that the hybridization allows to obtain a higher number of cycles to failure than those of basalt reinforced composites. This result may be related to a positive action of flax fibres. In general, several studies present in literature have compared the fatigue behaviour of natural fibre reinforced composites with that of glass fibre composites. Most of these works highlighted that the glass reinforced composites display a higher absolute resistance to fatigue than the natural fibre reinforced composites [Mahboob *et al.*, 2018]. This is mainly due to the superior tensile strength of glass fibre composites than plant fibre composites. Shah et al. [Shah *et al.*, 2013] performed a comparison between the fatigue behaviour of plant fibre (jute, hemp and flax) polyester matrix composites with the behaviour of a glass/polyester composite. The authors reported that the fatigue strength degradation rates are lower in plant fibre composites than in glass fibre composites. A slower fatigue stiffness degradation of plant fibres compared to that of glass fibres and the ability of plant fibre to absorb and deflect cracks, thanks to their complex microstructure, can be considered as possible explanations of the fatigue behaviour of natural fibre reinforced composites.

III.2.1.2 Modelling of the fatigue behaviour

Several models have been proposed over the years in order to predict the fatigue resistance of composite materials characterized by different stacking sequences, different types of fibres and matrices and under different loading conditions [Degrieck *et al.*, 2001; Sevenois *et al.*, 2015]. Among these, it is possible to find the model proposed by D'Amore et al. [D'Amore *et al.*, 1996] based on the residual strength degradation of the composite. This model was developed for continuous glass-mat-reinforced thermoset based composites, but it was proved to be able to successfully predict the fatigue behaviour of continuous fibre reinforced composites [Caprino *et al.*, 1998, , 1999]. The model proposed by D'Amore et al. was used as a basis for the development of the Epaarachchi and Clausen model [Epaarachchi *et al.*, 2003], used in the present study. The model proposed by Epaarachchi and Clausen describes the strength degradation of a glass fibre reinforced composite subject to constant amplitude and constant frequency cyclic loading. The starting point of the model is a deterministic equation to measure the rate of strength *S* degradation, Equation III.1:

$$\frac{dS}{dN} = -C_1 N^{-m_1} \qquad \text{(III.1)}$$

where σ is the residual strength after N cycles, C_1 and m_1 are material constants and N is the number of fatigue cycles. From Equation III.1 and assuming that the fatigue failure occurs when the residual strength remaining in the sample in the direction of applied load is equal to S_{max}, the number of cycles required to degrade the material strength from S_u (the ultimate tensile stress) to S_{max} (the maximum applied stress), corresponding to the number of failure cycles N_f, can be expressed using Equation III.2:

$$N_f = \left[1 + \left(\frac{S_{u,\theta}}{S_{max}} - 1\right) \frac{f^{\beta}}{\alpha(1-R)^{\lambda - R|\sin\theta|}} \left(\frac{S_{u,\theta}}{S_{max}}\right)^{\lambda - 1 - R|\sin\theta|}\right]^{\frac{1}{\beta}} \quad \text{(III.2)}$$

where:

θ: is the smallest angle between the fibre direction in loading and the load direction;

$S_{u,\theta}$: is the ultimate tensile stress;

S_{max}: is the maximum applied stress;

R: is the stress ratio (minimum applied stress/maximum applied stress);

f: fatigue frequency used;

α and β: are the material constants;

λ: is a constant value of 1.6.

This model then provides the number of cycles to fatigue failure N_f of a composite as a function of the frequency f, the stress ratio R, the ratio between the ultimate tensile stress $S_{u,\theta}$ and the maximum applied stress S_{max}. The advantage of this model is to predict the fatigue behaviour of a composite material using a well-defined minimum number of tests. For each sample, the constants α and β were calculated. In order to determine the two material constants α and β, Equation III.2 can be rewritten as Equation III.3:

$$\alpha\left({N_f}^{\beta} - 1\right) = \left(\frac{S_{u,\theta}}{S_{max}} - 1\right) \frac{f^{\beta}}{(1-R)^{1.6 - R|\sin\theta|}} \left(\frac{S_{u,\theta}}{S_{max}}\right)^{0.6 - R|\sin\theta|} \quad \text{(III.3)}$$

The value of β was determined in a way that, for the experimental results, the right side of the equation plotted as a function of $(N_f^{\beta}-1)$ formed a straight line passing through the origin. The slope of this line was the value of α. In Table III.6 are reported the α and β values found for the different composites.

Table III. 6 The α and β values calculated for the different composite laminates.

Ply orientation		**α**	**β**
0°/90°	Basalt	0.129	0.473
	Flax	0.095	0.323
	Hybrid	0.121	0.338
+45°/-45°	Basalt	0.655	0.044
	Flax	0.043	0.320
	Hybrid	0.245	0.210

Figure III.7 shows the Wöhler diagrams of the experimental results for each type of composite and the Epaarachchi and Clausen model, represented by the solid lines. The dashed lines represent the dispersion intervals, which are calculated from the dispersion of the ultimate tensile strength. From Figure III.7 it is possible to observe that the model is able to correctly predict the fatigue behaviour of flax fibre and hybrid composites. A good correspondence between the experimental values and the model is reported. On the contrary, a different result is found for the basalt fibre composites for both the 0°/90° and the +45°/-45° ply orientations. In particular, the latter configuration exhibits the worst results, specifically at the lower values of maximum applied stress. A possible explanation of this result can be found in an excessive internal heating of the sample during fatigue tests. It is important to stress that the model proposed by Epaarachchi and Clausen is based on the assumption that the temperature of the specimen is constant or close to constant during test [Epaarachchi *et al.*, 2003]. In this framework, a qualitative analysis of the temperature evolution of the specimen surfaces was performed by a Fluke Ti300^{+} Thermal Camera, with acquisition rate of 9 Hz. A similar analysis on woven hemp fibre reinforced epoxy composites was performed by De Vasconcellos et al. [De Vasconcellos *et al.*, 2014]. This previous study reported that the highest temperature gradient on the specimens' face was obtained for the highest fatigue loading values used. In addition, the authors highlighted that the temperature gradient is more significant for the ±45° laminates than for the 0°/90°. For these reasons, in order to address the worst heating conditions, in the present study, measurements were carried out during fatigue tests performed at the stress level of 85% and for the composite samples with the ±45° ply orientation. Results show the progressive appearance of hot areas in localised zones on specimen's surface, as shown in Figure III.8, where images were taken right before the specimen's failure. The basalt composite exhibits an excessive overheating, reaching a maximum temperature of 98.5°C.

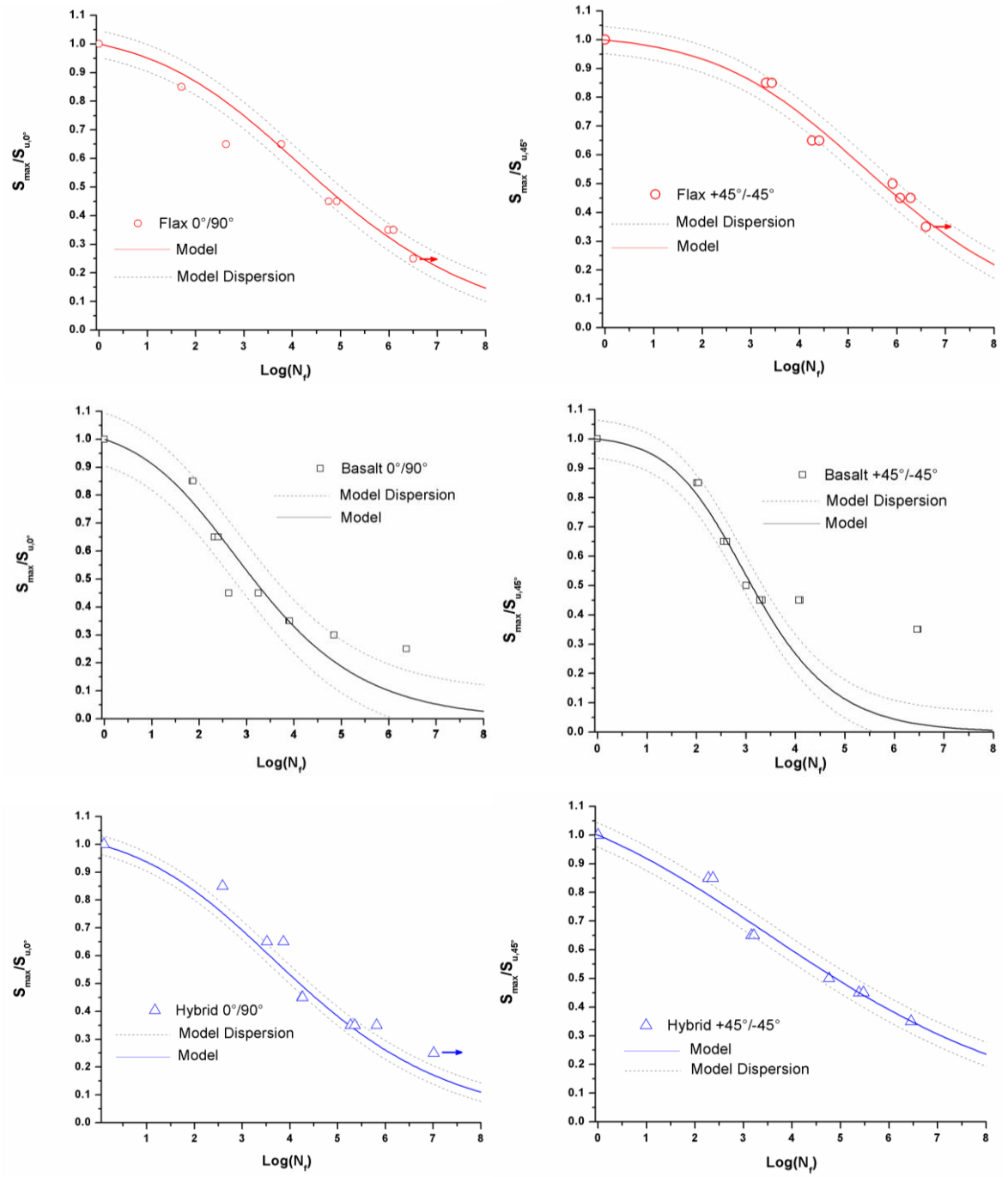

Figure III. 7 The normalized Wöhler diagrams and the curves of the Epaarachchi and Clausen model found for the different composites with 0°/90° and +45°/-45° reinforcement orientations.

A lower heating phenomenon is reported for the hybrid laminate, while for the flax composite the temperature can be approximated as constant during the fatigue test. The excessive basalt/epoxy composite heating is due to internal friction and damage initiation and propagation. Such a high temperature value is able to cause a change in the mechanical

behaviour of the material, whose fatigue behaviour will be difficult to predict by the model proposed by Epaarachchi and Clausen.

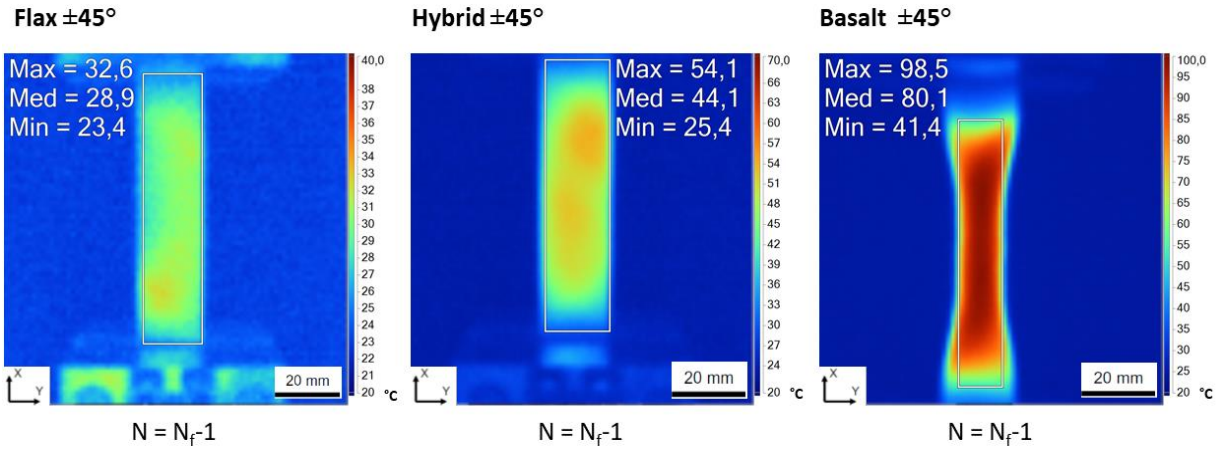

Figure III. 8 Temperature fields of specimen's surface measured by infrared camera during fatigue tests just before the failure for ±45° laminates at the stress level of 85% of S_u.

III.2.1.3 Fatigue fracture surface characterization

Post-mortem analysis of failed woven composites was performed by scanning electron microscopy. In particular, a morphological analysis of the fracture surface of both 0°/90° and ±45° laminates at the stress level of 45% of the ultimate tensile stress value was carried out. The micrographs show that the main failure modes are the matrix failure (brittle failure), basalt fibre and flax yarn pull-out, fibre failure (transverse failure of the fibre) and fibre-yarn debonding. All the different woven composites exhibit a poor interface quality between the reinforcement and the epoxy matrix. The morphological analysis points out that the interfacial degradation controls the fatigue resistance of all the different laminates. In Figure III.9 are reported the fracture surfaces found for the basalt/epoxy laminates. An intensive phenomena of basalt fibre pull-out and debonding with the epoxy matrix can be observed in Figure III.9-B,D. A strong interface debonding is also found for flax/epoxy composites (Figure III.10). An extensive flax yarn pull-out was observed, where the matrix crack runs around the yarns. Figure III.10-B shows a matrix transverse crack spreading around the flax fibre, producing a subsequent debonding at the fibre–matrix interface. Through cyclic loading, the matrix cracks can grow and initiate local debonding between the flax yarns thus causing a faster decrease in resistance of the laminate [Bensadoun, 2016]. In the case of flax fibre composites, where twist and crimp are present compared to the basalt composite

counterparts where only the crimp is present, extra matrix cracking can be initiated due to the more complex stress state in the twisted yarns oriented along the testing direction. The flax yarns can try to "untwist" creating shear and normal stresses relative to the fibre orientation and resulting in additional micro-cracks at the fibre/matrix interface. The FE-SEM observations highlighted the presence of a large amount of porosity, clearly visible in Figure III.10-A. The voids can provide a weak area, allowing cracks to propagate between them and weaken the flax composite laminate.

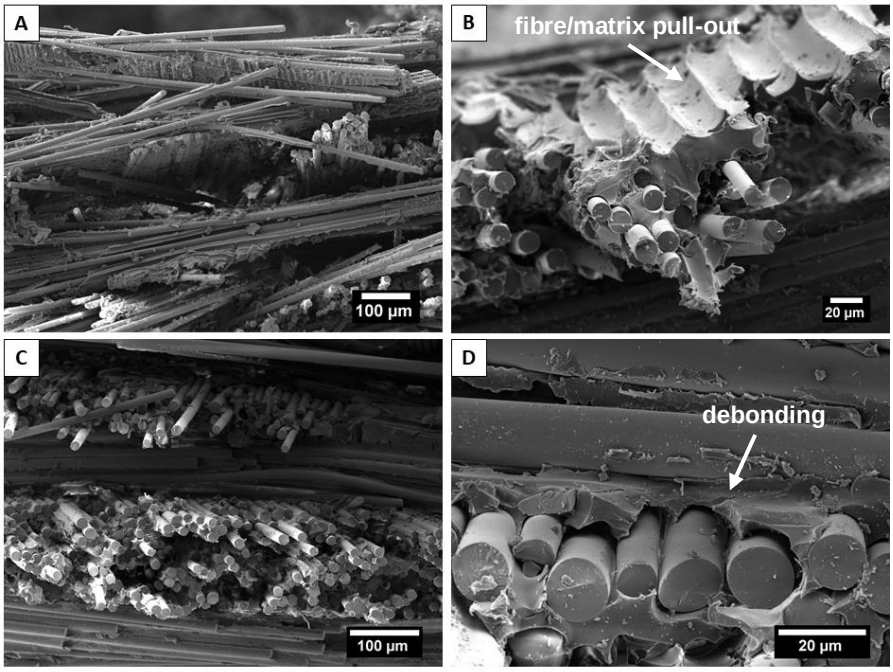

Figure III. 9 FE-SEM micrograohs of the basalt/epoxy composites after fatigue failure at stress level of 45% of S_u: (A-B) 0°/90° and ±45° (C-D) laminates.

Similar results were found for the hybrid composites. In fact, a poor interfacial adhesion between both basalt and flax fibres and the epoxy matrix was found (Figure III.11). A pull-out phenomenon of the single basalt fibres and the flax yarns confirmed the low compatibility between the reinforcement and the polymer matrix. These results show that a low interfacial adhesion can lead to the deterioration of fatigue behaviour for all the composites. It demonstrates the necessity to improve the adhesion quality at reinforcement/matrix interface in order to enhance the dynamic performances of these composites.

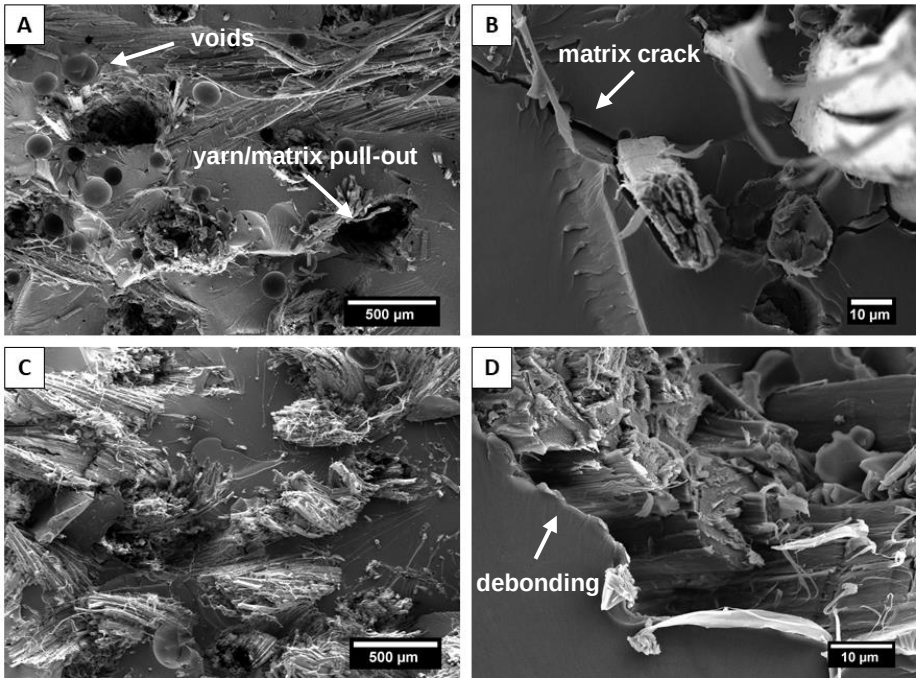

Figure III. 10 FE-SEM micrographs of the flax/epoxy composites after fatigue failure at stress level of 45% of S_u: (A-B) 0°/90° and ±45° (C-D) laminates.

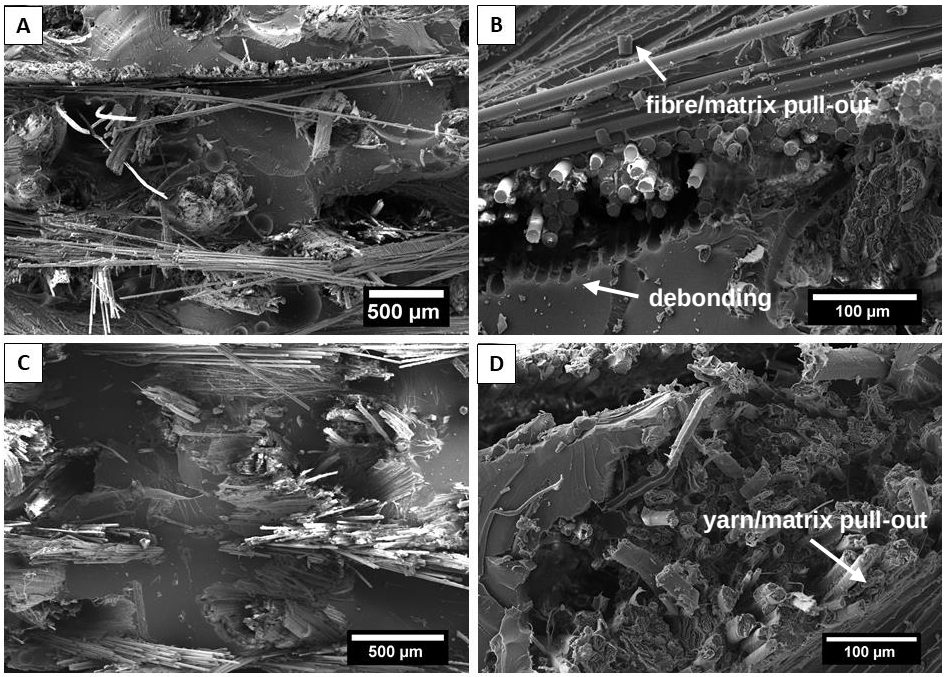

Figure III. 11 FE-SEM micrographs of the basalt-flax hybrid composites after fatigue failure at stress level of 45% of S_u: (A-B) 0°/90° and ±45° (C-D) laminates.

III.2.2 Impact behaviour of woven composites

Low-velocity impact tests were performed to compare the dynamic behaviour of the different woven composite materials. As reported in section II.2.5.2.4, an instrumented drop-weight CEAST/Instron 9340 impact testing machine was used, equipped with a hemispherical tip (diameter of 16 mm). Tests were performed on composite coupons measuring 8.5 × 8.5 cm^2. Several impact tests were performed under various target impact energies ranging from 1J to 40J in order to examine damage process in non-hybrid and hybrid laminates. The data acquisition system allowed the evaluation of some characteristic parameters such as impact load, sample displacement, impact velocity, impact energy and absorbed energy. In this section, the results of the low-velocity impact tests performed on the different woven composites are described in detail.

III.2.2.1 Force-displacement response of woven composites

In Figure III.12 are reported the typical load-deflection curves found for the different samples as a function of increasing impact energy. The area included in the closed loop of the curve corresponds to the energy absorbed E_a by the laminate. As reported by Dhakal et al. [Dhakal *et al.*, 2007], four different stages can be defined during the impact damage process. The first stage corresponds to a rapid load increase without the occurrence of visible damage. The second stage exhibits matrix cracking, which spreads rapidly and leads to the third stage characterized by the generation of interfacial debonding phenomena. Finally, the fourth and last stage corresponds to the stage where the laminate exhibited fibre breakage, delamination and perforation. The generation of matrix cracking and delamination phenomena can be related to the first load drop in the load-deflection curves. The second load drop, generally near or at the peak load, corresponds to the fibre breakage, more extensive matrix cracking and delamination [Sarasini *et al.*, 2016]. The basalt laminates exhibited the highest peak force values compared to the hybrid and flax configurations. From Figure III.12-B, it is possible to see how basalt composites showed all closed load-deflection curves, except for the curve at an impact energy of 40J indicating the material penetration. A dependence between the peak reaction load and the impact energy was found for both the basalt and the hybrid laminates. In fact, an increase in the peak force was produced with increasing impact energies. As reported by De Rosa et al. [De Rosa *et al.*, 2012], this effect

can be related to an increase in the elastically absorbed energy with increasing impact energy.

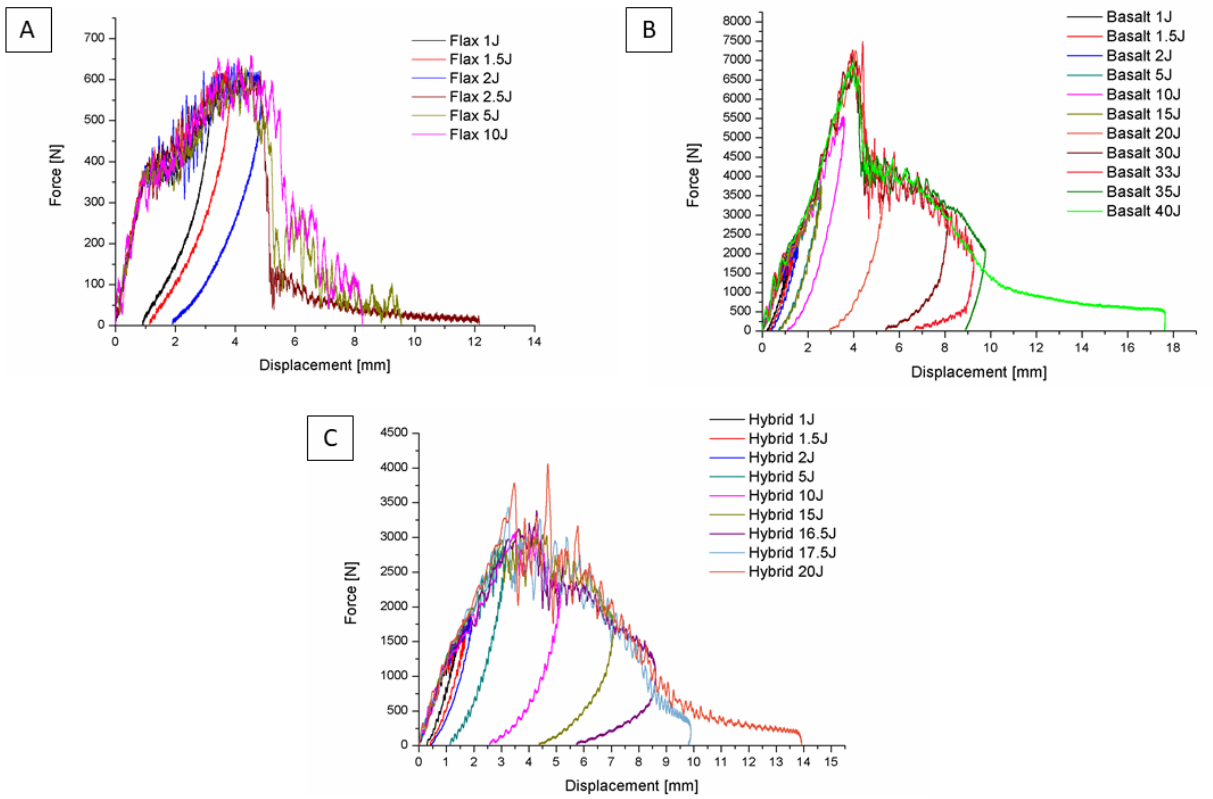

Figure III. 12 Force-displacement curves as a function of impact energy for the flax/epoxy (A), basalt/epoxy (B) and the hybrid (C) composite laminates.

Flax laminates showed an onset of penetration at 2.5J, a much lower value than that shown by both basalt (40J) and hybrid laminates (17.5J). In addition, much lower values of peak force are reported for the flax/epoxy composites. In general, the peak force represents an indicative value of the impact resistance of a material. This parameter indicates the maximum load that the material can bear for a given value of impact energy, before suffering important damage phenomena [Padaki *et al.*, 2008]. However, it is important to stress that this parameter is strongly influenced by several factors such as the thickness of the laminate, the geometry and the mass of the impactor used. In Section II.1.3, the microstructural characteristics of the different laminates have been reported. It has been highlighted that the tested composites are characterized by strongly different fibre volume fraction and thickness values. Specifically, the flax/epoxy laminate presents the lowest fibre volume fraction (0.26) and thickness (2.2 mm). It is therefore clear that these differences must be taken into account during the analysis of the impact behaviour of the different laminates. In Table III.7 are

summarized some key impact parameters such as absorbed energy E_a, maximum displacement and the peak force found for the different configurations.

Table III. 7 Parameters obtained from impact tests on flax, basalt and hybrid composite specimens.

Specimen	**E_a [J]**	**Max. Displacement [mm]**	**Peak Force [N]**	**E_a/E_i**
Energy 1J				
Flax	0.64 ± 0.03	2.97 ± 0.2	427.9 ± 160	0.64 ± 0.03
Basalt	0.36	1.1	1844	0.36
Hybrid	0.37 ± 0.02	1.36 ± 0.007	1468 ± 70	0.37 ± 0.02
Energy 1.5J				
Flax	1.06 ± 0.03	3.91 ± 0.09	642.5 ± 3.4	0.71 ± 0.02
Basalt	0.66 ± 0.03	1.36 ± 0.01	2216± 81	0.44 ± 0.02
Hybrid	0.66 ± 0.07	1.66 ± 0.01	1868 ± 70.4	0.44 ± 0.05
Energy 2J				
Flax	1.57 ± 0.02	4.84 ± 0.01	640.6 ± 0.7	0.78 ± 0.01
Basalt	0.95 ± 0.03	1.56 ± 0.007	2429 ± 208	0.47 ± 0.01
Hybrid	1.01 ± 0.02	1.61 ± 0.42	1890 ± 53	0.51 ± 0.01
Energy 2.5J				
Flax	2.47 ± 0.09	8.08 ± 0.04	675.5 ± 22.3	0.99 ± 0.03
Energy 5J				
Flax	2.68	9.55	630.1	1
Basalt	2.58 ± 0.03	2.56 ± 0.02	3849 ± 60	0.51 ± 0.007
Hybrid	3.24 ± 0.21	3.17 ± 0.03	2915 ± 75	0.64 ± 0.04
Energy 10J				
Flax	2.95	8.25	659.3	1
Basalt	5.53 ± 0.01	3.54 ± 0.05	5573± 23	0.55 ± 0.001
Hybrid	8.38 ± 0.04	5.05 ± 0.1	3219 ± 44	0.83 ± 0.004
Energy 15J				
Basalt	11.87 ± 0.09	4.38 ± 0.02	6457 ± 0.3	0.79 ± 0.006
Hybrid	13.86 ± 0.26	7.32 ± 0.35	3053 ± 70	0.92 ± 0.01
Energy 16.5J				
Hybrid	15.79 ± 0.08	8.41 ± 0.27	3382 ± 0.7	0.95 ± 0.005
Energy 17.5J				
Hybrid	17.83 ± 0.28	17.25 ± 10.41	3265 ± 250	1
Energy 20J				
Basalt	17.53 ± 0.22	5.43 ± 0.11	7262 ± 0.8	0.87 ± 0.01
Hybrid	20.21	13.92	4068	1
Energy 30J				
Basalt	28.1 ± 0.09	8.18 ± 0.08	6900 ± 342	0.93 ± 0.003
Energy 33J				
Basalt	31.86 ± 0.03	9.11 ± 0.02	7181 ± 60	0.96 ± 0.007
Energy 35J				
Basalt	34.22 ± 0.23	9.54 ± 0.31	7090 ± 513	0.97 ± 0.006
Energy 40J				
Basalt	40.38	17.64	6988.4	1

In order to evaluate the impact resistance of the different laminates, the damage degree was measured. This parameter is a measurement of the structural integrity deterioration of the

composite laminate and can be defined as the ratio between the E_a absorbed energy and the given impact energy E_i values [Suresh Kumar *et al.*, 2015]. At penetration, the laminate absorbs the maximum value of energy and the degree of damage is unity. From the values reported in Table III.7, it is clear that the flax laminates exhibited a better energy absorption capability and lower peak reaction force values compared to the other laminates. The superior capability to absorb energy during the impact phenomenon of flax laminates can be related to the high damping properties of flax and to the development of significant damage inside the laminate. In recent years, the combination of the damping properties of flax fibres with the high performance of basalt fibres has been extensively investigated [Petrucci *et al.*, 2015; Boria *et al.*, 2016; Zivkovic *et al.*, 2017; Papa *et al.*, 2018]. Several studies highlighted the advantages of the basalt/flax fibre hybridization, increasing the impact performance of flax fibre composites without a significant weight penalty. The results found in the present study confirm the positive effect produced by the combination of flax and basalt fibres. From Table III.7, it is possible to infer that the hybridisation was successful in enhancing the impact peak reaction load values compared to the flax configuration. In addition, hybridisation allowed to obtain an increase in the absorbed energy values compared to the basalt laminates. This behaviour is strongly related to the damping effect of flax fibres. In fact, damage mechanisms such as fibrillation, pull-out and debonding can lead to a decrease in the reaction force and an increase in the impact energy dissipation. From Figure III.12-C, it is possible to point out that the hybrid laminates showed a larger displacement at the load peak than the basalt composites. As reported by Papa et al. [Papa *et al.*, 2018], this behaviour is related to the capability of the flax reinforced composites to absorb the impact energy through not elastic mode and deflect the impact progression. To get a better insight into the different impact behaviours of laminates, an X-ray microtomography analysis of the flax, basalt and hybrid composites was carried out with a resolution of 14 μm. In order to assess the damage modes of the laminates at the same impact energy, the micro-CT observations were performed on laminates impacted at 2J energy. The x-slices for the different composites are presented in Figures III.13-A,B,C. It is well reported in literature that the low-velocity impact can lead to four significant damage events: the contact damage, delamination, matrix failure and fibre failure [Safri *et al.*, 2018]. From Figure III.13-A, it is possible to observe that the flax laminate exhibits all these damages. In particular, a very large matrix crack can be detected from the CT scan. A typical pine tree damage pattern can be observed from CT-scan, that increases from the impacted surface toward the non-impact side. In particular,

severe transverse matrix cracks can be detected that coalesced due to the presence of a significant level of porosity. On the contrary, no damage development is noticed for the basalt and the hybrid laminates at a low impact energy of 2J. These results are consistent with the force-displacement curves found for the different composites reported in Figure III.13. In the case of flax laminates, most of the energy is absorbed through non elastic mode. The load-deflection curve is characterized by a limited elastic recovery and a large plateau around the maximum load is observed, which suggests the development of a significant internal damage.

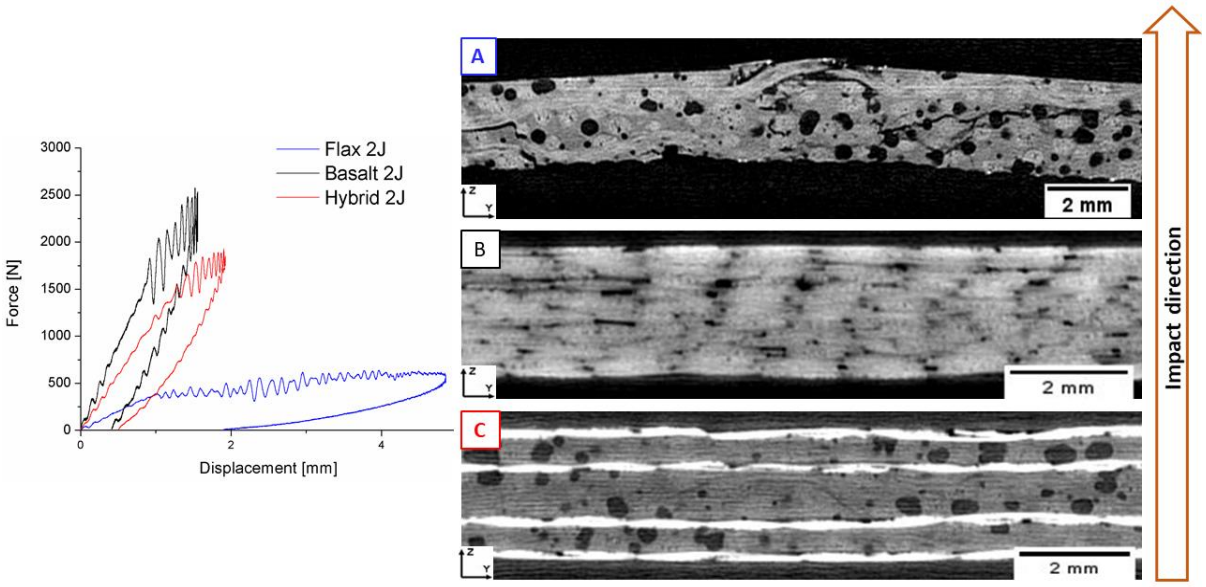

Figure III. 13 The force-displacement curves for the different composite laminates impacted at the energy of 2J. A post-mortem micro-CT analysis was performed on: flax/epoxy (A), basalt/epoxy (B) and basalt-flax hybrid (C) composites.

A superior impact behaviour is exhibited by both basalt and hybrid laminates. The superior elastic recovery and the absence of a plateau indicate that for these composites the impact energy of 2J is too low to promote the development of visible damages. In fact, it is important to stress that the 2J impact energy corresponds to the 80% of the penetration energy of flax laminates, but only the 11.4% and the 5.7% of the penetration energy for the hybrid and the basalt composites, respectively. From the comparison of the damage degree values obtained after the impact test at 2J (Table III.7), it is possible to point out that both basalt and hybrid laminates show the same value of 0.44, confirming the similar impact behaviour at this level of impact energy. A higher value of damage degree was obtained for flax laminates, specifically of 0.71, confirming once again the severe deterioration of structural integrity.

However, it is very important to stress that the microtomography observations also confirmed the presence of a large amount of porosity, especially in the flax and hybrid composites. From Figure III.13 it is possible to observe how the voids provide weak areas allowing cracks to propagate between them and weaken the flax composite laminate. The comparison of the different micro-CT scans highlights that the amount of porosity is concentrated into the flax layers. The voids content is one of the main problems affecting the natural and cellulose fibre composites [Meredith *et al.*, 2013; Phillips *et al.*, 2013; Li *et al.*, 2015]. The compaction behaviour of flax fabric as well as its difficult impregnation by the resin plays a key role in the formation of voids, affecting the resin pressure, which is an important parameter in diffusion controlled void growth due to moisture and air entrapment. Another aspect of great importance is the hydrophilic behaviour and the consequent high moisture content of flax fibres. It is well known that the water content of flax can be a critical variable in the formation of voids during the curing process of the composite material. In fact, the water molecules can be the source of gases which may be generated in the thermal process producing voids inside the laminate. It is therefore clear how necessary is the reduction of the hydrophilic behaviour of flax fibres in order to decrease the voids content of the resulting composites and, at the same time, improve their adhesion with the more hydrophobic polymer matrices.

III.2.2.2 Visual inspection of specimens for impact damages

In order to get more information on the effect of the impact on the different laminates, the damage patterns of the flax, basalt and hybrid composites were analysed. In Figure III.14 are reported damages on both front and back surfaces of flax laminate at the impact energy of 2.5J. At this energy the flax laminate is completely penetrated. The composite exhibits an extended damage characterized by the typical cross-shaped matrix crack pattern. This type of fracture pattern has been largely reported for natural fibre laminates [Dhakal *et al.*, 2007; Wang *et al.*, 2016; Ravandi *et al.*, 2017; Papa *et al.*, 2018]. It is well described that for natural fibre reinforced laminates, the damage can propagate in both the longitudinal and transverse directions due to the low impact resistance of plant fibres. The impacted front surface (Figure III.12-A) of flax/epoxy composite shows the presence of both a circumferential and a radial fracture close to the impact point, whereas a cross-shaped crack is found on the back side (Figure III.14-B). In order to carry out a comparison between the impact resistance exhibited

by the basalt fibre and the hybrid composites, the surfaces of the laminates impacted at an energy of 15J were analysed (Figure III.15).

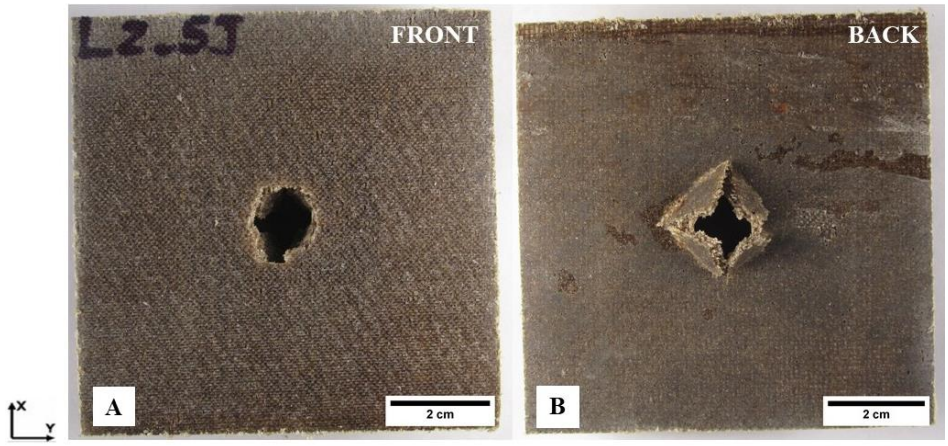

Figure III. 14 Fracture damage on front (A) and back (B) surface for the flax/epoxy laminate impacted at 2.5J.

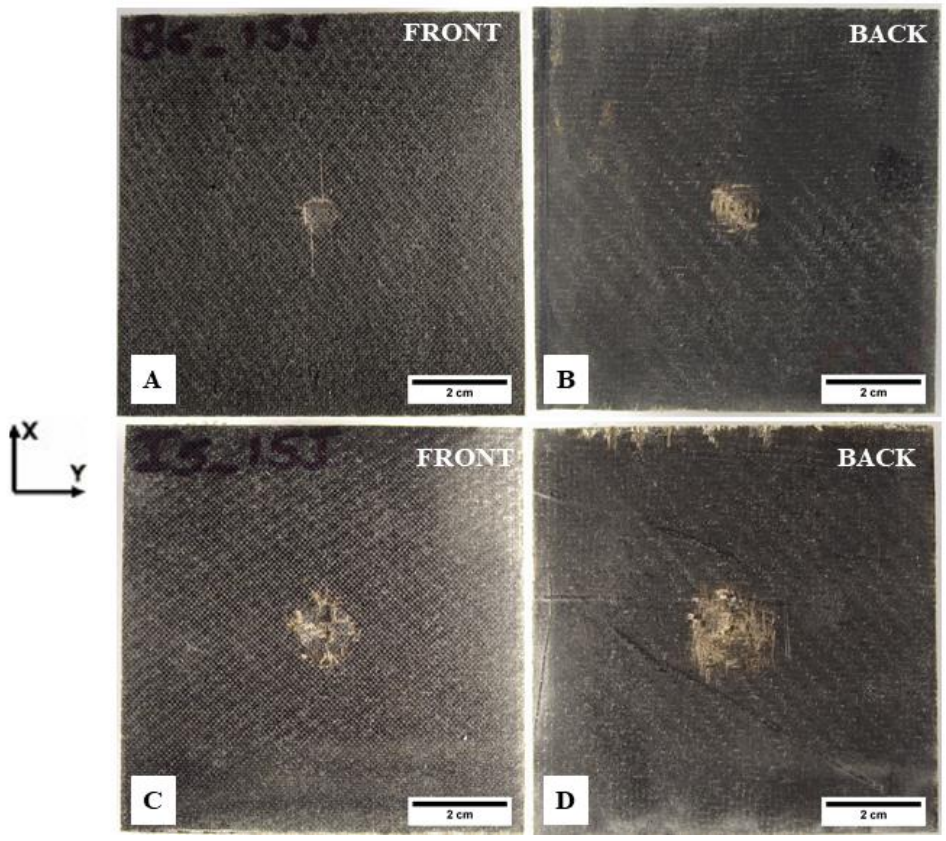

Figure III. 15 Damage on impacted and back surfaces at 15J for: basalt/epoxy (A-B) and hybrid (C-D) laminates.

From the values reported in Table III.7 it can be noted that the hybrid composite shows a high damage degree, close to the unit value, which indicates that the laminate is close to its

complete perforation. A much lower damage degree value is reported for the basalt composite. This result clearly indicates the presence of a greater damage inside the hybrid laminate compared to the composite reinforced with only basalt fibres. From the comparison of the different impacted surfaces, it can be pointed out that the hybrid composite exhibits a larger damage area (Figure III.15-C) than the more localized area of the basalt composite (Figure III.15-A). In particular, the latter displays a damage pattern characterized by the presence of a circular indentation due to the hemispherical head of the impactor used. From the back surface of the basalt/epoxy composite (Figure III.15-B) it is possible to notice that the damage is essentially due to a breakage of the matrix and the fibres. Differently, a combination of matrix failure, fibre breakage and delamination can be detected from the back surface of the hybrid laminate (Figure III.15-D). To get a better insight into the fracture patterns of the basalt and the hybrid composites, an analysis of both front and back surfaces was performed after penetration (Figures III.16,17).

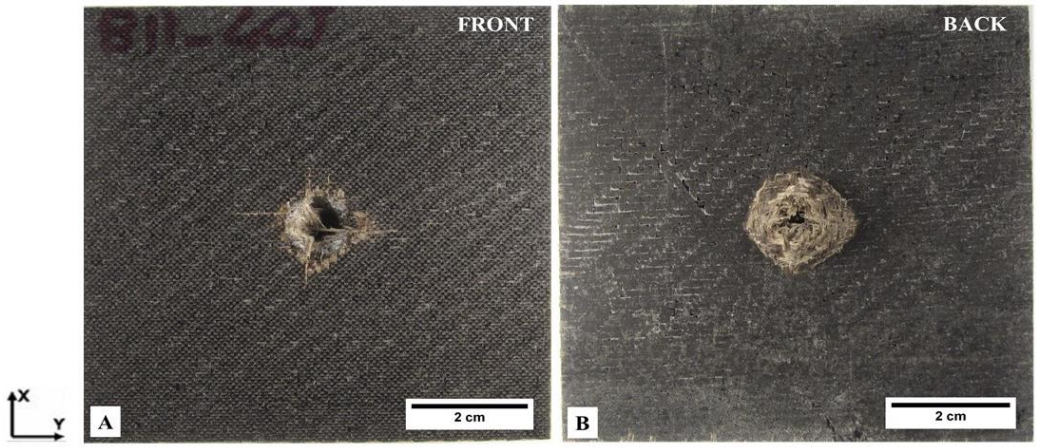

Figure III. 16 Fracture damage on impacted (A) and back (B) surface for the basalt/epoxy laminate impacted at 40J.

A similar fracture pattern can be observed for the basalt and the hybrid composites. A concentrated damage around the impact point is clear on the front surface of both the basalt and the hybrid composites, Figure III.16-A and Figure III.17-A, respectively. From the observation of the back side, a diamond shape damage was found for both laminates (Figure III.16-B and Figure III.17-B). This similarity in fracture pattern of the two composite materials can be related to the ply interface configurations of the two laminates. Specifically, the use of outer basalt layers in the hybrid type composites can allow to obtain a better

mechanical stability in dynamic loads, thanks to the greater stiffness of the basalt layer with respect to that of flax.

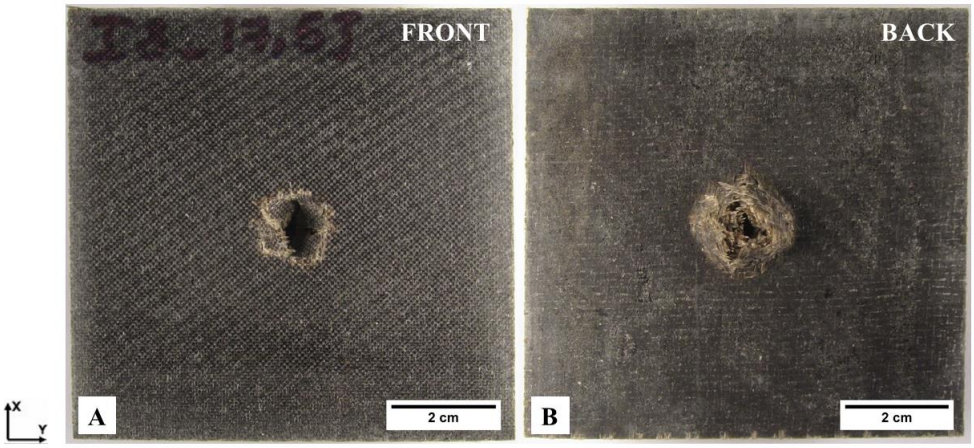

Figure III. 17 Fracture damage on impacted (A) and back (B) surface for the hybrid laminate impacted at 17.5J.

Conclusion of Part III

Part III was devoted to the analysis of the mechanical properties of basalt-flax/epoxy hybrid composite materials. The hybrids properties were compared with those obtained for basalt/epoxy and flax/epoxy composites. In a first phase, an analysis of the quasi-static mechanical behaviour of the different composites was carried out performing tensile tests and four-point bending tests. The results showed that the hybrid composites were characterized by intermediate mechanical properties between those exhibited by flax and basalt composites. The combination of basalt with flax fibres allowed to obtain a composite material characterized by greater tensile and flexural strengths than flax composites. A similar result was obtained after dynamic tests. Specifically, in order to carry out a dynamic characterization of composites, tensile-tensile fatigue tests and low-velocity impact tests were performed. The results pointed out that the hybridization was able to produce a positive effect on the fatigue resistance of basalt laminates. A slower fatigue stiffness degradation and the ability to absorb and deflect cracks of flax fibres allowed obtaining a hybrid composite with a better fatigue resistance compared to basalt laminates. The better ability of flax to absorb energy than basalt fibres was also confirmed by low-velocity impact tests. In particular, hybridization allows to improve the amount of absorbed energy during the impact phenomenon compared to that shown by basalt composites. On the other hand, because of their superior stiffness, basalt fibres allowed to enhance the impact resistance of flax laminates. The mechanical characterization of the different composite laminates highlighted the effective interest in combining the basalt fibres with flax fibres in order to produce a composite material characterized not only by limited cost and environmental impact but also by good mechanical performance. The positive results obtained in this work can encourage the possible application of flax-basalt hybrid composites in different sectors, such as: the automotive (for both interior and exterior parts), the aerospace (interior parts), the sport and leisure sectors.

However, a crucial issue raised in this first phase of study, is the need to improve the compatibility between the natural fibres and the epoxy matrix. It was observed that the compatibility between natural fibres and polymer matrices plays a key-role in the mechanical

performances of the resulting hybrid composites. The morphological analysis of the fracture surfaces after fatigue cycles showed a poor adhesion quality of both flax and basalt fibres with the epoxy matrix. In addition, the presence of a high porosity content inside the composite laminates was demonstrated by both FE-SEM observations on the fatigue fracture surfaces and by a X-Ray microtomographic analysis on low-velocity impacted samples. In particular, the micro-CT analysis showed that voids are present essentially in the flax layers. This result can be related to the high hydrophilic behaviour and the high moisture content of flax fibres along with the limited wettability of natural fabrics with traditional matrices optimized for synthetic reinforcements. These results aroused the need to modify the surface properties of natural fibres in order to improve their adhesion with polymer matrices and, therefore increase the mechanical performance of the resulting composite materials. In this framework, in the next Part IV and Part V, different surface modification treatments will be specifically designed and investigated for flax and basalt fibres with the aim of increasing their adhesion to two different thermoset matrices, namely epoxy and vinylester. Flax and basalt fibres were treated by the physical process of Plasma Enhanced Chemical Vapour Deposition (PECVD), while flax fibres were also subjected to two chemical treatments using enzymatic species and supercritical CO_2. An in-depth analysis of the effects of the different treatments on the wetting, morphological, compositional, and mechanical properties of flax yarns and basalt filaments will be described in Part IV. The adhesion quality of untreated and treated flax yarns and basalt fibres with both epoxy and vinylester matrices will be discussed in Part V.

Conclusion de la Partie III

(en français)

La partie III a été consacrée à l'analyse des propriétés mécaniques des matériaux composites hybrides basalte-lin/époxy. Les propriétés des hybrides ont été comparées à celles obtenues pour les composites basalte/époxy et lin/époxy. Tout d'abord, une analyse du comportement mécanique quasi-statique des différents composites a été réalisée en effectuant des essais de traction et des essais de flexion quatre points. Les résultats ont montré que les composites hybrides étaient caractérisés par des propriétés mécaniques intermédiaires entre celles des composites de lin et de basalte. La combinaison du basalte avec des fibres de lin a permis d'obtenir un matériau composite avec des résistances en traction et en flexion supérieures à celles des composites de lin. Un résultat similaire a été obtenu après des tests dynamiques. Notamment, afin de réaliser une caractérisation dynamique des composites, des tests de fatigue traction-traction et des tests d'impact à basse vitesse ont été réalisés. Les résultats ont montré que l'hybridation a pu produire un effet positif sur la résistance à la fatigue des stratifiés de basalte. Les propriétés amortissantes des fibres de lin ont permis d'obtenir un composite hybride avec une meilleure résistance à la fatigue par rapport aux stratifiés de basalte. La meilleure capacité du lin à absorber l'énergie a également été confirmée par les tests d'impact à faible vitesse. L'hybridation permet d'améliorer la quantité d'énergie absorbée lors de l'impact par rapport à celle obtenue pour les composites de basalte. D'autre part, en raison de leur rigidité supérieure, les fibres de basalte ont permis d'améliorer la résistance aux chocs des stratifiés de lin. Une question cruciale, soulevée dans cette première phase d'étude, est la nécessité d'améliorer la compatibilité entre les fibres naturelles et la matrice époxy. Il a été observé que la compatibilité entre les fibres naturelles et les matrices polymères joue un rôle clé dans les performances mécaniques des composites hybrides résultants. L'analyse morphologique des faciès de rupture après les cycles de fatigue a montré une mauvaise qualité d'adhérence des fibres de lin et de basalte avec la matrice époxy. De plus, la présence de porosités à l'intérieur des stratifiés composites a été mise en évidence à la fois par des observations FE-SEM sur les faciès de rupture en fatigue et par une analyse microtomographique sur des échantillons impactés. En particulier, l'analyse micro-CT a montré que des micro-vides sont présents essentiellement dans les couches de lin. Ce résultat peut être lié au comportement hydrophile prononcé, à la teneur élevée d'humidité dans les fibres de lin et à la mouillabilité limitée des tissus de lin avec une matrice traditionnelle optimisée pour les renforts synthétiques. Ces résultats montrent la nécessité de modifier les propriétés de surface des fibres naturelles afin d'améliorer leur adhérence aux matrices polymères et donc d'augmenter les performances mécaniques des matériaux composites. Dans les parties IV et V, différents traitements de modification de surface seront spécifiquement conçus et étudiés pour les fibres de lin et de basalte dans le but d'augmenter leur adhérence à deux matrices thermodures différentes, à savoir l'époxy et la vinylester. Les fibres de lin et de basalte ont été traitées par le processus physique de dépôt chimique en phase vapeur assisté par plasma (PECVD), tandis que les fibres de lin ont également été soumises à deux traitements

chimiques utilisant des espèces enzymatiques et du CO_2 supercritique. Une analyse approfondie des effets des différents traitements sur les propriétés mouillantes, morphologiques, compositionnelles et mécaniques des fils de lin et des fibres de basalte sera décrite dans la partie IV. La qualité d'adhérence des fils de lin et des fibres de basalte non traités et traités avec les matrices époxy et vinylester sera discutée dans la partie V.

PART IV

SURFACE MODIFICATION TREATMENTS AND THEIR EFFECTS ON FLAX AND BASALT FILAMENTS

The focus of Part IV is on describing the different surface modification treatments and providing a detailed analysis of their effects on the properties of flax and basalt filaments. The chemical and physical treatments performed on flax yarns will be described in Chapter IV.1. In particular, the section IV.1.3 will be focused on the investigation of the effects of enzymatic and supercritical CO_2 treatments on the wetting, morphological, compositional, and mechanical properties of flax yarns. The changes produced by the physical treatments of oxygen and a tetravinylsilane plasma deposition on flax yarns will be discussed in section IV.1.4. Finally, the Chapter IV.2 will address the effects of a thermal de-sizing treatment and a tetravinylsilane plasma deposition process on the properties of basalt fibres.

PART IV – SURFACE MODIFICATION TREATMENTS AND THEIR EFFECTS ON FILAMENTS

CHAPTER IV.1

SURFACE MODIFICATION TREATMENTS OF FLAX

In order to enhance the interfacial adhesion of flax with thermosetting resins, chemical and physical treatments were performed in this study. In the next sections, all the experimental procedures used to carry out the different treatments and an in-depth description of their effects on the wetting, compositional, morphological and mechanical properties of flax yarns will be reported.

IV.1.1 The chemical treatments

Among the chemical modification treatments widely reported in section I.3.1, an enzymatic biochemical treatment and a supercritical CO_2 treatment were selected in this experimental work. The effect, common to both treatments, is to perform and to catalyse the removal of undesirable substances such as pectin, hemicelluloses, lignin, fat, and waxes from the surface of flax fibres. Most of these components contribute to the surface polarity of flax, promoting a hydrophilic behaviour and thus a bad fibre/matrix interface with hydrophobic polymers. The enzymatic and the supercritical CO_2 treatments were selected due to their lower environmental impact than the traditional chemical treatments. The enzymatic process is characterized by a high selectivity, specificity and no chemicals are involved during the fibre modification treatment. In addition, the supercritical carbon dioxide is inexpensive, essentially nontoxic and can be easily recovered and recycled.

IV.1.1.1 Biochemical enzymatic treatment

The enzymatic treatments were performed at the laboratories of the “Department of Chemical Engineering Materials Environment”, (Sapienza University of Rome). In order to remove their pectin and hemicellulose content, flax fabrics and yarns were treated using

different commercial enzyme preparations of relatively low cost. A Feedlyve AXC 1500L and a Peclyve EXG commercial enzyme solutions, supplied by Lyven SA (Colombelles, France), were selected. The Feedlyve AXC 1500L preparation, rich in endo 1,4-β xylanase enzyme, is able to remove the hemicellulose content from flax, whereas the Peclyve EXG solution, rich in pectinases and xyloglucanases enzymes, can remove both pectin and hemicellulose. The biochemical treatment was performed on both flax fabric and flax yarns. Flax fabrics, with the dimension of 3×3 mm^2, and flax yarns, with a length of 80 mm, were treated in small borosilicate lab jars, placed into a thermostatic and a magnetically stirred water bath at the temperature of 50°C, (Figure IV.1).

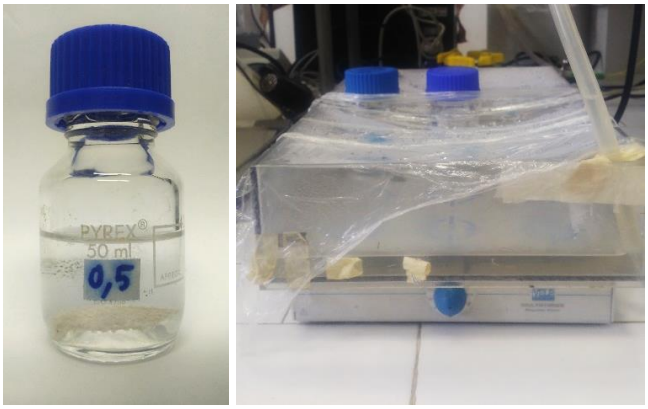

Figure IV. 1 An example of flax fabric inside the lab jar and the thermostated water bath system used during the treatment.

Different concentrations and times were selected, (Table IV.1). The optimum enzyme-specific pH values were used. A pH of 5.5 was used for the Feedlyve solution and a pH of 5 was used for the Peclyve one. Afterwards, drying was performed at 80°C for 24 hours.

Table IV. 1 Concentrations of the enzyme preparations and process parameters used.

Enzyme solution	**Biological source**	**Main enzymes components**	**Concentration [wt%]**	**Time [h]**	**T [°C]**	**pH**
Feedlyve AXC 1500 L	Trichoderma Longibrachiatum	Endo 1,4-β xylanase	2.5 - 5	2 – 3 – 6	50	5.5
Peclyve EXG	Trichoderma Longibrachiatum	Pectinases Xyloglucanases	2.5 – 5 – 7.5 -10	2 – 3 – 4.5 – 6	50	5

IV.1.1.2 Supercritical CO_2 treatment

The supercritical CO_2 (SC-CO_2) process was performed in collaboration with the "Institute Franche-Comté Electronics Mechanics Thermal Science and Optics – Sciences and Technologies (FEMTO-ST)" and the "Institute de Chimie Moléculaire", Bourgogne University. Flax yarns were treated using an equipment supplied by Separex (Figure IV.2-A). The flax yarns were first placed in a temperature and pressure-controlled enclosure. A schematic representation of the equipment setup used is reported in Figure IV.2-B. Gaseous carbon dioxide (1) was extracted from a bottle by a valve (2) at the beginning of the process. It was then cooled to a liquid state (3) and directed towards a pump (4), which controlled the pressure. When it reached the pressure needed for the supercritical state (up to the critical point of 73.8 bar), the carbon dioxide was heated by a heat exchanger (5). At the supercritical state, the CO_2 was directed towards the autoclave (6), which contained the flax yarn samples (7). Thermocouples were used to control the temperature (8). The treatment of flax in autoclave was carried out under high temperature and pressure conditions (130°C – 150 bar) for a duration of 170 min. When the treatment was finished, the carbon dioxide was recovered (9), cooled, and directed towards a recycling line. The amount of CO_2 injected in the reactor was measured and controlled using a balance. After the process, the reactor was depressurized from 150 bar to 0 bar to allow its opening and the samples were stored at room temperature for cooling.

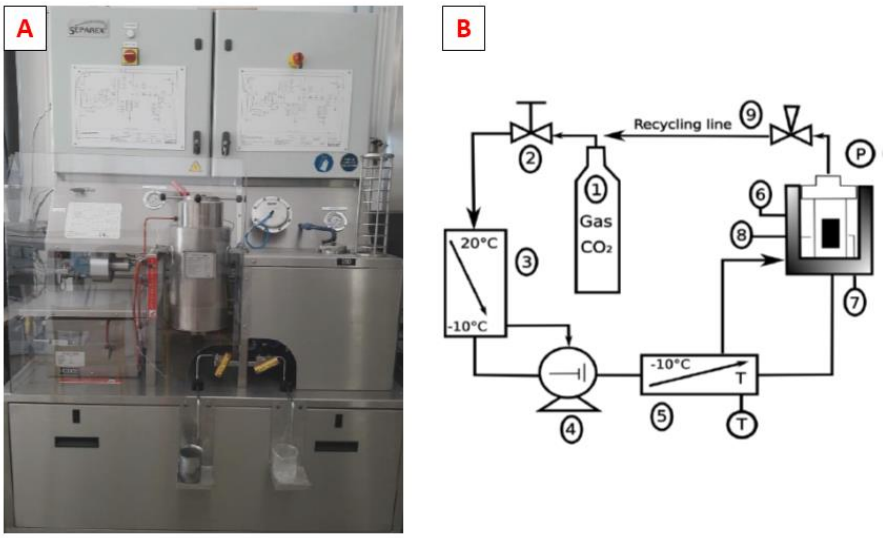

Figure IV. 2 Supercritical CO_2 equipment from Separex (A) and the schematic diagram of the supercritical equipment (B).

IV.1.2 The physical treatments

Physical treatments were also used to modify the flax fibre surfaces. Contrary to the chemical treatments, physical treatments modify the structural and the surface properties of fibres without producing a substantial change of their chemical composition.

In this work, the plasma technology was chosen to modify the surface properties of flax. In particular, the effects of two different plasma treatments were investigated: an oxygen plasma, able to increase the surface roughness and improve the fibre/matrix wetting; and a plasma polymerization treatment, which consists in the deposition of a polymer film onto the fibre surface. Both plasma treatments were performed in collaboration with the "Brno University of Technology", Czech Republic.

IV.1.2.1 Oxygen plasma treatment

The oxygen plasma treatment was carried out in a reactor consisting of a glass tube 100 cm long and with an inner diameter of 40 mm, (Figure IV.3). At first, flax yarns 1 m long were housed inside the reactor. Subsequentially, the plasma system was evacuated to a basic pressure of about 10^{-4} Pa. Argon gas (99.999%) was used to clean the plasma reactor and vacuum chambers. The oxygen plasma treatment was performed using different plasma power conditions: 2, 10, 20, 50 and 100 W. The surfaces of flax yarns were exposed to a continuous oxygen plasma ablation for 30 min at a pressure of 5.8 Pa. After the plasma treatment, the plasma apparatus was flushed with argon gas for 60 min and evacuated to a basic pressure of about 10^{-4} Pa. After approximately 12h the chamber was flooded with air to atmospheric pressure and the prepared specimen conveyed from the chamber.

Figure IV. 3 The PECVD reactor used.

IV.1.2.2 Plasma-Enhanced Chemical Vapour Deposition

The plasma polymerization treatment was performed in the same reactor used for the oxygen plasma treatment. The polymer deposition treatment was divided in two steps. At first, a non-polymerising oxygen gas plasma pre-treatment was performed in order to clean the surface of flax fibres, removing contaminants, and to improve the polymer film adhesion. Subsequently, a second step of polymerising gas plasma was realized. During this step, a tetravinylsilane monomer $Si(–CH=CH_2)_4$ (purity 97%, Sigma Aldrich) was fragmented and ionized in plasma producing excited species, free radicals and ions which were recombined forming a thin plasma polymer tetravinylsilane (pp-TVS) film onto the yarns surface. The plasma polymer deposition process was employed for a duration of 15 min. In order to assess the effect of the oxygen pre-treatment step on the deposition quality, oxygen plasma was excited using two different power conditions, 2 W and 100 W, at 5.8 Pa for 30 min. In both cases, the subsequent plasma deposition step was carried out using a power of 10 W at 3.8 Pa. After the film deposition, the plasma apparatus was flushed with argon gas for 60 min and finally evacuated to a basic pressure of about 10^{-4} Pa. The chamber was flooded with air to atmospheric pressure after 12h and the prepared specimen taken from the chamber.

IV.1.3 The influence of chemical treatments on flax properties

IV.1.3.1 Effects on wetting properties

In an initial phase of the study, the enzymatic biochemical treatments were carried out only on flax fabrics. For both Feedlyve and Peclyve enzymatic solutions, the fabrics were treated using a concentration of 0.5, 2.5 and 5 wt% and a duration of 2, 3 and 6 h. The aim of the first phase of the experimental investigation was to verify the actual effect of the two enzymatic preparations on the surface properties of flax and thus to select the solution able to produce the best results. In this framework, a study of the wetting properties of the untreated and treated flax fabrics was performed by a water drop test. As reported in section II.2.3, degassed water drops with a volume of 4 µl were applied to the different flax fabrics and the time until the applied drop is absorbed completely was measured. This measurement was repeated twice for each sample. Because of the large data dispersion, mainly due to the fabric irregularities, only representative values of absorption times are reported in Table IV.2. Due the presence of hydroxyl and strongly polar groups, the untreated flax fabrics

showed a marked hydrophilic behaviour. Water retention times lower than 1 s were found for the as-received flax. From the results reported in Table IV.2, it is possible to notice that flax fabrics show a wetting behaviour strongly dependent on the type of enzymatic preparation used.

Table IV. 2 Water absorption time values obtained for the untreated and enzymatically treated flax fabric surface.

Flax fabric	Absorption time t [s]	Absorption time t after 2h [s]	Absorption time t after 3h [s]	Absorption time t after 6h [s]
Neat	t < 1	-	-	-
Peclyve EXG 0.5 wt%	-	1	1.2	5.5
Peclyve EXG 2.5 wt%	-	1.4	2.2	1.5
Peclyve EXG 5 wt%	-	1.5	35	50
Feedlyve AXC 1500 L 0.5 wt%	-	t < 2	t < 1	1
Feedlyve AXC 1500 L 2.5 wt%	-	t < 2	1	t < 1
Feedlyve AXC 1500 L 5 wt%	-	1	t < 1	t < 1

A certain increase in the hydrophobic behaviour is produced after the Peclyve solution. On the contrary, the flax fabrics treated using the Feedlyve preparation maintain their strong hydrophilic behaviour. In figure IV.4 are compared the sequences of the water drop tests carried out for fabrics treated using the Feedlyve and Peclyve enzymatic solutions at 5 wt% and for a duration of 6 h. A maximum value of water retention time of 50 s was obtained after the treatment performed using the Peclyve solution. On the contrary, the flax fabric treated by the Feedlyve solution showed a water retention time lower than 1 s. According to George et al. [George *et al.*, 2014], the increase in hydrophobic behaviour may be explained as a consequence of the removal of pectin and hemicellulose fractions on the fibres surface produced by both pectinases and xyloglucanases enzymes. The better results obtained by the Peclyve solution can be linked to the synergic action of pectinases and xyloglucanases enzymes. In contrast, the only endo 1,4-β xylanase enzyme present in the Feedlyve preparation was not able to induce substantial modifications of the flax properties. The removal of pectin and hemicellulose components results in a decrease in the surface polarity of flax fibres, reducing the presence of hydroxyl groups distributed on their surface. Based

on these results, the Peclyve preparation was chosen as enzymatic solution able to successfully modify the surface properties of flax fibres. The subsequent enzymatic treatments were performed on flax yarns using this solution. In order to analyse in detail the action of the Peclyve solution, the subsequent enzymatic treatments were performed using solution concentrations of 2.5 – 5 – 7.5 – 10 wt% and treatment times of 4.5 and 6 h.

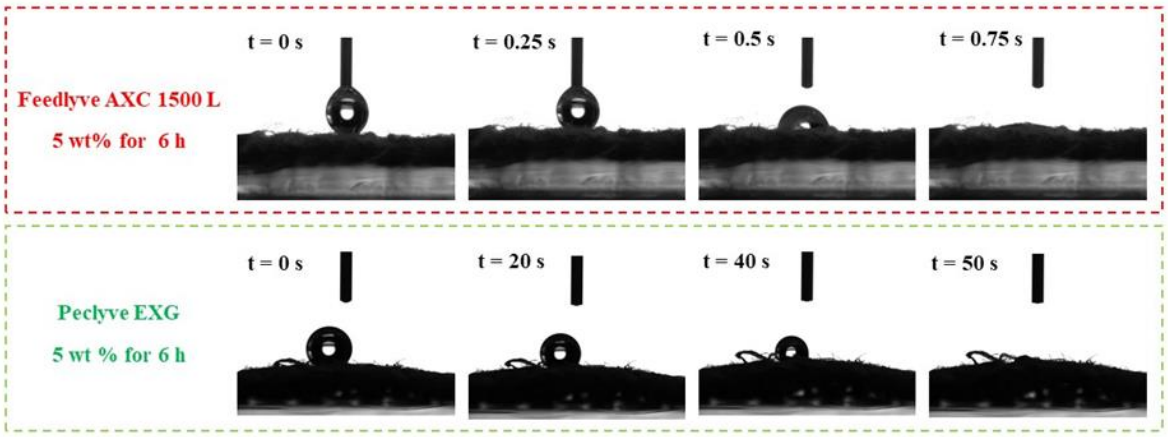

Figure IV. 4 The different sequences of the water drop test performed onto the flax fabrics treated using the Feedlyve and Peclyve enzymatic solutions at 5 wt% and for a duration of 6 h.

The water drop test was useful in order to obtain a qualitative analysis of the wetting behaviour of the different flax fabrics but, because the large data dispersion, it has proved to be inadequate to identify a precise relationship between process times and enzyme concentrations to be used.

IV.1.3.2 Effects on morphological and compositional characteristics

The changes in the surface morphology of flax yarns produced by the Peclyve solution were investigated in comparison with the untreated flax yarns. In Figure IV.5 are reported the FE-SEM micrographs of the as-received flax yarns. A large amount of impurities, such as fat and waxes, are present on the yarn surface. These non-cellulosic cementing materials can bind the flax bundles together, ensuring good mechanical properties for the yarn [Abdel-Halim *et al.*, 2010]. A comparison between the lateral surface of the as-received flax fibres and the flax fibres treated using the Peclyve solution at 5 wt% for 6h is reported in Figure IV.6. One of the main effects observed after the enzymatic treatment was the removal of a substantial part of the impurities present on the untreated fibres.

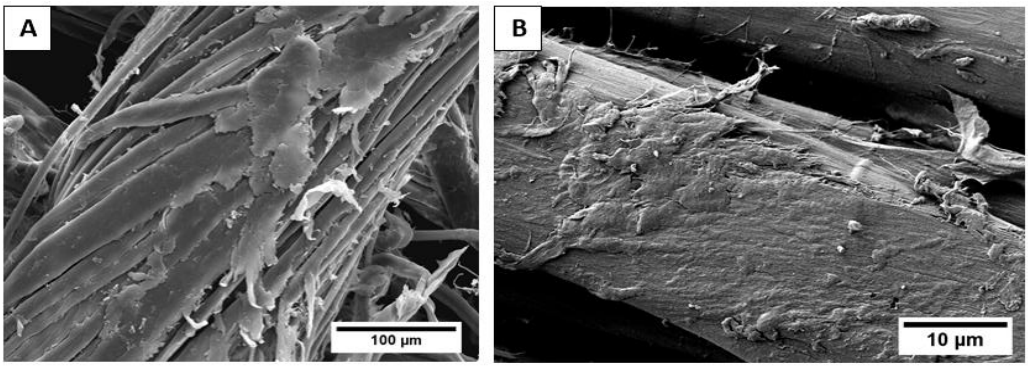

Figure IV. 5 SEM micrographs showing the untreated flax yarn (A) and a detail of the flax fibre surface (B).

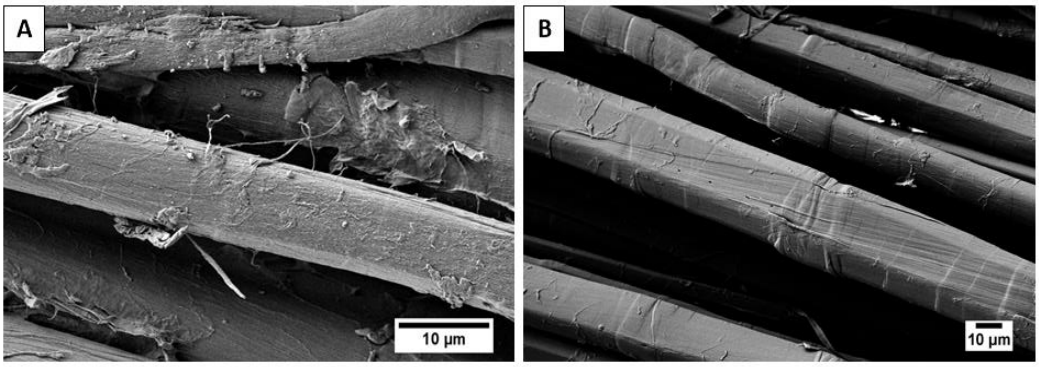

Figure IV. 6 Comparison between the lateral surface of the untreated flax fibres (A) and the flax fibres treated using the 5 wt% Peclyve enzymatic solution for 6h (B).

The FE-SEM micrographs reported in Figure IV.7 show the morphologies of the flax yarns after the different enzymatic treatments. Irrespective of treatment condition, flax yarn fibrillation was observed. It is important to highlight that, the greater the process time and the enzyme concentration, the higher the fibrillation of yarns. As reported by George et al. [George *et al.*, 2014], the pectinase is the enzyme which contributes the most to the separation of elementary fibres from their yarn. An enzymatic effect observed only at high solution concentration is the progressive breakage of the flax fibres present at the outer surface of the yarn. This effect was found for the yarns treated for 4.5h and 6h using a Peclyve concentration of 10 wt% (Figure IV.8). An investigation of the surface morphology of flax yarn after supercritical carbon dioxide treatment was carried out. Figure IV.9 shows the SEM micrographs for the treated flax yarn. Comparing the surface of the untreated flax yarn (Figure IV.5-A) and supercritical CO_2 treated flax yarn (Figure IV.9-A), it is possible to observe that the supercritical carbon dioxide treatment was able to remove impurities from the yarn surface.

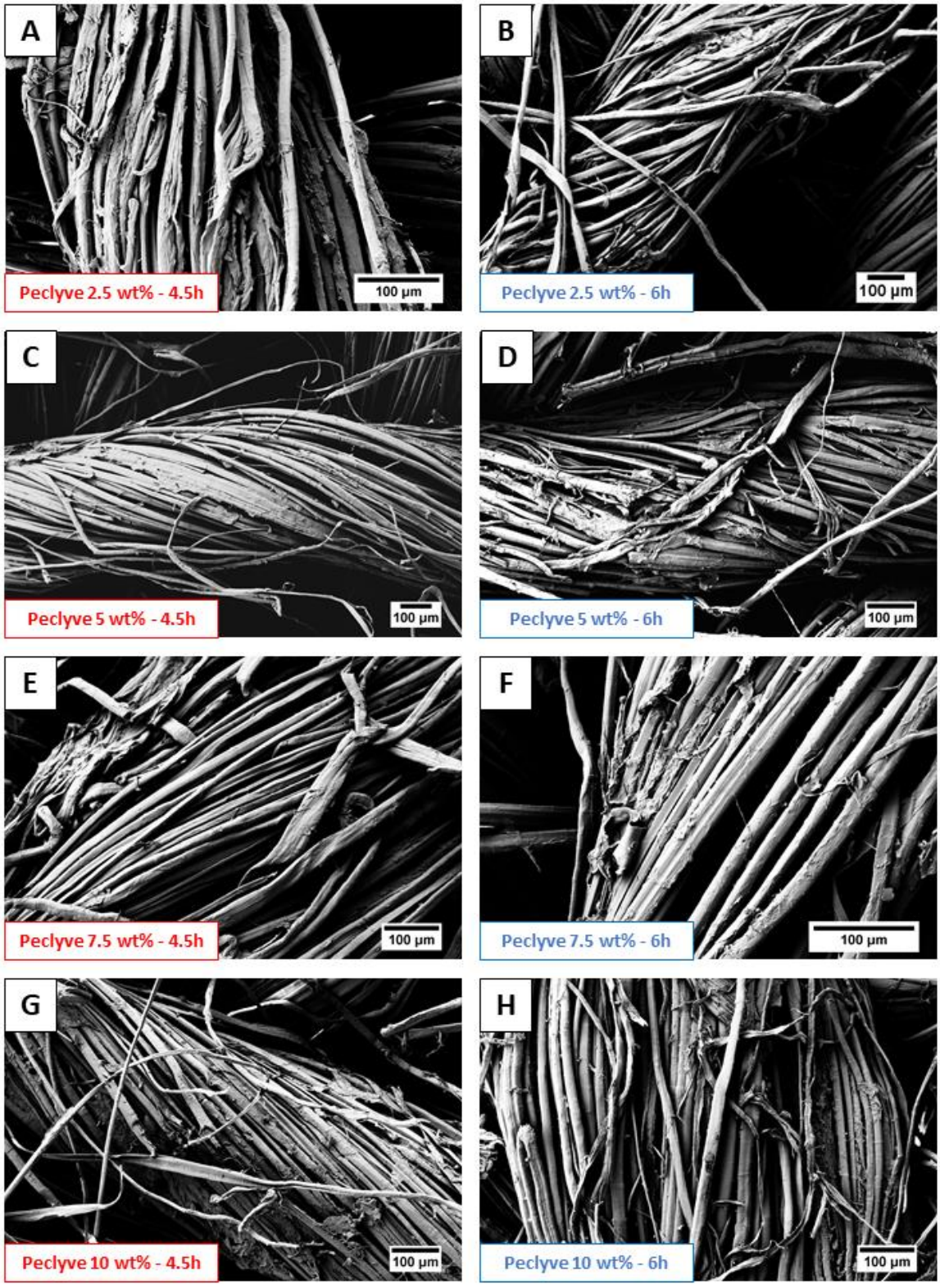

Figure IV. 7 SEM micrographs of the flax yarns as a function of the different enzymatic treatments.

The wax-like substances decreased after the supercritical CO_2 treatment, producing a relatively clean and smooth flax yarn surface. A phenomenon of surface peeling was visible

with higher magnifications, Figure IV.9-B. As reported by Zhang et al. [Zhang *et al.*, 2018] this peeling effect implies that some changes to the surface morphology of the flax fibres occurred in supercritical carbon dioxide. The micrographs indicate that non cellulosic constituents such as lignin, pectin and hemicellulose can be removed in supercritical carbon dioxide fluid.

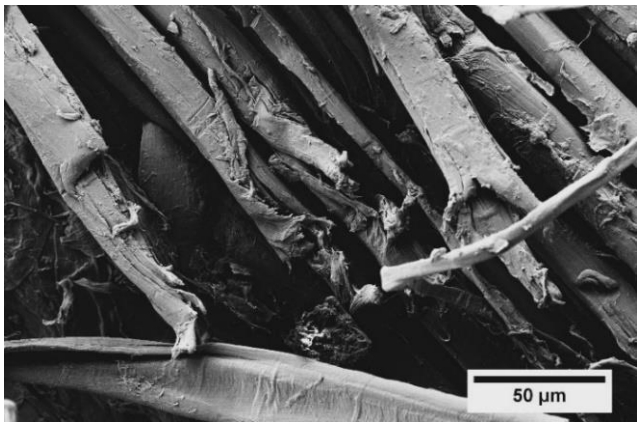

Figure IV. 8 SEM micrograph of the flax yarn treated with the 10 wt% Peclyve solution for a duration of 4.5 h. The micrograph shows the damage on the outer fibres of the flax yarn after the enzymatic treatment.

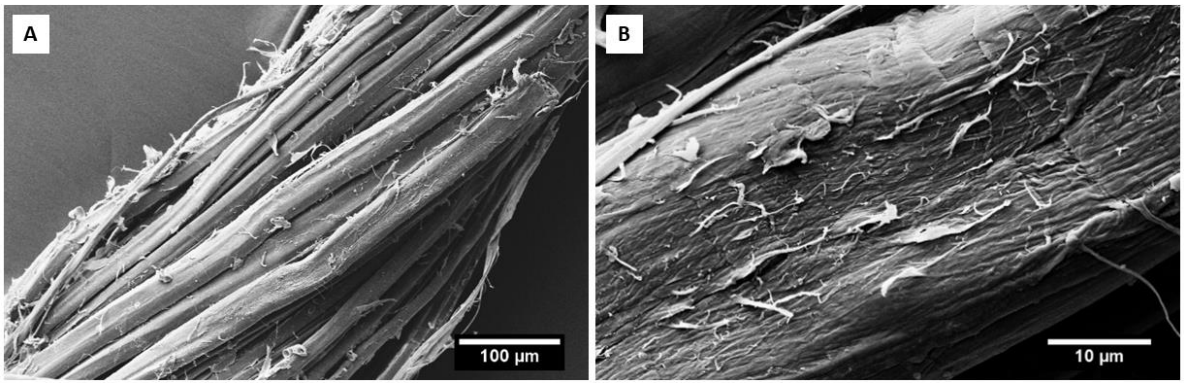

Figure IV. 9 SEM micrographs showing the supercritical CO_2 treated flax yarn (A) and a detail of the fibre surface (B).

The effect of the chemical treatments on the surface composition of flax fibres has been studied by Fourier-Transform Infrared (FTIR) analysis. A comparison between the FT-IR spectra of as-received, enzymatically and supercritical CO_2 treated flax yarns is shown in Figures IV.10-11-12, respectively. The spectral analysis revealed that the untreated flax fibre consists of alkene, esters, aromatics, ketone and alcohol belonging to cellulose, hemicellulose and lignin [Titok *et al.*, 2010; Bozaci *et al.*, 2013; Reddy *et al.*, 2015] (Table IV.3).

Table IV. 3 Assignment of the main ATR-FTIR bands of flax fibres.

Wavenumber (cm^{-1})	Band Assignments*
3700-3000	νOH
2990-2754	νCH of cellulose and hemicellulose
1742	νC=O of hemicellulose
1637	δHOH of water in crystalline cellulose
1597, 1514, 1450	νC=C and dCH in methyl, methylene and methoxyl groups of lignin
1427, 1368, 1314	δCH_2, δCH of cellulose and ωCH_2 in cellulose and hemicellulose
1278	τC-H_2 of cellulose
1248, 1160, 1104, 1029	νC-O-C and νC-C of polysaccharide components (mainly cellulose)
1053	νC-OH of cellulose and hemicellulose
897	β-glycosidic linkages between the sugars units in cellulose

* ν = stretching; δ = bending; d = deformation; ω = wagging; τ = twisting.

In order to assess the changes induced by the enzymatic treatment on the composition of flax fibre, the FTIR analysis was carried out on the samples treated using the minimum and maximum concentration of Peclyve solution. In particular, in Figure IV.10 are reported the infrared spectra of the enzymatically treated flax yarns using a 2.5 wt% Peclyve solution, whereas the infrared spectra obtained for flax yarns treated using a 10 wt% Peclyve solution are shown in Figure IV.11. The main effect produced by the enzymatic treatment is a strong reduction of the bands at 1742 cm^{-1} of hemicellulose and at 1596 cm^{-1}, 1512 cm^{-1} and 1451 cm^{-1} of the lignin. This reduction was observed for flax yarns treated with both 2.5 wt% and 10 wt% of Peclyve solution and confirms that the enzymatic treatment was able to successfully remove undesirable substances like hemicelluloses and lignin from the surface of the fibres. Comparing the infrared spectra obtained for the flax yarns enzymatically treated using a 2.5 wt% Peclyve solution for different duration (Figure IV.10-b, c, d), it is possible to notice that the longer the treatment time, the greater the removal efficiency of the enzymatic solution. The lowest hemicellulose and lignin peaks were obtained after a treatment duration of 6h (Figure IV.10-d). These results are confirmed by the values of crystallinity index (CI) of cellulose calculated for the different flax yarns.

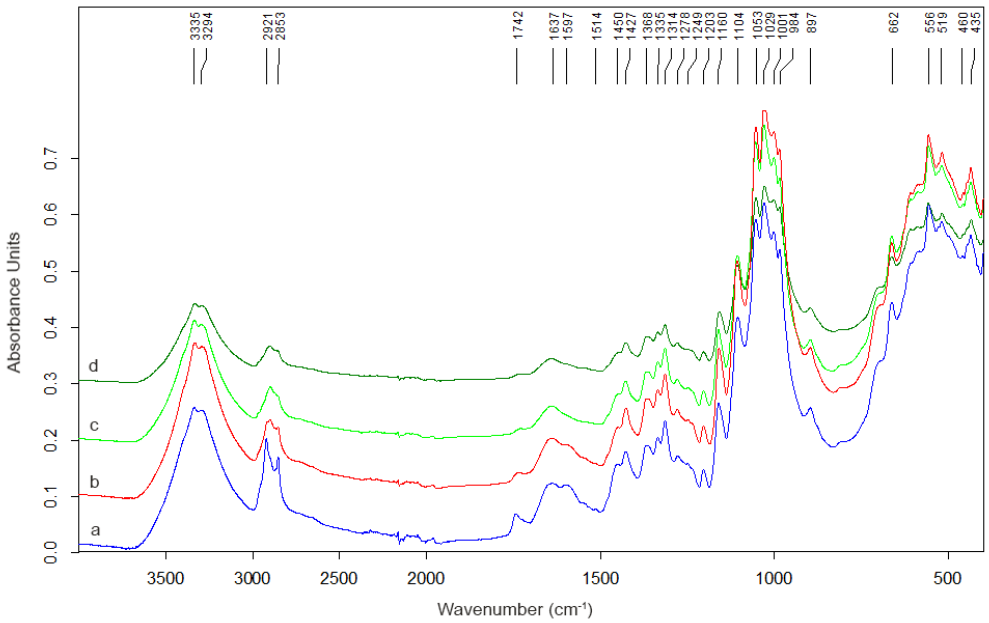

Figure IV. 10 Infrared spectra of as-received (a) and enzymatically treated flax yarns using a 2.5 wt% Peclyve solution for 3h (b), 4.5h (c) and 6h (d).

The CI is an important parameter which refers to the relative crystallinity of the fibre samples. The higher the value of CI, the greater the crystalline cellulose content and thus, the greater the efficiency of the enzymatic treatment in removing the amorphous components from flax [Abidi *et al.*, 2018; Zhang *et al.*, 2018]. The IR crystallinity index of cellulose was evaluated as the intensity ratio between the IR absorption bands at 1427 and 896 cm^{-1} (I_{1427}/I_{896}), which are assigned to CH_2 bending mode of cellulose, and of the CH in β-glycosidic linkages between monosaccharides (Table IV.4) [Abidi *et al.*, 2014].

Table IV. 4 The crystallinity index of cellulose for the untreated and enzymatically treated flax yarns using different times and concentrations of Peclyve solution.

Flax Yarn	Treatment Time	Cellulose Crystallinity index (CI)
Neat	-	1.01
Peclyve EXG 2.5 wt%	3 h	1
	4.5 h	1.15
	6 h	1.24
Peclyve EXG 10 wt%	3 h	1.36
	4.5 h	1.54
	6 h	1.54

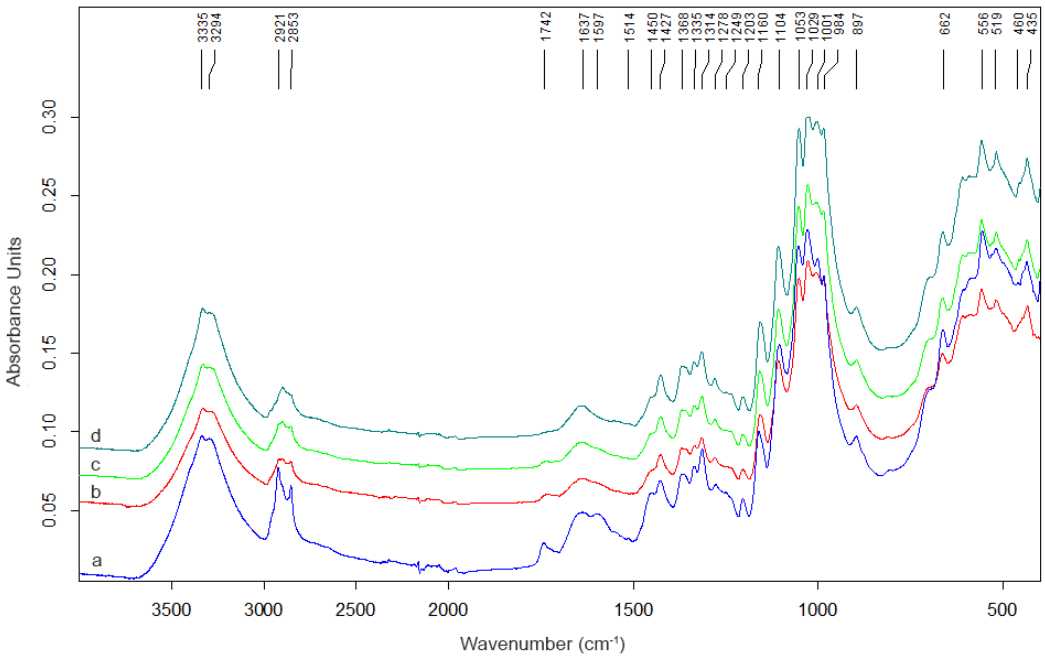

Figure IV. 11 Infrared spectra of as-received (a) and enzymatically treated flax yarns using a 10 wt% Peclyve solution for 3h (b), 4.5h (c) and 6h (d).

A progressive increase in the cellulose crystallinity index values was observed passing from 3h to 6h treatment. Concerning the infrared spectra obtained for the flax yarns treated using a 10 wt% Peclyve solution (Figure IV.11), an additional reduction in the hemicellulose and lignin bands occurred. Negligible differences can be found between the infrared spectra of the flax yarns treated for 4.5h and 6h and the same cellulose CI value was measured. These results highlight that the use of the Peclyve solution with a concentration of 10 wt% allowed to obtain the maximum efficiency after 4.5h of treatment. No further removal of amorphous components from the surface of flax fibres was produced using longer treatment times.

Upon CO_2 supercritical treatment, slight shifts could be observed for the characteristic bands of flax. The stretching vibration of C–O–C and the bending vibration of C–H were shifted from 1161 cm^{-1} to 1157 cm^{-1} and from 897 cm^{-1} to 896 cm^{-1}, respectively. Furthermore, a visible reduction of the bands at 1742 cm^{-1} and 1248 cm^{-1} of hemicellulose and at 1596 cm^{-1}, 1512 cm^{-1} and 1451 cm^{-1} of the lignin was observed. A possible explanation of these results may be found in the removal of amorphous non-cellulosic compounds produced by supercritical CO_2. Generally, in the treatment process, supercritical carbon dioxide fluid could infiltrate into flax fibres and swell them, which promote the re-arrangements and re-crystallization of the molecule chains, causing the shifts of the characteristic bands of treated flax fibres. On the other hand, the lignin structure in the flax fibres was easily destroyed and

hydrolyzed in supercritical carbon dioxide. Theoretically, carbon dioxide could swell and plasticize flax fibre to a certain degree in the supercritical state, which contributed to the interactions and movements of the macromolecular chains of the flax samples, thereby causing their rearrangement under high temperature conditions, and resulting in the increase in the crystallinity index [Gao *et al.*, 2015; Zhang *et al.*, 2018]. The presence of these phenomena was confirmed by the cellulose IR crystallinity index value calculated after the CO_2 treatment. In fact, a cellulose CI of 1.68 was found for the treated flax, higher than the value of 1.01 of the untreated flax.

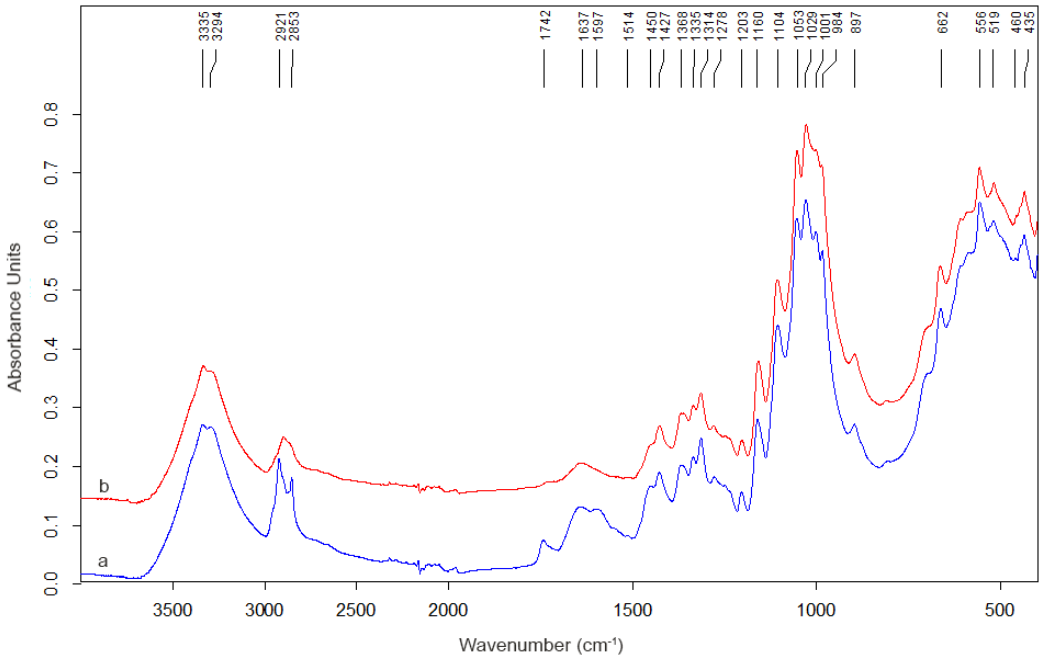

Figure IV. 12 Infrared spectra of as-received (a) and supercritical CO_2 treated flax yarns (b).

The influence of the enzymatic and the supercritical CO_2 treatment on the thermal properties of the flax yarns was also investigated using thermogravimetric analysis. In figure IV.13 are reported the thermograms for the as-received and the treated flax yarns. Weight changes versus temperature and the derivative of weight changes versus temperature have been measured. The thermogram of the untreated flax yarns reveals the presence of three peaks in the derivative curve: the first mass loss, at about 60-120°C, is related to the release of water occurring mostly in the amorphous region of cellulose; the second peak, at about 240-280°C, is attributed to the decomposition of the non-cellulosic components such as pectin and

hemicellulose; the third mass loss peak, at about 340-360°C, is due to the cellulose degradation [Velde *et al.*, 2001; Dong *et al.*, 2015; Mazian *et al.*, 2018].

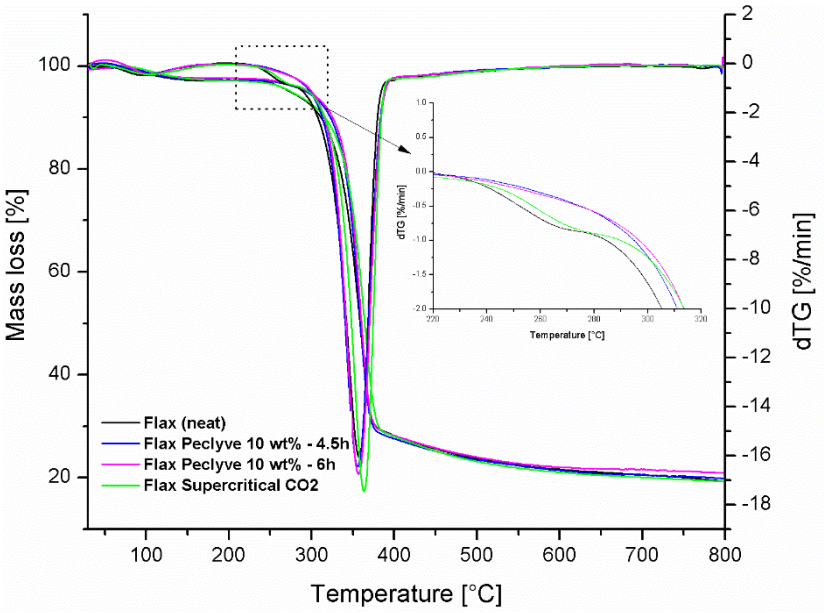

Figure IV. 13 Mass loss and derivative of the mass loss as a function of temperature for the untreated, enzymatically and supercritical CO_2 treated flax yarns.

After the enzymatic treatment, a change in the thermal stability of the flax yarns occurred. The thermogravimetric analysis confirmed the enzymatic removal of hemicellulose and pectin components from the flax surface. In particular, the thermal stability of flax yarns treated using the maximum concentration of 10 wt% of Peclyve solution was investigated. The thermograms reported in Figure IV.13 show that the peak related to water loss remains unchanged. However, the second and the third step of thermal degradation were changed. In fact, contrary to the as-received flax, both yarns treated for 4.5h and 6 h, do not show any step of weight loss associated with the hemicellulose and the pectin decomposition. This result can be related to the action of the Peclyve solution, which was able to effectively remove the non-cellulosic components. From the mass loss-temperature curves it can be also seen that the onset degradation temperatures tend to increase after the enzymatic treatment, compared with the untreated flax yarns. This effect can be partially due to the fact that non-cellulosic components, which degrade at a lower temperature, were removed during the enzymatic treatment, thus increasing the thermal stability of flax yarns.

Different results were obtained for the supercritical CO_2 treated flax yarns. If compared to the enzymatically treated yarns, a slight removal of hemicellulose and pectin components

was obtained after the supercritical CO_2 treatment. Table IV.5 shows the peak maximum temperature and the temperature of 10% weight loss values found for the untreated and the treated flax yarns. Both the enzymatically and the supercritical CO_2 treated flax yarns displayed a peak maximum temperature comparable to that obtained for the untreated one. An increase of the 10% of weight loss temperature values was obtained after both enzymatic treatments. In particular, the highest temperature value (325.5°C) was obtained for the flax yarn after a 6h treatment. On the contrary, the supercritical CO_2 treatment does not induce a significant change in the temperature value. The results obtained show that the treatment with supercritical CO_2 does not significantly affect the kinetics of thermal degradation of flax yarns.

Table IV. 5 Results of the thermogravimetric analysis for the different kinds of flax yarns.

	Peak maximum Temperature [°C]	**Temperature of 10% weight loss [°C]**
Flax yarn (neat)	357.2	311.3
Peclyve EXG 10 wt% - 4.5 h	355.7	322.8
Peclyve EXG 10 wt% - 6 h	356.7	325.5
Flax supercritical CO_2	363.4	313.9

Contrary to FT-IR results, the thermogravimetric analysis did not highlight a strong lignin degradation after both enzymatic and supercritical CO_2 treatments. In general, the weight loss of lignin occurs slowly over a broader temperature range than cellulose and hemicellulose components [Spinacé *et al.*, 2009]. The lignin decomposition starts at relatively low temperatures, (200-275°C), but the main process occurs around 400°C, with the formation of aromatic hydrocarbons, phenolics, hydroxyphenolics and guaiacyl-/syringyl-type compounds [Brebu *et al.*, 2010]. Comparing the thermograms obtained for the untreated and treated flax yarns, no difference was highlighted in a temperature range around 400°C.

IV.1.3.3 Influence on mechanical properties

A mechanical characterization of untreated and chemically treated flax yarns was performed in order to investigate the effect of the different treatments on their tensile behaviour. As

described in detail in section II.2.5, the tensile properties of individual flax yarns were determined by single filament tensile tests. Unlike synthetic fibres, one of the main characteristics of the plant ones is their remarkable heterogeneity. One of the parameters of greatest variability of this type of reinforcement is the diameter. A statistical analysis based on measurements at one hundred points was performed to define the diameter value of the untreated and chemically treated flax yarns. In particular, the Gaussian probability distribution was used in order to analyse the flax yarn diameter, according to the Equation IV.1 [Guillebaud-Bonnafous *et al.*, 2012]:

$$P(d) = \frac{1}{\sqrt{2\pi}\cdot\sigma} e^{-\frac{(d-\mu)^2}{2\cdot\sigma^2}} \qquad \text{(IV.1)}$$

where d is the diameter of flax yarn, μ is the mean of the distribution, and σ^2 is the variance of the distribution. In figure IV.14 is reported the Laplace-Gauss distribution obtained for the different yarn diameters.

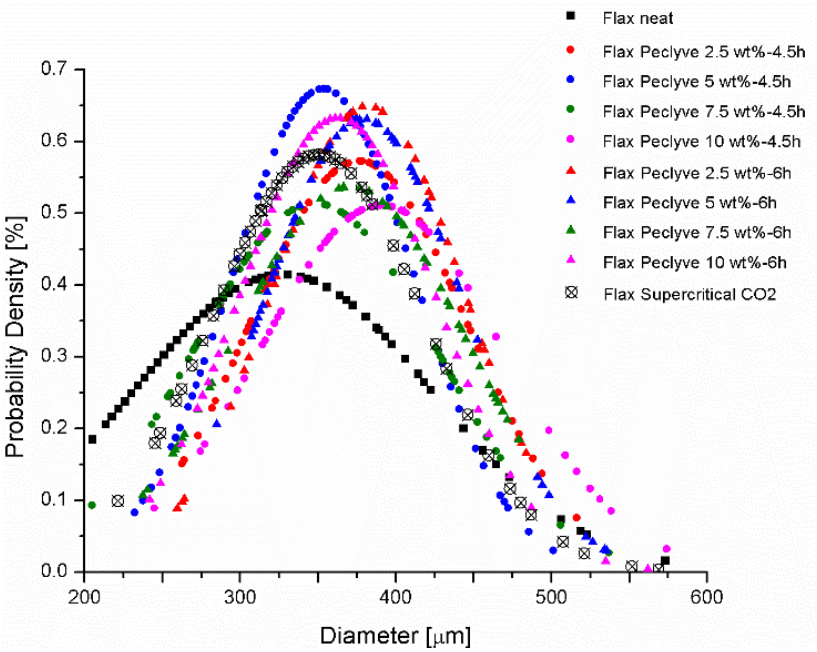

Figure IV. 14 Gaussian distribution of measured diameters of flax yarn.

From the statistical analysis it was possible to confirm the significant scattering in the measured diameter values. If compared with the chemically treated flax yarns, a very large diameter distribution was found for the untreated flax yarn, with an average value of 327 μm

and a standard deviation of 96 μm. In this study, the yarns were assumed to be characterized by a circular cross-section and the average values of diameters were used to evaluate their cross-sectional area. The scatter of the tensile strength of flax yarns was statistically analysed using a two-parameter Weibull distribution, according to the equation IV.2 [Sarasini *et al.*, 2018]:

$$\Pr(\sigma) = 1 - \exp\left[-\left(\frac{\sigma}{\sigma_0}\right)^m\right] \quad \text{(IV. 2)}$$

where *Pr(σ)* is the cumulative probability of failure as a function of applied stress *σ*, *m* is the Weibull modulus (related to the dispersion of the data) and σ_0 is the characteristic strength. Equation IV.3 gives the estimator, P_f, used for the evaluation of failure probability:

$$P_f = \frac{i-o.5}{N} \quad \text{(IV.3)}$$

where *N* is the number of filaments tested and *i* is the rank of data point for each filament. Concerning the as-received flax yarns, the tensile strength σ_f and the strain to failure ε_f values were measured at three different gauge lengths, namely 20 mm, 30 mm and 40 mm. In table IV.6 are reported the tensile properties measured for the untreated flax yarns. It can be seen that with longer gauge length there is a small decrease in the yarn strength, from 272 to 236 MPa. This result can be related to a greater probability to find defects in flax yarns as the gauge length increases. For all the yarns, a strain to failure value ranging between 3.4% and 3.8% was found.

Table IV. 6 Tensile properties of untreated flax yarns as a function of gauge length and the corresponding Weibull parameters.

Gauge length L_0 [mm]	F_{max} [N]	Diameter [μm]	σ_f [MPa]	ε_f [%]	Characteristic strength σ_0 [MPa]	Weibull Modulus m
20	22.9 ± 3.9	328 ± 77	271 ± 46	3.78 ± 0.57	292	6.83
30	20.7 ± 3.8	326 ± 69	249 ± 46	3.62 ± 0.62	265	6.36
40	19.8 ± 4.8	327 ± 96	236 ± 57	3.40 ± 0.42	257	5.02

Contrary to the untreated flax yarns, for both enzymatically and supercritical CO_2 treated yarns, the tensile properties were determined by single filament tensile tests performed using a gauge length of 40 mm. The effects of the enzymatic treatment on the mechanical

performances of flax are reported in Table IV.7. A decrease in the tensile strength of flax yarns was observed increasing both the concentration of the enzymatic solution used and the treatment time. The reduction in mechanical performance can be linked with the enzymatic effect of bundle fibrillation observed by FE-SEM analysis. A strong loss of tensile strength of about 58.5% was obtained after a treatment with the 10 wt% Peclyve solution for 6 h. This tensile strength drop can be connected to the progressive breakage of the fibres present at the outer surface of the yarn produced at high solution concentration (Figure IV.8).

Table IV. 7 Tensile properties of untreated and enzymatically treated flax yarns. In the table are also reported the parameters of the Weibull distribution for the tensile strength.

	Flax Yarn	F_{max} [N]	Diameter [µm]	σ_f [MPa]	ε_f [%]	Characteristic strength σ_0 [MPa]	Weibull Modulus m
	Neat	19.8 ± 4.8	327 ± 95	236 ± 57	3.4 ± 0.42	257.4	5
4.5h	Peclyve EXG 2.5 wt%	20.2 ± 3.5	376 ± 69	181 ± 31	3.55 ± 0.49	194	6.8
	Peclyve EXG 5 wt%	16.9 ± 3.6	353 ± 59	172 ± 36	2.99 ± 0.47	186	5.5
	Peclyve EXG 7.5 wt%	16.2 ± 4	348 ± 77	170 ± 41	2.95 ± 0.41	186	4.8
	Peclyve EXG 10 wt%	14.8 ± 3.5	390 ± 78	123 ± 29	3.04 ± 0.47	134	5
6h	Peclyve EXG 2.5 wt%	14.1 ± 3.4	382 ± 61	123 ± 29	3.03 ± 0.59	134	4.6
	Peclyve EXG 5 wt%	13.7 ± 2.1	379 ± 63	121 ± 19	3.19 ± 0.55	129	7.6
	Peclyve EXG 7.5 wt%	11.7 ± 3.6	370 ± 74	108 ± 33	2.93 ± 0.6	120	3.5
	Peclyve EXG 10 wt%	11.1 ± 2.8	362 ± 63	107 ± 27	3.02 ± 0.54	118	4.3

Another phenomenon able to produce a reduction in the mechanical performance of the yarns is likely to be the enzymatic removal of non-cellulosic constituents of flax, such as pectin, hemicellulose and lignin. Although they are not structural constituents of the fibre, the non-cellulosic components have the role to keep joined together the cellulose microfibrils. A similar result was found by Liu et al. [Liu *et al.*, 2016]. A reduction in the tensile properties of hemp fibres was reported after the enzymatic treatment using the polygalacturonase (EPG) enzyme. The authors proposed a "composite model" to explain the mechanical behaviour of plant fibres and the effect of the enzymatic solution on their properties. The hemp fibre can be assimilated to a composite material, in which the cellulose microfibrils are the reinforcing fibres and the non-cellulosic components the matrix. According to this model, the mechanical performances of the fibre are governed not only by the cellulose microfibrils but also by their adhesion with the non-cellulosic matrix. The enzymatic degradation of the non-cellulosic matrix produced during the treatment results in a reduction in fibre/matrix interface strength and in an overall decrease in the tensile properties of the

fibre. Similar conclusions have been found on pectinase treated hemp fibres by Saleem et al. [Saleem *et al.*, 2008]. In addition, lignin is a structural component and its degradation can result in a decrease in fibre tensile strength. The removal of amorphous non-cellulosic components from flax fibres has been confirmed by both FT-IR and thermogravimetric analysis. Several studies in literature studied the relationships between the tensile properties and the cellulose crystallinity index for plant fibres [Gassan *et al.*, 1999; Sawpan *et al.*, 2011]. In general, an increase in tensile strength and Young's modulus with increased crystallinity index was reported. As described previously, in this study an increase in the cellulose crystallinity index was observed after the different enzymatic treatments. The reduction in the tensile strength of enzymatically treated flax yarns can be related to an excessive degradation of the structural components of fibre, such as lignin. A similar behaviour was found by Mwaikambo et al. [Mwaikambo *et al.*, 2006] for alkali treated sisal fibres. A decrease in tensile strength and Young's modulus of sisal fibres with increased crystallinity index was reported. The authors suggested that the alkali treatment severity had a large influence on tensile properties and that higher levels of treatment can produce a strong degradation of the fibres. The effects of the supercritical CO_2 on the mechanical performances of flax are reported in Table IV.8.

Table IV. 8 Tensile properties of untreated and SC-CO_2 treated flax yarns. In the table are also reported the parameters of the Weibull distribution for the tensile strength.

Flax Yarn	F_{max} [N]	Diameter [µm]	σ_f [MPa]	ε_f [%]	Characteristic strength σ_0 [MPa]	Weibull Modulus m
Neat	19.8 ± 4.8	327 ± 95	236 ± 57	3.4 ± 0.42	257.4	5
Supercritical CO_2	20.4 ± 3.5	350 ± 68	211 ± 36	1.4 ± 0.15	226.1	7.1

If the maximum force values obtained for untreated and treated flax yarns are compared, it is possible to highlight that the supercritical CO_2 process does not produce a change of the load bearing ability of the yarns. However, a slight reduction in the tensile strength value was observed, passing from a value of 236 ± 57 MPa to a value of 211 ± 36 MPa for the as-received and the CO_2 treated flax yarns, respectively. This decrease is strictly dependent on the increase in the average diameter of yarns produced by the exposure to the supercritical fluid. In addition, from results reported in Table IV.8, it is possible to notice that an increase in brittleness of flax yarns is produced after the exposure of supercritical fluid. In fact, the SC-CO_2 treated flax yarns exhibit a strain to failure value of 1.4 ± 0.15%, lower than the

value of 3.4 ± 0.42% found for the untreated ones. The experimental results, obtained for the as-received and the chemically treated flax yarns, were statistically analysed using a two-parameter Weibull distribution, according to the equation IV.2. In Tables IV.6-7-8 are reported all the Weibull modulus and the Weibull characteristic strength values found for the untreated, enzymatically and SC-CO_2 treated flax yarns. The curves reported in Figure IV.15 represent the results of the two-parameter Weibull distribution applied to all the analysed flax yarns.

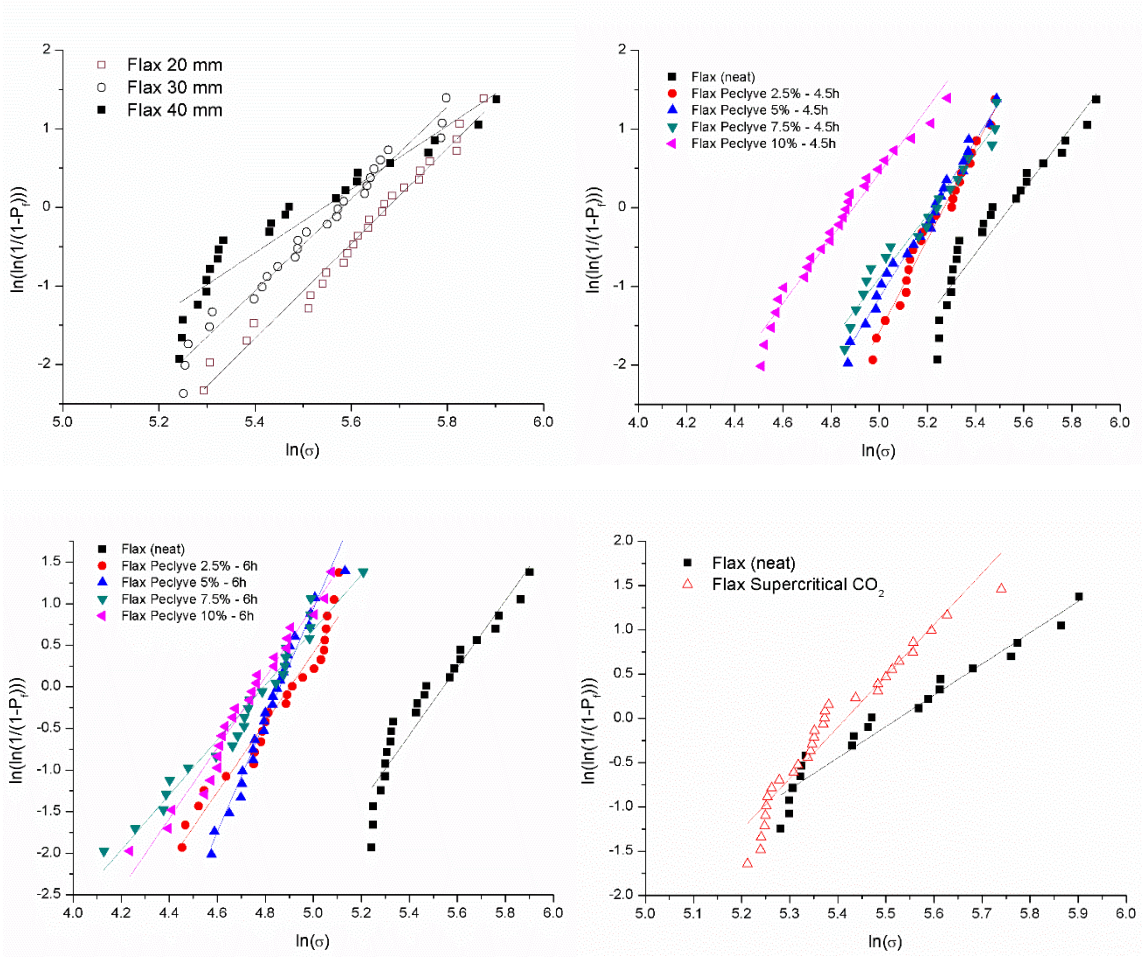

Figure IV. 15 Weibull distribution plots of strength measured for: (a) untreated flax yarns as a function of gauge lengths, (b) enzymatically treated flax yarns for a duration of 4.5 h, (c) enzymatically treated flax yarns for a duration of 6h and (d) supercritical CO_2 treated flax yarns.

A quasi-linear trend was found for both untreated and treated flax yarns. This trend indicates that the yarn failure depends on the presence of a single population of flaws on the flax yarn surface. Both enzymatic and supercritical CO_2 treatments do not result in a change in the nature of the fibres defects, but rather they cause an increase in their concentration and severity.

IV.1.4 The influence of physical treatments on flax properties

IV.1.4.1 Effects on wetting properties

The efficiency of the plasma treatment in changing the wetting properties of flax was investigated. At first, water drop tests were performed on the surface of flax fabrics treated by plasma polymerization process. Before the plasma deposition, flax fabrics were pretreated using a 100 W oxygen plasma step. The wetting analysis highlighted the ability of plasma polymerization process to produce an increase in hydrophobic behaviour of the flax fabric. After the pp-TVS coating deposition, flax fabrics showed a strong hydrophobic nature with water retention time longer than 1 minute. However, as mentioned for the enzymatic treatment, due to a large data dispersion, the water drop test can be considered only as a qualitative test. In order to carry out a more accurate and quantitative analysis of the wetting properties of flax, a tensiometric method was used to determine contact angles and surface energies of untreated and plasma treated flax yarns. As described in detail in section II.2.3, a force tensiometer – K100SF (Kruss) with a resolution of 0.1 µg was used to perform contact angle measurements. Single elementary fibres were carefully extracted from flax yarns and immersed in two test liquids, namely water and diiodomethane, for the wetting analysis. The advancing θ_a, static θ_s and receding contact angles θ_r were measured using the Wilhelmy equation (Eq. II.6). Advancing and receding contact angle values were used in order to have supplementary information about angle hysteresis and then on physico-chemical properties of fibre surface [Extrand, 1998]. Contact angle hysteresis is a crucial element of wetting. The hysteresis of the contact angle is calculated as the difference between the advancing and the receding contact angle values, Equation IV.4:

$$\Delta\theta = \theta_a - \theta_r \qquad \text{(IV.4)}$$

This difference can be attributed to different effects such as surface roughness, solid heterogeneity, inter-diffusion or the surface deformation. In general, ideal flat surfaces are characterized by a contact angle hysteresis equal to zero. For real surfaces, as in the case of flax fibres, the contact angle hysteresis assumes a value greater than zero. Table IV.9 reports the average values and the standard deviation values of static and dynamic contact angles found for the as-received and the plasma coated flax fibres.

Table IV. 9 Static and dynamic contact angles derived from measurements on untreated and plasma treated flax yarns. The contact angle hysteresis is also reported.

		Advancing Contact Angle θ_a [°]	Receding Contact Angle θ_r [°]	Static Contact Angle θ_s [°]	Hysteresis $\theta_a - \theta_r$ [°]
Flax	Water	59.8 ± 4.7	35.8 ± 4.3	40.6 ± 6.8	23.9 ± 1.6
(Neat)	Diiodomethane	61.1 ± 2.12	26.8 ± 13.4	50.4 ± 4.3	34.3 ± 13
PECVD	Water	84.9 ± 6.8	8.6 ± 7.7	58.2 ± 4	76.3 ± 9.9
(100W O_2)	Diiodomethane	63.7 ± 5.2	35.8 ± 2.9	42.6 ± 7.6	27.9 ± 4.3

The Owens and Wendt (Eq. II.9) equation was used to measure the dispersive γ_s^d and the polar γ_s^p components of flax fibres surface energy γ_s, (Table IV.10). Figure IV.16 shows the plots obtained with values of contact angles following the Owens and Wendt method for water and diiodomethane test liquids. The values of static and dynamic contact angles and the surface energy values found for the as-received flax fibres are consistent with those reported in literature [Pucci *et al.*, 2017]. The fundamental aspect that emerged from this analysis is the strong decrease in the polar component of the flax fibres after the deposition of the pp-TVS layer on their surface. The ratio between the dispersive γ_s^d component and the total surface energy γ_s of flax was measured in order to assess the dispersivity degree of the different yarns. Unlike the untreated flax fibres, which showed a dispersion degree equal to 56.28%, the plasma treated fibres exhibited a reduced polar component of surface energy with a dispersion degree of 73.12%. These results were confirmed by the measured contact angle values. The increase in the dispersive behaviour of flax fibres produced a reduction in their surface wetting with strongly polar liquid such as water. From the values reported in table IV.9, it is possible to notice that after the plasma treatment, flax showed an increase in the static contact angle with water, passing from 40.6 ° for the untreated fibres to a value of 58.2 ° for the plasma treated fibres.

Table IV. 10 Dispersive and polar components of the total surface energy of untreated and treated flax yarns.

	γ^p [mN/m]	γ^d [mN/m]	γ [mN/m]	Dispersivity degree [%]
Flax (Neat)	26.58 ± 3.96	33.97 ± 3.38	60.35 ± 7.34	56.28 ± 1.25
PECVD (100W O_2)	13.99 ± 1.06	38.07 ± 5.49	52.06 ± 6.55	73.12 ± 1.36

An opposite behaviour was observed using diiodomethane as test liquid. This strongly dispersive liquid tends to better wet the surface of fibres covered by the pp-TVS. A

consequent reduction of the fibre contact angle with diiodomethane was observed after the plasma deposition of the polymeric TVS film. These results confirmed the ability of plasma polymerization process to reduce the hydrophilic behaviour of the flax yarns.

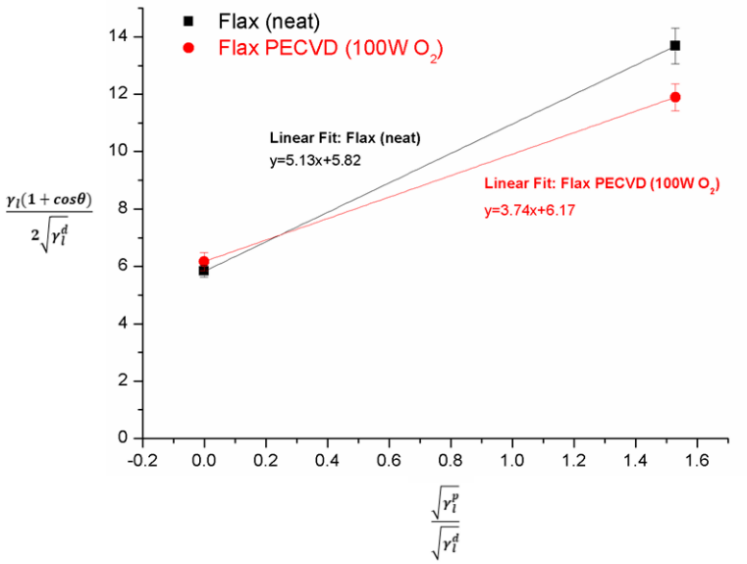

Figure IV. 16 Linear fits for surface energies of flax fibres in the as-received state and after the plasma deposition process.

As reported by Bismarck et al. [Bismarck *et al.*, 1999], according to the model proposed by Wenzel [Wenzel, 1949], the lower the surface roughness of a solid, the smaller the value of the contact angle hysteresis. From the values reported in Table IV.9, it is possible to note that a strong increase in the contact angle hysteresis of flax fibres is produced after the plasma deposition of the polymer TVS coating. It is possible to assume that this phenomenon depends on the increase in the surface roughness of flax fibres. As will be discussed in the next section, the oxygen plasma pre-treatment and the subsequent plasma deposition can promote an increase in the surface irregularities of flax fibres. It is well known that the roughness of a solid surface can represent a barrier to the motion of the solid-liquid contact line. Surface irregularities can pin the motion of the liquid front as it advances, causing an increase in the advancing contact angle and, at the same time, these irregularities can hold back the contracting motion of the liquid front when it recedes, thus leading to a decrease in the receding contact angle [Yuan *et al.*, 2013]. A lower contact angle hysteresis is reported with the diiodomethane probe liquid, Table IV.9. This result can be related to the liquid properties. In fact, as reported by Chibowski et al. [Chibowski *et al.*, 2013], the contact angle hysteresis depends not only on the solid properties but also on the properties of the probe

liquid, such as vapour pressure, size of liquid molecules etc.. The authors report that the contact angle hysteresis is larger with polar liquids (water) than with apolar liquids (diiodomethane). For this reason, it is possible to point out that the development of surface heterogeneity plays only a minor role with diiodomethane.

IV.1.4.2 Effects on morphological and compositional characteristics

A morphological analysis was carried out on the surface of the different plasma treated flax yarns. In figure IV.17 are reported the micrographs of the lateral surface of untreated flax yarns and oxygen plasma treated flax yarns using the power of 2, 10, 20, 50 and 100 W. The main effect produced by the oxygen plasma treatment is an enhancement in the surface roughness of the flax yarns. This effect is essentially linked to the ability of the reactive plasma gas to perform a surface ablation of the flax fibres. From figure IV.17 it is possible to observe that the greater the plasma power, the greater the surface roughness of yarns. Ablation occurs by a chemical etching process during the plasma treatment. In fact, the oxygen plasma is a chemically reactive plasma in which the inorganic oxygen gas is not able to form any polymeric deposition. The ionization and dissociation reactions of oxygen gas are reported in Equation IV.5 and Equation IV.6:

$$e + O_2 \rightarrow O_2^- \quad \text{(IV.5)}$$

$$e + O_2 \rightarrow O + O^- \quad \text{(IV.6)}$$

The reaction of these high energy oxygen ions with the flax surface is able to produce changes in the surface morphology. As reported by Sun and Stylios [Sun *et al.*, 2006], after the oxygen plasma treatment, fibre surface became rougher with the presence of pits, voids and spaces. This effect is clearly visible by comparing the micrograph of the untreated flax fibres (Figure IV.17-A) with that of the treated fibres using an oxygen plasma power of 100 W (Figure IV.17-F). Similar results were found by De Farias et al. [De Farias *et al.*, 2017]. They showed that the oxygen plasma treatment of coir fibres led to a partial removal of the surface amorphous layer, revealing the inner structure with long valleys and peaks. A morphological analysis has been carried out also after the plasma deposition of the polymeric TVS film. This analysis showed that the quality of the polymeric coating strictly depends on

the plasma power used during the first oxygen non-polymerising gas plasma step. Oxygen power values of 100 W and 2 W have been tested. By comparing the SEM micrographs reported in Figures IV.18-A,B and Figures IV.19-A,B, it can be seen that the oxygen pre-treated flax yarns with a plasma power of 2 W are characterized by the presence of a very homogeneous polymeric layer. A much more uneven coating was obtained for the flax yarns treated using a power of 100 W. The morphological analysis highlights that the final characteristics of the polymer film strongly depend on the finishing of lateral surface of flax yarn as a result of the oxygen pre-treatment. The higher the plasma oxygen power used, the greater the roughness of the flax fibres and so the lower the homogeneity of the polymeric film.

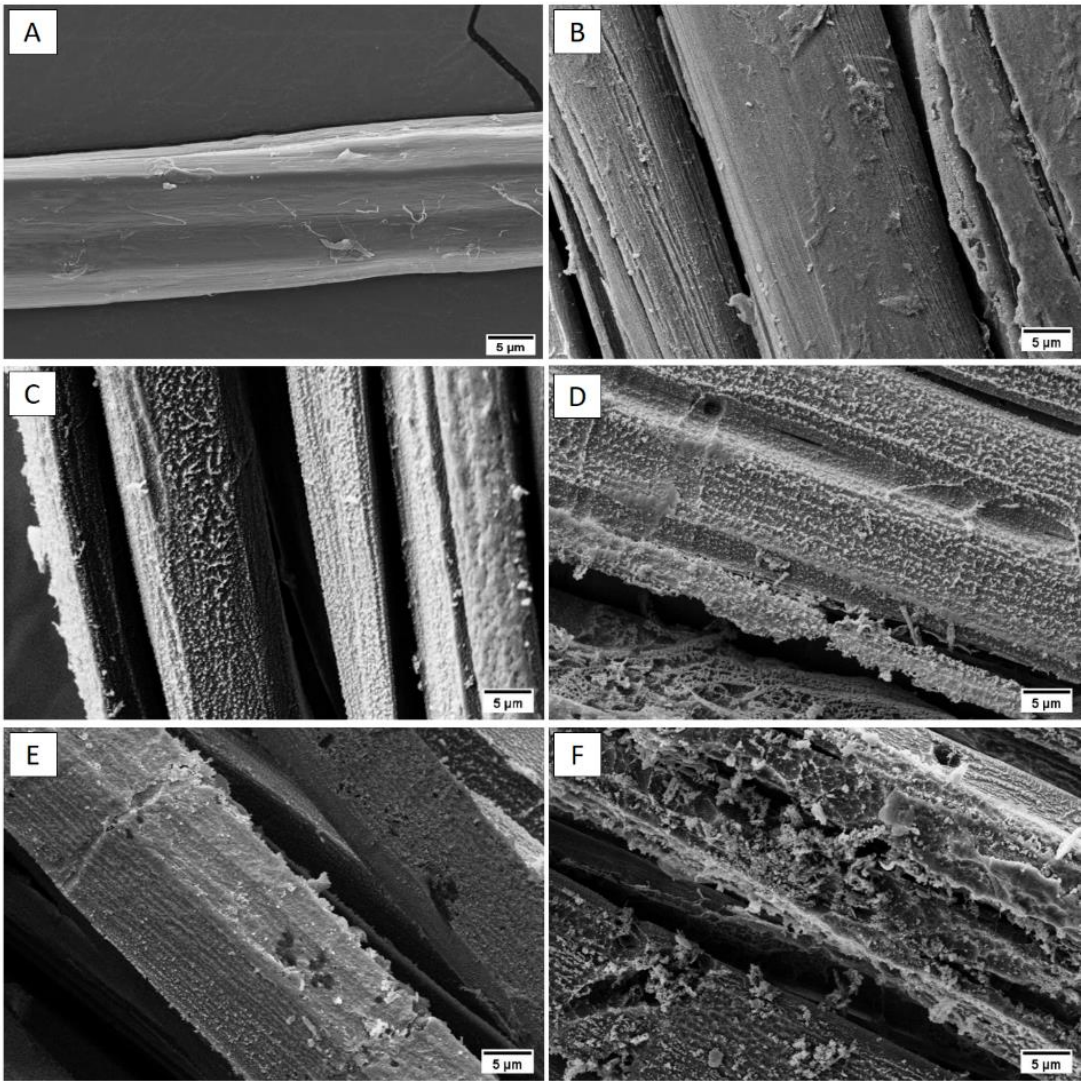

Figure IV. 17 SEM micrographs detailing the lateral surface of untreated flax yarn (A) and oxygen plasma treated flax yarn using a power of 2 W (B), 10W (C), 20 W (D), 50 W (E) and 100 W (F), [Seghini et al., 2019].

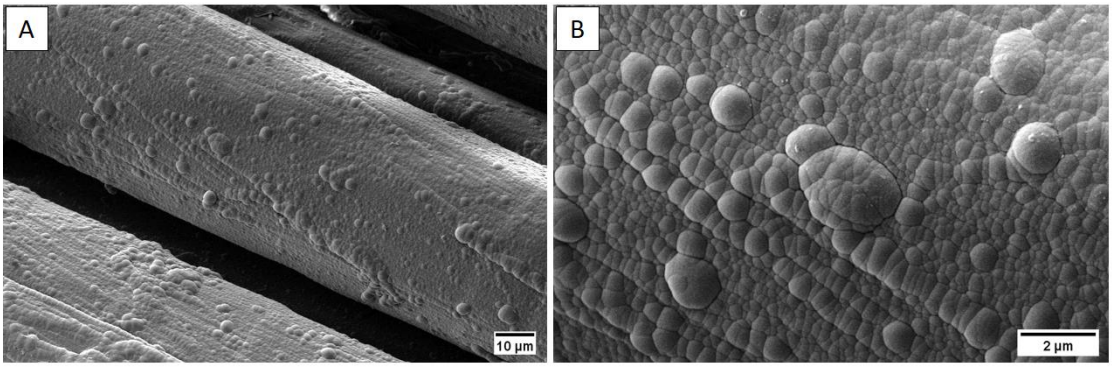

Figure IV. 18 SEM micrographs of flax yarns after the plasma polymer tetravinylsilane deposition, using a plasma power of 2 W for the oxygen pre-treatment. Lateral surface of treated flax fibres (A) and a detailed view of the polymer film (B), [Seghini et al., 2019].

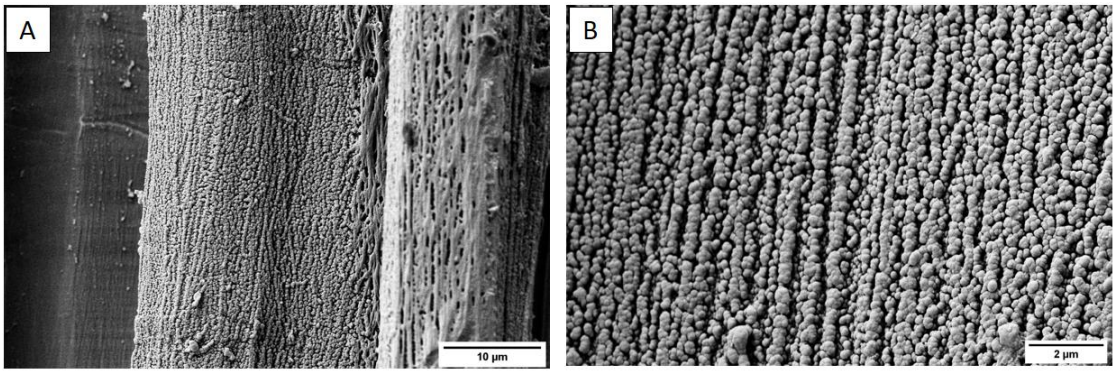

Figure IV. 19 SEM micrographs of flax yarns after the plasma polymer tetravinylsilane deposition using a plasma power of 100 W for the oxygen pre-treatment. Lateral surface of treated flax fibres (A) and a detailed view of the polymer film (B), [Seghini et al., 2019].

The effect of the different plasma treatments on the chemical composition of flax fibres has been studied by Fourier-transform infrared (FT-IR) analysis. FT-IR spectra in Figure IV.20 show the untreated and the oxygen plasma treated flax fibres using 2 W and 100 W power values. Upon plasma pre-treatment, the bands in the range 1780-1520 cm^{-1} changed, indicating that hemicellulose and lignin in the fibres were degraded as shown by the decrease of the bands at 1734 and 1597, 1511 cm^{-1}, respectively. This is in agreement with previous studies, which demonstrated that the amorphous regions are more susceptible to chemical and ion etching [De Souza Lima *et al.*, 2004; Donaldson *et al.*, 2004; Jamali *et al.*, 2011]. In addition, with O_2 pre-treatment at 100 W, an increase at ≈ 1630 cm^{-1} can be attributed to the breakage of the β-1,4 glycosidic bonds of cellulose macromolecules in the oxidation reaction of the cellulose as confirmed by the reduction in the integrated intensity of the band at 897 cm^{-1} (2 W: 0.085; 100 W: 0.076). Indeed this latter, as previously reported, was found to be

linearly correlated with the percentage of cellulose [Abidi *et al.*, 2017] and degree of crystallinity [Abidi *et al.*, 2014].

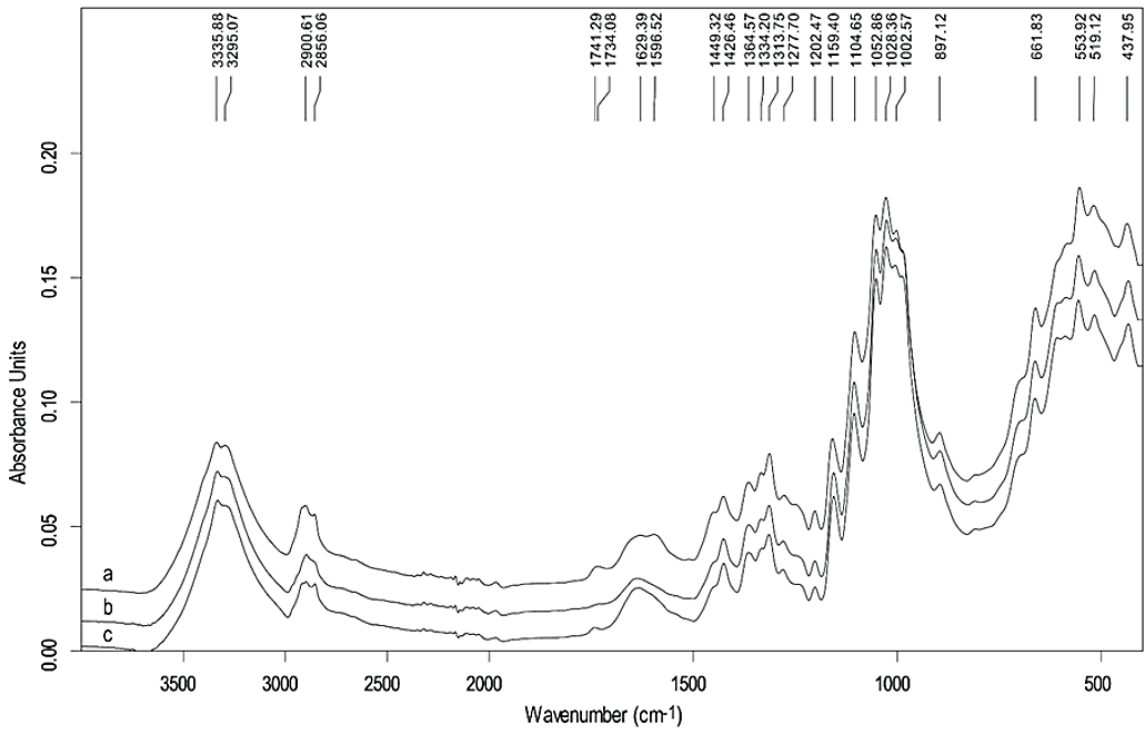

Figure IV. 20 Infrared spectra of different flax yarns: untreated (a), O_2-plasma treated at 2 W (b) and 100 W (c).

Moreover, a new band at 1741 cm^{-1}, probably due to the formation of oxidized species rich in hydroxyl, carbonyl, carboxyl groups and phenoxy radicals, appeared after O_2 plasma treatment at 100 W [Demirkir *et al.*, 2017]. The presence of the polymeric layer has been confirmed also by infrared spectroscopy analysis. Typical infrared bands of plasma-polymerized tetravinylsilane (pp-TVS) film deposited on flax fibres are shown in Figure IV.21. In the wavenumber range 3700-3200 cm^{-1} a significant band of -OH and harmonic vibration of C=C in vinyl group at 3286 cm^{-1} occurs. Following, wide bands in the range 3100-2750 cm^{-1} can be ascribed to vibrations of $-CH_2$ groups. Significant bands are the ones related to Si-H and C=O vibration at 2112 cm^{-1} and 1696 cm^{-1}, respectively. Four bands contribute to $Si-CH=CH_2$ vibrations, such as: $-CH_2$ scissoring (1451 cm^{-1}), $=CH_2$ deformation in vinyl group (1404 cm^{-1}), $-CH_2$ wagging in $Si-CH_2-R$ (1250 cm^{-1}) and =CH (1021 cm^{-1}), CH_2 wagging (shoulder at 950 cm^{-1}) of $=CH_2$ bond. Finally, a multiband in the range 1100-1000 cm^{-1} belongs to Si-O-Si stretching (1097 cm^{-1}), Si-O-C stretching (1050 cm^{-1}) and Si-O (869 cm^{-1}) bending [Davidson, 1971; Cech *et al.*, 2014].

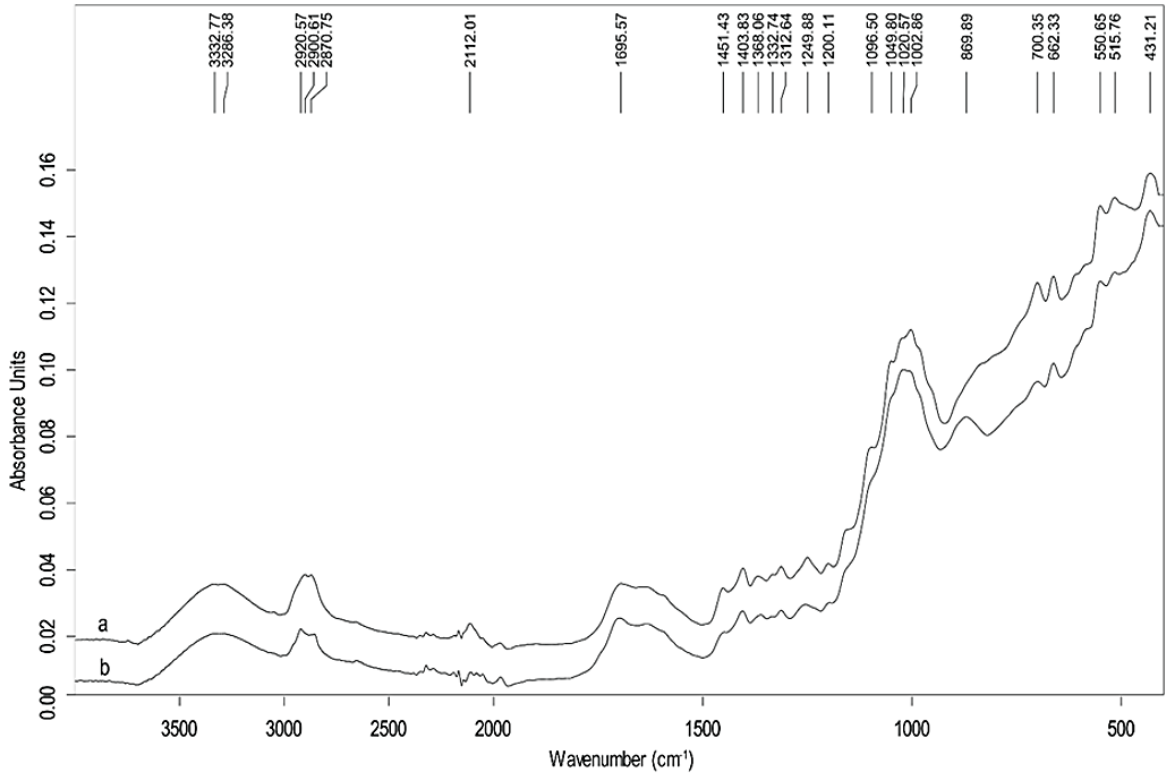

Figure IV. 21 Infrared spectra of pp-TVS films deposited on pre-treated flax yarns at 2 W (a) and 100 W (b).

Thermogravimetric analysis has been used to assess the thermal stability of untreated and both oxygen and tetravinylsilane plasma treated flax yarns. In figure IV.22 are reported the thermograms for the as-received and the plasma treated flax yarns. From the results reported in Table IV.11, it can be noticed that the flax fibres treated using an oxygen plasma power of 2 W show similar behaviour to the untreated one. A strong influence on thermal stability of flax can be instead detected starting from oxygen plasma power of 10 W. De Oliveira et al. [De Oliveira *et al.*, 2017] highlighted how the oxygen plasma exposure can be able to perform a partial removal of non-cellulosic substances like hemicellulose, lignin, pectin, waxes and impurities from coconut surfaces. The decrease in both decomposition peak temperature and 10% weight loss temperature of flax after the oxygen plasma exposure may be ascribed to an excessive value of plasma power used. In fact, the surface etching produced by oxygen can generate an overall degradation of flax fibres, with a consequent reduction in their thermal stability. By comparing the results found for the neat and the treated flax yarns using an oxygen plasma power of 100 W, a 10°C reduction can be observed for the two representative temperatures.

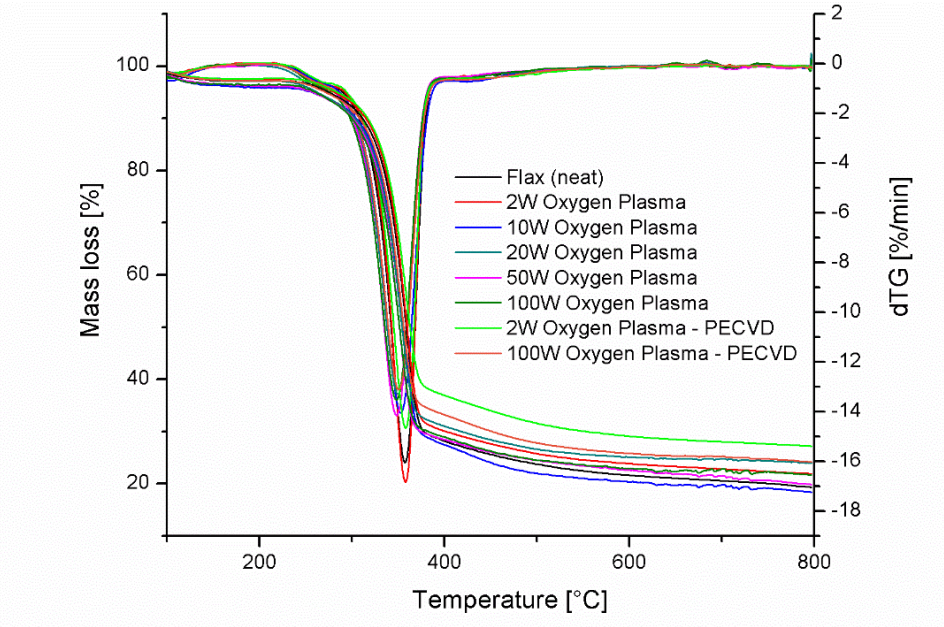

Figure IV. 22 Mass loss and derivative of the mass loss as a function of temperature for the untreated and plasma treated flax yarns.

Similar decomposition peak temperature values may be found for the 2 W and the 2 W-PECVD treated flax yarns, whereas an increase has been measured for the 100 W-PECVD treated yarns with respect to the 100 W oxygen treated ones. The increase in thermal stability is essentially linked to the presence of the polymeric coating on the yarn surface, which allows a small recovery of the thermal resistance, strongly reduced due to the excessive plasma power used during the oxygen pre-treatment.

Table IV. 11 Results of the thermogravimetric analysis for the different kinds of flax yarns.

Flax yarn	**Peak maximum Temperature [°C]**	**Temperature of 10% weight loss [°C]**
Neat	357.2	311.3
2W O_2 Plasma	357.7	314.7
10W O_2 Plasma	352.5	304.3
20W O_2 Plasma	349.6	303.4
50W O_2 Plasma	348.0	301.0
100W O_2 Plasma	347.9	299.7
PECVD (2W O_2)	357.9	316.9
PECVD (100W O_2)	350.3	308.1

IV.1.4.3 Influence on mechanical properties

In order to evaluate the effects of the different physical surface modification treatments on the mechanical performance of the single flax yarns, a mechanical characterization has been carried out by single yarn tensile tests. A statistical analysis based on the Gaussian probability distribution was used in order to analyse the flax yarn diameter, (Equation IV.1). As previously reported for the untreated and chemically treated flax yarns, a significant scattering in the measured diameter values was found after the plasma treatments (Figure IV.23). These values were used to measure the cross-sectional area of the different flax yarns and to evaluate their tensile strength values.

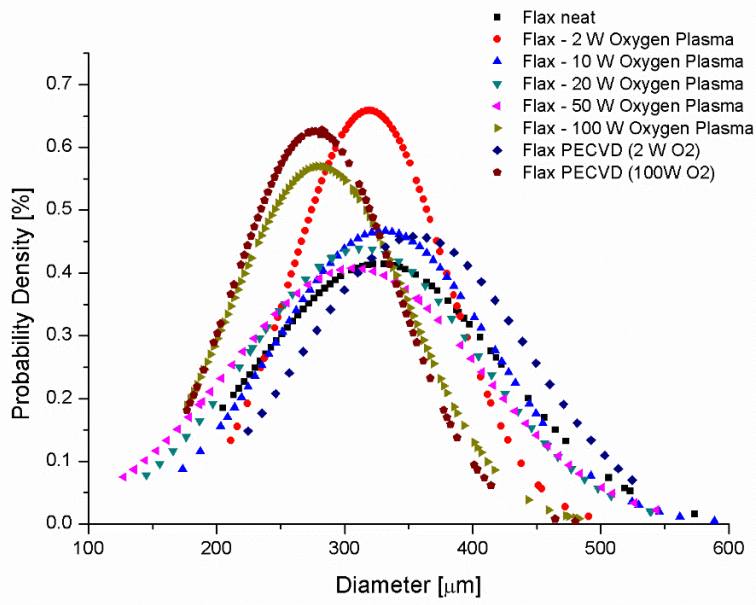

Figure IV. 23 Gaussian distribution of measured diameters of untreated and plasma treated flax yarns.

A brittle behaviour under tensile loading has been found for all the different families of flax yarns. From the results reported in Table IV.12, it is possible to notice a decrease in the maximum force and strength values with increasing power of oxygen plasma. For the 2 W oxygen plasma, the measured strength value can be considered similar to the one obtained for untreated flax yarns because of the large scattering. Then, for higher power, the strength values decrease, until a reduction of 36.4% for the 100 W condition. This result can be explained by the outcomes of the morphological analysis (Figure IV.17): the oxygen plasma carries out a surface ablation of flax fibres, generating defects such as pits, voids and spaces.

Moreover, as shown in the thermogravimetric analysis, exposure of flax fibres to increasing plasma powers leads to a removal of hemicellulose, pectin and waxes but also to a strong degradation of structural components such as lignin and cellulose. The mechanical performance of flax yarns is thus closely linked to the oxygen plasma treatment.

Table IV. 12 Tensile properties of flax yarns after different oxygen plasma power conditions and plasma deposition processes. In the table are also reported the parameters of the Weibull distribution for the tensile strength.

Flax Yarn	F_{max} [N]	Diameter [µm]	σ_f [MPa]	ε_f [%]	Characteristic strength σ_0 [MPa]	Weibull Modulus m
Neat	19.8 ± 4.8	327 ± 95	236 ± 57	3.4 ± 0.42	257.4	5
2W O_2 Plasma	20.9 ± 2.8	319 ± 60	262 ± 35	3.67 ± 0.33	277	8.8
10W O_2 Plasma	17 ± 3.4	330 ± 85	199 ± 39	3.39 ± 0.33	215	6.1
20W O_2 Plasma	17.9 ± 4.5	314 ± 90	231 ± 58	3.49 ± 0.44	253.6	4.5
50W O_2 Plasma	10.6 ± 4	307 ± 97	143 ± 54	2.71 ± 0.5	160	3.1
100W O_2 Plasma	9.2 ± 2.9	280 ± 69	150 ± 48	2.62 ± 0.56	167.1	3.4
PECVD (2W O_2)	21 ± 3.9	355 ± 87	212 ± 39	2.96 ± 0.35	228.8	6
PECVD (100W O_2)	14.7 ± 4.1	277 ± 63	244 ± 68	2.81 ± 0.59	272.5	3.6

Concerning the results obtained for flax yarns treated with the TVS plasma, the average strength value measured for the yarns pretreated at 2 W is very similar to the one obtained for the yarns only treated with the 2 W power oxygen plasma. On the contrary, significantly higher strength values have been found for the 100 W pretreated flax (244 MPa ± 68 MPa) than for the yarns treated only with the 100 W power oxygen plasma (150 MPa ± 48 MPa). This enhancement of the mechanical properties of the TVS plasma treated flax yarn may be related to the filling and healing process of superficial defects by the polymeric layer deposited on flax yarns [Zinck *et al.*, 1999], as explained later in section IV.2.3.3. The experimental results appear to be well-fitted by a two-parameter Weibull distribution (Equation IV.1). In Table IV.12 are reported all the Weibull moduli and the characteristic strength values found for the treated and untreated flax yarns. The curves reported in Figure IV.24 represent the results of the two-parameter Weibull distribution applied to all the analysed flax yarns. A quasi-linear trend was found for both untreated and treated flax yarns. This trens indicates that the yarn failure depends on the presence of a single population of flaws in the flax yarn.

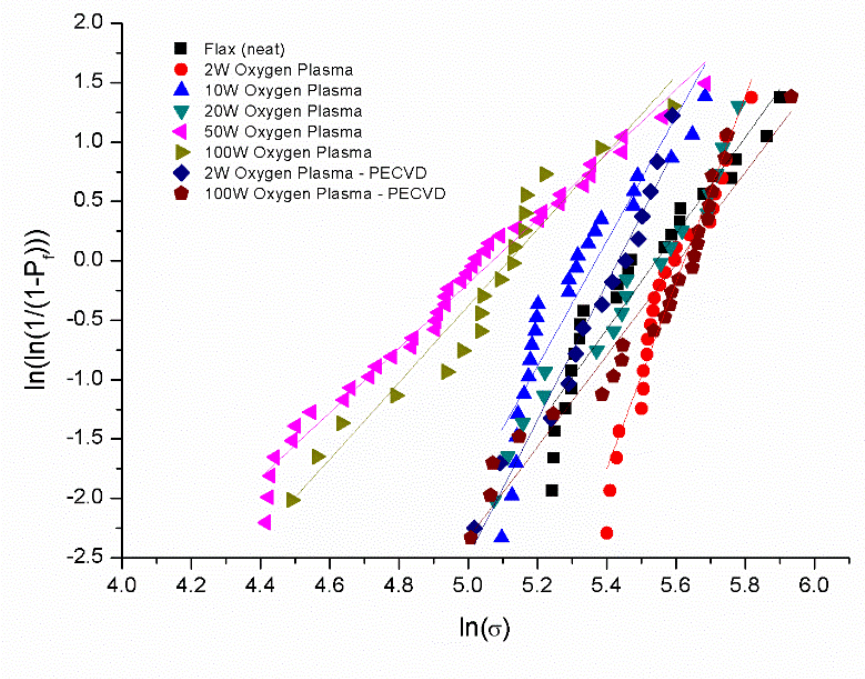

Figure IV. 24 Weibull distribution plots of strength measured for the different families of flax yarns.

CHAPTER IV.2

SURFACE MODIFICATION TREATMENTS OF BASALT

As reported in section II.1.1, the basalt fibres used in this study are characterized by the presence of a commercial sizing optimized for epoxy matrices. In the same way as glass fibres, basalt fibres are coated during their manufacturing steps with a sizing commonly by contacting an applicator roll [Thomason *et al.*, 1999]. The applied sizing consists in a mixture of organosilane polymer and a film former agent. The organosilane structure contains a reactive functional group and a hydrolizable group (like the alkoxy group). The functional group has the capability to react with an appropriate polymer and, the hydrolizable group can react with the fibre surface [Shokoohi *et al.*, 2008]. In this way, the organosilane is able to promote the production of bond bridges between the fibre and the organic matrix, improving the adhesion between them [Petersen *et al.*, 2013]. However, it is important to stress that much of the sizing normally used on basalt fibres is inherited directly from glass fibre technology, thus it is not necessarily designed for basalt fibres [Jenkins *et al.*, 2018]. Tailoring the sizing chemical composition is crucial in order to obtain a successful reinforcement product able to generate an appropriate fibre/matrix interface. In addition, mainly because of the application conditions used, the resulting coating is frequently non-uniform in all three dimensions of the fibres. The molecules of silane coupling agents are prone to self-condense, forming siloxane oligomers rather than a complete bonding with the fibre surface and, most notably, only a limited fraction (in the range 10–20%) of the total sizing is bonded to the fibre surface [Thomason, 1995]. In general, the amount of the applied sizing layer is comprised between 0.2–2% of the total fibre weight [Thomason *et al.*, 1999]. Variations in the structure or distribution of the coupling agent on the fibre surface may lead to a difference in the properties of the interface and thus of the composite performances. With the aim to analyse the effect of the sizing agents on the properties of basalt fibres, a thermal de-sizing treatment was performed. The thermal treatment was also considered as a

preliminary step in order to perform a subsequent plasma polymerization treatment. A tetravinylsilane coating was deposited on the surface of the thermally treated basalt fibres through Plasma-Enhanced Chemical Vapour Deposition (PECVD) process. In the next sections the experimental procedures used to perform both thermal and PECVD treatments will be described. Subsequently, the effects of the different treatments on the wetting, compositional, morphological and mechanical properties of basalt fibres will be discussed.

IV.2.1 Thermal de-sizing treatment

Several studies in literature have investigated the effect of different methods in order to remove the sizing agents from the surface of synthetic fibres. Petersen et al. [Petersen *et al.*, 2013] and Feih et al. [Feih *et al.*, 2005] reported that a soxhlet extraction is able to remove the physisorbed and soluble part of the sizing while the covalently bound part can be removed only performing a thermal treatment on fibres. Recently, a comparison between the effects of a sizing extraction using acetone and a thermal de-sizing process on basalt fibre properties has been carried out [Sarasini *et al.*, 2018]. The study highlighted that the soxhlet extraction was not able to completely remove the sizing, whereas a better effect was obtained after the thermal exposure of fibres. Based on these findings, in this experimental work the as-received basalt fibre bundles were thermally treated in order to remove their commercial sizing. The thermal de-sizing treatment was performed in a tube furnace (Lenton Thermal Designs Ltd, Figure IV.25) at a temperature of 400°C in air for 1 h.

Figure IV. 25 The Lenton Thermal tube furnace used.

The temperature of 400°C was selected in order to mimic the conditions typically experienced in an end-of-life composite thermal recycling process [Pickering, 2006]. In general, the fibres strength loss produced by the thermal exposure is not only temperature

but also time dependent. A strong decrease in the mechanical performances of basalt fibres was reported after a thermal de-sizing treatment carried out at 400°C for 4h [Sarasini *et al.*, 2018]. For this reason, in this experimental work, the shorter duration of 1h was selected in order to ensure a reduced drop in the mechanical performances of basalt fibres.

IV.2.2 Plasma-Enhanced Chemical Vapour Deposition

After the thermal treatment, a thin polymer film has been deposited on the unsized basalt fibres by Plasma-Enhanced Chemical Vapour Deposition (PECVD) process. Plasma deposition has been carried out in the same reactor used for the flax yarns described in section IV.1.1.2.1. As for the flax yarns, the polymer deposition treatment has been divided in two steps: a first non-polymerising oxygen plasma step, and a second step of polymerising gas plasma. During this last step a homogeneous tetravinylsilane (pp-TVS) coating was produced on the surface of basalt fibres. The pre-treatment with oxygen plasma was performed at 5.8 Pa and 100 W for 30 min, whereas the subsequent pp-TVS deposition was carried out at 3.8 Pa and 10 W for 15 min.

IV.2.3 The influence of thermal de-sizing and PECVD treatments on basalt properties

IV.2.3.1 Effects on wetting properties

To investigate the influence of sizing agents and polymer tetravinylsilane coating, a wetting analysis has been performed on as-received, thermally treated and plasma treated basalt fibres. Static and dynamic contact angles were measured through tensiometric method using water and diiodomethane as test liquids and results are reported in Table IV.13 and Table IV.14, respectively.

Table IV. 13 Advancing, receding and static contact angles values found for the different basalt fibres in water. The value of the contact angle hysteresis is also reported.

WATER	**Advancing Contact Angle [°]**	**Receding Contact Angle [°]**	**Static Contact Angle [°]**	**Hysteresis θ_a - θ_r [°]**
As-received Basalt	56.40 ± 7.25	36.87 ± 4.79	39.68 ± 5.77	19.5 ± 3
Basalt 400°C - 1h (sizing removal)	97.55 ± 0.18	46.20 ± 7.08	47.02 ± 7.77	50.6 ± 7.6
Basalt 400°C - 1h + PECVD	92.58 ± 9.03	69.32 ± 6.27	80.47 ± 2.61	23.2 ± 3

Table IV. 14 Advancing, receding and static contact angles values found for the different basalt fibres in diiodomethane. The value of the contact angle hysteresis is also reported.

DIIODOMETHANE	**Advancing Contact Angle [°]**	**Receding Contact Angle [°]**	**Static Contact Angle [°]**	**Hysteresis $\theta_a - \theta_r$ [°]**
As-received Basalt	70.95 ± 3.3	46.77 ± 11.78	52.36 ± 3.61	30.6 ± 18.1
Basalt 400°C - 1h (sizing removal)	82.93 ± 2	74.71 ± 2.45	76.25 ± 3.58	7.5 ± 1.6
Basalt 400°C - 1h + PECVD	69.29 ± 0.74	49.25 ± 7.48	53.28 ± 3.4	20 ± 7.2

Knowing contact angles, fibre surface energy and its dispersive and polar components, before and after thermal and plasma treatments, were determined through the Owens and Wendt equation (Eq. II.9). In Table IV.15 are reported all the dispersive γ_s^d and polar γ_s^p components of basalt fibres surface energy γ_s. The plots obtained with values of contact angles following the Owens and Wendt method for water and diiodomethane test liquids are reported in Figure IV.26.

Table IV. 15 Dispersive and polar components and the total surface energies of the different basalt fibres.

	γ^p [mN/m]	**γ^d [mN/m]**	**γ [mN/m]**	**Dispersivity degree [%]**
As-received Basalt	27.45 ± 3.41	33.06 ± 2.6	60.52 ± 6.01	54.63 ± 1.12
Basalt 400°C - 1h (sizing removal)	32.37 ± 5.06	19.71 ± 2.45	52.08 ± 7.51	37.84 ± 0.77
Basalt 400°C - 1h + PECVD	4.88 ± 0.72	32.37 ± 2.65	37.26 ± 3.37	86.83 ± 0.74

The first aspect emerging from the wetting analysis is a strong decrease in the polar component of surface energy after the plasma treatment. Basalt fibres present a quasi-totally dispersive behaviour proving that the plasma deposition process was able to make basalt fibres more hydrophobic. From the contact angle values found with diiodomethane (Table IV.14), the as-received and the plasma treated basalt fibres exhibit a very similar behaviour. On the contrary, a strong increase in advancing, receding and static contact angle values was measured with water after the plasma deposition process (Table IV.13). These results are confirmed by the surface energy estimation. From the values reported in Table IV.15, it is possible to notice that a strong reduction in the polar component of the surface energy was produced after the deposition of the pp-TVS film.

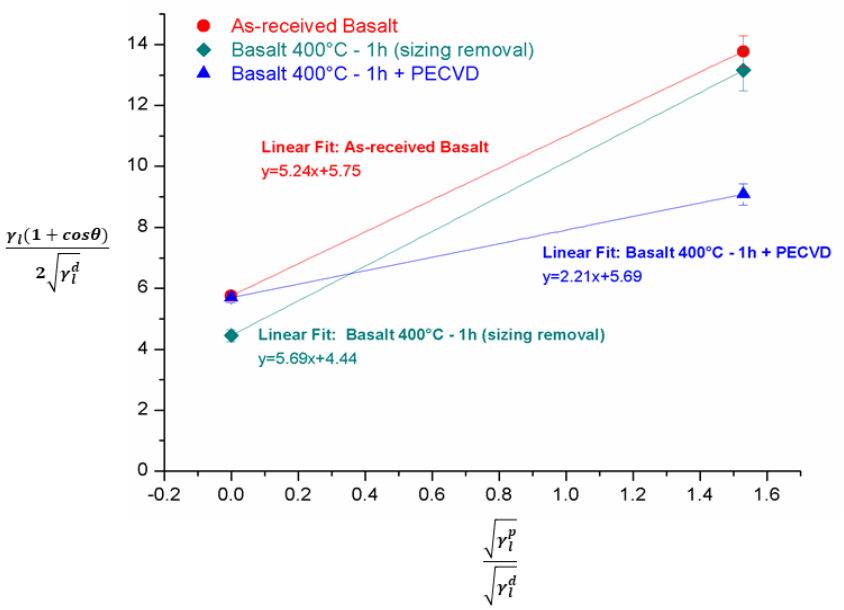

Figure IV. 26 Linear fits for surface energies obtained for the different basalt fibres tested.

The plasma treated basalt fibres showed a more dispersive and hydrophobic behaviour, with a dispersivity degree of 86.8%, compared to the untreated fibres, characterized by a dispersivity degree of 54.3%. Advancing and receding contact angle values were used in order to measure the contact angle hysteresis of the different basalt fibres. From values reported in Table IV.13, a strong increase in the contact angle hysteresis with water can be observed after the thermal exposure of basalt fibres. As described previously for flax fibres, the roughness of a solid surface can strongly influence the dynamic contact angles values, and consequently, the contact angle hysteresis. The reported high hysteresis value can be linked to the increase surface roughness promoted by the partial thermal removal of sizing. A strong increase in the advancing contact angle is produced after the plasma deposition of the TVS coating. However, in this case, the contact angle hysteresis is less pronounced than the thermally treated fibres. This is mainly due to the higher receding contact angle value. The dynamic contact angles are influenced by the presence of both high and low energy components on a solid surface [Bismarck *et al.*, 1999; Della Volpe *et al.*, 2001]. In general, the advancing contact angle should be characteristic for the low energy part of the fibre surface (i.e. organic groups) and the receding contact angle for the high energy part (i.e. inorganic groups). The deposition of the organic tetravinylsilane coating can produce an increase in the low energy surface part of basalt fibres and lead to an increase in their receding contact angle. From the different values reported in Table IV.14, it is possible to

notice that a little hysteresis is observed for both thermally and plasma treated fibres with diiodomethane. As described previously for flax fibres, the lower contact angle hysteresis depends on the properties of the diiodomethane probe liquid. A strong increase in advancing and receding contact angle values has been measured with diiodomethane after the thermal treatment (Table IV.14). In particular, the increase in the static contact angle highlights an enhancement of polarity of these fibres. This result is confirmed by both dispersive and polar surface energies components found (Table IV.15). The thermally treated basalt fibres showed a lower dispersivity degree, specifically 37.84%, than the untreated, 54.63%, and plasma treated, 86.83%, fibres. A similar result was found in literature [Pucci *et al.*, 2017]. The authors reported that basalt fibres show a polar nature after a thermal removal of the sizings. In particular, a polar component of the surface energy of 46.36 ± 12.32 mN/m was found, higher than the value of 32.37 ± 5.06 mN/m reported in the present study. This difference can be due to the longer exposure at the temperature of 400 ° C, 4h compared to 1h used in this work, and thus to a more complete removal of the sizing from the basalt surface.

IV.2.3.2 Effects on morphological and compositional characteristics

A morphological investigation of the lateral surfaces of the different basalt fibres was performed by FE-SEM. Figure IV.27 shows the micrographs for the untreated and treated basalt fibres. The comparison between Figure IV.27-a and Figure IV.27-b highlights the ability of the heat treatment in removing or at least deteriorating the protective sizing layer, exposing the superficial defects present on the as-received fibres. From figure IV.27-c it is possible to see that a continuous pp-TVS film has been produced by plasma polymerization process, which is able to spread homogeneously all over the lateral surface of basalt fibre. Some surface irregularities of pp-TVS film randomly dispersed along the fibre surface have been found, (Figure IV.27-c). As reported by Cech et al. [Cech *et al.*, 1999], the presence of these surface features may be connected with the plasma polymerization mechanism. In particular, it is possible that defects or surface irregularities present on the surface of the thermally treated basalt fibers may operate as nucleation centers of pp-TVS deposits. The presence of the pp-TVS film has been demonstrated by intentionally producing some scratches on the fibre surface (Figure IV.28-a,b).

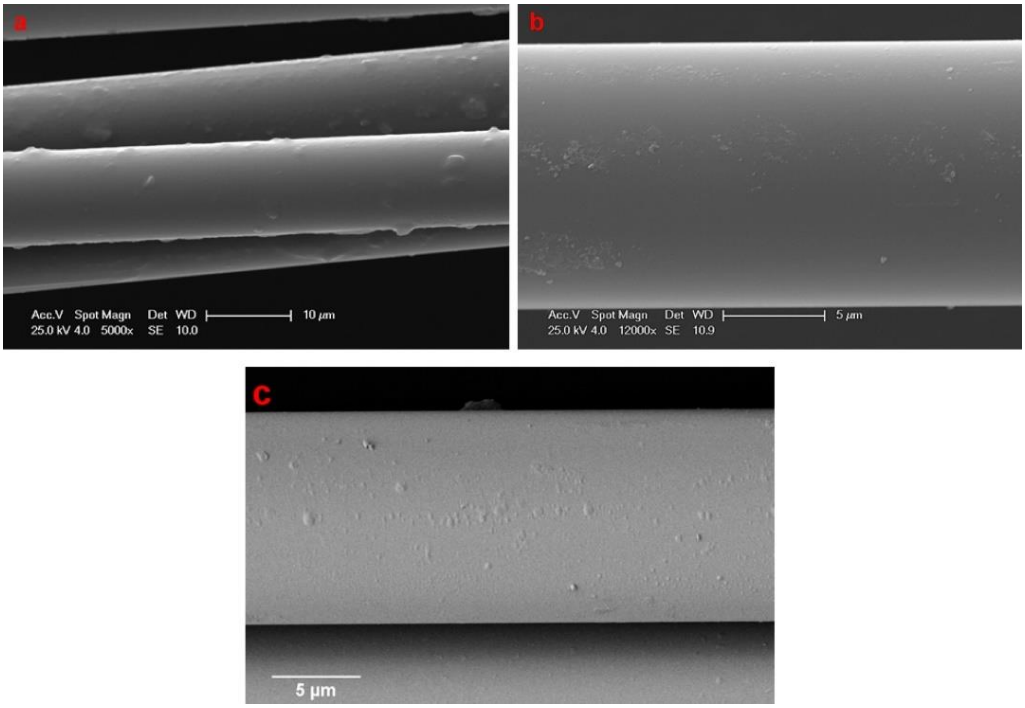

Figure IV. 27 Scanning electron micrographs detailing the lateral surface of untreated (a), thermally treated (b), plasma treated (c) basalt fibres.

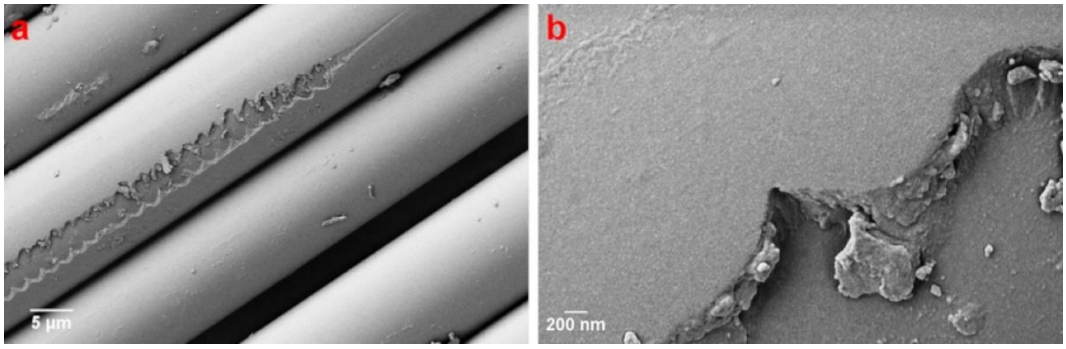

Figure IV. 28 Scanning electron micrographs of plasma polymer coated basalt fibres: (a) micrograph showing several uniformly plasma treated fibres and an intentionally scratched fibre, (b) with a detailed view of the damaged polymer film [Seghini et al., 2019].

The chemical composition of the treated and untreated basalt fibres was investigated by Fourier Transform Infrared Spectroscopy. The FT-IR spectra of as-received, thermally treated and plasma treated basalt fibres are shown in Figure IV.29. The spectral analysis revealed that in all samples a group of very strong absorption bands is observed in the region of 1270-600 cm^{-1}, due to the stretching vibrations of the Al\O\Si network. In particular, the absorption bands at 929 cm^{-1} and 763 cm^{-1} are due to the Si–O asymmetric stretching vibrational mode of SiO_4 tetrahedra and Si–O or Si–O–Al symmetric bending, respectively [Preston *et al.*, 2011]. Furthermore, the characteristic bands of O=C-NH of imine at 1650

cm^{-1}, the -NH bending at 1510 cm^{-1} and small peaks of -CH at 2852 and 2924 cm^{-1} were also visible in the as-received sample (Figure IV.29-a) [Kim *et al.*, 2009]. The latter should be due to the presence of the sizing in the as-received basalt fibre and, it disappeared after the thermal treatment (Figure IV.29-b). Typical infrared bands of plasma-polymerized tetravinylsilane (pp-TVS) films deposited on thermally treated basalt fibres can be seen in Figure IV.29-c. At the wavenumber range 3700-3100 cm^{-1} a significant band of -OH occurs. Following, wide bands in the range 3100-2750 cm^{-1} are due to vibrations of $-CH_2$ and $-CH_3$ groups. Significant bands due to C=O vibration at 1699 cm^{-1}, C=C stretching at 1651 cm^{-1}, $-CH_2$ scissoring at 1455 cm^{-1} and $=CH_2$ deformation at 1418 cm^{-1} in vinyl group can be observed. Finally, an increase in the band belonging to Si-O-Si stretching at 980 cm^{-1} is clearly visible in plasma-coated sample [Davidson, 1971; Cech *et al.*, 2007, 2014].

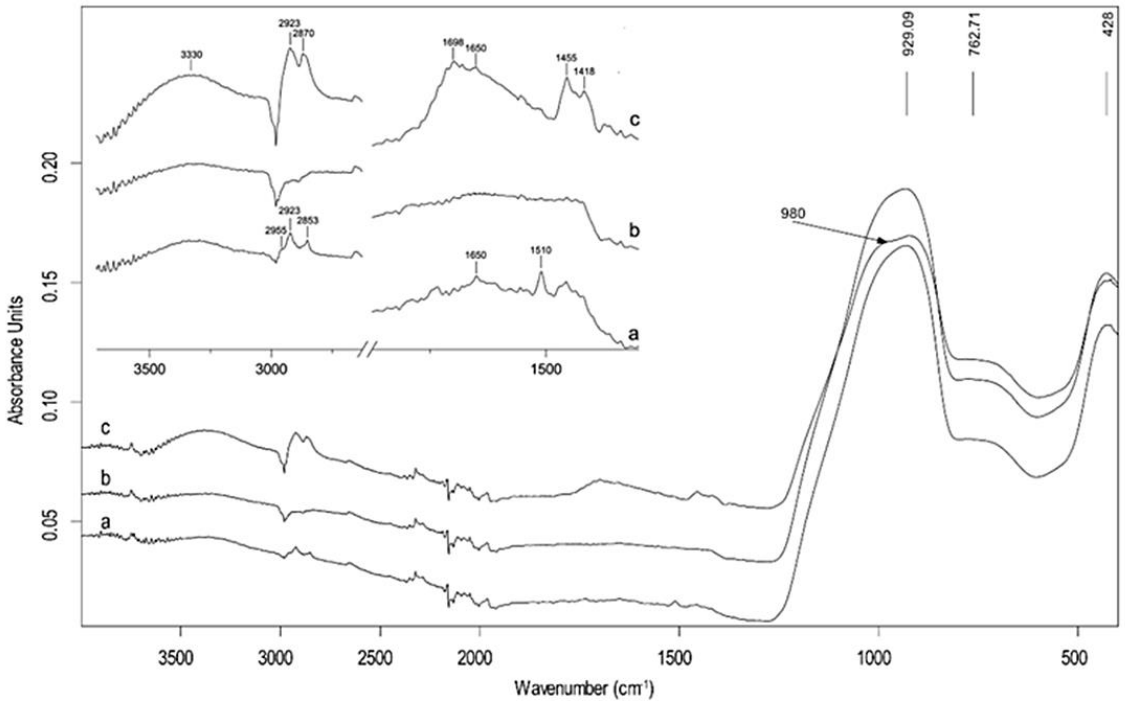

Figure IV. 29 Infrared spectra of as-received (a), thermally treated (b) and plasma treated (c) basalt fibres.

The surface roughness of the untreated and treated basalt fibres has been measured by AFM. Differences in the surface topography of the different basalt fibres have been found. The RMS roughness results from AFM data are reported in Table IV.16 while Figure IV.30 shows the different surface roughness plots for the different basalt fibres.

Table IV. 16 Average RMS roughness values for the as-received, thermally treated and plasma treated basalt fibres.

	Average RMS roughness [nm]
As-received Basalt	3.72 ± 0.45
Basalt 400°C - 1h (sizing removal)	7.57 ± 2.79
Basalt 400°C - 1h + PECVD	7.46 ± 2.23

A lower surface roughness has been found locally for the untreated basalt fibres, while an increase in surface roughness has been found for both thermally treated and plasma treated basalt fibres. In the first case, these results indicate that the heat treatment is able to remove, at least partially, the sizing layer present in the commercial fibres, thus exposing surface defects. After the plasma polymer deposition, the presence of a rougher surface has been highlighted, (Figure IV.30-c), likely due to the surface irregularities of pp-TVS film randomly dispersed along the fibre surface previously described (Figure IV.27-c).

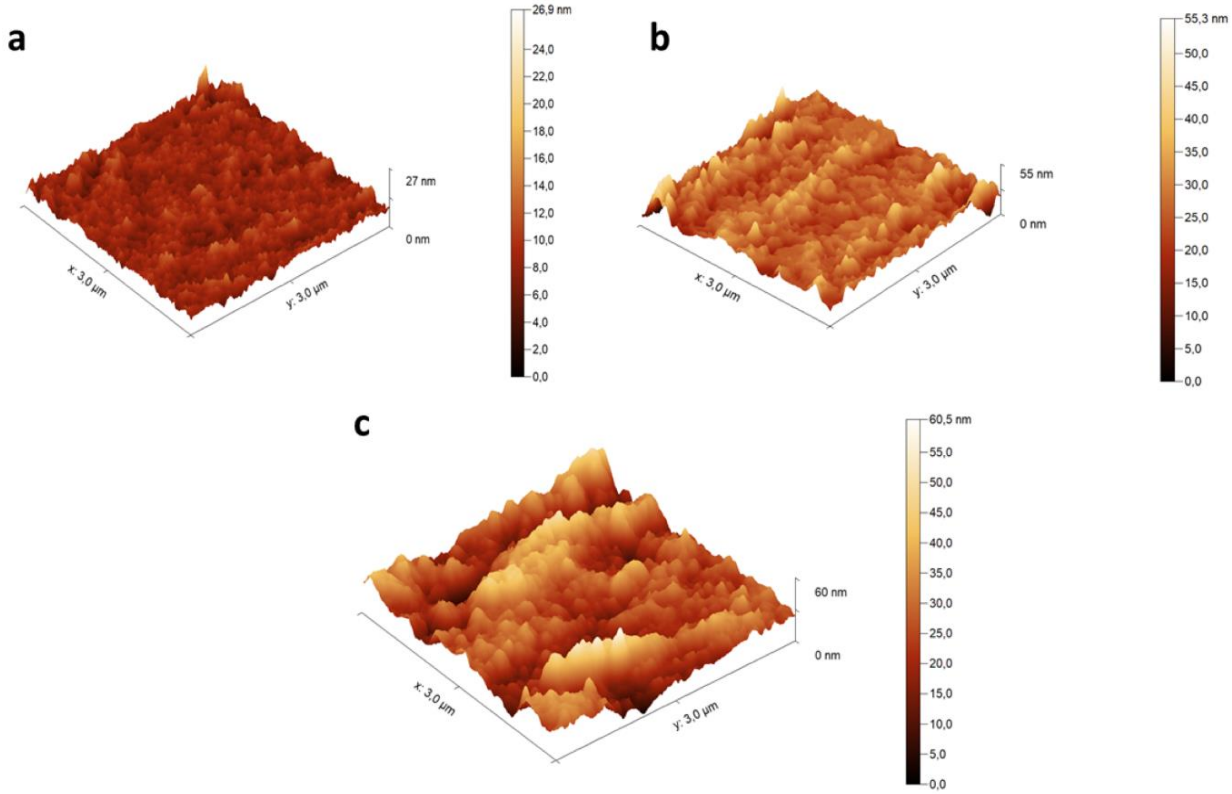

Figure IV. 30 3D topography plots of basalt fibres (BFs): (a) as-received BFs, (b) BFs treated at 400°C for 1h and (c) BFs thermally treated at 400°C for 1h and subsequently treated by PECVD [Seghini et al., 2019].

IV.2.3.3 Influence on mechanical properties

A mechanical characterization of untreated and treated basalt fibres was performed in order to investigate the effect of the different treatments on their tensile behaviour. The results found for the commercially sized basalt fibres, the thermally treated and the plasma treated basalt fibres are presented in Table IV.17. A strong dependence of tensile strength on gauge length was observed for all the different types of fibres. From results it is possible to observe that the failure strength tends to decrease with an increase of fibre gauge length. This decreasing trend can be linked to a "dimension effect" on the tensile strength of the brittle basalt fibres. The longer the fibres, the higher the probability to find defects on their surface [Berger *et al.*, 2003; Yang *et al.*, 2013]. By comparing the tensile results found for the as-received and treated basalt fibres, it is possible to notice that the thermal exposure was able to induce a decrease in the tensile strength of basalt fibres. If the strength values of the untreated and the thermally treated basalt fibres are compared, a significative reduction is found after the treatment at 400°C. This result can be linked to the loss of protective effect of the sizing agents present on the surface of the commercial basalt fibre. Several studies investigated the effect produced by the sizing coating on the mechanical properties of fibres [Zinck *et al.*, 1999; Feih *et al.*, 2005; Jenkins *et al.*, 2018]. These works showed that the sizing can influence the fibre mechanical properties because it can fully or partially fill the surface cavities, producing a sort of "flaw healing" effect. In a previous experimental work, the influence of temperature on the tensile behaviour of basalt fibres was investigated [Sarasini *et al.*, 2018]. The thermal removal of the organic coating from the basalt surface was considered as one of the responsible mechanisms of the fibre strength loss. The thermogravimetric results highlithed that a complete volatilization of the sizing coating was produced at temperatures ranging between 160°C and 400°C. This phenomenon produces a loss of the sizing healing effect of surface flaws, and thus leads to a reduction of mechanical properties. As highlighted by the morphological analysis (Fig. IV.27-b), the thermal de-sizing treatment was able to deteriorate the protective sizing layer of basalt fibre, producing an exposure of the superficial defects. On the contrary, the exposure to the plasma polymerization process after the heating treatment results in a partial recovery of the tensile properties of fibres. By comparing the results found for the thermally treated and plasma treated basalt fibres, an increase in the tensile strength has been detected after the pp-TVS

film deposition. The recovery phenomenon is significant in particular for the basalt fibres tested at a gauge length of 20 mm.

Table IV. 17 Tensile properties of untreated and treated basalt fibres.

	Gauge Length l_0 [mm]	σ_f [MPa]	εf [%]
As-received Basalt	20	2515 ± 277	2.41 ± 0.32
	30	2440 ± 164	2.6 ± 0.24
	40	2410 ± 277	2.5 ± 0.4
Basalt 400°C - 1h	20	1197 ± 311	1.47 ± 0.43
	30	1231 ± 387	1.42 ± 0.44
	40	1113 ± 296	1.36 ± 0.34
Basalt 400°C - 1h + PECVD	20	2218 ± 450	2.07 ± 0.62
	30	1763 ± 409	1.83 ± 0.48
	40	1478 ± 349	1.81 ± 0.41

Once again, this result may be ascribed to the healing effect of the pp-TVS deposited film on the surface defects of the thermally treated basalt fibres. The experimental results were statistically analysed using a two-parameter Weibull distribution, according to the equation IV.1. In table IV.18 are reported all the Weibull moduli and the characteristic strength values for the treated and untreated basalt fibres.

Table IV. 18 Weibull distribution parameters for untreated and treated basalt fibres.

	Gauge Length l_0 [mm]	Weibull modulus *m*	Characteristic strength σ_0 [MPa]
As-received Basalt	20	10.85	2634
	30	18.02	2513
	40	10.27	2530
Basalt 400°C - 1h	20	4.44	1312
	30	3.39	1373
	40	4.19	1226
Basalt 400°C - 1h + PECVD	20	5.78	2395
	30	5.32	1913
	40	4.84	1612

Weibull distribution plots of strength as a function of gauge length, for treated and untreated basalt fibres, are reported in Figure IV.31. A quasi-linear trend was found for all the Weibull distribution graphs, which indicates a mechanical behaviour influenced by the presence of a single population of defects. The thermal and the plasma treatments do not result in a change in the nature of the fibre defects, but rather they cause an increase in their concentration and severity.

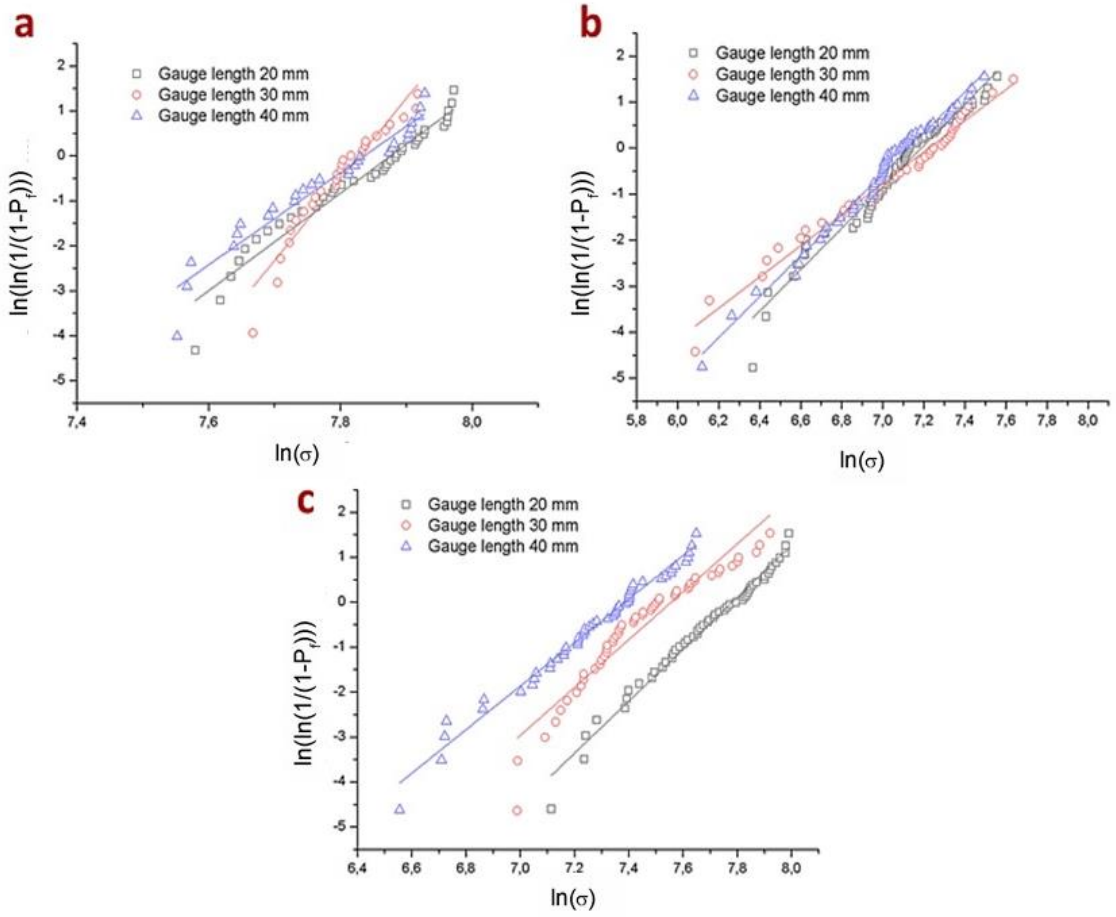

Figure IV. 31 Weibull plots of single fibre strength for the as-received (a), thermally treated (b) and plasma treated basalt fibres (c).

Conclusion of Part IV

The results obtained from the mechanical characterization of the different composites, discussed previously in Part III, have revealed the need to optimize the fibre/matrix interface adhesion quality, in order to increase the mechanical performance of the hybrid composites. The peculiar chemical composition, hydrophilic properties and surface characteristics of plant fibres prevent them from achieving a proper interfacial adhesion with the more hydrophobic polymer matrices. In this study, a careful analysis of the wetting properties of as-received flax yarns was carried out by performing a water drop test and a more accurate tensiometric test. The results proved that flax yarns are characterized by a strongly hydrophilic nature. This behaviour depends essentially on the chemical composition of flax. A FT-IR analysis highlighted that the untreated flax fibres consist of hydroxyl and strongly polarized groups, belonging to hemicellulose and cellulose, which confer a hydrophilic character to flax fibres limiting their compatibility with polymeric matrices.

In the same way as synthetic fibres, the basalt fibres are commercially available with the presence of specific coatings optimized to promote their adhesion with the polymer matrices. In general, these fibres are coated during their manufacturing steps. However, the resulting coating is not always characterized by a consistent thickness and uniformity. In addition, much of the sizing used on basalt fibres is inherited from glass fibre technology, thus being not necessarily designed for basalt fibres. All these issues can result in a low compatibility between basalt fibres and polymeric matrices.

In this framework, different surface modification treatments have been specifically designed and investigated for flax and basalt fibres with the aim of increasing their adhesion to thermoset matrices. Chemical and physical treatments were selected in order to modify the surface properties of flax. Among the chemical treatments, an enzymatic biochemical treatment and a supercritical CO_2 treatment were performed to promote the removal of undesirable substances such as pectin, hemicelluloses, lignin, fat, and waxes from the surface of flax fibres. The physical treatments including oxygen plasma and plasma polymerization were also used to modify the flax fibre surfaces. A wetting analysis performed through water drop test on enzymatically treated flax fabrics showed that pectinases and xyloglucanases

enzymes can successfully remove the pectin and hemicellulose content from flax, increasing its hydrophobic character. The major changes in wetting properties of flax were obtained after the deposition of the tetravinylsilane polymer film produced by the physical treatment of plasma polymerization process. A tensiometric method was used to measure contact angles and surface energies of flax yarns. The deposition of the polymer film produces a strong increase in the dispersive behaviour of flax fibres and a reduction in their surface wetting with polar liquid. The increased hydrophobicity of plasma treated flax yarn, compared to the untreated flax, was confirmed by an increase of about 30% in the static contact angle with water. Compositional and thermogravimetric analyses have confirmed the ability of both chemical and oxygen plasma treatments to produce a removal of hemicellulose, pectin and waxes. Despite these positive aspects, this experimental study showed the need to carry out an optimization of the different process parameters used, i.e. treatment times, enzyme solution concentrations and plasma power. In fact, except supercritical CO_2 treatment, all the different surface modification treatments resulted in a reduction in the tensile strength of flax yarns. In the case of enzymatic treatments, this decrease may be linked to an excessive enzymatic removal of non-cellulosic constituents of flax. In particular, lignin is a structural component and its degradation can result in a decrease in fibre tensile strength. A morphological analysis performed by FE-SEM showed that the enzymatic solution leads to bundle fibrillation of the treated flax yarns. This phenomenon could result in a decay in the mechanical performance of the yarn. A close connection was proved to exist between the oxygen plasma treatment and the mechanical properties of flax. FE-SEM micrographs showed that oxygen plasma involves a surface ablation of flax fibres, generating defects such as pits, voids and spaces. A strength value decrease, until a reduction of 36.4%, was obtained after the oxygen plasma treatment using a plasma power of 100 W. The effect of the different chemical and physical treatments on the adhesion properties of flax yarns with both epoxy and vinylester matrices will be discussed in the next Part V. The interfacial adhesion was explored by single filament fragmentation test (SFFT). This analysis was performed only for the treatment conditions considered as the most interesting in the perspective of an effective interfacial adhesion enhancement. Specifically, the SFFTs were performed on:

- as-received flax yarns;
- enzymatically treated flax yarns using the 5 wt% of Peclyve solution for 4.5h;
- enzymatically treated flax yarns using the 10 wt% of Peclyve solution 6h;

- flax yarns treated by supercritical CO_2 treatment;
- oxygen plasma treated flax yarns using the minimum plasma power of 2 W;
- oxygen plasma treated flax yarns using the maximum plasma power of 100 W;
- PECVD treated flax yarns, with an oxygen plasma pre-treatment performed at 2W;
- PECVD treated flax yarns, with an oxygen plasma pre-treatment performed at 100 W.

The physical treatment of plasma polymerization process was also used in order to modify the surface properties of basalt fibres. The effects produced by the plasma deposition of a tetravinylsilane polymer film on to the basalt surface were compared with those obtained by using a commercial coupling agent optimized for epoxy resins and a thermal de-sizing treatment performed at 400°C for 1 h. The crucial aspect that emerged from this study is the ability of the plasma polymer deposition to produce a strong increase in the hydrophobic behaviour of the basalt fibres, in comparison to both the commercial and the thermally treated fibres. After the deposition of the tetravinylsilane, basalt fibres showed a strong increase in the static contact angle with water, passing from a value of 39.68 ° for the commercial fibres to a value of 80.47 ° for the plasma treated fibres. The effective ability of the plasma treatment to produce a continuous tetravinylsilane coating on the basalt surface was confirmed by both morphological and compositional analysis. Due to an exposure of surface defects, an increase in roughness was measured for the thermally and plasma treated basalt fibres. This effect combined with the increase in hydrophobic behaviour may constitute a key factor in order to promote the adhesion of the fibres with the polymeric matrix. In fact, a greater fibre/matrix compatibility can be promoted not only by the creation of chemical interactions, but also by the production of mechanical interlocking between the fibre and matrix surfaces. Similarly to commercial sizing, the tetravinylsilane coating protects the fibre surfaces and performs an “healing” effect of the existing fibre defects. In fact, the mechanical characterization carried out on single basalt fibres has shown how, despite the loss of strength due to the thermal exposure, the plasma polymerization treatment allows to obtain a partial recovery of the mechanical performance of the fibres. In order to assess the effect of the different treatments on the adhesion properties of basalt fibres with both the epoxy and vinylester matrices, SFFTs were performed. In particular, tests were carried out on:

- as received basalt fibres;
-thermally treated basalt fibres, at 400°C for 1h;

-thermally treated (400°C for 1h) ad subsequentially PECVD treated basalt fibres.

The results will be in depth discussed in the next Part V.

Conclusion de la Partie IV

(en français)

Les résultats obtenus à partir de la caractérisation mécanique des différents composites, discutés précédemment dans la partie III, ont révélé la nécessité d'optimiser la qualité d'adhésion de l'interface fibre/matrice, afin d'augmenter les performances mécaniques des composites hybrides. La composition chimique particulière, les propriétés hydrophiles et les caractéristiques de surface des fibres végétales empêchent d'obtenir une bonne adhésion interfaciale avec les matrices polymères plus hydrophobes. Dans cette étude, une analyse des propriétés de mouillage des fils de lin reçus a été réalisée en effectuant le test de la goutte d'eau et des mesures tensiométriques plus précises. Les résultats ont prouvé que les fils de lin se caractérisent par une nature fortement hydrophile. Ce comportement dépend essentiellement de la composition chimique du lin. Une analyse FT-IR a mis en évidence que les fibres de lin non traitées sont constituées de groupes hydroxyles fortement polarisés, appartenant à l'hémicellulose et à la cellulose, qui confèrent un caractère hydrophile aux fibres de lin limitant leur compatibilité avec les matrices polymères. De la même manière que les fibres synthétiques, les fibres de basalte sont disponibles dans le commerce avec la présence de revêtements spécifiques optimisés pour favoriser leur adhésion avec les matrices polymères. En général, ces fibres sont enrobées lors de leur fabrication. Cependant, le revêtement résultant est caractérisé par une épaisseur et une uniformité variables. De plus, une grande partie des techniques de traitement de surface utilisées sur les fibres de basalte est héritée de la technologie des fibres de verre, et n'est donc pas nécessairement conçue pour les fibres de basalte. Tous ces problèmes peuvent entraîner une faible compatibilité entre les fibres de basalte et les matrices polymères. Dans ce cadre, différents traitements de modification de surface ont été spécifiquement conçus et étudiés pour les fibres de lin et de basalte dans le but d'augmenter leur adhésion aux matrices thermodures. Des traitements chimiques et physiques ont été sélectionnés afin de modifier les propriétés de surface du lin. Parmi les traitements chimiques, un traitement biochimique enzymatique et un traitement au CO_2 supercritique ont été effectués pour favoriser l'élimination des substances indésirables telles que la pectine, les hémicelluloses, la lignine, les graisses et les cires de la surface des fibres de lin. Les traitements physiques, dont le plasma d'oxygène et la polymérisation plasma, ont également été utilisés pour modifier les surfaces des fibres de lin. Une analyse de mouillabilité effectuée par le test de la goutte d'eau sur des tissus de lin traités par enzymes a montré que les pectinases et les xyloglucanases peuvent éliminer avec succès la teneur en pectine et hémicellulose du lin, augmentant son caractère hydrophobe. Les changements majeurs dans les propriétés de mouillage du lin ont été obtenus après le dépôt du film polymère de tétravinylsilane produit par le traitement physique du procédé de polymérisation plasma. Une méthode tensiométrique a été utilisée pour mesurer les angles de contact et les énergies de surface des fils de lin. Le dépôt du film polymère produit une forte augmentation du comportement dispersif des fibres de lin et une diminution de leur mouillage superficiel par le liquide polaire. L'hydrophobicité accrue du fil de lin traité au plasma, par rapport au lin non traité, a été confirmée par une augmentation

d'environ 30% de l'angle de contact statique avec l'eau. Des analyses de composition et de thermogravimétrie ont confirmé la capacité des traitements chimiques et des traitements au plasma d'oxygène de produire une élimination de l'hémicellulose, de la pectine et des cires. Malgré ces aspects positifs, cette étude expérimentale a montré la nécessité de réaliser une optimisation des différents paramètres du procédé utilisé, à savoir les temps de traitement, les concentrations de solution enzymatique et la puissance du plasma. En fait, à l'exception du traitement au CO_2 supercritique, les différents traitements de modification de surface ont entraîné une réduction de la résistance à la traction des fils de lin. Dans le cas des traitements enzymatiques, cette diminution peut être liée à une élimination enzymatique excessive des constituants non cellulosiques du lin. En particulier, la lignine est un composant structurel et sa dégradation peut entraîner une diminution de la résistance à la traction des fibres. Une analyse morphologique réalisée par FE-SEM a montré que la solution enzymatique conduit à une fibrillation des faisceaux des fils de lin traités. Ce phénomène pourrait entraîner une dégradation des performances mécaniques du fil. Il a été prouvé qu'un lien étroit existait entre le traitement au plasma d'oxygène et les propriétés mécaniques du lin. Les micrographies FE-SEM ont montré que le plasma d'oxygène implique une ablation de surface des fibres de lin, générant des défauts tels que des creux, des vides et des espaces. Une diminution de la valeur de résistance en traction, jusqu'à 36,4%, a été obtenue après le traitement au plasma d'oxygène en utilisant une puissance de plasma de 100 W. L'effet des différents traitements chimiques et physiques sur les propriétés d'adhésion des fils de lin avec des matrices époxy et vinylester sera discuté dans la partie V. Dans cette partie, l'adhésion interfaciale sera analysée grâce à des tests de fragmentation sur composite monofilamentaire (SFFT). Cette analyse sera réalisée uniquement pour les conditions de traitement considérées comme les plus intéressantes dans la perspective d'une amélioration efficace de l'adhésion interfaciale. Des tests seront donc réalisés sur :

- fils de lin non traités ;
- fils de lin traités par voie enzymatique en utilisant la solution de Peclyve à 5% en masse pendant 4,5 heures ;
- fils de lin traités par voie enzymatique en utilisant la solution de Peclyve à 10% en masse pendant 6h ;
- fils de lin traités au CO_2 supercritique ;
- fils de lin traités au plasma d'oxygène avec une puissance de 2W ;
- fils de lin traités au plasma d'oxygène avec une puissance de 100W ;
- fils de lin traités par PECVD, avec un prétraitement au plasma d'oxygène effectué à 2W ;
- fils de lin traités par PECVD, avec un prétraitement au plasma d'oxygène effectué à 100W.

Le procédé de polymérisation par plasma a également été utilisé afin de modifier les propriétés de surface des fibres de basalte. Les effets produits par le dépôt d'un film de polymère de tétravinylsilane sur la surface du basalte ont été comparés à ceux obtenus en utilisant un agent de couplage commercial optimisé pour les résines époxy et à ceux obtenus après un traitement thermique effectué à 400°C pendant 1h pour enlever cet agent de couplage. L'aspect crucial qui est ressorti de cette étude est la capacité du dépôt de polymère par plasma à produire une forte augmentation du comportement hydrophobe des fibres de basalte, par rapport aux fibres

commerciales et aux fibres traitées thermiquement. Après le dépôt du tétravinylsilane, les fibres de basalte ont montré une forte augmentation de l'angle de contact statique avec l'eau, passant d'une valeur de 39,68° pour les fibres commerciales à une valeur de 80,47° pour les fibres traitées au plasma. La capacité effective du traitement au plasma à produire un revêtement continu de tétravinylsilane sur la surface du basalte a été confirmée par l'analyse morphologique et chimique. À cause d'une exposition des défauts de surface, une augmentation de la rugosité a été mesurée pour les fibres de basalte traitées thermiquement et par plasma. Cet effet associé à l'augmentation du comportement hydrophobe peut constituer un facteur clé pour favoriser l'adhésion des fibres à la matrice polymère. Une plus grande compatibilité fibre/matrice peut être favorisée non seulement par la création d'interactions chimiques, mais également par la production d'un ancrage mécanique entre la fibre et la matrice. De façon similaire au procédé commercial, le revêtement de tétravinylsilane protège les surfaces des fibres et effectue un effet «cicatrisant» des défauts de surface des fibres existants. En effet, la caractérisation mécanique réalisée sur des fibres de basalte seules a montré comment, malgré la perte de résistance en traction due à l'exposition thermique, le traitement de polymérisation par plasma permet d'obtenir une récupération partielle des performances mécaniques des fibres. Afin d'évaluer l'effet des différents traitements sur les propriétés d'adhésion des fibres de basalte avec les matrices époxy et vinylester, des SFFT seront réalisés. En particulier, des tests seront effectués sur:

- les fibres de basalte non traitées ;
- les fibres de basalte traitées thermiquement à 400°C pendant 1h ;
- les fibres de basalte traitées thermiquement à 400°C pendant 1h puis traitées par PECVD.

Les résultats sont présentés et discutés dans la partie V.

PART V

INTERFACIAL PROPERTIES OF FLAX AND BASALT FILAMENTS IN THERMOSET MATRIX COMPOSITES

The Part V is focused on the assessment of the adhesion properties of flax yarns and basalt fibres with both epoxy and vinylester matrices. In particular, the effect of the different chemical and physical treatments on the filament/matrix interface properties will be investigated. The interfacial adhesion will be explored by single filament fragmentation test. The Chapter V.1 will focus on the interfacial properties of flax/epoxy and flax/vinylester composites. The first part of the chapter will address the effects of enzymatic and supercritical CO_2 treatments on the compatibility of flax yarns, while the assessment of the effect of oxygen and tetravinylsilane plasma treatments will be discussed in the second part of the chapter. Concerning the basalt fibres, the interfacial adhesion of plasma-polymerized basalt fibres in epoxy and vinylester based composites will be investigated in Chapter V.2. The results obtained from the single filament fragmentation tests will be compared with those obtained for commercially sized basalt fibres and basalt fibres after sizing removal.

PART V – INTERFACIAL PROPERTIES OF FLAX AND BASALT FILAMENTS IN THERMOSET MATRIX COMPOSITES

CHAPTER V.1

INTERFACIAL ADHESION ASSESSMENT IN FLAX/EPOXY AND IN FLAX/VINYLESTER COMPOSITES

V.1.1 Effects of chemical modification treatments on interfacial properties of flax yarns in thermoset matrix composites

As discussed in depth in Part IV, different surface modification treatments were performed in order to enhance the interfacial adhesion of flax yarns with thermoset resins. The effect of the chemical treatments, both enzymatic and supercritical CO_2 (SC-CO_2), on the compatibility of flax yarns with epoxy and vinylester matrices will be discussed in the next sections of the present chapter. Regarding the enzymatically treated flax yarns, the interfacial adhesion analysis was focused on two specific treatment conditions. In fact, according to the wetting test results (section IV.1.3.1) and to the obtained tensile strength values (section IV.1.3.3), single filament fragmentation tests were performed on flax yarns treated using the 5 wt% and the 10 wt% of Peclyve enzymatic solution for 4.5h and 6 h, respectively. From the water retention time values reported in Table IV.2, it was possible to notice that flax fabrics showed an increase in their hydrophobic behaviour starting from a solution concentration of 5 wt% and a duration of 3 h. The 5 wt% - 4.5h condition was selected because it allowed to obtain changes in the wetting properties of flax yarns without significantly affecting their mechanical performance. Indeed, this enzymatic treatment condition produced a reduction in the tensile strength of the yarns of approximately 27% (Table IV.7). On the other hand, the condition of 10 wt% for 6h was selected in order to assess the effects of the maximum concentration of Peclyve solution and of the maximum treatment duration on the adhesion quality between flax yarns and thermoset matrices.

V.1.1.1 Determination of critical fragment length

The critical fragment length plays an essential role in determining the adhesion quality in a composite. The measurement of the critical fragment length is directly correlated to the shear stress value transferred at filament/matrix interface. As reported by Zafeiropoulos et al. [Zafeiropoulos *et al.*, 2002; Zafeiropoulos, 2007], a very interesting approach to assess the interface properties in a composite material is the model proposed by Fraser et al. [Fraser *et al.*, 1983]. In this approach, the adhesion quality is not estimated from the measurement of the interfacial shear stress but rather by the fragment length values. The principle of the approach introduced by Fraser and co-authors is that, at saturation level, the critical fragment length reflects the stress transfer efficiency at the interface and thus it offers a qualitative value of the interfacial bond. As reported in section I.2.2.1, according to Ohsawa et al. [Ohsawa *et al.*, 1978] the critical fragment length value was evaluated using Equation I.18. After fragmentation tests, optical microscopy was used to measure the fragment filament length values in the gauge length region of the different monofilament specimens. In Figure V.1 is reported a typical micrograph obtained for the fragmented flax yarn. In particular, the fragment lengths have been determined as the average values between the internal and the central points of the breaking zones.

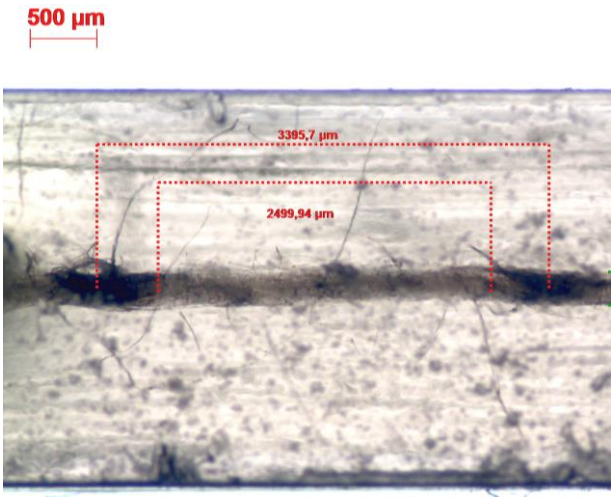

Figure V. 1 Typical optical micrographs of a fragmented flax yarn: measurement of the yarn fragment length.

A comparison between the critical fragment lengths measured for the untreated and the chemically treated single yarn composites is shown in Table V.1. For each family of monofilament composites, at least 10 fragmentation tests were carried out and, a

measurement of about 80 critical fragment lengths was performed. From the results it is possible to observe that the enzymatic and the SC-CO_2 treatments produced a slight reduction in the critical fragment length of flax yarns in both epoxy and vinylester matrices.

Table V. 1 Critical fragment length values for the untreated and chemically treated single yarn composites.

Matrix	Flax yarn	l_c [µm]
Epoxy	Neat	2687 ± 631
	Peclyve EXG 5 wt% - 4.5 h	2628 ± 531
	Peclyve EXG 10 wt% - 6 h	2511 ± 203
	Supercritical CO_2	2587 ± 623
Vinylester	Neat	3942 ± 807
	Peclyve EXG 5 wt% - 4.5 h	3962 ± 243
	Peclyve EXG 10 wt% - 6 h	3554 ± 776
	Supercritical CO_2	3345 ± 490

With reference to the enzymatic treatment, the results indicate that the best adhesion quality was produced after the treatment performed using the maximum concentration value of 10 wt% and the maximum treatment duration of 6 h. Differently, the flax/epoxy and the flax/vinylester systems with the flax yarn treated using the 5 wt% of Peclyve solution for 4.5h showed a critical fragment length value almost equal to that obtained for the untreated single yarn composites. However, it must be emphasized that the approach proposed by Fraser and co-authors, to assess the adhesion properties of different filament/matrix systems through the comparison of critical fragment length values, can be applied only in the case the filament strength values are the same for all the systems. As already described, as the tensile load increases during the fragmentation test, the filament inside the resin will break repeatedly into increasingly smaller fragments, at locations where the filament axial stress reaches its failure tensile strength. Therefore, it is easy to deduce that there is a strong dependence between the fragment length value and the filament tensile strength. The greater the failure strength value of a filament, the greater the length needed to reach this load and provide fragmentation. In this study, the as-received and the chemically treated flax yarns are characterized by significantly different tensile strength values. The results of the single yarn tensile tests, reported in section IV.1.3.3, showed that both the enzymatic and supercritical CO_2 modification treatments affected the mechanical performance of flax yarns. In particular, a marked loss of tensile strength was obtained after the enzymatic treatment performed by a 10 wt% Peclyve solution for 6 h. For these reasons, it should not

be proper to evaluate the differences in interfacial bond of the different flax yarn/epoxy and flax yarn/vinylester systems in terms of critical fragment length. However, a comparison between the different values found for a same flax yarn family with the epoxy and vinylester matrices is admissible. The two thermoset systems exhibited different results. From values reported in Table V.1, it is possible to see how the flax/epoxy samples are characterized by smaller values of critical fragment lengths than the flax/vinylester ones, indicating a better adhesion quality between flax yarn and epoxy resin than that observed for the vinylester matrix. This difference in adhesion quality between the epoxy and vinylester systems can be related to the different ability of the two polymer resins to wet the surface of flax yarns. As reported in section II.1.2, it is important to stress that the vinylester resin selected for this experimental work is an innovative styrene-free resin in which the styrene monomer is replaced by 1,4-butanediol dimethacrylate (BDDMA). Recently, Bénéthuilière et al. [Bénéthuilière et al., 2015] investigated the potential of a styrene-free resin on the adhesion level of E-glass fibres performing the microbond test. As in the present study, the BDDMA was used as reactive diluent for the styrene-free resin and the results were compared with those found with a conventional vinylester resin. The authors reported that the styrene-free resin displayed a lower ability than a conventional vinylester resin to wet E-glass fibres having a vinylester -compatible sizing. This phenomenon could be due to the fully dispersive nature of the styrene-free resin, while the E-glass fibres have a much higher polar characteristic. As described in detail in Chapter IV.1, flax yarns are characterized by a strongly polar behaviour which can explain the low compatibility with the fully dispersive styrene-free vinylester resin.

V.1.1.2 Calculation of interfacial shear strength

The interfacial shear strength value (IFSS) was estimated in order to describe the yarn/matrix interface adhesion quality. This value was determined for the different untreated and treated flax yarn/epoxy systems using the Equation I.19, according to the model proposed by Kelly and Tyson [Kelly *et al.*, 1965]. Because of the small l_c values, it was impossible to measure experimentally the tensile strength of a single yarn at a length equal to the critical one. To overcome this problem, an extrapolation of strength at critical length l_c was realized. Two different ways of extrapolation have been taken into consideration in this study. The first method has been proposed by El Asloun et al. [El Asloun *et al.*, 1989]. According to this

study, it is possible to extrapolate the maximum stress of flax yarn at small gauge lengths from tensile tests performed at several large gauge lengths. It is possible to do this extrapolation by taking the logarithm of stress in Equation V.1:

$$ln(\sigma_f) = -\frac{1}{m_i} ln(L_0) + ln[\sigma_0^i \Gamma\left(1 + \frac{1}{m_i}\right)] \quad \text{(V.1)}$$

where m_i and σ^i_0 are the shape and the scale parameters of the equivalent Weibull distribution, respectlively, L_0 the gauge length, σ_f the tensile strength and Γ the Gamma function. Thus, the tensile strength of a flax yarn at a given gauge length can be easily estimated by linear extrapolation using Equation V.1.

The second extrapolation method taken into account in this study is based on the Weibull cumulative distribution function determined for only one given filament gauge length L_0. This method has been widely used in literature [Joffe *et al.*, 2003, 2005; Zafeiropoulos, 2007; Ramirez *et al.*, 2008; Guillebaud-Bonnafous *et al.*, 2012]. According to these studies, using the obtained two-parameter Weibull distribution, the average filament strength may be evaluated by Equation V.2:

$$< \sigma_f > = \sigma_0 L_0^{-\frac{1}{m}} \left[\Gamma\left(1 + \frac{1}{m}\right)\right] \quad \text{(V.2)}$$

where Γ is the Gamma function and σ_0 and m are the characteristic life and the Weibull modulus for the tested gauge length L_0, respectively. By applying equation (V.2) to L_0 and to the critical length l_c, it was possible to obtain the following Equation V.3:

$$\sigma_f(l_c) = \sigma_f(L_0) \left(\frac{L_0}{l_c}\right)^{-\frac{1}{m}} \quad \text{(V.3)}$$

As reported in section IV.1.3.3, the tensile strength of the as-received flax yarn was evaluated at three different gauge lengths, namely 20 mm, 30 mm and 40 mm. For these yarns it was thus possible to use both the linear extrapolation method (with equation V.1) and the Weibull weakest link theory (with equation V.3), in order to determine the yarn strength at a length equal to the critical yarn length, $\sigma_f(l_c)$, and so the IFSS values. Concerning the first method,

in Figure V.2 is reported the graph plotting $ln(\sigma_f)$ against $ln(L_0)$. A linear trend was found, characterized by a slope of $-\frac{1}{m_i} = -0.2$.

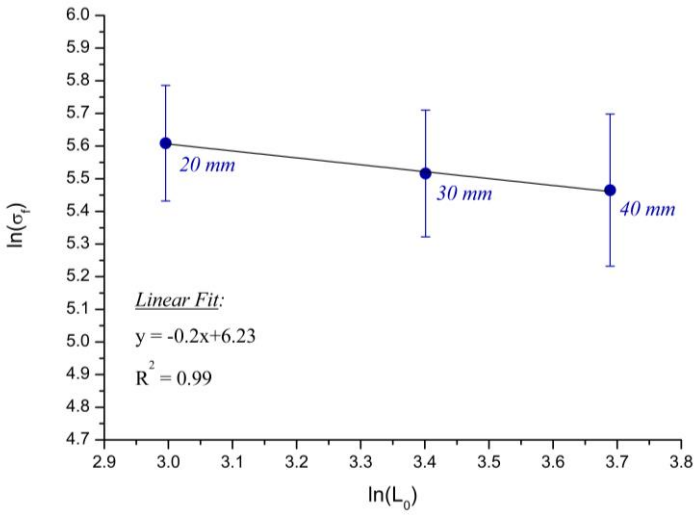

Figure V. 2 Evolution of tensile strength of flax yarn versus gauge length.

In Table V.2 are reported the results obtained with both linear extrapolation and Weibull methods. The negligible difference found for the different flax yarn $\sigma_f(l_c)$ and IFSS values proves the validity of both calculation methods. Concerning the analysis of the untreated flax yarn/matrix adhesion quality, from Table V.2 it is possible to see that the IFSS values reflect the results already found by comparing the critical filaments lengths. In fact, from the IFSS values, it is possible to point out that the flax yarn/epoxy system is characterized by a better interface quality than the flax/vinylester one.

Table V. 2 Interfacial shear strength values for the untreated flax/epoxy and flax/vinylester single yarn composites: 1- linear extrapolation method; 2- two-parameter Weibull theory.

	l_c/d mean	**$\sigma_f(l_c)$ 1 [MPa]**	**$\sigma_f(l_c)$ 2 [MPa]**	**IFSS 1 [MPa]**	**IFSS 2 [MPa]**
Flax/Epoxy Resin	10.75 ± 1.61	416 ± 19	406 ± 18	19.8 ± 3.8	19.3 ± 3.7
Flax/Vinylester Resin	13.7 ± 1.81	383 ± 16	376 ± 15	14.1 ± 2.9	13.9 ± 2.8

Contrary to the as-received flax yarns, the tensile properties of the different treated flax yarns were measured by single filament tensile tests performed at the single gauge length L_0 of 40 mm. Therefore, for these yarns, the Weibull method was used in order to determine the yarn strength at a length equal to the critical yarn length, $\sigma_f(l_c)$, and so the IFSS values. The used

Weibull parameters for this method are those obtained from single filaments tensile tests on the different flax yarns, reported in Table IV.7-8. The strength values at critical fragment length and the IFSS values found for the untreated and the chemically treated flax/epoxy and flax/vinylester systems are reported in Table V.3. By comparing the results found after the enzymatic treatment with those obtained for the as-received flax yarns, it is possible to highlight that a reduction in the IFSS values was produced after both surface modification treatments. This is especially true for the flax yarns enzymatically treated using the 10 wt% of Peclyve solution for 6 h.

Table V. 3 Strength values at critical fragment length and IFSS values for the untreated and chemically treated flax/epoxy and flax/vinylester systems.

Matrix	Flax Yarn	$\sigma_f(l_c)$ [MPa]	IFSS [MPa]
Epoxy	Neat	406 ± 18	19.3 ± 3.7
	Peclyve EXG 5 wt% - 4.5 h	283 ± 10	18.1 ± 2.7
	Peclyve EXG 10 wt% - 6 h	203 ± 3	12.2 ± 1.1
	Supercritical CO_2	312 ± 10	15.7 ± 2.1
Vinylester	Neat	376 ± 15	13.9 ± 2.8
	Peclyve EXG 5 wt% - 4.5 h	262 ± 2	10. 5 ± 1.4
	Peclyve EXG 10 wt% - 6 h	188 ± 9	7.8 ± 2
	Supercritical CO_2	300 ± 6	14.3 ± 2.6

A bad interfacial adhesion betwenn the treated flax yarns and both epoxy and vinylester matrices could be deduced from these results. However, as highlighted previously for the critical fragment length values, it is important to stress that the IFSS results are strictly dependent on the strong reduction in the mechanical properties of flax yarns produced by the chemical treatments. After the 10 wt% Peclyve – 6h treatment, the tensile strength at a length equal to the critical yarn length was reduced by 50%, producing a strong decrease in the interfacial shear strength value with the epoxy and the vinylester resin. Particularly interesting are the interfacial shear strength values obtain for the supercritical CO_2 treated flax yarn/vinylester system. It is important to recall that this treatment did not produce a strong change of the tensile properties of flax yarns (Table IV.8). It is therefore possible to directly compare the IFSS values obtained after the SC-CO_2 treatment with those found for the as-received flax yarn. Considering the flax/vinylester system, a sligth increase in the interfacial adhesion is produced after the exposure of flax yarn to the supercritical fluid. On

the contrary, a decrease in IFSS value is reported with the epoxy matrix. However it has to be noted that, as reported previously in section IV.1.3.3, an increase in the average diameter of yarns was produced by the exposure to the supercritical fluid, causing a slight reduction in the tensile strength value. This reduction can be considered as the possible explanation of the decrease in the IFSS values found for the flax/epoxy system. From values reported in Table V.3 it is possible to highlight that the two thermoset systems exhibited different IFSS results. The flax/epoxy samples are characterized by higher values of interfacial shear strength than the flax/vinylester ones. This result confirmed once again the better adhesion quality between flax yarn and epoxy resin than that observed for the vinylester matrix.

V.1.1.3 Fragment debonding analysis

In the previous sections, it was pointed the difficulty in performing a comparative analysis of critical fragment lengths and the IFSS values obtained from fragmentation tests performed on monofilament composites characterized by yarns with different mechanical performances. This is because these values are strongly affected by the failure stress value of the yarn embedded into the matrix. The method of Fraser et al. can only be applied when the flax yarn strength remains unaffected after the application of surface treatments. To overcome this problem, another parameter can be taken into account in order to compare the adhesion quality between the different flax yarns and the thermoset matrix: the length of the debonding zone between the flax yarns and the polymer resin. According to Kim et al. [Kim et al., 2002] and Ramirez et al. [Ramirez et al., 2008], debonding represents a very important phenomenon in studying the interface quality of polymer composites. These authors have performed fragmentation tests on single carbon and glass fibre composites. They measured the debonding length around each fragment by using photoelastic birefringence patterns. As explained by Kim et al. [Kim et al., 2002], the interfacial zone between the filament and the polymer matrix may be considered as a set of bonding lines (Figure V.3-a). When the monofilament composite is loaded, the molecular bonded lines become tense until filament fractures and some lines near the filament break are disconnected. The authors defined the debonding zone as the region containing both the filament breaking gap and the breaking zone of the molecular bonding lines (Figure V.3-b). They showed that a large debonding zone is typical for weak interfacial bonds. The higher is the debonding length value found, the lower is the adhesion quality between the filament and the polymer matrix. In this

framework, optical microscopy was used in this work to measure the length of the debonding zone between the different flax yarns and the epoxy/vinylester resin. In Figure V.4 is reported a typical optical micrograph obtained for the fragmented flax yarn.

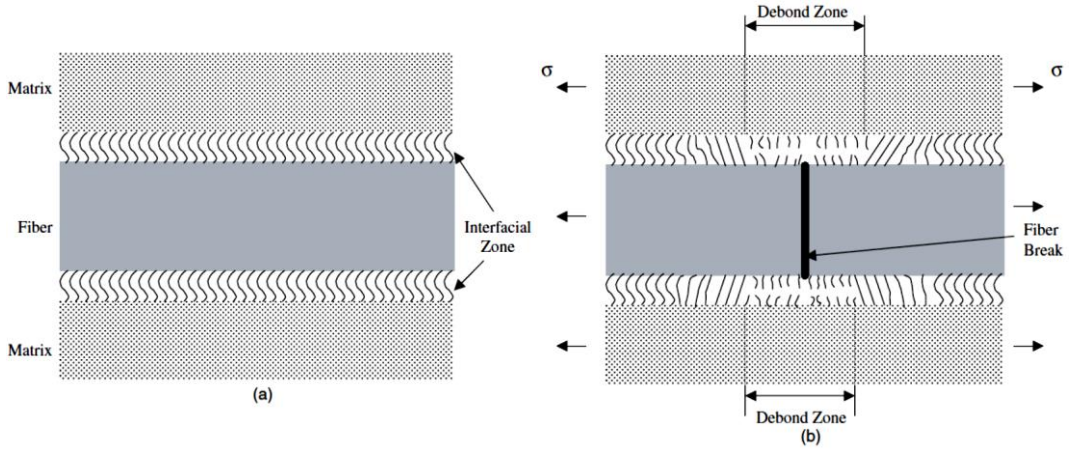

Figure V. 3 Schematic description of the debonding microstructure of filament and matrix interface: (a) the microstructure before the loading of the sample, no filament break occurs; (b) the microstructure after the loading of the sample, filament break occurs [Kim et al., 2002].

From Figure V.4, it is possible to notice that around the yarn break a black zone is formed. The length of this specific zone was measured, and its value was considered as the debonding length ($l_{debonding}$) between the flax yarn and the polymer matrix.

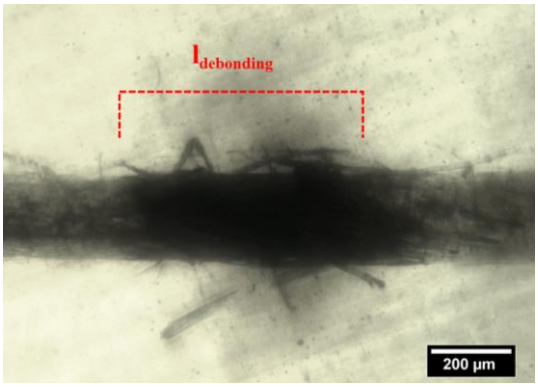

Figure V. 4 Measurement of the debonding length ($l_{debonding}$).

Comparisons between the debonding lengths measured for the untreated and the chemically treated single yarn composites are reported in Table V.4. For each family of monofilament composites, a measurement of about 80 debonding lengths was performed. The results showed that both the enzymatic and the SC-CO_2 treatments produced a decrease in the length of the debonding zone, promoting the interfacial adhesion of flax yarns with the epoxy and

the vinylester resin. By comparing the different values reported in Table V.4, it is possible to highlight that the best results in terms of debonding length are obtained for the enzymatically treated flax yarns. The decrease in debonding length found for the enzymatically treated flax yarn with both epoxy and vinylester matrices can be linked to the increase in hydrophobic behaviour produced by the Peclyve enzymatic solution. As reported in section IV.1.3, the pectinases and xyloglucanases enzymes, contained in Peclyve solution, are able to successfully remove the pectin and hemicellulose content from flax fibres, increasing their hydrophobic character and consequently their compatibility with the thermoset resins. Regarding the effect of the Peclyve solution on the interfacial adhesion of flax yarn with the epoxy resin, similar debonding lengths values were measured for both the 5 wt% - 4.5h and 10 wt% - 6h treatment conditions. A decrease in debonding length of about 18% was found for both the enzymatically treated flax yarns in the epoxy-based composites. This result indicates that the different solution concentrations and treatment durations used affect in the same way the adhesion quality between the flax yarn and the epoxy matrix. Different are the results found for the flax yarn/vinylester system. In this case, the enzymatic treatment performed by a 10 wt% of Peclyve solution for 6h produces better adhesion results than the treatment performed using the 5 wt% Peclyve - 4.5h condition. If compared with the as-received flax yarn/vinylester system, a decrease in debonding length of about 36% was found for the Peclyve 10 wt% - 6h flax yarn/vinylester composite. Unlike the enzymatic treatment, the flax yarns treated by SC-CO_2 did not show noticeable changes in their compatibility with the epoxy matrix. An average value of debonding length of 429 ± 39 µm was measured, comparable with the value of 444 ± 49 µm found for the as-received flax yarn/epoxy systems.

Table V. 4 Debonding length values for the untreated and chemically treated single yarn in both epoxy and vinylester based composites.

Matrix	Flax yarn	$l_{debonding}$ [µm]
Epoxy	Neat	444 ± 49
	Peclyve EXG 5 wt% - 4.5 h	353 ± 89
	Peclyve EXG 10 wt% - 6 h	365 ± 46
	Supercritical CO_2	429 ± 39
Vinylester	Neat	830 ± 343
	Peclyve EXG 5 wt% - 4.5 h	628 ± 128
	Peclyve EXG 10 wt% - 6 h	529 ± 65
	Supercritical CO_2	673 ± 145

On the contrary, a positive effect on the adhesion properties of flax yarn with the vinylester matrix is produced by the supercritical CO_2 fluid. This result is consistent with the critical fragment lengths value previously reported, and it points out that the supercritical carbon dioxide fluid is able to successfully promote the adhesion of flax yarns with the vinylester matrix. This positive effect produced on the flax yarn/matrix adhesion can be linked to the non-cellulosic constituents removal, such as lignin, pectin and hemicellulose, occurred during the SC-CO_2 process. As it is possible to see in Table V.4, the debonding length values found for the epoxy matrix samples are lower than the values found for the vinylester matrix ones. These results are consistent with the critical fragment length and IFSS values reported in Table V.2 and Table V.3 respectively and, they highlight once again the better adhesion of flax yarns with the epoxy matrix than with the vinylester one.

The debonding length results were also confirmed by micro computed tomography. A post-mortem examination of the monofilament composites has been performed through the use of high resolution micro computed tomography, which allowed a precise measurement of the yarn/matrix debonding zone. It is important to point out the great novelty of the use of this type of analysis for the assessment of the interfacial properties in monofilament composites. For each flax yarn/epoxy and flax yarn/vinylester specimen, microtomographic image acquisitions have been made with a resolution of 1.5 µm. The debonding length was identified by the black voxels corresponding to voids between the periphery of the flax yarn and the matrix. In Figure V.5-6-7 are reported examples of x-slices obtained for the untreated and chemically treated flax/epoxy and flax/vinylester single yarn samples. In particular, concerning the enzymatically treated flax yarns, only the samples treated with the Peclyve 10 wt% - 6h were analysed. Concerning the untreated samples, debonding length values of 530µm ± 70µm and 624µm ± 76µm were found for the flax/epoxy (Figure V.5-A) and the flax/vinylester (Figure V.5-B) monofilament composites, respectively. These values of the debonding lengths are consistent with the black zone lengths measured by optical microscopy on the same samples: 504µm ±102µm for flax/epoxy and 599µm ±181µm for the flax/vinylester. This result demonstrates that the observed black zone in optical micrographs (Figure V.4) coincides with the debonding zone between the flax yarn and the polymer matrix. The microtomographic images for the enzymatically and supercritical CO_2 treated flax/matrix samples confirmed the decrease in debonding length produced by the different chemical processes with both epoxy and vinylester resin. Interesting results were found for the supercritical CO_2 treated flax yarn. In fact, as reported previously, also the

micro computed tomography observations point out the better adhesion of the SC-CO_2 treated flax yarn with the vinylester matrix than that obtained with untreated flax yarns.

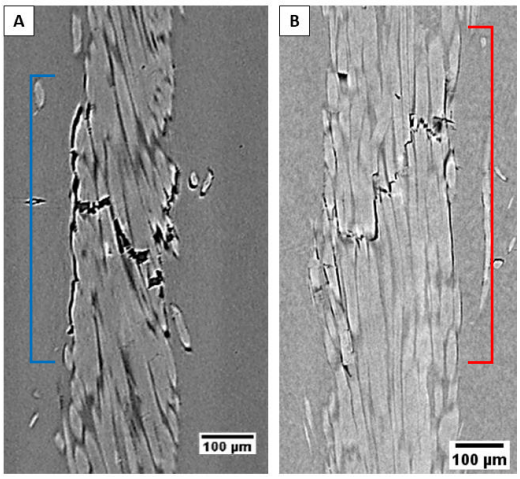

Figure V. 5 Debonding length observation by micro computed tomography. High resolution micro-CT images for untreated flax/epoxy (A) and untreated flax/vinylester (B) single yarn samples.

Comparison between Figure V.5-B with Figure V.7-B highlights the decrease in the debonding length thanks to the exposure of flax yarns to the supercritical fluid, producing an enhancement of the yarn/matrix interfacial adhesion. The presence of some resin cracks inside the vinylester matrix, identified by a blue arrow in Figure V.7-B, confirms the increase in compatibility, so the enhancement in load transfer ability, between the treated flax yarn and the vinylester polymer matrix.

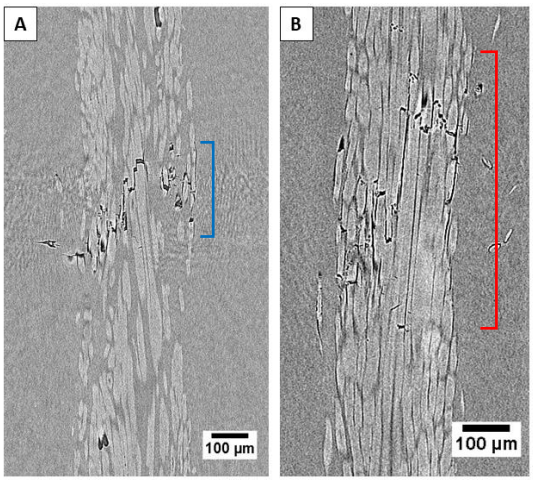

Figure V. 6 Debonding length observation by micro computed tomography. High resolution micro-CT images for Peclyve EXG 10 wt% - 6h treated flax/epoxy (A) and flax/vinylester (B) single yarn samples.

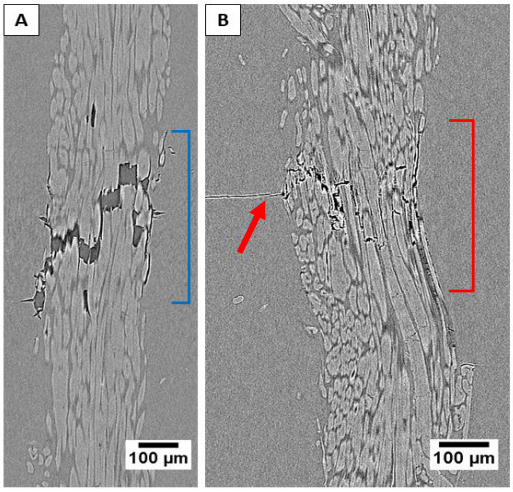

Figure V. 7 Debonding length observation by micro computed tomography. High resolution micro-CT images for supercritical CO_2 treated flax/epoxy (A) and flax/vinylester (B) single yarn samples.

Using the AVIZO 9.0 software, it was possible to perform a post-mortem 3-D reconstruction of the fracture zone distribution along the flax yarn (Figure V.8).

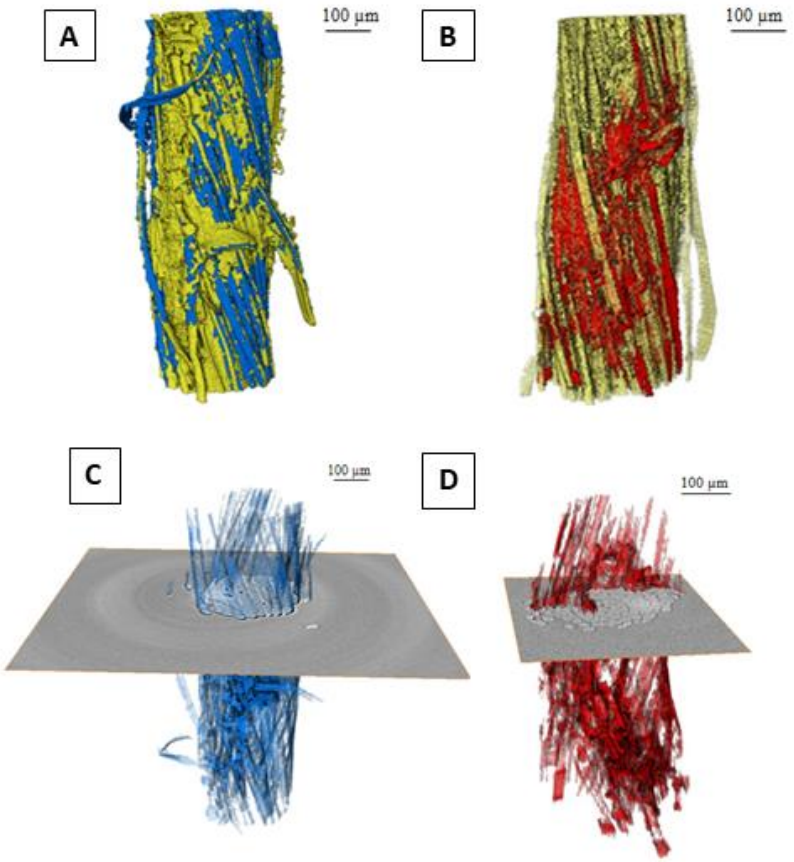

Figure V. 8 Volumetric reconstruction of the as-received flax yarn and the fracture zone for both untreated flax/epoxy (A-C) and untreated flax/vinylester (B-D) systems. The flax yarn is represented in yellow, the fracture zone in blue and red for flax/epoxy and flax/vinylester samples, respectively [Seghini et al., 2018].

This analysis permitted an easier viewing of fine detail that would be difficult to evaluate using only the axial reconstruction images. Raw images were pre-treated using smoothing filters and an image segmentation was carried out. Black voids (breaking and debonding zone) were identified from the background (the rest of flax yarn) on the basis of the different grey threshold values. The volumetric reconstruction was carried out on both epoxy and vinylester types of samples with the untreated flax yarn. In order to simplify the identification, the yellow colour was used for the flax yarn, the blue and red colours for the fracture zones of flax/epoxy and flax/vinylester samples respectively. A large debonding zone is clearly visible from the volumetric reconstructions of both flax/epoxy and flax/vinylester systems. The black voids are mainly concentrated at the peripheral zone of flax yarn and can be related to the debonding phenomenon between the flax yarn and the thermoset resin. This result is clearly visible in the V.8-C and V.8-D images that show the 3-D reconstruction of the breaking zone and it can be considered as a further confirmation of the low adhesion quality between the flax yarn and both thermoset matrices.

V.1.1.4 Fractographic analysis

After fragmentation tests, a morphological investigation of the fracture surface has been performed using the FE-SEM. The fracture surface of the as-received and chemically treated single flax yarn samples with epoxy and vinylester resins was investigated. Figure V.9 presents a comparison of the FE-SEM-micrographs showing the fracture surface for the untreated flax/epoxy and flax/vinylester systems. In both cases, an extensive flax fibre debonding was observed, confirming the low adhesion quality between the flax yarn and the polymer matrices. From the comparison between Figure V.9-B and Figure V.9-D, it is possible to see that there are differences between the two systems at the fibre/matrix interface. Indeed, for the flax/epoxy sample the presence of little resin ligaments, albeit minimal, was found between the matrix and the flax fibres. It has not been observed for the flax/vinylester composite. These little connections may explain the better adhesion that the flax yarn displays in presence of the epoxy resin. Regarding the effects of enzymatic treatment on the adhesion properties of flax yarns with the two thermoset matrices, Figure V.10 reports the FE-SEM micrographs found for the monofilament composites with the yarns treated using the Peclyve 5 wt% - 4.5h and Peclyve 10 wt% - 6h conditions.

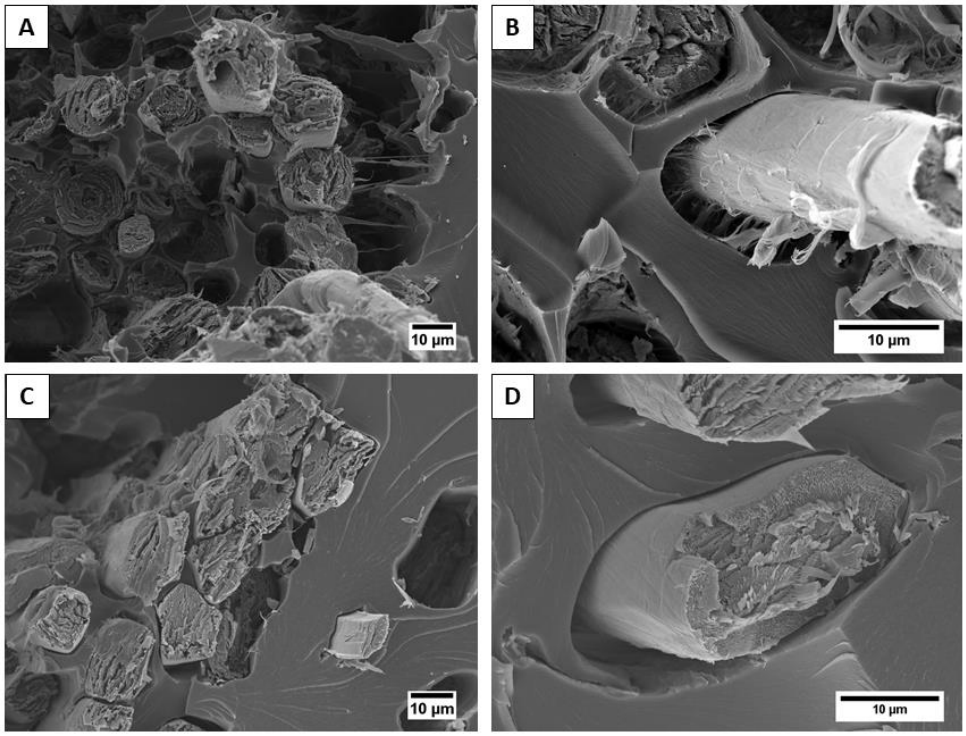

Figure V. 9 FE-SEM micrographs showing the fracture surface for the untreated flax/epoxy (A-B) and for the untreated flax/vinylester (C-D) single yarn composite.

Despite the results of debonding length reported in the previous section, the morphological analysis showed that the enzymatic treatment carried out using a Peclyve concentration of 5 wt% for 4.5h did not produce a significant change in the adhesion properties of flax yarns with the thermoset matrices. Both flax/epoxy and flax/vinylester single yarn composite samples showed a quality of adhesion between the flax fibres and the polymer matrix (Figure V.10-A,B and Figure V.10-C,D) comparable to that found for the untreated flax yarn composites, with the exception of lower pull-out lengths and increased tendency toward multiple fibre failures on the fracture plane. A slight improvement in the compatibility between the treated flax yarns and the polymer matrices is produced using higher concentration and treatment time conditions. The gap in the fibre/matrix interfacial adhesion seems to decrease for both the epoxy and the vinylester matrices. A possible explanation of this behaviour may be found in the Peclyve solution capacity to modify the surface chemical composition of flax. Although a phenomenon of pull-out of flax fibres from the matrix can be identified, the presence of some flax fibre residues attached to the surface of the epoxy matrix was observed. These residues are visible in the micrograph reported in Figure V.10-

F (denoted by a white arrow) and they can confirm the slight increase in compatibility between the treated flax yarn and the epoxy resin.

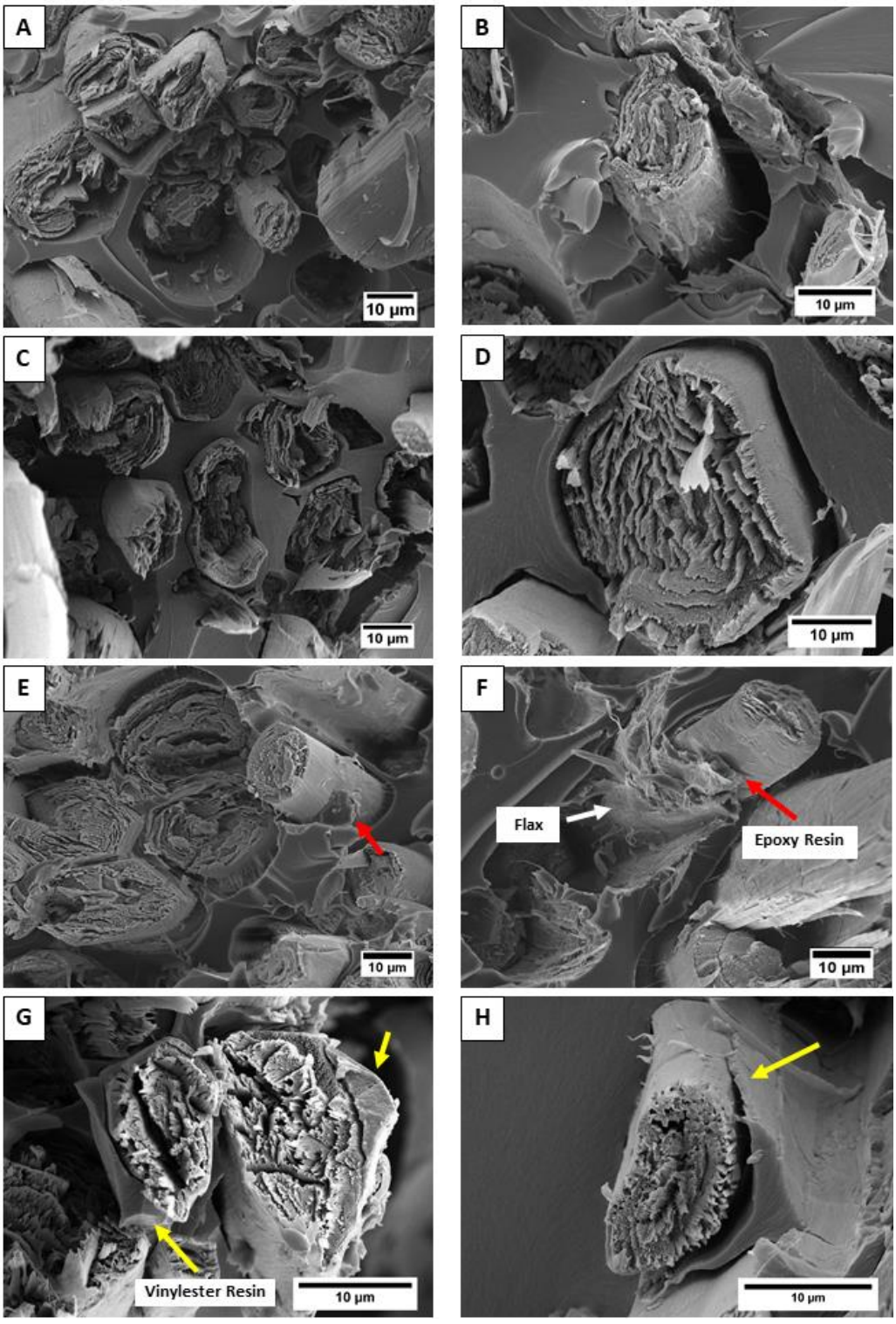

Figure V. 10 FE-SEM micrographs showing the fracture surface for the different enzymatically treated flax yarn/matrix composites: (A-B) Peclyve 5 wt% - 4.5h treated flax/epoxy system; (C-D) Peclyve 5 wt% - 4.5h treated flax/vinylester system; (E-F) Peclyve 10 wt% - 6h treated flax/epoxy system; (G-H) Peclyve 10 wt% - 6h treated flax/vinylester system.

Small fragments of epoxy and vinylester resin remained attached to the lateral surface of flax fibres as highlighted in Figure V.10-E,F with red arrows and in Figure V.10-G,H with yellow arrows, respectively. As reported in the previous sections, the supercritical CO_2 treatment did not produce noticeable changes in the compatibility of flax yarns with the epoxy matrix. This behaviour is clearly visible in micrographs reported in Figure V.11-A,B, which show an interfacial behaviour similar to that obtain for the as-received flax/epoxy samples. On the contrary, a different behaviour was found from observation of the fracture surface of flax/vinylester system. From the comparison of Figure V.11-B with Figure V.11-C it is possible to highlight that a positive effect on the adhesion properties of flax yarn with the vinylester matrix is produced by the supercritical CO_2 fluid. In particular, the micrograph reported in Figure V.11-D shows how the SC-CO_2 treated flax yarns exhibit a strongly reduced gap with the vinylester matrix. In addition, an in-plane fibres failure with a reduced fibre pull-out phenomenon were reported. These results are consistent with the reduction in debonding length reported in the previous section and represents an additional proof of the enhanced fibre/matrix adhesion.

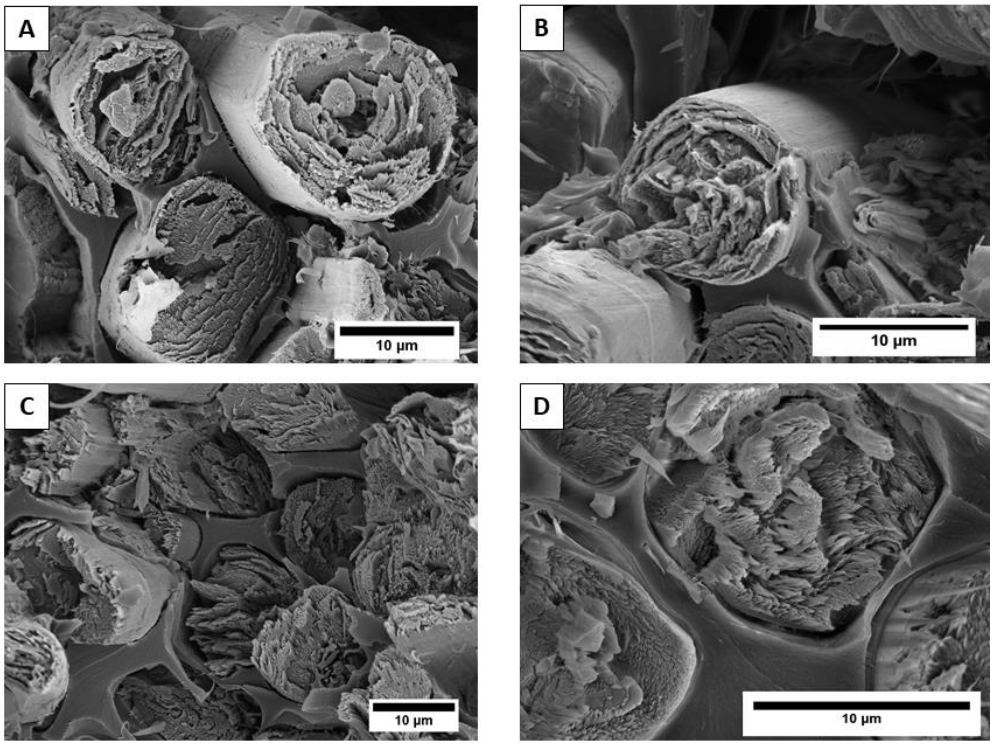

Figure V. 11 FE-SEM micrographs showing the fracture surface for the supercritical CO_2 treated flax/epoxy (A-B) and flax/vinylester (C-D) single yarn composite.

V.1.2 Effects of physical modification treatments on interfacial properties of flax yarns in thermoset matrix composites

In order to investigate the effect of plasma treatment on the adhesion quality of flax with the epoxy and vinylester thermosets matrices, fragmentation tests were performed on the as-received and plasma treated flax yarns. Specifically, the effect of both oxygen plasma and plasma polymerization process, in terms of critical fragment length, IFSS and debonding lengths values, will be discussed in the next sections of the present chapter.
Concerning the oxygen plasma treatment, in order to assess the effect of the plasma process on the adhesion quality of flax yarn with the epoxy matrix, fragmentation tests have been performed only on flax yarns treated with the maximum and minimum oxygen plasma power values, 100 W and 2 W, respectively. On the contrary, the effect of the tetravinylsilane plasma deposition on the adhesion properties of flax yarns was investigated with both the epoxy and the vinylester matrices.

V.1.2.1 Determination of critical fragment length

Fragmentation tests have been performed for the untreated flax yarns and for the flax yarns treated using oxygen and tetravinylsilane plasma with both epoxy and vinylester resins. As reported previously, the critical fragment length value reflects the stress transfer efficiency between the flax yarn and the matrix at the interface and its estimation plays a crucial role in the assessment of the adhesion quality in a composite material. The critical fragment lengths were measured by optical microscopy for the different systems, and results are reported in Table V.5. When comparing the length values found for the untreated flax yarns with those for the oxygen plasma treated yarns in epoxy resin systems, only the 100 W process is able to reduce the critical filaments length values. The oxygen plasma treatment performed at a plasma power of 2 W seems to be not able to decrease the critical length of the flax yarn in the epoxy matrix. These results could lead to the conclusion that only an oxygen plasma treatment with a power of 100 W is able to effectively modify the surface of flax yarns and increase the adhesion with the epoxy matrix. For the flax yarn/vinylester systems, it can be seen that critical length values are significantly higher than those obtained for the epoxy resin. These results show that the flax yarn/epoxy system is characterized by a better interface quality than the flax/vinylester one. The deposition of the plasma polymer tetravinylsilane (TVS) coating results in an increase in compatibility between flax yarn and

both thermoset matrices. However, it is important to stress that the plasma polymerization process exhibited a strong dependence on the oxygen plasma pre-treatment. Results reported in Table V.5 show that, for both thermoset matrices, only the TVS deposition after the 100 W oxygen pre-treatment was able to produce a strong enhancement of the yarn/matrix interfacial adhesion. Indeed, a reduction of about 30% of the critical fragment length was produced after the TVS deposition onto the flax yarn surface.

Table V. 5 Critical fragment length values for the different single yarn composites.

Matrix	Flax yarn	l_c [µm]
Epoxy	Neat	2687 ± 631
	2 W Oxygen Plasma	2950 ± 731
	100 W Oxygen Plasma	1885 ± 204
	2 W Oxygen Plasma – PECVD	2473 ± 399
	100 W Oxygen Plasma - PECVD	1899 ± 377
Vinylester	Neat	3938 ± 804
	2 W Oxygen Plasma – PECVD	4175 ± 702
	100 W Oxygen Plasma - PECVD	3075 ± 600

V.1.2.2 Calculation of interfacial shear strength

The interfacial shear strength value (IFSS) of the different flax/epoxy and flax/vinylester systems was estimated according to the Kelly and Tyson theory, using Equation I.19. For the plasma treated flax yarns the tensile properties were determined performing single filament tensile tests using a single gauge length L_0 of 40 mm. Therefore, for these yarns, the extrapolation of strength at critical length l_c has been performed by using the Weibull cumulative distribution function (Guillebaud-Bonnafous et al. 2012; R. Joffe, Andersons, and Wallström 2005; Roberts Joffe, Andersons, and Wallström 2003; Zafeiropoulos 2007). The Weibull parameters used for this method are those obtained with tensile tests on the different flax yarns reported in Table IV.13. In Table V.6 are reported all the $\sigma_f(l_c)$ values and the IFSS results obtained for the different flax/epoxy and flax/vinylester systems. The oxygen plasma treatment increases the IFSS values and this is particularly true in the case of the 100 W plasma power. This reflects the results already found by comparing the critical length and the debonding length values. Concerning the PECVD process, from the results reported in Table V.6 it may be observed that, for both thermoset matrices, a significant

increase in the values of IFSS was produced due to the deposition of the polymeric film after the 100 W oxygen pre-treatment. By comparing the IFSS values found for the epoxy and vinylester systems with the 100 W oxygen-PECVD treated flax yarns, it is possible once again to conclude that the flax yarn/epoxy system has a better interface quality than the flax/vinylester one.

Table V. 6 Strength values at critical fragment length and IFSS values for the different flax/epoxy and flax/vinylester systems.

Matrix	Flax Yarn	$\sigma_f(l_c)$ [MPa]	IFSS [MPa]
Epoxy	Neat	406 ± 18	19.3 ± 3.7
	2 W Oxygen Plasma	353 ± 9	20 ± 3.8
	100 W Oxygen Plasma	363 ± 11	24.8 ± 2.8
	2 W Oxygen Plasma – PECVD	336 ± 8	21.2 ± 1.6
	100 W Oxygen Plasma - PECVD	573 ± 31	41.3 ± 11.6
Vinylester	Neat	376 ± 15	13.9 ± 2.8
	2 W Oxygen Plasma – PECVD	309 ± 8	12.4 ± 2.1
	100 W Oxygen Plasma - PECVD	501 ±26	23 ± 6.7

In order to better understand the interfacial phenomena, a photoelasticity analysis has also been performed. It allowed to carry out a qualitative study of stress state near yarn breaks and at the interface between the yarn and the matrix. This analysis has been performed for the untreated flax yarn/epoxy and the 100 W oxygen-PECVD treated flax yarn/epoxy systems. The vinylester resin used in this work does not exhibit birefringence phenomena, therefore no photoelasticity analysis has been carried out. Figure V.12 presents the different isochromatic patterns observed for the two different yarn/epoxy systems at the saturation of the fragmentation process. Around each yarn break, the stress redistribution occurs at 45° of the tensile loading, showing a cross-shape profile. This type of stress transfer at the interface has been also observed in carbon/epoxy composites [Wang *et al.*, 2010]. Isochromatic patterns exhibit different fringe orders in Figure V.12-A and Figure V.12-B. Fringes are more pronounced, with a higher stress level, in the case of the untreated flax yarn than in the case of the PECVD treated one. This dissimilar stress distribution confirms the lower interface quality and the lower IFSS value measured for the untreated specimen.

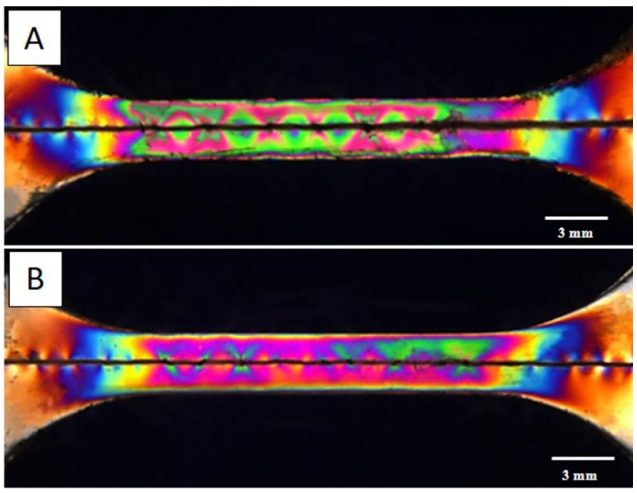

Figure V. 12 Comparison of experimental photoelastic patterns after yarn fragmentation test for the neat flax yarn/epoxy (A) and the 100 W oxygen-PECVD treated flax yarn/epoxy (B) composite specimens.

V.1.2.3 Fragment debonding analysis

In the previous sections, it was emphasized that the comparison of the adhesion properties of different filament/matrix systems by referring to their critical fragment length and IFSS values is very dependent on the mechanical properties of the different filaments. As in the case of enzymatic and supercritical CO_2 treatments, the oxygen plasma and TVS plasma deposition treatments affected the mechanical performances of flax yarns. The results obtained from the mechanical characterization of the plasma treated flax yarns (section IV.1.4.3), showed that the increase in the power of oxygen plasma can produce a strong decrease in the maximum force and strength values of yarns. In particular, a tensile strength reduction up to 36.4% was found after the oxygen plasma treatment performed using a plasma power of 100 W. To overcome this problem, the length of the debonding zone between the flax yarns and both the epoxy and vinylester resins was considered. In Table V.7 are reported the different values obtained for the different single yarn composites by optical microscopy. A slight decrease in the length of the debonding zone between the flax yarn and the epoxy matrix was produced after the oxygen plasma treatment using a plasma power of 2 W. This is in contrast with the results previously found. In fact, an IFSS and a critical fragment length values comparable with those found for the untreated yarn indicated that the 2 W oxygen plasma power was not able to produce any changes in the flax/matrix adhesion quality. The best results in terms of debonding length were found after the oxygen plasma treatment performed at a plasma power of 100 W. By comparing the results found for the untreated flax yarns with those for the oxygen plasma treated yarns in epoxy resin

systems, the 100 W process is able to produce a decrease of about 28.6% in the debonding length values. These results are perfectly in agreement with those found for the critical fragment length and IFSS, and they highlighted that only an oxygen plasma treatment with a power of 100 W is able to effectively modify the surface of flax yarns and increase the adhesion with the epoxy matrix.

Table V. 7 Debonding length values for the untreated and plasma treated single yarn in both epoxy and vinylester composites.

Matrix	Flax yarn	$l_{debonding}$ [µm]
Epoxy	Neat	444 ± 49
	2 W Oxygen Plasma	335 ± 41
	100 W Oxygen Plasma	317 ± 44
	2 W Oxygen Plasma – PECVD	355 ± 30
	100 W Oxygen Plasma - PECVD	247 ± 63
Vinylester	Neat	830 ± 343
	2 W Oxygen Plasma – PECVD	680 ± 182
	100 W Oxygen Plasma - PECVD	460 ± 116

Concerning the PECVD process, from the results reported in Table V.7, it may be observed that a decrease in the debonding length was produced after the deposition of the TVS polymeric film onto the yarn surface. Results show that, for both the epoxy and vinylester resins, the best results were found for the TVS deposition after the 100 W oxygen pre-treatment. The debonding length values found indicate a strong enhancement of the yarn/matrix interfacial adhesion. A decrease in the debonding length zone of 44.3% and 44.6% was produced with the epoxy and vinylester matrices, respectively.

This tendency has been confirmed by micro computed tomography. A post-mortem 3-D reconstruction of the fracture zone distribution along the flax yarn was carried out using the AVIZO 9.0 software. This analysis has been performed for both epoxy and vinylester systems with untreated or 100 W oxygen - PECVD treated flax yarns (Figure V.13). In order to simplify the identification, the dark grey and the green colours have been used for yarn representation, and the blue and red colours have been chosen for damage reconstruction. The 3D reconstructions for both epoxy and vinylester composites highlight the decrease in the debonding length thanks to the pp-TVS film deposition treatment.

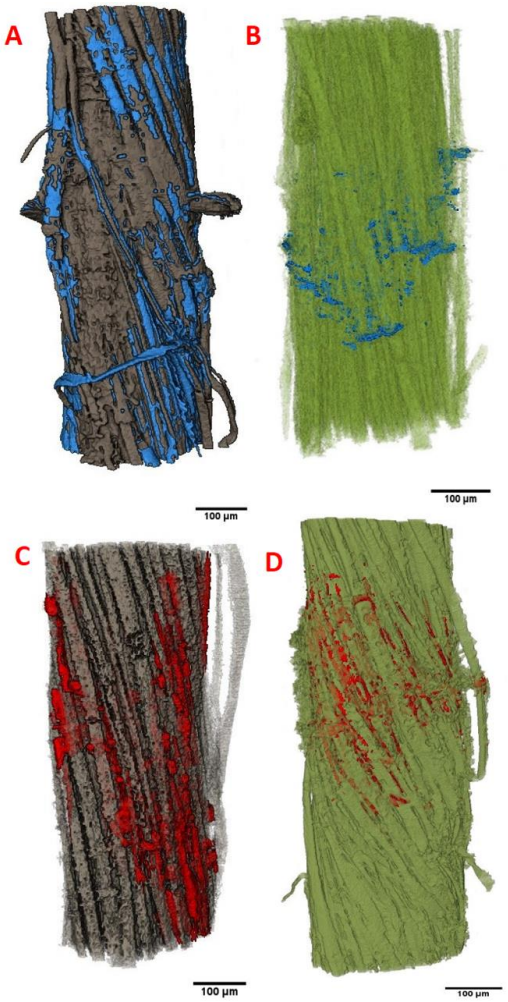

Figure V. 13 Volumetric reconstruction of the flax yarn and the fracture zone for neat flax/epoxy (A), 100W oxygen - PECVD flax/epoxy (B), neat flax/vinylester (C), 100W oxygen - PECVD flax/vinylester (D) systems [Seghini et al., 2019].

By comparing the volumetric reconstructions reported in Figure V.13-B and Figure V.13-D, it is possible to see that the flax yarn/epoxy system shows a better interface quality than the flax/vinylester one. High resolution micro-CT observations allowed a precise measurement of the yarn/matrix debonding zone. The debonding length has been identified by the black voxels corresponding to voids between the periphery of the flax yarn and the matrix (Figures V.14 and Figure V.15). Comparison of debonding lengths confirms that for both thermoset matrices, the polymer deposition on flax yarn after the 100 W oxygen pre-treatment allows a significant increase in the yarn/matrix interfacial adhesion. Comparison of Figure V.14-C and Figure V.15-C also confirms that the flax yarn/epoxy monofilament composite shows a better interface quality than the flax/vinylester one.

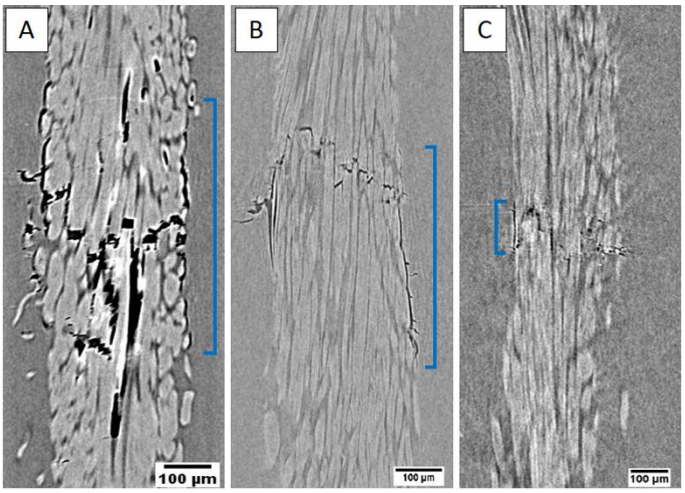

Figure V. 14 Debonding length observation by micro computed tomography for: neat flax/epoxy (A), 2 W oxygen - PECVD flax/epoxy (B) and 100 W oxygen - PECVD flax/epoxy (C) samples.

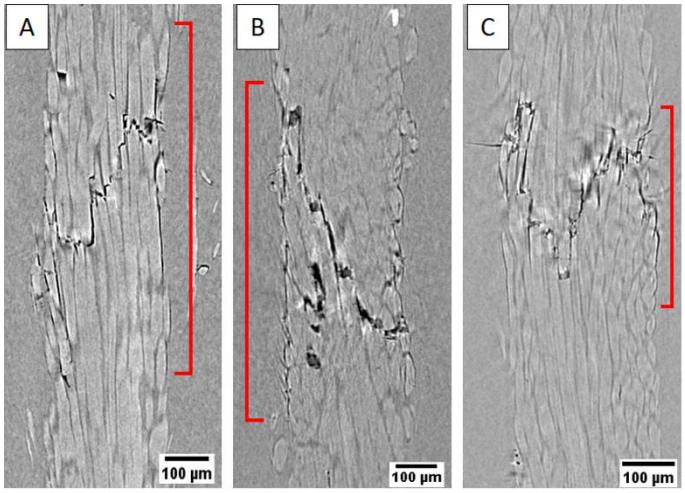

Figure V. 15 Debonding length observation by micro computed tomography for: neat flax/vinylester (A), 2 W oxygen - PECVD flax/vinylester (B) and 100 W oxygen - PECVD flax/vinylester (C).

V.1.2.4 Fractographic analysis

A post mortem morphological investigation of the fracture surface has been performed using the FE-SEM. The fracture surfaces of both single flax yarn samples with epoxy and vinylester resins have been investigated. Figure V.16 presents a comparison of the FE-SEM micrographs showing the fracture surface for the untreated and the different oxygen plasma treated flax/epoxy systems. Observations show that there is a gap in the yarn/matrix interfacial adhesion for both untreated and 2 W oxygen plasma treated specimens. Indeed, extensive flax fibre debonding can be seen in Figures V.16-A and V.16-B. On the contrary,

for the 100 W oxygen plasma treated flax/epoxy system, it is possible to notice an increase in the yarn/matrix interfacial adhesion (Figure V.16-C). These results are completely in agreement with the critical yarn lengths, the debonding lengths and the IFSS values found. A possible explanation of this behaviour may be found in the plasma oxygen capacity to modify the superficial morphology and the chemical composition of flax.

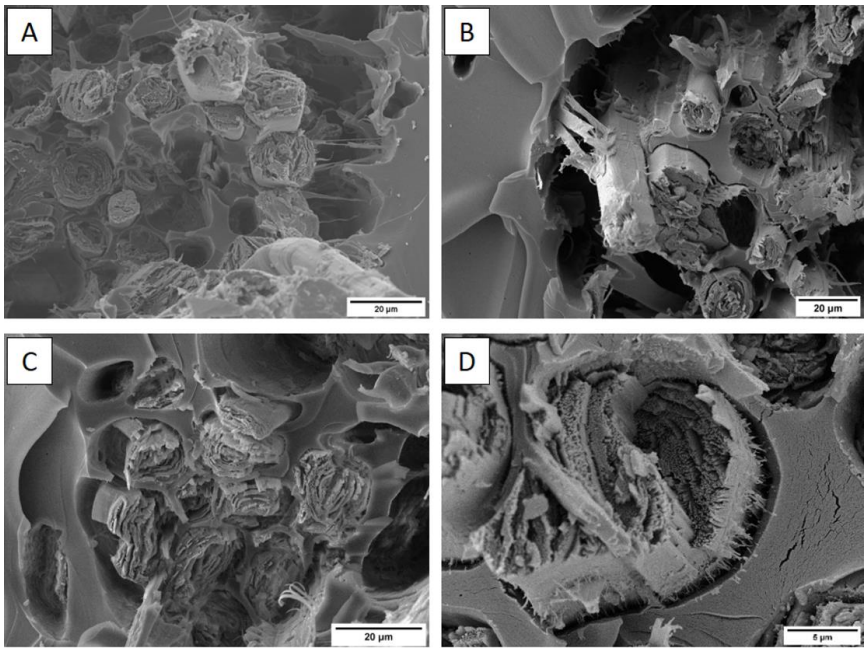

Figure V. 16 FE-SEM micrographs showing the fracture surface for the different flax/epoxy single yarn composites: neat flax/epoxy (A), 2 W oxygen plasma flax/epoxy (B), and 100 W oxygen plasma flax/epoxy (C-D).

As discussed in section IV.1.4.2, the oxygen plasma treatment is able to perform a surface ablation of the flax fibres and to enhance their surface roughness (Figure IV.17). Different studies in literature have analysed the influence of frictional forces on the interfacial adhesion between the synthetic fibres and the polymeric matrices [Beggs *et al.*, 2015; Gao *et al.*, 2015; Thomason *et al.*, 2018; Fu *et al.*, 2019]. These studies showed that the mechanical interlocking action between the fibre surface and the polymer matrix may lead to an increase in the interfacial strength. The increase in mechanical interlocking after plasma treatment can have a great effect on the load transfer between the matrix and the fibres [Kafi *et al.*, 2011; Bozaci *et al.*, 2013; De Oliveira *et al.*, 2017]. For this reason, it is possible to state that the roughness enhancement produced by the oxygen plasma treatment may increase the surface energy of the fibres, increasing the contact area with the polymer

matrix and creating static frictional stresses able to enhance the adhesion quality of flax. It is important to highlight also the effect of the oxygen plasma on the chemical composition of flax fibres. During the chemical and ion etching performed by the oxygen plasma treatment, hydrophilic species like hemicelluloses may be degraded. Moreover, the FT-IR analysis (section IV.1.4.2) showed that the oxygen plasma treatment performed at 100 W may promote the formation of oxidized species rich in hydroxyl, carbonyl, carboxyl groups and phenoxy radicals. All these modifications of the surface chemistry of the fibres induced by the oxygen plasma process may have a positive effect on the flax/epoxy adhesion quality. For example, the presence of little resin ligaments between the epoxy matrix and the 100 W oxygen treated flax fibres can be observed in Figure V.16-D. These little connections may further explain the better adhesion of the 100 W oxygen treated flax fibres than the 2 W treated ones. After fragmentation tests, a morphological investigation of the fracture surface has been performed also for the epoxy and vinylester composite samples with PECVD treated flax yarns (Figures V.17 and V.18, respectively). From an in-depth analysis of the different fracture surfaces, it is possible to confirm the higher adhesion of the 100 W oxygen plasma-PECVD treated flax (Figure V.17-D) with respect to the 2 W oxygen plasma-PECVD treated one (Figure V.17-A) with the epoxy resin. The morphological analysis shows that the pp-TVS film, deposited on the flax yarn surface after an oxygen pre-treatment at a plasma power of 2 W, has a good adhesion with epoxy matrix but is completely detached from the surface of the flax fibre (red arrows in Figures V.17-B and V.17-C). On the contrary, for the 100 W oxygen plasma-PECVD treated flax, not only the pp-TVS film is attached to the surface of the epoxy matrix but an improvement in adhesion between the polymeric film and the treated flax fibre surface may be also observed (Figure V.17-E). From this result, it may be concluded that the oxygen pre-treatment plays a fundamental role in the adhesion between the deposited pp-TVS film and the flax surface. Only the 100 W oxygen plasma treatment is able to remove contaminants and improve film adhesion. The morphological analysis allowed to highlight also the effect of the flax yarn roughness on the adhesion with epoxy resin. The higher the plasma oxygen power used, the greater the roughness of the flax fibres. In Figure V.17-F, it is possible to see that the epoxy surface that has been directly in contact with the pp-TVS film is highly irregular (yellow arrow) and it may increase the frictional force and the mechanical interlocking between the fibre surface and the polymer matrix.

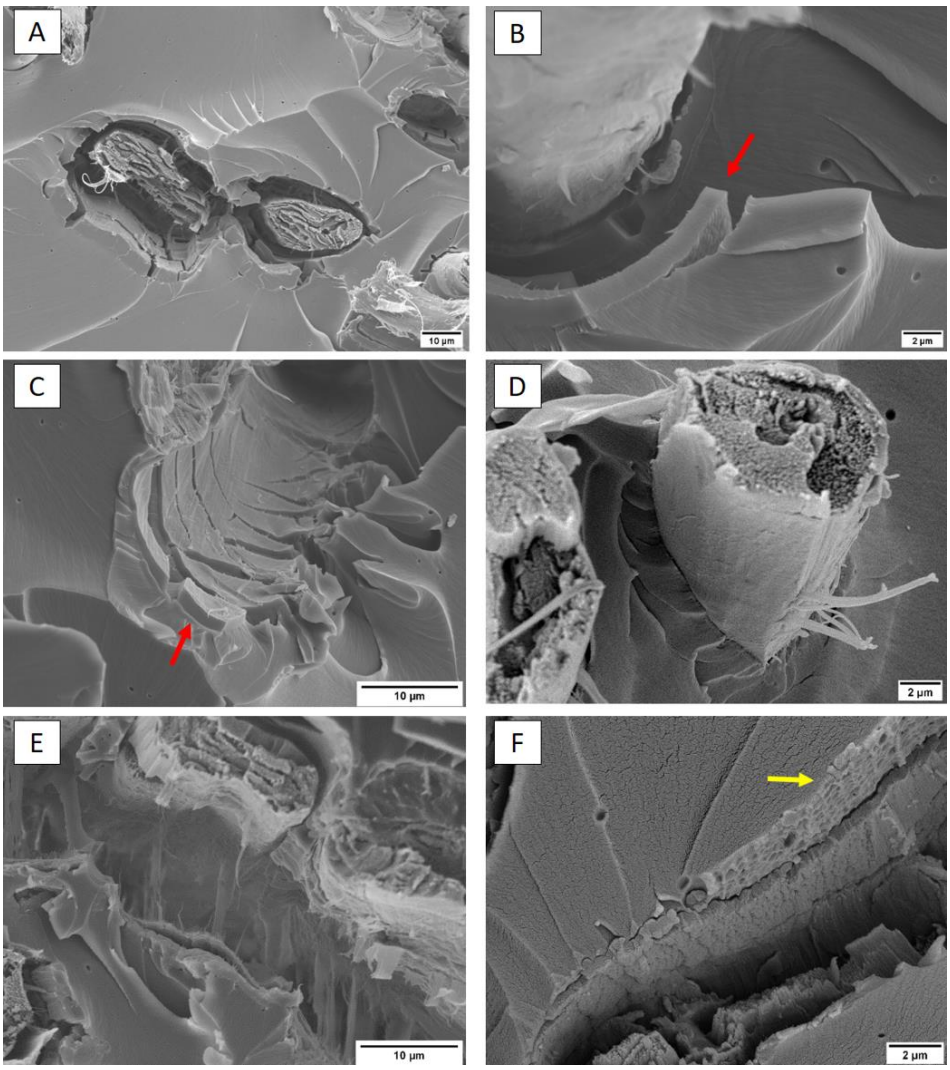

Figure V. 17 FE-SEM-micrographs showing the fracture surface for the different flax/epoxy single yarn composites: 2 W oxygen - PECVD flax/epoxy (A-B-C) and 100 W oxygen - PECVD flax/epoxy (D-E-F).

By comparing the fracture surfaces found for the neat flax/vinylester (Figure V.18-A) and for the 100 W oxygen - PECVD flax/vinylester (Figure V.18-D) systems, it is possible to see once again that the plasma polymer deposition process is able to produce a strong increase in the fibre/matrix adhesion. Concerning the 2 W oxygen - PECVD flax/vinylester system, contrary to what has been found for the epoxy resin, the deposited polymer film shows a good adhesion with the fibre surface but, on the contrary, a decohesion towards vinylester resin (red arrows in Figures V.18-B,C). This behaviour may explain the lower interfacial adhesion of the 2 W oxygen - PECVD flax/vinylester composite compared to the 100 W oxygen - PECVD flax/vinylester system.

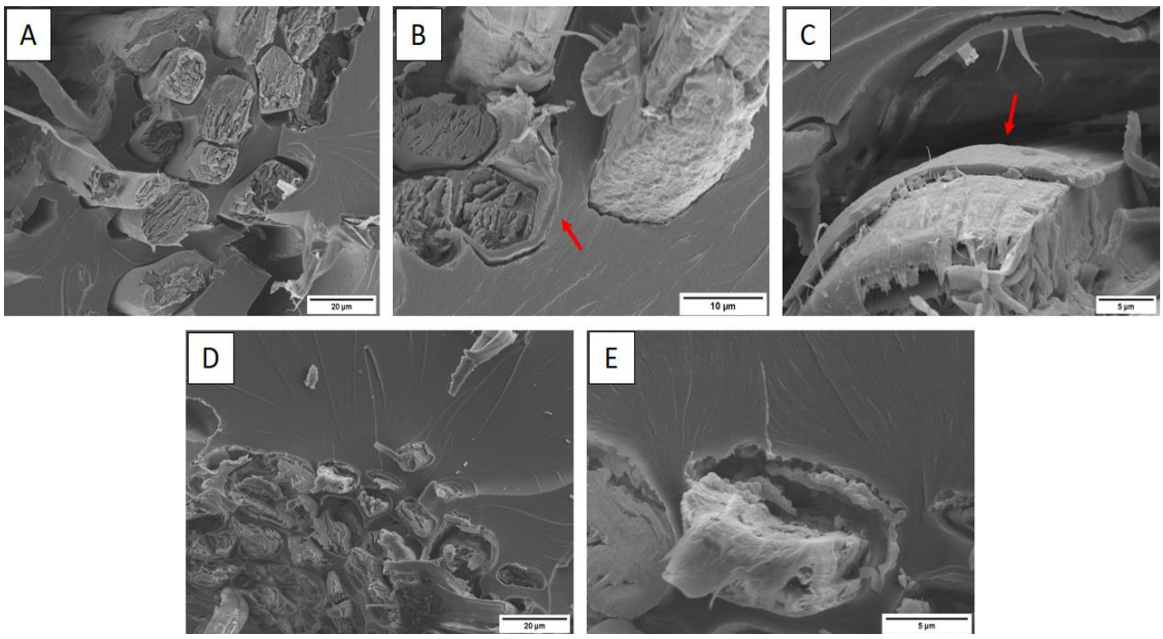

Figure V. 18 FE-SEM micrographs showing the fracture surface for the different flax/vinylester single yarn composites: neat flax/vinylester (A), 2 W oxygen -PECVD flax/vinylester (B-C) and 100 W oxygen - PECVD flax/vinylester (D-E).

The strong increase in the flax yarn/matrix adhesion properties promoted by the plasma deposition of the TVS coating is in accordance with the results found from the wetting analysis and described in depth in section IV.1.4.1. Although the surface tension values for the Gurit Prime 27 epoxy resin and for the Advalite VH-1207 vinylester resin used in this work are not known, some values found for different epoxy and vinylester resins are reported in literature [Dirand *et al.*, 1996; Cheng *et al.*, 2013; Pucci *et al.*, 2017]. The epoxy resin is characterized by surface energy value between 28 and 40 mN/m and a dispersive component greater than the polar one. A similar behaviour is reported for the conventional vinylester resin, in which the styrene monomer is used as reactive diluent. For these resins, a surface energy value of 50.5 mN/m, a dispersive component of 41.5 mN/m and a polar component of 9 mN/m is reported. In addition, as described previously, a fully dispersive behaviour is reported for the more unconventional styrene-free vinylester resin [Bénéthuilière *et al.*, 2015]. In general, it can be asserted that the higher the dispersive behaviour of a fibre, the greater will be its wettability with a thermoset resin. For this reason, the increase in the surface energy dispersive component and the decrease in polarity of flax fibres after the plasma deposition treatment confirms the results found by fragmentation tests.

CHAPTER V.2

INTERFACIAL ADHESION ASSESSMENT IN BASALT/EPOXY AND IN BASALT/VINYLESTER COMPOSITES

V.2.1 Effects of thermal de-sizing and PECVD treatments on interfacial properties of basalt fibres in thermoset matrix composites

As discussed in-depth in Chapter IV.2, a tetravinylsilane coating was deposited through Plasma-Enhanced Chemical Vapour Deposition (PECVD) process onto the basalt fibres surface in order to improve their interfacial adhesion in epoxy and vinylester based composites. The surface, morphological and mechanical properties of plasma-polymerized basalt fibres with the tetravinylsilane film were investigated. In particular, the reported results pointed out that the plasma deposition process is able to realize an homogeneous polymeric coating on the surface of basalt fibres. In order to assess accurately the effect of the pp-TVS coating on the adhesion quality of basalt fibres with both epoxy and vinylester matrices, single fibre fragmentation tests were performed. The next sections of the present chapter will provide a comparison between the interfacial adhesion properties of plasma treated basalt fibres with commercially sized basalt fibres and basalt fibres after sizing removal.

V.2.1.1 Shape of fibre breaks and fragment debonding length analysis

The shape of the fibre breaks inside polymer resin is an indicative factor of the adhesion between fibre and matrix. In general, systems characterized by a strong fibre/matrix bond exhibits extensive cracks propagation into the polymer matrix which leads to the specimen's failure. On the contrary, in a weak interface system, the fibre crack does not damage the matrix but a widening of the breaking gap between the fibre and the matrix will be produced [Feih *et al.*, 2004]. After the fragmentation test, an analysis of the shape of the basalt fibre

breaks inside both epoxy and vinylester resin was performed by optical microscopy. Figures V.19 and V.20 report the optical micrographs obtained for the fragmented epoxy and vinylester samples reinforced with the as-received (Figure V.19-A, Figure V.20-A), thermally treated (Figure V.19-B, Figure V.20-B) and plasma treated basalt fibres (Figure V.19-C, Figure V.20-C). As reported by Kim et al. [Kim *et al.*, 2002], when a fibre fractures earlier than the polymer matrix during the fragmentation test, the fibre ends may slip leaving empty space at the point of the fibre break. These gaps between the fibre ends are in general of the order of the fibre diameter, but with increasing stress, most of them may expand more than twice their initial length, in particular in systems characterized by a low fibre/matrix interfacial bond. For both the epoxy and vinylester samples, these empty spaces are clearly visible in the three different optical micrographs as black areas.

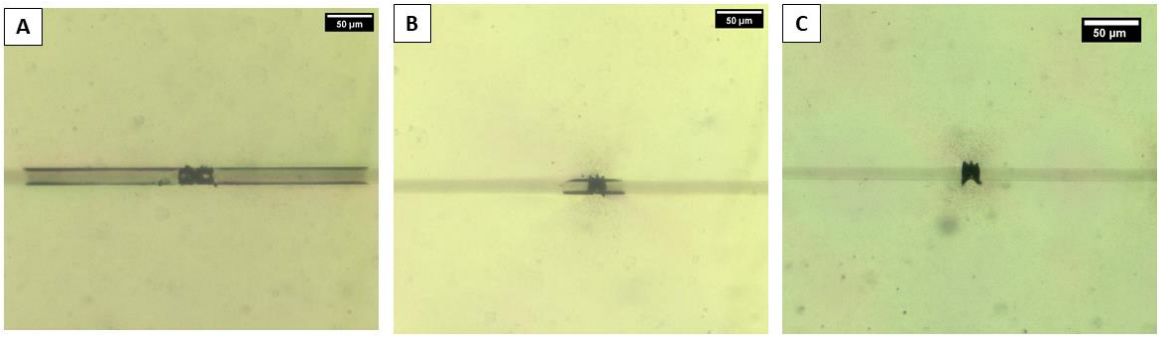

Figure V. 19 Optical micrographs of the fragmented basalt fibres in epoxy matrix: (A) as-received, (B) thermally treated and (C) plasma treated basalt fibres.

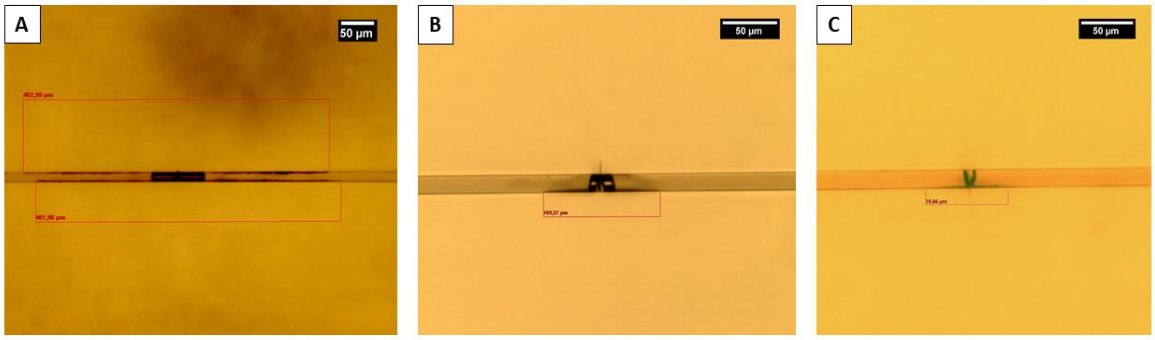

Figure V. 20 Optical micrographs of the fragmented basalt fibres in vinylester matrix: (A) as-received, (B) thermally treated and (C) plasma treated basalt fibres.

Micro-CT analysis has been performed on the as received basalt and plasma treated basalt fibre/epoxy and basalt/vinylester systems. The results confirmed that the black area found

during the optical microscopy investigation corresponds to the empty zone inside the matrix produced during tensile loading (Figures V.21 and V.22).

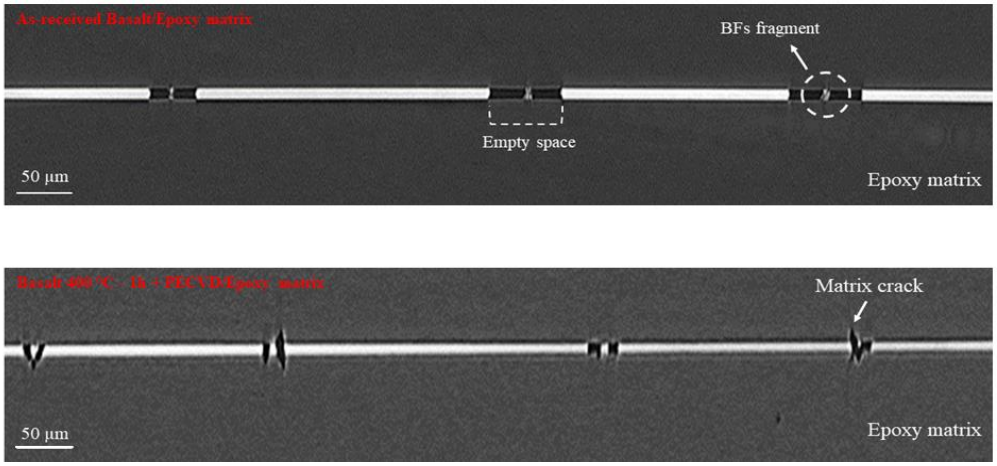

Figure V. 21 High resolution micro-CT images for as-received basalt fibre/epoxy and plasma treated basalt fibre/epoxy systems.

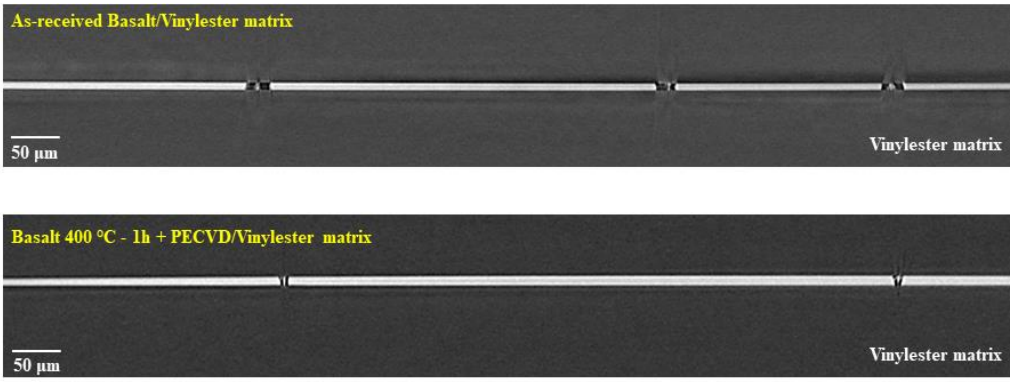

Figure V. 22 High resolution micro-CT images for as-received basalt fibre/vinylester and plasma treated basalt fibre/vinylester systems.

The microtomography analysis also showed the presence of basalt fibre fragments inside the empty zones, impossible to be detected by optical microscopy. The untreated basalt fibre/epoxy samples exhibited a shape of breaks characteristic of a weak interface system, characterized by a wide breaking gap. For all the untreated basalt/epoxy samples, no breakage extending in the matrix has been observed. Moreover, both the epoxy samples reinforced with thermally treated and plasma treated basalt fibres showed the presence of a reduced break gap between the fibre ends (Figure V.19-B,C). As it is possible to see from the micrographs, in these samples, the epoxy matrix cracks form a characteristic “bat-shape” break zone [Schutte *et al.*, 1994]. This particular shape is clearly visible in Figure V.19-C

and it is distinctive of a strong interface system. In fact, as reported by Feih et al. [Feih *et al.*, 2004], in systems characterized by a strong bonding between the fibre and the polymer matrix, a damage of the matrix is introduced in the area around the fibre break producing a narrow breaking area able to propagate towards the matrix. Concerning the analysis of the fibre break shape inside the vinylester resin, the untreated basalt fibre/vinylester samples exhibited a shape of break zone with a wide breaking gap and no matrix cracks (Figure V.20-A). This result is similar to that obtained for the untreated basalt/epoxy system and it is characteristic of a weak interface system. On the contrary, a strong reduction of the break zone between the basalt fibre ends was produced after the thermal and plasma treatments. In fact, from Figure V.20-B,C, it is possible to observe that both the vinylester samples reinforced with thermally treated and plasma treated basalt fibres showed a reduced break gap with a breakage extending in the vinylester matrix. However, contrary to what displayed by the epoxy samples, no "bat-shape" break zone may be observed for the vinylester matrix cracks (Figure V.20-B,C).

The birefringence method has been used to observe the interfacial debonding phenomena between the different basalt fibres and the epoxy matrix. According to Kim et al. [Kim *et al.*, 2002], when the debonding phenomena occur, photoelastic birefringence is formed near the stressed fibre ends. During the load application (Figure IV.23-A), two birefringence zones are produced: a first zone at the matrix/fibre interface, and a second larger zone surrounding the first one.

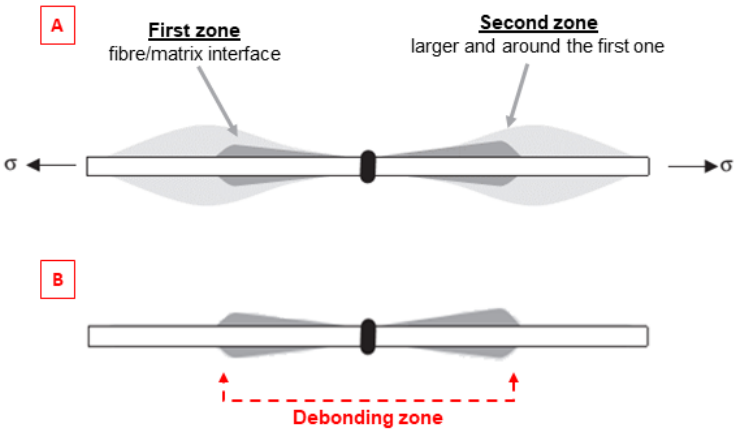

Figure V. 23 The schematic representation of the photoelastic birefringence pattern of shear stress around a fibre break with debonding phenomenon: A) under tensile loading; B) when the tensile loading is released [Kim et al., 2002] .

When the applied stress is removed (Figure IV.23-B), the second birefringence zone disappears, and the first zone remains unchanged. The length of this second zone corresponds to the length of the debonding zone. Figure V.24-A,B and Figure V.25-A,B show the birefringence patterns found for the as-received basalt fibre/epoxy system and for the single filament epoxy specimens with the thermally and plasma treated basalt fibres. From Figure V.24-B it is possible to note that the maximum of the flat colour birefringence zone coincides with the black line present at the interface between the fibre and the epoxy matrix. The length of this zone has been considered for the debonding length measurement. The as-received basalt fibre/epoxy samples have shown the highest debonding length values. A symmetrical birefringence pattern has been found, Figure V.24-A, which confirms that the saturation level occurred at the end of fragmentation test. After the thermal treatment and the polymer plasma deposition process, a decrease and a lack in the flat colour zone were detected (Figure V.25-A and Figure V.25-B, respectively).

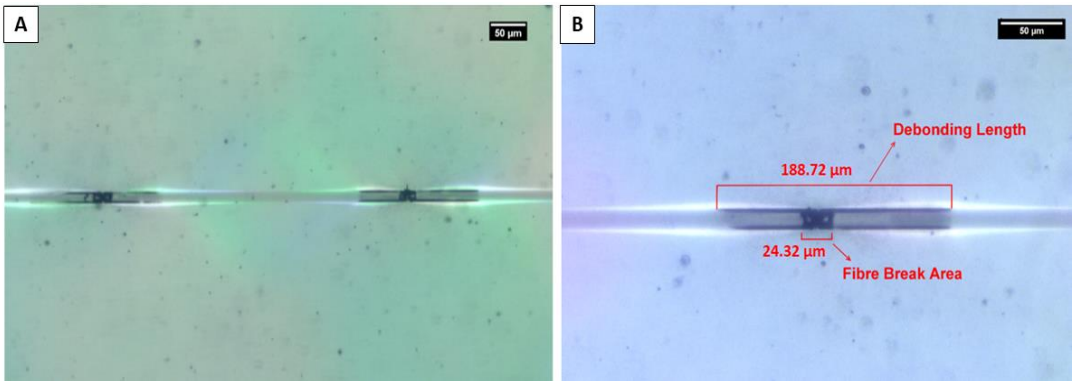

Figure V. 24 Optical micrographs showing the interface patterns (A) and the debonding length measurement (B) for the as-received basalt fibre/epoxy samples.

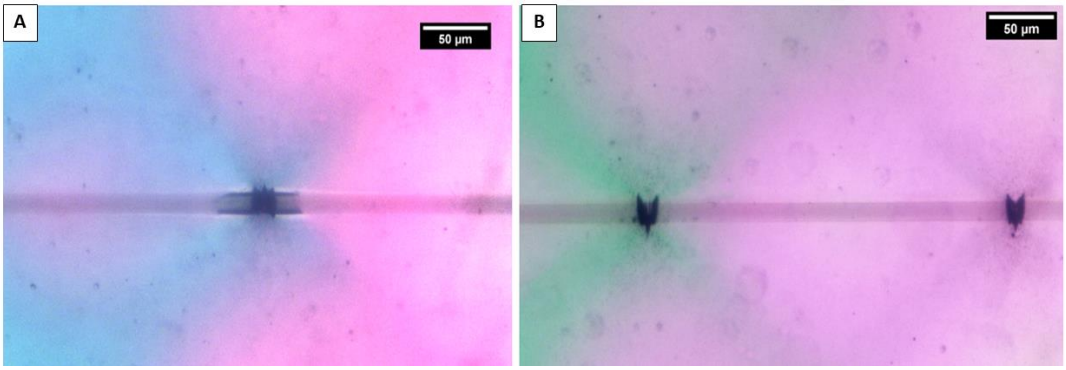

Figure V. 25 Optical micrographs showing the interface patterns for the thermally treated basalt fibre/epoxy (A) and the plasma treated basalt fibre/epoxy systems (B).

Contrary to the epoxy matrix samples, some difficulties have been encountered during the measurement of the debonding length values for the basalt/vinylester systems. It was not possible to use the birefringence method to observe the interfacial debonding phenomena between the different basalt fibres and the vinylester matrix, because of the no-birefringence character of this resin. In order to overcome this problem and carry out an accurate debonding zone assessment, a new technique was optimized by optical microscopy. As it is possible to see in Figure V.26, modifying the light transmittance parameters, it was possible to identify the debonding zone between the fibre and the vinylester resin in the brightest areas around basalt fibres.

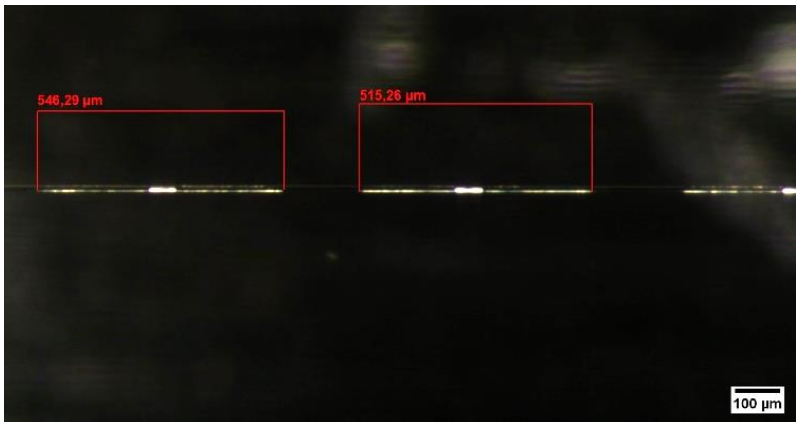

Figure V. 26 An example of an optical micrograph showing the debonding length pattern for the untreated basalt fibre/vinylester matrix sample.

Table V.8 reports all the debonding length values measured for the different specimens. Concerning the basalt/epoxy samples, the different values found confirm the results highlighted by birefringence analysis. After the pp-TVS deposition, basalt fibres showed a clear increase in compatibility with the epoxy matrix, evidenced by a significant reduction in the debonding phenomenon. In particular, a debonding length reduction of about 88% was found for the plasma treated basalt fibres with respect to the untreated ones. Similar results were found for the different basalt/vinylester single fibre composites. The thermal exposure of basalt fibres seems to produce a positive effect on their adhesion properties with the vinylester matrix. Indeed, a reduction of the debonding length was noticed after the thermal treatment. However, as already found for the epoxy matrix, the lowest values of debonding lengths were found for the composites containing plasma treated basalt fibre. A reduction of 67% of the fibre/matrix debonding length was found after the pp-TVS deposition. This result confirms the ability of the plasma polymerization process to successfully increase the

adhesion of basalt fibres with both the thermoset matrices. When comparing the results found for the basalt/epoxy and the basalt/vinylester composites, it is important to highlight that, for each family of basalt fibre, the basalt/vinylester systems are characterized by a lower adhesion compared to the basalt/epoxy ones. Wider fibre/matrix debonding zones were found with the vinylester resin than with the epoxy one.

Table V. 8 Debonding length values of the untreated and treated basalt fibres in epoxy and vinylester matrix samples.

Matrix	Basalt fibre	$l_{debonding}$ [µm]
Epoxy	As-received Basalt	192 ± 80
	Basalt 400°C - 1h	48 ± 8
	Basalt 400°C - 1h + PECVD	23.5 ± 14
Vinylester	As-received Basalt	387 ± 89
	Basalt 400°C - 1h	159 ± 92
	Basalt 400°C - 1h + PECVD	125 ± 68

V.2.1.2 Determination of critical fragment length and interfacial shear strength values

The measurement of the critical fibre fragment length has been performed through optical microscopy. As reported in section I.2.2.1, according to Ohsawa et al. [Ohsawa *et al.*, 1978], the critical fragment length value was evaluated using Equation I.18. The interfacial shear strength value (IFSS) was estimated in order to analyse the basalt fibre/matrix interface adhesion quality. This value was determined for the different systems using the Equation I.19, according to the model proposed by Kelly and Tyson [Kelly et al., 1965]. As already analysed in detail for flax yarns, also for the basalt fibres it was impossible to determine directly the tensile strength at a length equal to the critical fragment length because of its small value. To overcome this problem, the extrapolation method based on the Weibull cumulative distribution function has been used (Equation V.3). The Weibull parameters used are those obtained from tensile tests carried out at the gauge length L_0 of 40 mm, (Table IV.19). In Table V.9 are reported all the critical fragment length values, the $\sigma_f(l_c)$ values and the IFSS results obtained for the untreated and treated basalt/epoxy and basalt/vinylester composites. For both the epoxy and vinylester systems, it is possible to highlight that the

best results in terms of both critical fragment length and IFSS were found for the basalt fibres treated by the TVS plasma. From the results reported in Table V.9 it may be observed that a marked increase in the values of IFSS was produced after the deposition of the polymeric film for the basalt/epoxy samples. This reflects the results already discussed concerning break shape and debonding analysis.

Table V. 9 Critical fragment length and Interfacial Shear Strength of the untreated and treated basalt fibres in epoxy and vinylester matrix samples.

Matrix	Basalt fibre	l_c [µm]	$\sigma_f(l_c)$ [MPa]	IFSS [MPa]
Epoxy	As-received Basalt	675.2 ± 109	3591 ± 55	35.4 ± 6
	Basalt 400°C - 1h	353 ± 13	3282 ± 27	60.5 ± 3
	Basalt 400°C - 1h + PECVD	346 ± 48	3948 ± 101	75.4 ± 10
Vinylester	As-received Basalt	812 ± 114	3526 ± 46	28.6 ± 4
	Basalt 400°C - 1h	734 ± 119	2791 ± 99	25.3 ± 4.7
	Basalt 400°C - 1h + PECVD	705 ± 115	3412 ± 122	32.4 ± 7

A less pronounced increase in the IFSS value is obtained in the basalt/vinylester system. The increase in the compatibility between the plasma treated flax yarns and both epoxy and vinylester matrices is in accordance with the contact angles and the surface energy values found from the wetting analysis, section IV.2.3.1. As reported previously, both epoxy and vinylester resin are characterized by a strongly dispersive behaviour. A decrease in the polar component of the surface energy and a consequent enhancement of the dispersive behaviour of basalt fibres was found after the plasma polymerization treatment. These results highlighted that the TVS coating is able to promote the wetting of basalt fibres with the thermoset resin, increasing the fibre/matrix interfacial adhesion. By comparing the critical fragment lengths and the IFSS values obtained for the thermally treated and the plasma treated basalt fibres, it is possible to note that the thermal treatment seems to have a positive effect on the interfacial adhesion of the basalt fibre with the epoxy matrix. Despite the sizing degradation carried out by the thermal exposure, a decrease in the critical length and an increase in the IFSS values was produced compared to the values found for the as-received fibres. This is an interesting result because the sizing formulations are studied and optimized in order to promote the chemical bonding across the fibre/matrix interface. A possible

explanation of this result may be ascribed to the topography modification produced after the fibre thermal exposure. As discussed in section IV.2.3.2, an increase in the surface roughness of the thermally treated basalt fibres has been measured (Table IV.17). A mechanical interlocking action between the surface of the treated basalt fibre and the epoxy matrix may lead to the increase in the interfacial strength. In a recent study, Thomason et al. [Thomason *et al.*, 2018] observed that compressive radial stress, generated during the cooling step of composites production, may create static frictional stresses able to affect the IFSS value. For this reason, it may be assumed that the increase in the fibres surface roughness leads to a growing importance of the friction stresses in the fibre/matrix adhesion measurement. Concerning the vinylester polymer resin, a slight reduction in the interfacial shear strength value is found for the thermally treated basalt fibres. This result can be linked to the drop in tensile strength at the critical fragment length of basalt fibres. In fact, although the reduction in the critical fibre length indicates an enhancement in the fibre/matrix adhesion quality, the degradation of the mechanical properties of thermally treated basalt fibres can affect the IFSS measurement.

V.2.1.3 Fractographic analysis

A morphological investigation of the fracture surface has been performed using the FE-SEM. Concerning the different basalt/epoxy systems, from an in-depth analysis of the different fracture surfaces, once again it can be possible to confirm the higher adhesion of the plasma treated basalt fibre with the epoxy resin. Despite the positive values of critical fragment length, IFSS and debonding length reported previously, from Figure V.27-B, it can be inferred that a debonding phenomenon between the basalt fibre and the epoxy matrix is still present after the thermal treatment. However, the thermally treated fibres exhibited an in-plane failure without a pull-out phenomenon with the epoxy matrix, contrary to what was found for the untreated fibres (Figure V.27-A). This phenomenon can support the enhancement of adhesion quality between the basalt fibres and the epoxy matrix after the thermal de-sizing process. Unlike the untreated and thermally treated fibres, the specimens with the plasma treated fibres exhibit a total fibre/matrix adhesion. Figure V.28 shows how the plasma polymerization process is able to coat homogeneously the fibre surface. A measurement of the thickness of the polymer plasma TVS coating has been carried out through FE-SEM. Maximum and minimum thickness values of 1.4 µm and 0.8 µm,

respectively, have been measured. This difference in thickness values is caused by the shadowing effect of the other fibres present in the bundle during the plasma deposition process.

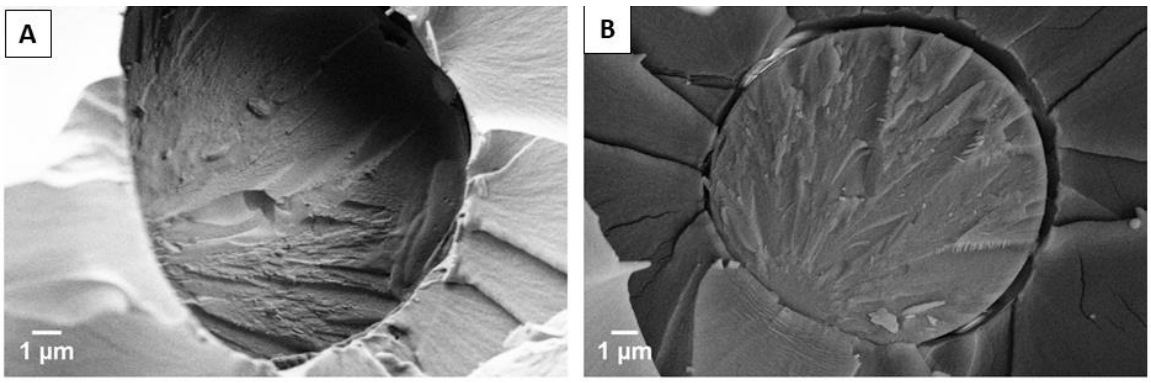

Figure V. 27 FE-SEM micrographs detailing the fracture surface for the untreated (A) and thermally treated (B) single basalt fibre/epoxy systems.

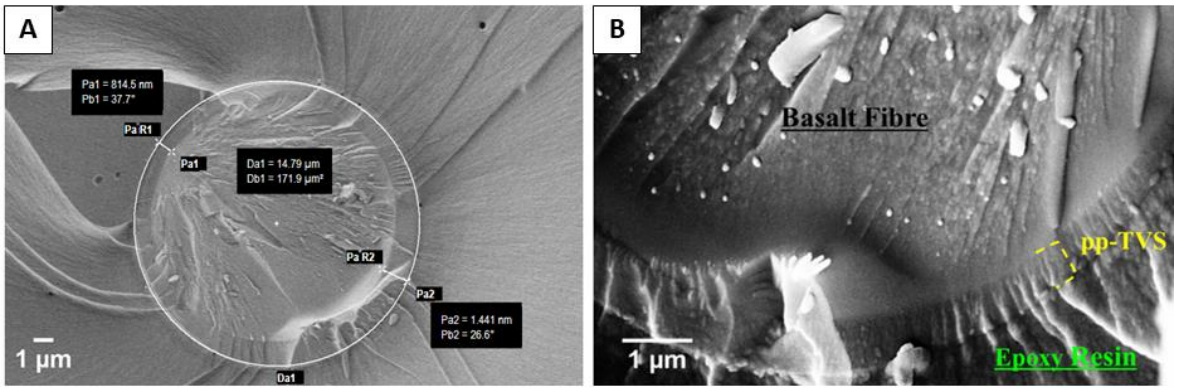

Figure V.28 FE-SEM micrographs detailing the fracture surface for the plasma treated single basalt fibre/epoxy systems: micrograph showing the thickness measurement of the pp-TVS deposited coating (A), a detailed view of the deposited pp-TVS coating at the fibre/matrix interface (B) [Seghini et al., 2019].

The FE-SEM micrographs obtained for the as-received and plasma treated basalt/vinylester composites are reported in Figure V.29. The micrographs confirmed the results observed for the basalt/epoxy systems. A poor interfacial adhesion for the untreated basalt fibres with vinylester matrix was observed, with the presence of pull-out and a debonding phenomenon (Figure V.29-A). As already reported for the basalt/epoxy system, the thermally treated fibres exhibited an in-plane failure without a pull-out phenomenon with the vinylester matrix (Figure V.29-B), proving the increase in interfacial adhesion quality between the basalt fibres and the vinylster matrix after the thermal de-sizing process.

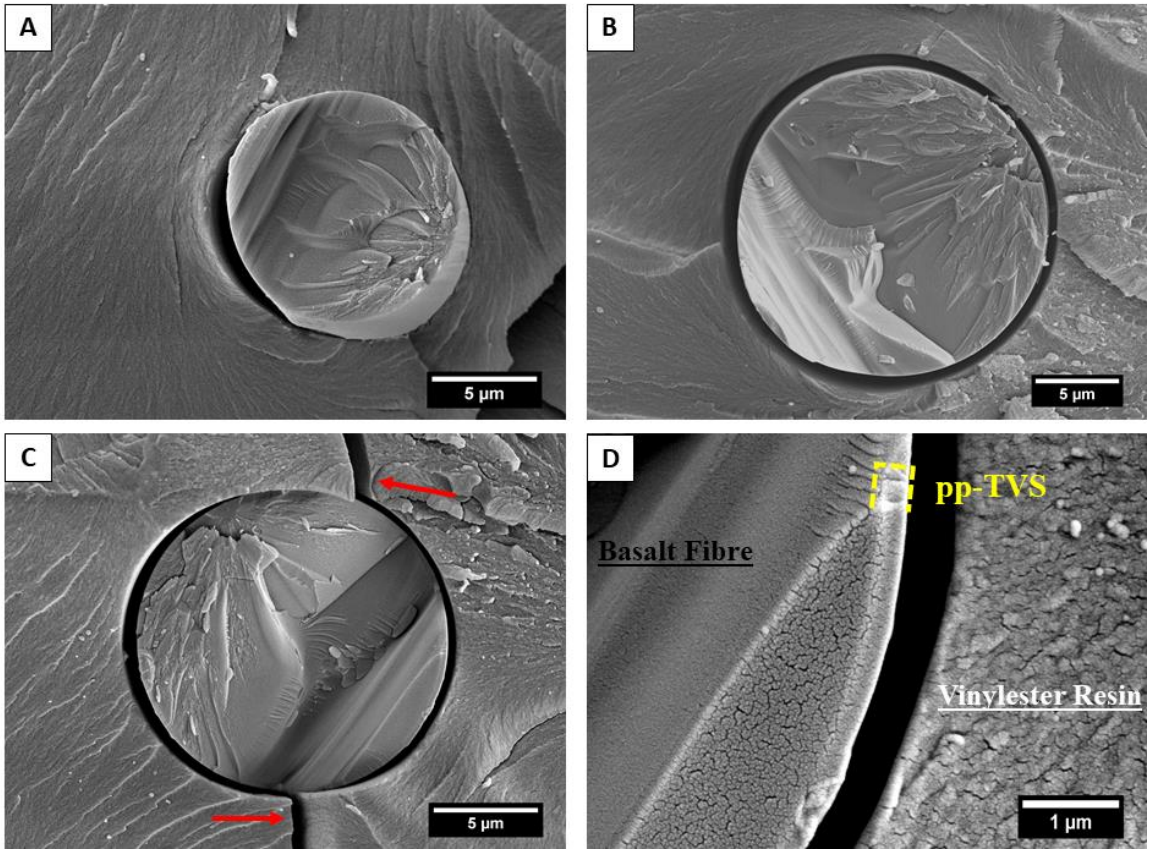

Figure V. 29 FE-SEM micrographs detailing the fracture surface for the untreated (A) thermally treated (B) and plasma treated (C) single basalt fibre/vinylester systems. A detailed view of the deposited pp-TVS coating at the fibre/matrix interface is also reported (D).

Differently from what observed previously for the epoxy matrix composites, the plasma polymerization treatment does not seem to produce a strong increase in the adhesion of basalt fibres with the vinylester matrix. From Figure V.29-C it is possible to notice a debonding zone between the plasma treated fibre and the matrix. Despite this fibre/matrix debonding, the presence of some matrix cracks, originated from the fibre failure zone (red arrows in Figure V.29-C), and an in-plane fibre failure can be linked to an increased load transfer ability from the vinylester matrix to the treated basalt fibre, thus to a slightly better interfacial strength. A detailed view of the deposited pp-TVS coating at the fibre/matrix interface is reported in Figure V.29-D. Finally, by comparing the different FE-SEM micrographs obtained for the basalt/epoxy and the basalt/vinylester systems, it is possible to highlight, once again, that both the as-received and the treated basalt fibres exhibit a better interfacial adhesion with the epoxy matrix than with the vinylester one.

Conclusion of Part V

The compatibility between natural fibres and polymer matrices plays a key-role in determining the mechanical performance of the resulting hybrid composites. In previous sections, it was shown how the chemical composition as well as the surface characteristics of natural fibres can prevent them from achieving good interfacial adhesion properties with polymer matrices. The results reported in Part IV have proven that it was possible to effectively modify the surface properties of both flax and basalt filaments by performing tailored chemical and physical treatments. In particular, a biochemical enzymatic and a supercritical CO_2 (SC-CO_2) treatments were able to successfully remove the undesirable substances which contribute to the hydrophilic behaviour of flax fibres, producing a bad interfacial adhesion with the more hydrophobic polymers. In addition, the physical treatments of oxygen plasma and plasma-enhanced chemical vapour deposition can respectively increase the surface roughness and deposit a homogeneous polymeric coating onto the surfaces of both flax and basalt filaments, promoting their interfacial bond with the polymer matrix.

Once analysed the effects on the chemical, mechanical and morphological properties of both flax and basalt filaments, it was of crucial importance to assess the actual effects of both the chemical and the physical treatments on the filament/matrix interfacial adhesion. In this framework, an in-depth analysis of the interfacial strength of both the untreated and treated filaments with the polymer matrices was performed. The single fibre fragmentation test (SFFT) was selected in order to evaluate the adhesion quality of flax and basalt filaments with epoxy and vinylester thermoset matrices. The filament/matrix adhesion quality was assessed in terms of critical fragment length and Interfacial Shear Strength (IFSS), according to the Kelly and Tyson theory. The as-received flax yarns and the commercial grade of basalt fibres showed better adhesion properties with the thermoset epoxy resin than with the vinylester one. The lowest values of critical fragment lengths and the highest values of IFSS were reported for both the untreated flax and basalt filaments in the epoxy matrix composite samples. An increase of the filament/matrix interface adhesion was produced by both the chemical and the physical modification treatments. The chemical enzymatic and the SC-CO_2

treatments have produced a reduction in the critical fragment length of flax yarns in both epoxy and vinylester matrices. The best result was reported after the enzymatic treatment carried out using the maximum concentration of the Peclyve solution and the maximum treatment duration, specifically 10 wt% and 6 h. A possible explanation of this result can be found in a greater ability of the Peclyve enzymatic solution at high concentration and treatment time, to successfully remove the more hydrophilic components from flax fibres, increasing their compatibility with polymer matrix. However, a reduction in the IFSS values was produced after both enzymatic and SC-CO_2 chemical treatments. This result pointed out the strong dependence of the critical fragment lengths and of IFSS values on the drop in the mechanical properties of flax yarns produced by the different treatments. To overcome this problem, the length of the debonding zone between the filament and the polymer matrix was considered. For the first time, the micro-computed tomography was used in the study of the interfacial properties. Specifically, a high-resolution microtomography was performed as support analysis to confirm the debonding lengths measurements observed by optical microscopy. The microtomographic images found for the enzymatically and SC-CO_2 treated flax/matrix samples confirmed the ability of these treatments to increase the adhesion properties of flax yarns with both epoxy and vinylester resin. This result can be linked to the removal of pectin and hemicellulose content produced after the exposure of flax yarn to the enzymatic solution and the supercritical fluid. The oxygen plasma treatment seems also to have a beneficial effect on the adhesion of flax yarns with polymer matrices, but the best results were obtained after the plasma modification treatments. The plasma polymer deposition produced a significant improvement of the adhesion property of flax yarns with both epoxy and vinylester matrices. An increase in the IFSS values of 114% and 71% was found after the TVS film deposition in epoxy and vinylester composites respectively, in comparison with the untreated yarn samples. In the case of basalt fibres, the adhesion qualities of the plasma-treated basalt fibres have even been superior to those of commercial fibres. A reduction in critical fragmentand debonding lengths as well as an increase in the value of IFSS have been obtained as a result of the pp-TVS with both the epoxy and the vinylester resins. In particular, an IFSS increase of about 113% was obtained for the plasma treated basalt/epoxy sample. These results were also confirmed by a morphological investigation by FE-SEM, performed on the different fracture surfaces after fragmentation test. This analysis pointed out that the presence of the pp-TVS coating onto the basalt fibre surface results in a total adhesion between the basalt fibres and the epoxy resin. The

interfacial adhesion properties of the plasma treated basalt fibres were compared with those found for thermally de-sized basalt fibres. The comparison highlighted that the surface topography of basalt fibres can also play a significant role in the fibre/matrix interfacial adhesion. Despite the thermal degradation of the optimized commercial sizing, an increase in the compatibility between the basalt fibre and both the epoxy and vinylester matrices was reported. As described in Part IV, the thermal treatment was able to produce an increase in the surface roughness of basalt fibres. It was assumed that the roughness enhancement can lead to an increase in the frictional stresses between the treated fibres and the polymer matrix, causing a mechanical interlocking effect between the fibre surface and the polymer matrix. The good results obtained for both flax and basalt filaments after the deposition of the plasma polymer TVS coating make the PECVD treatment extremely promising for a better interfacial adhesion in basalt-flax composites.

Conclusion de la Partie V

(en français)

La compatibilité entre les fibres naturelles et les matrices polymères joue un rôle clé dans les performances mécaniques des composites hybrides. Dans les sections précédentes, il a été montré comment la composition chimique ainsi que les caractéristiques de surface des fibres naturelles peuvent les empêcher d'atteindre de bonnes propriétés d'adhésion interfaciale avec les matrices polymères. Les résultats présentés dans la partie IV ont prouvé qu'il était possible de modifier efficacement les propriétés de surface des renforts de lin et de basalte en effectuant des traitements chimiques et physiques adaptés. En particulier, un traitement enzymatique biochimique et un traitement au CO_2 supercritique (SC-CO_2) ont réussi à éliminer les substances indésirables qui contribuent au comportement hydrophile des fibres de lin, produisant une mauvaise adhésion interfaciale avec les polymères les plus hydrophobes. De plus, les traitements physiques par plasma d'oxygène et par PECVD peuvent respectivement augmenter la rugosité de surface et déposer un revêtement polymère homogène sur les surfaces des renforts de lin et de basalte, favorisant leur liaison interfaciale avec la matrice polymère. Après avoir analysé les effets sur les propriétés chimiques, mécaniques et morphologiques des renforts de lin et de basalte, il était d'une importance cruciale d'évaluer les effets réels de ces traitements sur l'adhésion interfaciale fibre/matrice. Dans ce cadre, une analyse approfondie de la résistance interfaciale des renforts non traités et traités avec les matrices polymères a été réalisée. Le test de fragmentation sur composite monofilamentaire (SFFT) a été utilisé afin d'évaluer la qualité d'adhésion des renforts de lin et de basalte avec les matrices thermodures époxy et vinylester. La qualité d'adhésion fibre/matrice a été évaluée en termes de longueur critique de fragment et de résistance au cisaillement interfacial (IFSS), selon la théorie de Kelly et Tyson. Les fils de lin non traités et les fibres de basalte avec le revêtement commercial ont montré de meilleures propriétés d'adhésion avec la résine époxy qu'avec la vinylester. Les valeurs les plus faibles des longueurs critiques de fragments et les valeurs les plus élevées d'IFSS ont été obtenues pour les renforts de lin et de basalte non traités dans les échantillons composites à matrice époxy. Une augmentation de l'adhésion de l'interface fibre/matrice a été produite par les traitements de modification de surface. Les traitements par enzyme biochimique et par SC-CO_2 ont permis d'obtenir une réduction de la longueur critique des fragments pour les fils de lin dans les matrices époxy et vinylester. Le meilleur résultat a été atteint après le traitement enzymatique effectué en utilisant la concentration maximale de la solution de Peclyve et la durée maximale du traitement, c'est à dire 10% en masse pendant 6h. Cela peut s'expliquer par la plus grande capacité de la solution enzymatique Peclyve avec cette concentration élevée et pendant un temps de traitement long, pour éliminer avec succès les composants les plus hydrophiles des fibres de lin, augmentant ainsi leur compatibilité avec la matrice polymère. Cependant, une réduction des valeurs d'IFSS a été constatée après les traitements chimiques enzymatiques et par SC-CO_2. Ce résultat a mis en évidence la forte dépendance des longueurs critiques des fragments et des valeurs d'IFSS à la baisse des propriétés mécaniques des fils de lin produits par les différents traitements. Pour surmonter ce

problème, la longueur de la zone de décohésion entre le renfort et la matrice polymère a été considérée. Pour la première fois, la microtomographie par rayons X a été utilisée dans l'étude des propriétés interfaciales. Plus précisément, une microtomographie à haute résolution a été réalisée afin de confirmer les mesures de longueurs de décohésion observées par microscopie optique. Les images microtomographiques des échantillons de composite monofilamentaire élaborés avec des fils de lin traités enzymatiquement ou par SC-CO_2 ont confirmé la capacité de ces traitements à augmenter les propriétés d'adhésion des fils de lin avec la résine époxy et vinylester. Ce résultat peut être lié à l'élimination de la teneur en pectine et hémicellulose après l'exposition du fil de lin à la solution enzymatique et au fluide supercritique. Le traitement au plasma d'oxygène semble également avoir un effet bénéfique sur l'adhésion des fils de lin avec les matrices polymères, mais les meilleurs résultats ont été obtenus après les traitements de polymérisation par plasma. Le dépôt de polymère plasma a produit une amélioration significative l'adhésion des fils de lin avec les matrices époxy et vinylester. Une augmentation des valeurs d'IFSS de 114% et 71% a été trouvée après le dépôt de film de TVS dans les composites époxy et vinylester respectivement, en comparaison avec les échantillons contenant des fils non traités. Dans le cas des fibres de basalte, les qualités d'adhésion des fibres de basalte traitées au plasma ont même été supérieures à celles des fibres du commerce. Une réduction de la longueur critique de fragment et de la longueur de décohésion ainsi qu'une augmentation de la valeur de l'IFSS ont été obtenues à la suite des dépôts de film de TVS. En particulier, une augmentation de l'IFSS d'environ 113% a été obtenue pour l'échantillon de basalte/époxy traité au plasma. Ces résultats ont également été confirmés par une étude morphologique par FE-SEM, réalisée sur les différents faciès de rupture après les tests de fragmentation. Cette analyse a souligné que la présence du revêtement pp-TVS sur la surface des fibres de basalte entraîne une adhésion totale entre les fibres de basalte et la résine époxy. Les propriétés d'adhésion interfaciale des fibres de basalte traitées au plasma ont été comparées à celles trouvées pour les fibres de basalte après traitement thermique. La comparaison a mis en évidence que la topographie de surface des fibres de basalte peut également jouer un rôle important dans l'adhésion interfaciale fibre/matrice. Malgré la dégradation thermique de l'agent de couplage commercial, une augmentation de la compatibilité entre la fibre de basalte et les matrices époxy et vinylester a été obtenue. Comme décrit dans la partie IV, le traitement thermique a pu produire une augmentation de la rugosité de surface des fibres de basalte. Il a été supposé que l'amélioration de la rugosité peut entraîner une augmentation des contraintes de friction entre les fibres traitées et la matrice polymère, provoquant un effet d'ancrage mécanique entre la surface des fibres et la matrice polymère. Les bons résultats obtenus pour les renforts de lin et de basalte après le dépôt du revêtement polymère par plasma rendent le traitement PECVD extrêmement prometteur pour une meilleure adhésion interfaciale dans les composites hybrides basalte-lin.

Conclusions and Future Perspectives

The present work was focused on the optimization of the fibre/matrix interfacial adhesion for the development of basalt-flax hybrid composites with the twofold objective of obtaining more environmentally friendly and low-cost composites for semi-structural applications. Therefore, in this study different types of treatments were applied on plant (flax) and mineral (basalt) fibres, selecting the more efficient one by performing specific single fibre fragmentation tests.

In a first phase of the study, the mechanical properties of basalt-flax hybrid composites were determined in order to highlight the interest of hybridization. The hybrid composites were produced through vacuum infusion moulding using epoxy matrix. For comparison purposes, flax/epoxy and basalt/epoxy woven composites were also manufactured. Tensile and four-point bending tests were performed to assess the quasi-static mechanical behaviour of composites, whereas tensile-tensile fatigue tests and low-velocity impact tests were carried out to investigate their dynamic performances. The results pointed out that hybridization was able to produce a composite material with intermediate mechanical properties between those owned by flax and basalt composites. Specifically, the combination of basalt with flax fibres has proven to be a possible solution to overcome with success the typical limitations shown by flax fibre reinforced laminates, such as a low tensile and flexural strength and a low impact resistance. At the same time, a positive effect on the fatigue resistance of basalt laminates was produced by hybridization. In particular, hybrid composites exhibited a higher number of cycles to failure than that of basalt reinforced composites. However, the mechanical characterization confirmed the need to optimize the interfacial adhesion between the natural fibres and the epoxy matrix in order to exploit the full potential of the resulting hybrid composites. A post-fatigue morphological analysis of the fracture surfaces of the different laminates highlighted the low adhesion quality of both flax and basalt fibres with the epoxy matrix. It is well known that the low compatibility of natural fibres with polymer matrices is strongly dictated by their chemical composition and their surface characteristics. An analysis of the wetting properties of the as-received flax yarns, used in this study, confirmed the strong hydrophilic nature of these fibres, depending essentially on their

chemical composition. Indeed, a FT-IR analysis highlighted that flax fibres consist of hydroxyl and strongly polarized groups, belonging to hemicellulose and cellulose, which confer a hydrophilic character to flax fibres and prevent them from achieving a proper interfacial adhesion with hydrophobic polymer matrices. In addition, concerning the basalt fibres, it is important to stress that the commercial sizing present on the fibre surfaces is not only characterized by a variable thickness and uniformity, but it is inherited from glass fibre technology, thus not necessarily designed for basalt fibres.

In this framework, the next phase of the study was focused on the design and investigation of different surface modification treatments able to enhance the interfacial strength between both flax and basalt fibres and thermoset matrices. Chemical and physical "green treatments" were selected with a view to reducing their impact on the environment. In particular, an enzymatic biochemical process and a supercritical CO_2 modification treatment were used to modify the surface properties of flax. Concerning the physical treatments, an oxygen plasma and a tetravinylsilane (TVS) plasma treatments by Plasma Enhanced Chemical Vapour Deposition (PECVD) were performed in order to enhance the adhesion quality of flax and basalt filaments with different thermoset resins. The compositional and the thermogravimetric analyses performed on untreated and chemically treated flax yarns highlighted the ability of both enzymatic and supercritical CO_2 treatments to remove hemicellulose, pectin and waxes from flax fibres. In particular, the Peclyve enzymatic solution, rich in pectinases and xyloglucanases enzymes, successfully removed the pectin and hemicellulose constituents from flax, increasing its hydrophobic character. A similar effect was found after the oxygen plasma treatment. A morphological and compositional analysis showed that the oxygen plasma can increase the surface roughness and introduce functional groups in the surface of flax fibres. These effects are important for the enhancement of the fibre/matrix wetting properties and play a key role in promoting the plasma TVS polymer film deposition. It was found that the greater the plasma power used during oxygen treatment, the better the adhesion of the polymeric film to the surface of flax fibre. The plasma polymerization process has proven to be the most performing treatment in changing the wetting properties of flax. The deposition of the TVS polymer film resulted in an increase in the dispersive behaviour of flax fibres and in a strong reduction in their surface wetting with polar liquid. Similar results were found for the basalt fibres. The effects produced by the plasma process were compared with those obtained by using a commercial coupling agent optimized for epoxy resins and a thermal de-sizing treatment performed at

400°C for 1 h. An increase of about 103% in the static contact angle with water was found after the deposition of the tetravinylsilane coating. The morphological analysis of the lateral surfaces of the different basalt fibres showed that an increase in roughness was produced after the thermal treatment. This effect combined with the increase in hydrophobic behaviour may constitute a key factor in order to promote the adhesion of the fibres with the polymeric matrix, producing mechanical interlocking between the fibre and the matrix surfaces. The study also demonstrated how the plasma treatment can deposit a homogeneous polymer coating on the surface of the fibres, protecting the fibre surface and covering the existing fibre defects.

Once analysed the effects of both chemical and physical treatments on the properties of flax and basalt filaments, it was of crucial importance to assess the actual effects of these treatments on the filament/matrix interfacial adhesion. The degree and extent of filament/matrix adhesion were investigated by micromechanical fragmentation tests (Single Fibre Fragmentation Test - SFFT). The adhesion quality of untreated and treated flax yarns and basalt fibres with an epoxy and a vinylester matrix was discussed in terms of critical fragment length, debonding length and interfacial shear strength (IFSS). High-resolution μ-CT has been used to support the analysis of the damage mechanisms during fragmentation tests, and to confirm the debonding length measurements observed by optical microscopy. The results revealed that both enzymatic and supercritical CO_2 treatments were able to increase the filament/matrix interfacial adhesion. This result can be linked to the removal of pectin and hemicellulose after the exposure of flax yarn to the enzymatic solution and the supercritical fluid. Concerning the physical treatments, the oxygen plasma treatment seems to have a beneficial effect on the adhesion of flax yarns with both epoxy and vinylester matrices. However, the best results in terms of critical filament, debonding lengths and IFSS were obtained after the plasma polymer deposition treatment. This treatment produced a significant improvement of the adhesion property of flax yarns and basalt fibres with both epoxy and vinylester matrices. In particular, the best results were found with the epoxy matrix. An increase in the IFSS values of 114 % and 113 % was found after the TVS film deposition in flax/epoxy and basalt/epoxy composites, respectively, in comparison with the untreated samples. These results were also confirmed by a morphological investigation by FE-SEM, performed on the different fracture surfaces after fragmentation test. Despite the thermal degradation of the optimized commercial sizing, an increase in the compatibility between the basalt fibre and both the epoxy and vinylester matrices was reported. This result

demonstrated how surface topography can play a significant role in the domain of fibre/matrix interfacial adhesion. In fact, the increase in the fibre surface roughness produced by the thermal treatment can promote the formation of mechanical interactions between the fibre and the polymer matrix.

The present work demonstrates how both chemical and physical treatments can successfully modify the surface properties of natural fibres, producing a positive effect on their adhesion quality with polymer matrices. Among the different treatments, the plasma polymer deposition process has proved to be of particular interest. The satisfactory results obtained for both flax and basalt filaments after the deposition of the plasma polymer tetravinylsilane coating make the plasma polymerization treatment extremely promising for a better interfacial adhesion in basalt-flax composites. Despite these positive aspects, this study showed the need to carry out an optimization of the different process parameters used. In fact, all the different surface modification treatments resulted in a reduction in the tensile strength of flax yarns. Specifically, a close connection was proved to exist between the oxygen plasma treatment and the mechanical properties of flax. Results of fragmentation tests highlighted that only the TVS deposition after the 100 W oxygen pre-treatment was able to produce a strong enhancement of the flax yarn/matrix interfacial adhesion. However, the oxygen plasma power of 100 W results in a strong degradation of the tensile resistance of flax yarns. A future perspective will be certainly the optimization of the plasma power for oxygen pre-treatment, in order to maximize the adhesion of the TVS coating on the fibre surface while not reducing the fibre mechanical performance. Manufacturing hybrid composites with the optimized fibre/matrix interface treatment will represent an important future development of this research. It will be of crucial importance to assess the actual effects of these treatments on the mechanical performance of the resulting hybrid composites. Based on the good results obtained, the plasma polymerization treatment can be selected as the treatment able to produce the best increase in the filament/matrix interfacial adhesion, even considering its potential scalability in manufacturing systems. Commercial production requires continuous surface modification using a roll-to-roll plasma device. Plasma coating in low-pressure plasmas allows for a wide variability of physical, chemical, and topographic properties for the functionalization of the fibre surface. Roll-to-roll devices with PECVD reactors that operate at low pressure and focus on the surface modification of fibres are becoming available, thus being potentially attractive from a manufacturing point

of view. Finally, an increased fibre/matrix wettability will provide an optimization of the manufacturing process of composite materials, in order to reduce the porosity content present inside the laminates and obtain better mechanical performances and less variable properties. All these improvements can promote the industrial exploitation of the future generation of basalt-flax hybrid composites in semi-structural applications.

Conclusion et perspectives

(en français)

Ce travail de thèse avait pour objectif l'optimisation de l'adhésion interfaciale fibre/matrice pour le développement de composites hybrides basalte-lin afin d'obtenir des composites plus respectueux de l'environnement et à faible coût pour des applications semi-structurelles. Par conséquent, dans cette étude, différents types de traitements ont été appliqués sur les fibres végétales (lin) et minérales (basalte), en sélectionnant le traitement le plus efficace grâce à des tests de fragmentation sur composites monofilamentaires. Dans une première phase de l'étude, les propriétés mécaniques des composites hybrides basalte-lin ont été déterminées afin de mettre en évidence l'intérêt de l'hybridation. Les composites hybrides ont été élaborés par moulage par infusion sous vide en utilisant une matrice époxy. À des fins de comparaison, des composites tissés lin/époxy et basalte/époxy ont également été fabriqués. Des tests de traction et de flexion quatre points ont été effectués pour évaluer le comportement mécanique quasi-statique des composites, ainsi que des tests de fatigue en traction-traction et des tests d'impact à basse vitesse pour étudier leurs performances dynamiques. Les résultats ont montré que l'hybridation a permis d'obtenir un matériau composite avec des propriétés mécaniques intermédiaires entre celles des composites 100% à fibres de lin et celles des composites 100% à fibres de basalte. Plus précisément, la combinaison du basalte avec les fibres de lin s'est avérée être une solution possible pour surmonter avec succès les limitations des stratifiés renforcés uniquement de fibres de lin, telles qu'une faible résistance à la traction et à la flexion et une faible résistance aux chocs. Dans le même temps, un effet positif sur la résistance à la fatigue des stratifiés à fibres de basalte a été obtenu par hybridation. En particulier, les composites hybrides ont montré un nombre de cycles à rupture plus élevé que celui des composites renforcés à 100% de basalte. Cependant, la caractérisation mécanique a confirmé la nécessité d'optimiser l'adhésion interfaciale entre les fibres naturelles et la matrice époxy afin d'exploiter tout le potentiel des composites hybrides. Une analyse morphologique post-fatigue des faciès de rupture des différents stratifiés a mis en évidence la faible qualité d'adhésion des fibres de lin et de basalte avec la matrice époxy. Il est bien connu que la faible compatibilité des fibres naturelles avec les matrices polymères est fortement dictée par leur composition chimique et leurs caractéristiques de surface. Une analyse des propriétés de mouillage des fils de lin non traités a confirmé la forte nature hydrophile de ces fibres, liée essentiellement à leur composition chimique. En effet, une analyse FT-IR a mis en évidence que les fibres de lin sont constituées de groupes hydroxyles et fortement polarisés, appartenant à l'hémicellulose et à la cellulose, qui confèrent un caractère hydrophile aux fibres de lin et les empêchent de créer une adhésion interfaciale correcte avec les matrices polymères hydrophobes. En outre, en ce qui concerne les fibres de basalte, il est important de souligner que le traitement commercial présent à la surface des fibres achetées présente une épaisseur et une uniformité variables, et est hérité de la technologie des fibres de verre, donc pas nécessairement conçu pour les fibres de basalte. Dans ce cadre, la phase suivante de l'étude s'est concentrée sur la conception et l'étude de différents traitements de modification de surface

capables d'améliorer l'adhésion interfaciale entre les fibres de lin et de basalte et les matrices thermodures étudiées. Des «traitements verts» chimiques et physiques ont été sélectionnés en vue de réduire leur impact sur l'environnement. En particulier, un processus biochimique enzymatique et un traitement par CO_2 supercritique ont été utilisés pour modifier les propriétés de surface du lin. Concernant les traitements physiques, un plasma d'oxygène et un dépôt de tétravinylsilane (TVS) par plasma (Plasma Enhanced Chemical Vapor Deposition - PECVD) ont été réalisés afin d'améliorer la qualité d'adhésion des renforts de lin et de basalte avec les résines thermodurcissables. Les analyses de la composition de la surface des renforts et les analyses thermogravimétriques effectuées sur les fils de lin non traités et traités chimiquement ont mis en évidence la capacité des traitements enzymatiques et au CO_2 supercritique à éliminer l'hémicellulose, la pectine et les cires des fibres de lin. En particulier, la solution enzymatique Peclyve, riche en enzymes pectinases et xyloglucanases, a réussi à éliminer la pectine et l'hémicellulose du lin, augmentant ainsi son caractère hydrophobe. Un effet similaire a été constaté après le traitement au plasma d'oxygène. Une analyse morphologique et chimique a montré que le plasma d'oxygène peut augmenter la rugosité de surface et introduire des groupes fonctionnels à la surface des fibres de lin. Ces effets sont importants pour l'amélioration des propriétés de mouillage fibre/matrice et jouent un rôle clé pour le dépôt du film polymère de TVS par plasma. Il a été constaté que plus la puissance du plasma utilisée pendant le traitement à l'oxygène est élevée, meilleure est l'adhérence du film polymère à la surface de la fibre de lin. Le processus de polymérisation au plasma s'est avéré être le traitement le plus performant pour modifier les propriétés de mouillage du lin. Le dépôt du film polymère de TVS a entraîné une augmentation du comportement dispersif des fibres de lin et une forte réduction de leur mouillage superficiel par le liquide polaire. Des résultats similaires ont été trouvés pour les fibres de basalte. Les effets produits par le procédé plasma ont été comparés à ceux obtenus en utilisant un agent de couplage commercial optimisé pour les résines époxy et un traitement thermique effectué à 400°C pendant 1h. Une augmentation d'environ 103% de l'angle de contact statique avec l'eau a été observée après le dépôt du revêtement de tétravinylsilane. L'analyse morphologique des surfaces des différentes fibres de basalte a montré qu'une augmentation de la rugosité s'est produite après le traitement thermique. Cet effet combiné à l'augmentation du comportement hydrophobe peut constituer un facteur clé pour favoriser l'adhésion des fibres à la matrice polymère, produisant un ancrage mécanique entre la fibre et la matrice. L'étude a également montré comment le traitement au plasma peut déposer un revêtement polymère homogène à la surface des fibres, protégeant la surface des fibres et couvrant les défauts initiaux des fibres.

Après avoir analysé les effets des traitements chimiques et physiques sur les propriétés des renforts de lin et de basalte, il était important d'évaluer les effets réels de ces traitements sur l'adhésion interfaciale fibre/matrice. La qualité de l'adhésion fibre/matrice a été étudiée en réalisant des tests de fragmentation micromécanique (Single Fibre Fragmentation Test - SFFT). La qualité d'adhésion des fils de lin et des fibres de basalte non traités et traités avec une matrice époxy et vinylester a été discutée en termes de longueur critique de fragment, de longueur de décohésion et de résistance au cisaillement interfacial (IFSS). La microtomographie haute résolution a été utilisée pour compléter l'analyse des mécanismes d'endommagement lors des tests de fragmentation et pour confirmer les mesures de longueur de décohésion déterminées par microscopie optique. Les résultats ont révélé que les traitements

enzymatiques et au CO_2 supercritique étaient capables d'augmenter l'adhésion interfaciale fibre/matrice. Ce résultat peut être lié à l'élimination de la pectine et de l'hémicellulose après exposition du fil de lin à la solution enzymatique et au fluide supercritique. Concernant les traitements physiques, le traitement plasma d'oxygène semble avoir un effet bénéfique sur l'adhésion des fils de lin aux matrices époxy et vinylester. Cependant, les meilleurs résultats ont été obtenus après le traitement PECVD. Ce traitement a produit une amélioration significative de l'adhésion des fils de lin et des fibres de basalte avec les matrices époxy et vinylester. En particulier, les meilleurs résultats ont été obtenus avec la matrice époxy. Une augmentation des valeurs d'IFSS de 114% et 113% a été observée après le dépôt du film de TVS dans les composites lin/époxy et basalte/époxy, respectivement, par rapport aux échantillons non traités. Ces résultats ont également été confirmés par une étude morphologique par FE-SEM, réalisée sur les différents faciès de rupture après tests de fragmentation. Malgré la dégradation thermique de l'agent de couplage commercial, une augmentation de la compatibilité entre la fibre de basalte et les matrices époxy et vinylester a été constatée. Ces résultats ont montré comment la topographie de surface peut jouer un rôle important au niveau de l'adhésion interfaciale fibre/matrice. En effet, l'augmentation de la rugosité de surface des fibres produite par le traitement thermique peut favoriser la formation d'interactions mécaniques entre la fibre et la matrice polymère.

Le présent travail montre comment les traitements chimiques et physiques peuvent modifier avec succès les propriétés de surface des fibres naturelles, produisant un effet positif sur leur qualité d'adhésion avec les matrices polymères. Parmi les différents traitements, le procédé de dépôt de polymère par plasma s'est révélé particulièrement intéressant. Les résultats satisfaisants obtenus pour les renforts de lin et de basalte après le dépôt du revêtement de polymère de tétravinylsilane par plasma rendent ce traitement extrêmement prometteur pour une meilleure adhésion interfaciale dans les composites basalte-lin. Malgré ces aspects positifs, cette étude a montré également la nécessité de réaliser une optimisation des différents paramètres des procédés utilisés. En fait, les différents traitements de modification de surface ont entraîné une réduction de la résistance à la traction des fils de lin. Plus précisément, il a été montré qu'un lien étroit existait entre le traitement au plasma d'oxygène et les propriétés mécaniques du lin. Les résultats des tests de fragmentation ont mis en évidence que seul le dépôt de TVS après le prétraitement à l'oxygène de 100 W était capable de produire une forte amélioration de l'adhésion interfaciale fil de lin/matrice. Cependant, la puissance du plasma d'oxygène de 100 W entraîne une forte dégradation de la résistance à la traction des fils de lin. Une perspective sera certainement l'optimisation de la puissance du plasma pour le prétraitement à l'oxygène, afin de maximiser l'adhérence du revêtement de TVS sur la surface de la fibre sans réduire les performances mécaniques de la fibre. La fabrication de composites hybrides avec le traitement optimisé constitue une perspective importante de cette recherche. Il sera d'une importance cruciale d'évaluer les effets réels de ces traitements sur les performances mécaniques des composites hybrides optimisés. Sur la base des résultats obtenus, le traitement de polymérisation par plasma peut être sélectionné comme le traitement capable de produire la meilleure augmentation d'adhésion interfaciale. La production commerciale nécessitera de pouvoir effectuer une modification de surface en continu à l'aide par exemple d'un appareil à plasma de type rouleau à rouleau (roll-to-roll). Des dispositifs rouleau à rouleau avec des réacteurs PECVD qui fonctionnent à basse pression pour modifier la surface

des fibres sont en cours de développement, rendant possible un traitement à l'échelle industrielle. De plus, une mouillabilité fibre/matrice accrue permettra également d'optimiser le processus de fabrication des matériaux composites, afin de réduire la porosité présente à l'intérieur des stratifiés et d'obtenir de meilleures performances mécaniques et des propriétés moins variables. Toutes ces améliorations peuvent favoriser le développement industriel de la future génération de composites hybrides basalte-lin pour des applications semi-structurelles.

References

[Abdel-Halim et al., 2010] Abdel-Halim, E. S., Konczewicz, W., Zimniewska, M., Al-Deyab, S. S. and El-Newehy, M. H. (2010) ‘‘Enhancing hydrophilicity of bioscoured flax fabric by emulsification post-treatment’’, Carbohydrate Polymers, 82(1), pp. 195–201. doi: 10.1016/j.carbpol.2010.04.065.

[Abdullah-Al-Kafi et al., 2006] Abdullah-Al-Kafi, Abedin, M., Beg, M. and Al., E. (2006) ‘‘Study on the mechanical properties of jute/glass fiber-reinforced unsaturated polyester hybrid composites: effect of surface modification by ultraviolet radiation.’’, Journal of Reinforced Plastics and Composites, 25(6), pp. 575–588.

[Abidi et al., 2014] Abidi, N., Cabrales, L. and Haigler, C. H. (2014) ‘‘Changes in the cell wall and cellulose content of developing cotton fibers investigated by FTIR spectroscopy’’, Carbohydrate Polymers. Elsevier Ltd., 100, pp. 9–16. doi: 10.1016/j.carbpol.2013.01.074.

[Abidi et al., 2018] Abidi, N. and Manike, M. (2018) ‘‘X-ray diffraction and FTIR investigations of cellulose deposition during cotton fiber development’’, Textile Research Journal, 88(7), pp. 719–730.

[Adamsen et al., 2002] Adamsen, A. P. S., Akin, D. E. and Rigsby, L. L. (a2002) ‘‘Chelating Agents and Enzyme Retting of Flax’’, Textile Research Journal, 72(4), pp. 296–302.

[Adamsen et al., 2002] Adamsen, A. P. S., Akin, D. E. and Rigsby, L. L. (b2002) ‘‘Chemical retting of flax straw under alkaline conditions’’, Textile Research Journal, 72(9), pp. 789–794.

[Ageorges et al., 1999] Ageorges, C., Friedrich, K., Schüller, T. and Lauke, B. (1999) ‘‘Single-fibre Broutman test: Fibre-matrix interface transverse debonding’’, Composites Part A: Applied Science and Manufacturing, 30(12), pp. 1423–1434. doi: 10.1016/S1359-835X(99)00045-7.

[Akash. et al., 2018] Akash., Gupta, N. S. V. and Rao, K. V. S. (2018) ‘‘An experimental study on sisal/hemp fiber reinforced hybrid composites.’’, Materials Today: Proceedings, 5, pp. 7383–7387.

[Akil et al., 2014] Akil, H., Santulli, C., Sarasini, F., Tirillò, J. and Valente, T. (2014) ‘‘Environmental effects on the mechanical behaviour of pultruded jute / glass fibre-reinforced polyester hybrid composites’’, Composite Science and Technology. Elsevier Ltd, 94, pp. 62–70. doi: 10.1016/j.compscitech.2014.01.017.

[Akin et al., 2001] Akin, D. E., Foulk, J. A., Dodd, R. B. and McAllister, D. D. (2001) ‘‘Enzyme-retting of flax and characterization of processed fibers’’, Journal of Biotechnology, 89(2–3), pp. 193–203.

[Alavudeen et al., 2015] Alavudeen, A., Rajini, N. and Karthikeyan, S Thiruchitrambalam, M Venkateshwaren, N. (2015) ‘‘Mechanical properties of banana/kenaf fiber-reinforced hybrid polyester composites: Effect of woven fabric and random orientation.’’, Materials & Design, 66, pp. 246–57.

[Alexander et al., 2017] Alexander, J. and Elphej Churchill, S. J. (2017) ‘‘Mechanical Characterization of Baslat Based Natural Hybrid Composites for Aerospace Applications’’, IOP

Conference Series: Materials Science and Engineering, 197, pp. 1–8. doi: 10.1088/1757-899X/197/1/012008.

[Andrew et al., 2019] Andrew, J. J., Srinivasan, S. M., Arockiarajan, A. and Dhakal, H. N. (2019) ‘‘Parameters influencing the impact response of fiber-reinforced polymer matrix composite materials: A critical review’’, Composite Structures, 224, p. 111007. doi: 10.1016/j.compstruct.2019.111007.

[Arbelaiz et al., 2005] Arbelaiz, A., Cantero, G., Fernández, B., Mondragon, I., Gañán, P. and Kenny, J. M. (2005) ‘‘Flax fiber surface modifications: Effects on fiber physico mechanical and flax/polypropylene interface properties’’, Polymer Composites, 26(3), pp. 324–332. doi: 10.1002/pc.20097.

[Arberlaiz et al., 2007] Arberlaiz, A., Fernandez, B., Cantero, G., Llano-Ponte, R., Valea, A. and Mondragon, I. (2007) ‘‘Mechanical properties of flax fibre/polypropylene composites. Influence of fibre/matrix modification and glass fibre hybridization.’’, Composites: Part A, 36, pp. 1637–44.

[Asadi et al., 2016] Asadi, A., Miller, M., Moon, R. J. and Kalaitzidou, K. (2016) ‘‘Improving the interfacial and mechanical properties of short glass fiber/epoxy composites by coating the glass fibers with cellulose nanocrystals’’, Express Polymer Letters, 10(7), pp. 587–597. doi: 10.3144/expresspolymlett.2016.54.

[Ashik et al., 2015] Ashik, K. P. and Sharma, R. S. (2015) ‘‘A Review on Mechanical Properties of Natural Fiber Reinforced Hybrid Polymer Composites’’, Journal of Minerals and Materials Characterization and Engineering, 3, pp. 420–426.

[Assarar et al., 2015] Assarar, M., Zouari, W., Sabhi, H., Ayad, R. and Berthelot, J. (2015) ‘‘Evaluation of the damping of hybrid carbon – flax reinforced composites’’, Composite Structures. Elsevier Ltd, 132, pp. 148–154. doi: 10.1016/j.compstruct.2015.05.016.

[Atiqah et al., 2014] Atiqah, A., Maleque, M. A., Jawaid, M. and Iqba, M. (2014) ‘‘Development of kenaf-glass reinforced unsaturated polyester hybrid composite for structural applications.’’, Composites Part B: Engineering, 56, pp. 68–73.

[Awal et al., 2011] Awal, A., Cescutti, G., Ghosh, S. B. and Müssig, J. (2011) ‘‘Interfacial studies of natural fibre/polypropylene composites using single fibre fragmentation test (SFFT)’’, Composites Part A: Applied Science and Manufacturing. Elsevier Ltd, 42(1), pp. 50–56. doi: 10.1016/j.compositesa.2010.10.007.

[Aydın et al., 2011] Aydın, M., Tozlu, H., Kemaloglu, S., Aytac, A. and Ozkoc, G. (2011) ‘‘Effects of Alkali Treatment on the Properties of Short Flax Fiber-Poly(Lactic Acid) Eco-Composites’’, Journal of Polymers and the Environment, 19(1), pp. 11–17. doi: 10.1007/s10924-010-0233-9.

[Baltazar-y-Jimenez et al., 2008] Baltazar-y-Jimenez, A., Bistritz, M., Schulz, E. and Bismarck, A. (a2008) ‘‘Atmospheric air pressure plasma treatment of lignocellulosic fibres: Impact on mechanical properties and adhesion to cellulose acetate butyrate’’, Composites Science and Technology, 68(1), pp. 215–227. doi: 10.1016/j.compscitech.2007.04.028.

[Barouni et al., 2019] Barouni, A. K. and Dhakal, H. N. (2019) ‘‘Damage investigation and assessment due to low-velocity impact on flax/glass hybrid composite plates’’, Composite Structures. Elsevier, 226, pp. 111224. doi: 10.1016/j.compstruct.2019.111224.

[Beckermann et al., 2009] Beckermann, G. W. and Pickering, K. L. (2009) ‘‘Engineering and evaluation of hemp fibre reinforced polypropylene composites: Micro-mechanics and strength

prediction modelling'', Composites Part A: Applied Science and Manufacturing. Elsevier Ltd, 40(2), pp. 210–217. doi: 10.1016/j.compositesa.2008.11.005.

[Beg et al., 2008] Beg, M. D. H. and Pickering, K. L. (2008) ''Mechanical performance of kraft fibre reinforced polypropylene composites: influence of fibre length, fibre beating and hygrothermal ageing.'', Composites Part A: Applied Science and Manufacturing, 39, pp. 1748–1755.

[Beggs et al., 2015] Beggs, K. M., Servinis, L., Gengenbach, T. R., Huson, M. G., Fox, B. L. and Henderson, L. C. (2015) ''A systematic study of carbon fi bre surface grafting via in situ diazonium generation for improved interfacial shear strength in epoxy matrix composites'', Composites Science and Technology. Elsevier Ltd, 118, pp. 31–38. doi: 10.1016/j.compscitech.2015.08.001.

[Belgacem et al., 1994] Belgacem, M. N., Bataille, P. and Sapieha, S. (1994) ''Effect of Corona Modification on the Mechanical Properties of Polypropylene Cellulose Composites'', Journal of Applied Polymer Science, 53, pp. 379–385.

[Bénéthuilière et al., 2015] Bénéthuilière, T., Duchet-Rumeau, J., Gérard, J. F., Dubost, E. and Peyre, C. (2015) ''Physico-chemistry of vinylester/glass fiber interfaces used in SMC composites'', in ICCM20 - 20th International Conference on Composite Materials. Copenhagen, pp. 1–12.

[Bensadoun, 2016] Bensadoun, F. (2016) "In-service behaviour of flax fibre reinforced composites for high performance applications", PhD Thesis, KU Leuven.

[Berger et al., 2003] Berger, M. H. and Jeulin, D. (2003) ''Statistical analysis of the failure stresses of ceramic fibres: Dependence of the Weibull parameters on the gauge length, diameter variation and fluctuation of defect density'', Journal of Materials Science, 38(13), pp. 2913–2923. doi: 10.1023/A:1024405123420.

[Bismarck et al., 1999] Bismarck, A., Kumru, M. E., Song, B., Springer, J., Moos, E. and Karger-Kocsis, J. (1999) ''Study on surface and mechanical fiber characteristics and their effect on the adhesion properties to a polycarbonate matrix tuned by anodic carbon fiber oxidation'', Composites Part A: Applied Science and Manufacturing, 30(12), pp. 1351–1366. doi: 10.1016/S1359-835X(99)00048-2.

[Bledzki et al., 1999] Bledzki, A. K. and Gassan, J. (1999) ''Composites Reinforced with Cellulose Based Fibres'', Progress in Polymer Science, 24, pp. 221–274.

[Bledzki et al., 2010] Bledzki, A. K., Mamun, A. A., Jaszkiewicz, A. and Erdmann, K. (2010) ''Polypropylene composites with enzyme modified abaca fibre'', Composites Science and Technology. Elsevier Ltd, 70(5), pp. 854–860. doi: 10.1016/j.compscitech.2010.02.003.

[Bonnafous, 2011] Bonnafous, C. (2011) ''Analyse multi echelle des mecanismes dendommagement de composites chanvre/epoxy a renforts tissés. Caractérisation de l'interface fibre/matrice'' PhD Thesis, ISAE-ENSMA.

[Boria et al., 2016] Boria, S., Pavlovic, A., Fragassa, C. and Santulli, C. (2016) ''Modeling of Falling Weight Impact Behavior of Hybrid Basalt / Flax Vinylester Composites'', Procedia Engineering. The Author(s), 167, pp. 223–230. doi: 10.1016/j.proeng.2016.11.691.

[Bousfield et al., 2018] Bousfield, G., Morin, S., Jacquet, N. and Richel, A. (2018) ''Extraction and refinement of agricultural plant fibers for composites manufacturing'', Comptes Rendus Chimie, 21(9), pp. 897–906. doi: 10.1016/j.crci.2018.07.001.

[Bouzouita et al., 2010] Bouzouita, S., Salvia, M., Ben Daly, H., Doui, A. and Forest, E. (2010) ‘‘Effect of Fiber Treatment on Fiber Strength and Fiber/Matrix Interface of Hemp Reinforced Polypropylene Composites’’, Advanced Materials Research, 112(1), pp. 1–8.

[Bozaci et al., 2013] Bozaci, E., Sever, K., Sarikanat, M., Seki, Y., Demir, A. and Ozdogan, E. (2013) ‘‘Effects of the atmospheric plasma treatments on surface and mechanical properties of flax fiber and adhesion between fiber – matrix for composite materials’’, Composites Part B: Engineering. Elsevier Ltd, 45(1), pp. 565–572. doi: 10.1016/j.compositesb.2012.09.042.

[Brebu et al., 2010] Brebu, M. and Vasile, C. (2010) ‘‘Thermal degradation of lignin - A review’’, Cellulose Chemistry and Technology, 44(9), pp. 353–363.

[Caliendo, 2016] Caliendo, H. (2016) “CARBIO project produces carbon/flax hybrid automotive roof”, CompositesWorld. Available at: https://www.compositesworld.com/news/carbio-project-produces-carbonflax-hybrid-automotive-roof.

[Caprino et al., 1998] Caprino, G. and D’Amore, A. (1998) ‘‘Flexural fatigue behaviour of randomcontinous-fibre-reinforced thermoplastic composites’’, Composites Science and Technology, 58(6), pp. 957–965. doi: 10.1016/s0266-3538(97)00221-2.

[Caprino et al., 1999] Caprino, G. and Giorleo, G. (1999) ‘‘Fatigue lifetime of glass fabric/epoxy composites’’, Composites Part A: Applied Science and Manufacturing, 30(3), pp. 299–304. doi: 10.1016/S1359-835X(98)00124-9.

[Carré, 2007] Carré, A. (2007) ‘‘Polar interactions at liquid/polymer interfaces.’’, Journal of Adhesion Science and Technology, 21(10), pp. 961–81.

[Cech et al., 1999] Cech, V., Horvath, P., Jancar, J., Schauer, F. and Nespurek, S. (1999) ‘‘Characterization of poly(methylphenylsilane) prepared by plasma polymerization’’, Macromolecular Symposia, 148, pp. 321–332. doi: 10.1002/masy.19991480124.

[Cech et al., 2003] Cech, V., Prikryl, R., Balkova, R., Vanek, J. and Grycova, A. (2003) ‘‘The influence of surface modifications of glass on glass fiber/polyester interphase properties’’, Journal of Adhesion Science and Technology, 17(10), pp. 1299–1320. doi: 10.1163/156856103769172751.

[Cech et al., 2007] Cech, V., Studynka, J., Janos, F. and Perina, V. (2007) ‘‘Influence of oxygen on the chemical structure of plasma polymer films deposited from a mixture of tetravinylsilane and oxygen gas’’, Plasma Processes and Polymers, 4, pp. S776–S780. doi: 10.1002/ppap.200731903.

[Cech, 2007] Cech, V. (2007) ‘‘Plasma-polymerized organosilicones as engineered interlayers in glass fiber / polyester composites’’, Composite Interfaces, 14, pp. 321–334. doi: 10.1163/156855407780452850.

[Cech et al., 2014] Cech, V., Knob, A., Hosein, H., Babik, A., Lepcio, P., Ondreas, F. and Drzal, L. T. (2014) ‘‘Enhanced interfacial adhesion of glass fibers by tetravinylsilane plasma modification’’, Composites Part A: Applied Science and Manufacturing, Elsevier Ltd, 58, pp. 84–89. doi: 10.1016/j.compositesa.2013.12.003.

[Cech et al., 2017] Cech, V., Knob, A., Lasota, T., Lukes, J. and Drzal, L. T. (2017) ‘‘Surface modification of glass fibers by oxidized plasma coatings to improve interfacial shear strength in GF/polyester composites’’, Polymer Composites, pp. 1–8. doi: 10.1002/pc.24573.

[Cheng et al., 2013] Cheng, C. and Lin, H. (2013) ‘‘Measurement of Surface Tension of Epoxy Resins Used in Dispensing Process for Manufacturing Thin Film Transistor-Liquid Crystal

Displays'', IEEE Transactions on advanced packaging, 31, pp. 100–106. doi: 10.1109/TADVP.2007.901767.

[Chibowski et al., 2013] Chibowski, E. and Jurak, M. (2013) ''Comparison of contact angle hysteresis of different probe liquids on the same solid surface'', Colloid and Polymer Science, 291(2), pp. 391–399. doi: 10.1007/s00396-012-2777-9.

[Council of the European Union, 1999] Council of the European Union (1999) ''Council Directive 1999/31/EC of 26 April 1999 on the landfill of waste'', Official Journal of the European Communities.

[Cruz et al., 2016] Cruz, J. and Fangueiro, R. (2016) ''Surface Modification of Natural Fibers: A Review'', Procedia Engineering. Elsevier B.V., 155, pp. 285–288. doi: 10.1016/j.proeng.2016.08.030.

[D'Amore et al., 1996] D'Amore, A., Caprino, G., Stupak, P. and et al. (1996) ''Effect of stress ratio on the flexural fatigue behaviour of continuous strand mat reinforced plastics'', Science and Engineering of Composite Materials, 5(1), pp. 1–8.

[Daggumati et al., 2010] Daggumati, S., Van Paepegem, W., Degrieck, J., Praet, T., Verhegghe, B., Xu, J., Lomov, S. V. and Verpoest, I. (2010) ''Local strain in a 5-harness satin weave composite under static tension: Part I-Experimental Analysis'', Composites Science and Technology, 70(13), pp. 1926–1933. doi: 10.1016/j.compscitech.2011.03.020.

[Dai et al., 2013] Dai, D., Fan, M. and Collins, P. (2013) ''Fabrication of nanocelluloses from hemp fibers and their application for the reinforcement of hemp fibers'', Industrial Crops and Products. Elsevier B.V., 44, pp. 192–199. doi: 10.1016/j.indcrop.2012.11.010.

[Das, 2017] Das, S. (2017) ''Mechanical properties of waste paper/jute fabric reinforced polyester resin matrix hybrid composites.'', Carbohydrate Polymers, 172, pp. 60–67.

[Davidson, 1971] Davidson, G. (1971) ''The vibrational spectrum of tetravinylsilane'', Spectrochimica Acta Part A: Molecular Spectroscopy, 27A(7), pp. 1161–1169. doi: 10.1016/0584-8539(71)80198-8.

[De Farias et al., 2017] De Farias, J. G. G., Cavalcante, R. C., Canabarro, B. R., Viana, H. M., Scholz, S. and Simão, R. A. (2017) ''Surface lignin removal on coir fibers by plasma treatment for improved adhesion in thermoplastic starch composites'', Carbohydrate Polymers. Elsevier Ltd., 165, pp. 429–436. doi: 10.1016/j.carbpol.2017.02.042.

[De Oliveira et al., 2017] De Oliveira, D. M., Cioffi, M. O. H., De Carvalho Benini, K. C. C. and Voorwald, H. J. C. (2017) ''Effects of plasma treatment on the sorption properties of coconut fibers'', Procedia Engineering. Elsevier B.V., 200, pp. 357–364. doi: 10.1016/j.proeng.2017.07.050.

[De Prez et al., 2018] De Prez, J., Van Vuure, A. W., Ivens, J., Aerts, G. and Van de Voorde, I. (2018) ''Enzymatic treatment of flax for use in composites'', Biotechnology Reports. Elsevier B.V., 20, pp. 1–17. doi: 10.1016/j.btre.2018.e00294.

[De Rosa et al., 2012] De Rosa, I. M., Dhakal, H. N., Santulli, C., Sarasini, F. and Zhang, Z. Y. (2012) ''Post-impact static and cyclic flexural characterisation of hemp fibre reinforced laminates'', Composites Part B: Engineering. Elsevier Ltd, 43(3), pp. 1382–1396. doi: 10.1016/j.compositesb.2011.09.012.

[De Souza Lima et al., 2004] De Souza Lima, M. M. and Borsali, R. (2004) ‘‘Rodlike Cellulose Microcrystals: Structure, Properties, and Applications’’, Macromol.ecular Rapid Communications, 25, pp. 771–787. doi: 10.1002/marc.200300268.

[De Vasconcellos et al., 2014] De Vasconcellos, D. S., Touchard, F. and Chocinski-Arnault, L. (2014) ‘‘Tension-tension fatigue behaviour of woven hemp fibre reinforced epoxy composite: A multi-instrumented damage analysis’’, International Journal of Fatigue. Elsevier Ltd, 59, pp. 159–169. doi: 10.1016/j.ijfatigue.2013.08.029.

[Degrieck et al., 2001] Degrieck, J. and Van Paepegem, W. (2001) ‘‘Fatigue damage modeling of fibre-reinforced composite materials: Review’’, Applied Mechanics Reviews, 54(4), pp. 279–300.

[Della Volpe et al., 2001] Della Volpe, C., Maniglio, D., Siboni, S. and Morra, M. (2001) ‘‘An experimental procedure to obtain the equilibrium contact angle from the Wilhelmy method’’, Oil and Gas Science and Technology - Revue d’IFP Energies nouvelles, Institut Français du Pétrole, 56(1), pp. 9–22. doi: 10.2516/ogst:2001002.

[Demirkir et al., 2017] Demirkir, C., Colak, S. and Ozturk, H. (2017) ‘‘Effects of plasma surface treatment on bending strength and modulus of elasticity of beech and poplar plywood’’, Maderas. Ciencia y Tecnologia, 19(2), pp. 195–202. doi: 10.4067/S0718-221X2017005000017.

[Dhakal et al., 2007] Dhakal, H. N., Zhang, Z. Y., Richardson, M. O. W. and Errajhi, O. A. Z. (2007) ‘‘The low velocity impact response of non-woven hemp fibre reinforced unsaturated polyester composites’’, Composites Structures, 81(4), pp. 559–567. doi: 10.1016/j.compstruct.2006.10.003.

[Dhakal et al., 2015] Dhakal, H., Sarasini, F., Calabrese, L., Valenza, A. and Proverbio, E. (2015) ‘‘Effect of basalt fibre hybridisation on post-impact mechanical behaviour of hemp fibre reinforced composites.’’, Composites Part A: Applied Science and Manufacturing, 75, pp. 54–67.

[Dirand et al., 1996] Dirand, X., Hilaire, B., Soulier, J. P. and Nardin, M. (1996) ‘‘Interfacial shear strength in glass-fiber/vinylester-resin composites’’, Composites Science and Technology, 56(5), pp. 533–539. doi: 10.1016/0266-3538(96)00040-1.

[Donaldson et al., 2004] Donaldson, L. and Frankland, A. (2004) ‘‘Ultrastructure of iodine treated wood’’, Holzforschung, 58, pp. 219–225.

[Dong et al., 2015] Dong, Z., Ding, R., Zheng, L., Zhang, X. and Yu, C. (2015) ‘‘Thermal properties of flax fiber scoured by different methods’’, Thermal Scienece, 19(3), pp. 939–945. doi: 10.2298/TSCI130329005Z.

[Dong, 2018] Dong, C. (2018) ‘‘Review of Natural Fibre Reinforced Hybrid Composites’’, Journal of Reinforced Plastics and Composites, 37(5), pp. 331–348.

[Drzal et al., 1983] Drzal, L. T., Rich, M. J. and Lloyd, P. F. (1983) ‘‘Adhesion of graphite fibers to epoxy matrices, part I. The role of fiber surface treatment.’’, Journal of Adhesion Science and Technology, 16, pp. 1–30.

[Edhirej et al., 2017] Edhirej, A., Sapuan, S. M., Jawaid, M. and Zahari, N. I. (2017) ‘‘Cassava/sugar palm fiber reinforced cassava starch hybrid composites: Physical, thermal and structural properties.’’, International Journal of Biological Macromolecules, 101, pp. 75–83.

[El Asloun et al., 1989] El Asloun, M., Donnet, J. B., Guilpain, G., Nardin, M. and Schultz, J. (1989) ‘‘On the estimation of the tensile strength of carbon fibres at short lengths’’, Journal of Materials Science, 24(10), pp. 3504–3510. doi: 10.1007/BF02385732.

[Epaarachchi et al., 2003] Epaarachchi, J. A. and Clausen, P. D. (2003) ‘‘An empirical model for fatigue behavior prediction of glass fibre-reinforced plastic composites for various stress ratios and test frequencies’’, Composites Part A: Applied Science and Manufacturing, 34(4), pp. 313–326. doi: 10.1016/S1359-835X(03)00052-6.

[European Commission, 2019] European Commission (2019) ‘Rgulation (EU) 2019/631 Of the European Parliament and of the Council of 17 April 2019 setting CO2 emission performance standards for new passenger cars and for new light commercial vehicles, and repealing Regulations (EC) No 443/2009 and (EU) No 510/201’, Official Journal of the European.

[European Parliament and Council of the European Union, 2000] European Parliament and Council of the European Union (2000) ‘‘Directive 2000/53/EC of the European Parliament and of the Council of 18 September 2000 on end-of-life vehicles (OJ L 269 21.10.2000 p. 34)’’, Official Journal of the European Communities.

[Extrand, 1998] Extrand, C. W. (1998) ‘‘A Thermodynamic Model for Contact Angle Hysteresis’’, Journal of Colloid and Interface Science, 207, pp. 11–19.

[Feih et al., 2004] Feih, S., Wonsyld, K., Minzari, D., Westermann, P. and Lilholt, H. (no date b2004) ‘‘Testing procedure for the single fiber fragmentation test’’, Forskningscenter Risø. (Denmark. Forskningscenter Risoe. Risoe-R; No. 1483(EN)). Roskilde, pp. 1–30.

[Feih et al., 2005] Feih, S., Thraner, A. and Lilholt, H. (2005) ‘‘Tensile strength and fracture surface characterisation of sized and unsized glass fibers’’, Journal of Materials Science, 40(7), pp. 1615–1623. doi: 10.1007/s10853-005-0661-4.

[Feih et al., 2005] Feih, S., Wei, J., Kingshott, P. and Sørensen, B. F. (2005) ‘‘The influence of fibre sizing on the strength and fracture toughness of glass fibre composites’’, Composites Part A: Applied Science and Manufacturing, 36, pp. 245–255. doi: 10.1016/j.compositesa.2004.06.019.

[Ferrante et al., 2015] Ferrante, L., Tirillò, J., Sarasini, F., Touchard, F., Ecault, R., Vidal Urriza, M. A., Chocinski-arnault, L. and Mellier, D. (2015) ‘‘Behaviour of woven hybrid basalt-carbon / epoxy composites subjected to laser shock wave testing : Preliminary results’’, Composites Part B: Engineering, 78, pp. 162–173.

[Fiore et al., 2016] Fiore, V., Scalici, T., Calabrese, L., Valenza, A. and Proverbio, E. (2016) ‘‘Effect of external basalt layers on durability behaviour of flax reinforced composites.’’, Composites Part B: Engineering, 84, pp. 258–65.

[Fragassa et al., 2018] Fragassa, C., Pavlovic, A. and Santulli, C. (2018) ‘‘Mechanical and impact characterisation of flax and basalt fibre vinyl - ester composites and their hybrids.’’, Composites Part B: Engineering, 137, pp. 247–259.

[Francois et al., 2017] Francois, C., Plasseraud, L., Pourchet, S., Boni, G., Fontaine, S., Beaugrand, J., Champion, D., Francois, C., Plasseraud, L., Pourchet, S., Boni, G. and Placet, V. (2017) ‘‘Étude d ’ un procédé de traitement innovant des fibres de chanvre sous condition de fluide supercritique et propriétés induites’’, in Comptes Rendus des JNC 20 – Ecole des Ponts ParisTech – 28-30 Juin 2017. Paris, pp. 1–10.

[Fraser et al., 1983] Fraser, W. A., Ancker, F. H., Dibenedetto, A. T. and Elbirli, B. (1983) ‘‘Evaluation of Surface Treatments for Fibers in Composite Materials’’, Polymer Composites, 4(4).

[Fu et al., 2019] Fu, J., Zhang, M., Jin, L., Liu, L., Li, N., Shang, L., Li, M., Xiao, L. and Ao, Y. (2019) ‘‘Applied Surface Science Enhancing interfacial properties of carbon fi bers reinforced epoxy

composites via Layer-by-Layer self assembly GO / SiO 2 multilayers fi lms on carbon fi bers surface'', Applied Surface Science, 470, pp. 543–554. doi: 10.1016/j.apsusc.2018.11.168.

[Gao et al., 2015] Gao, S. H. and Yu, C. W. (2015) ''Effects of supercritical carbon dioxide on morphology of apocynum venetum fibers'', Thermal Science, 19(4), pp. 1279–1282. doi: 10.2298/TSCI1504279G.

[Gao et al., 2015] Gao, X., Jr, J. W. G., Jensen, R. E., Li, W., Haque, B. Z. G. and Mcknight, S. H. (2015) ''Effect of fiber surface texture on the mechanical properties of glass fiber reinforced epoxy composite'', Composites Part A, 74, pp. 10–17. doi: 10.1016/j.compositesa.2015.03.023.

[Gassan et al., 1999] Gassan, J. and Bledzki, A. K. (1999) ''Alkali treatment of jute fibers: Relationship between structure and mechanical properties'', Journal of Applied Polymer Science, 71(4), pp. 623–629. doi: 10.1002/(sici)1097-4628(19990124)71:4<623::aid-app14>3.3.co;2-b.

[Gassan et al., 2000] Gassan, J. and Gutowski, V. S. (2000) ''Effects of corona discharge and UV treatment on the properties of jute-fibre expoxy composites'', Composites Science and Technology, 60(15), pp. 2857–2863. doi: 10.1016/S0266-3538(00)00168-8.

[George et al., 1999] George, J., Ivens, J. and Verpoest, I. (1999) ''Mechanical properties of flax fibre reinforced epoxy composites.'', Macromolecular Materials and Engineering, 272(1), pp. 41–45.

[George et al., 2001] George, J., Sreekala, M. S., Thomas, S., George, J., Sreekala, M. S. and Thomas, S. (2001) ''A Review on interface modification and characterization of natural fiber reinforced plastic composites.'', Polymer Engineering & Science, 41, pp. 1471–1485.

[George et al., 2014] George, M., Mussone, P. G. and Bressler, D. C. (2014) ''Surface and thermal characterization of natural fibres treated with enzymes'', Industrial Crops and Products. Elsevier B.V., 53, pp. 365–373. doi: 10.1016/j.indcrop.2013.12.037.

[George et al., 2014] George, M., Mussone, P. G., Abboud, Z. and Bressler, D. C. (2014) ''Characterization of chemically and enzymatically treated hemp fibres using atomic force microscopy and spectroscopy'', Applied Surface Science. Elsevier B.V., 314, pp. 1019–1025. doi: 10.1016/j.apsusc.2014.06.080.

[George et al., 2016] George, M., Mussone, P. G., Alemaskin, K., Chae, M., Wolodko, J. and Bressler, D. C. (2016) ''Enzymatically treated natural fibres as reinforcing agents for biocomposite material: mechanical, thermal, and moisture absorption characterization'', Journal of Materials Science, 51, pp. 2677–2686. doi: 10.1007/s10853-015-9582-z.

[Grand View Research, 2018] Grand View Research (2018) 'Natural Fiber Composites (NFC) Market Size, Share & Trends Analysis Report By Raw Material, By Matrix, By Technology, By Application, And Segment Forecasts, 2018 - 2024'. doi: 978-1-68038-890-9.

[Guillebaud-Bonnafous et al., 2012] Guillebaud-Bonnafous, C., Vasconcellos, D., Touchard, F. and Chocinski-Arnault, L. (2012) ''Experimental and numerical investigation of the interface between epoxy matrix and hemp yarn'', Composites Part A: Applied Science and Manufacturing. Elsevier Ltd, 43(11), pp. 2046–2058. doi: 10.1016/j.compositesa.2012.07.015.

[Gulati et al., 2006] Gulati, D. and San, M. (2006) ''Fungal-modification of Natural Fibers: A Novel Method of Treating Natural Fibers for Composite Reinforcement'', Journal of Polymer and the Environment, 14(4), pp. 347–352.

[Gupta, 2009] Gupta, K. (2009) ‘‘Experimental investigation of the behavior of dual fiber hybrid composite under different stacking sequence.’’, in 17th International Conference on Composite Materials (ICCM-17). Edinburg, UK.

[Gurdag et al., 2013] Gurdag, G. and Sarmad, S. (2013) ‘‘Cellulose Graft Copolymers: Synthesis, Properties, and Applications’’, in Polysaccharide Based Graft Copolymers. doi: 10.1007/978-3-642-36566-9.

[Gutiérrez et al., 2012] Gutiérrez, M. C., Rosa, P. de T. V., De Paoli, M. A. and Felisberti, M. I. (2012) ‘‘Biocompósitos de acetato de celulose e fibras curtas de Curauá tratadas com CO2 supercrítico’’, Polimeros, 22(3), pp. 295–302. doi: 10.1590/S0104-14282012005000037.

[Hashim et al., 2012] Hashim, M. Y., Roslan, M. N., Amin, A. M., Mujahid, A. and Zaidi, A. (2012) ‘‘Mercerization Treatment Parameter Effect on Natural Fiber Reinforced Polymer Matrix Composite: A Brief Review’’, International Journal of Materials and Metallurgical Engineering, 6(8), pp. 1638–1644.

[Hayashi, 1972] Hayashi, T. (1972) ‘‘On the improvement of mechanical properties of composites by hybrid composition.’’, in Proc 8th int reinforced plastics conference, pp. 149–52.

[Hedgepeth, 1961] Hedgepeth, J. (1961) ‘Stress concentrations in filamentary structures’, NASA Technical Note.

[Henriksson et al., 1997] Henriksson, G., Akin, D. E. and Rigsby, L. L. (1997) ‘‘Influence of Chelating Agents and Mechanical Pretreatment on Enzymatic Retting of Flax’’, Textile Research Journal, 67(11), pp. 829–836.

[Huda et al., 2008] Huda, M. S., Drzal, L. T., Mohanty, A. K. and Misra, M. (2008) ‘‘Effect of fiber surface treatments on the properties of laminated biocomposites from poly(lactic acid) (PLA) and kenaf fibers.’’, Composites Science and Technology, 68, pp. 424–432.

[Jähn et al., 2002] Jähn, A., Schröder, M. W., Füting, M., Schenzel, K. and Diepenbrock, W. (2002) ‘‘Characterization of alkali treated flax fibres by means of FT Raman spectroscopy and environmental scanning electron microscopy’’, Spectrochimica Acta - Part A: Molecular and Biomolecular Spectroscopy, 58(10), pp. 2271–2279. doi: 10.1016/S1386-1425(01)00697-7.

[Jamali et al., 2011] Jamali, A. and Evans, P. D. (2011) ‘‘Etching of wood surfaces by glow discharge plasma’’, Wood Science and Technology, 45, pp. 169–182. doi: 10.1007/s00226-010-0317-7.

[Jawaid et al., 2014] Jawaid, M., Alothman, O., Paridah, M. and Khalil, H. (2014) ‘‘Effect of Oil Palm and Jute Fiber Treatment on Mechanical Performance of Epoxy Hybrid Composites.’’, International Journal of Polymer Analysis and Characterization, 19(1), pp. 62–9.

[Jenkins et al., 2018] Jenkins, P. G., Yang, L. and Thomason, J. L. (b2018) ‘‘Investigation of the effect of sizing on the tensile and interface properties of continuous basalt fibre and polypropylene’’, in Proceedings of ECCM18 - 18th European Conference on Composite Materials, Athens, Greece, 24-28th June 2018.

[Ji et al., 1985] Ji, X., Liu, X. and Chou, T. (1985) ‘‘Dynamic stress concentration factors in unidirectional composites.’’, Journal of Composite Materials, 19(3), pp. 269–75.

[Joffe et al., 2003] Joffe, R., Andersons, J. A. and Wallström, L. (2003) ‘‘Strength and adhesion characteristics of elementary flax fibres with different surface treatments’’, Composites Part A: Applied Science and Manufacturing, 34(7), pp. 603–612. doi: 10.1016/S1359-835X(03)00099-X.

[Joffe et al., 2005] Joffe, R., Andersons, J. and Wallström, L. (2005) ‘‘Interfacial shear strength of flax fiber/thermoset polymers estimated by fiber fragmentation tests’’, Journal of Materials Science, 40(9–10), pp. 2721–2722. doi: 10.1007/s10853-005-2115-4.

[John et al., 2001] John, S., Herszberg, I. and Coman, F. (2001) ‘‘Longitudinal and transverse damage taxonomy in woven composite components’’, Composites Part B: Engineering, 32(8), pp. 659–668. doi: 10.1016/S1359-8368(01)00047-6.

[John et al., 2007] John, K. and Venkata Naidu, S. (2007) ‘‘Chemical resistance of sisal/glass reinforced unsaturated polyester hybrid composites.’’, Journal of Reinforced Plastics and Composites, 26(4), pp. 373–376.

[John et al., 2008] John, M. J. and Anandjiwala, R. D. (2008) ‘‘Recent Developments in Chemical Modification and Characterization of Natural Fiber-Reinforced Composites.’’, Polymer Composites, 29, pp. 187–207.

[Joseph et al., 2003] Joseph, P., Joseph, K., Thomas, S., Pillai, C., Prasad, V., Groeninckx, G. and Al., E. (2003) ‘‘The thermal and crystallisation studies of short sisal fibre reinforced polypropylene composites.’’, Composites - Part A: Applied Science and Manufacturing, 34(3), pp. 253–266.

[Jumaidin et al., 2017] Jumaidin, R., Sapuan, S. M., Jawaid, M., Ishak, M. R. and Sahari, J. (2017) ‘‘Thermal, mechanical, and physical properties of seaweed/sugar palm fibre reinforced thermoplastic sugar palm starch/agar hybrid composites.’’, International Journal of Biological Macromolecules, 97, pp. 606–615.

[Kabir et al., 2012] Kabir, M. M., Wang, H., Lau, K. T. and Cardona, F. (2012) ‘‘Chemical treatments on plant-based natural fibre reinforced polymer composites: An overview.’’, Composites Part B: Engineering, 43(7), pp. 2883–92.

[Kafi et al., 2011] Kafi, A. A., Magniez, K. and Fox, B. L. (2011) ‘‘A surface-property relationship of atmospheric plasma treated jute composites’’, Composites Science and Technology. Elsevier Ltd, 71(15), pp. 1692–1698. doi: 10.1016/j.compscitech.2011.07.011.

[Kaith et al., 2008] Kaith, B. S. and Kalia, S. (2008) ‘‘Graft copolymerization of MMA onto flax under different reaction conditions: A comparative study’’, Express Polymer Letters, 2(2), pp. 93–100. doi: 10.3144/expresspolymlett.2008.13.

[Kalia et al., 2009] Kalia, S., Kaith, B. S. and Kaur, I. (2009) ‘‘Pretreatments of Natural Fibers and their Application as Reinforcing Material in Polymer Composites — A Review.’’, Polymer Engineering & Science, 49(7), pp. 1253–1272.

[Kalia et al., 2011] Kalia, S., Dufresne, A., Cherian, B. M., Kaith, B. S., Avérous, L., Njuguna, J. and Nassiopoulos, E. (2011) ‘‘Cellulose-based bio- and nanocomposites: A review’’, International Journal of Polymer Science, pp. 1–35. doi: 10.1155/2011/837875.

[Kalia et al., 2013] Kalia, S., Thakur, K., Celli, A., Kiechel, M. A. and Schauer, C. L. (2013) ‘‘Surface modification of plant fibers using environment friendly methods for their application in polymer composites, textile industry and antimicrobial activities: A review’’, Journal of Environmental Chemical Engineering. Elsevier B.V., 1(3), pp. 97–112. doi: 10.1016/j.jece.2013.04.009.

[Karaduman et al., 2013] Karaduman, Y., Gokcan, D. and Onal, L. (2013) ‘‘Effect of enzymatic pretreatment on the mechanical properties of jute fiber-reinforced polyester composites’’, Journal of Composite Materials, 47(10), pp. 1293–1302. doi: 10.1177/0021998312446826.

[Karger-Kocsis et al., 2015] Karger-Kocsis, J., Mahmood, H. and Pegoretti, A. (2015) ‘‘Recent advances in fiber/matrix interphase engineering for polymer composites’’, Progress in Materials Science, 73, pp. 1–43. doi: 10.1016/j.pmatsci.2015.02.003.

[Kelly et al., 1965] Kelly, A. and Tyson, W. R. (1965) ‘‘Tensile properties of fibre-reinforced metals: Copper/Tungsten and Copper/Molybdenum’’, Journal of the Mechanics and Physics of Solids, 13(6), pp. 329–350. doi: 10.1016/0022-5096(65)90035-9.

[Kim et al., 1998] Kim, J.-K. and Mai, Y.-W. (1998) ‘‘Chapter 2: Characterization of interfaces’’, in Engineered Interfaces in Fiber Reinforced Composites, pp. 5–41. doi: 10.1016/0250-6874(81)80012-1.

[Kim et al., 2002] Kim, B. W. and Nairn, J. a (b2002) ‘‘Observations of Fiber Fracture and Interfacial Debonding Phenomena Using the Fragmentation Test in Single Fiber Composites’’, Journal of Composite Materials, 36(15), pp. 1825–1858. doi: 10.1106/002199802026243.

[Kim et al., 2009] Kim, J., Seidler, P., Wan, L. S. and Fill, C. (2009) ‘‘Formation, structure, and reactivity of amino-terminated organic films on silicon substrates’’, Journal of Colloid and Interface Science. Elsevier Inc., 329(1), pp. 114–119. doi: 10.1016/j.jcis.2008.09.031.

[Kim et al., 2011] Kim, M. T., Kim, M. H., Rhee, K. Y. and Park, S. J. (2011) ‘‘Study on an oxygen plasma treatment of a basalt fiber and its effect on the interlaminar fracture property of basalt /epoxy woven composites’’, Composites Part B: Engineering. Elsevier Ltd, 42(3), pp. 499–504. doi: 10.1016/j.compositesb.2010.12.001.

[Kiruthika, 2017] Kiruthika, A. V (2017) ‘‘A review on physico-mechanical properties of bast fi bre reinforced polymer composites’’, Journal of Building Engineering. Elsevier Ltd, 9, pp. 91–99. doi: 10.1016/j.jobe.2016.12.003.

[Koronis et al., 2013] Koronis, G., Silva, A. and Fontul, M. (2013) ‘‘Green composites: A review of adequate materials for automotive applications’’, Composites Part B: Engineering. Elsevier Ltd, 44(1), pp. 120–127. doi: 10.1016/j.compositesb.2012.07.004.

[Lee et al., 2011] Lee, K.Y., Delille, A. and Bismarck, A. (2011) ‘‘Greener Surface Treatments of Natural Fibres’’, in Cellulose Fibers: Bio- and Nano- Polymer Composites, Springer, Berlin, Heidelberg, pp. 155–178.

[Li et al., 2009] Li, Y., Pickering, K. L. and Farrell, R. L. (a2009) ‘‘Analysis of green hemp fibre reinforced composites using bag retting and white rot fungal treatments’’, Industrial Crops and Products, 29(2–3), pp. 420–426. doi: 10.1016/j.indcrop.2008.08.005.

[Li et al., 2009] Li, Y., Pickering, K. L. and Farrell, R. L. (b2009) ‘‘Determination of interfacial shear strength of white rot fungi treated hemp fibre reinforced polypropylene’’, Composites Science and Technology. Elsevier Ltd, 69(7–8), pp. 1165–1171. doi: 10.1016/j.compscitech.2009.02.018.

[Li et al., 2015] Li, Y., Li, Q. and Ma, H. (2015) ‘‘The voids formation mechanisms and their effects on the mechanical properties of flax fiber reinforced epoxy composites’’, Composites Part A: Applied Science and Manufacturing. Elsevier Ltd, 72, pp. 40–48. doi: 10.1016/j.compositesa.2015.01.029.

[Li et al., 2007] Li, X., Tabil, L. G. and Panigrahi, S. (2007) ‘‘Chemical treatments of natural fiber for use in natural fiber-reinforced composites: A review’’, Journal of Polymers and the Environment, 15(1), pp. 25–33. doi: 10.1007/s10924-006-0042-3.

[Lisle et al., 2015] Lisle, T., Bouvet, C., Pastor, M. L., Rouault, T. and Marguerès, P. (2015) ‘‘Damage of woven composite under tensile and shear stress using infrared thermography and micrographic cuts’’, Journal of Materials Science, 50, pp. 6154–6170. doi: 10.1007/s10853-015-9173-z.

[Liu et al., 2016] Liu, M., Meyer, A. S., Fernando, D., Alexandre, D., Silva, S., Daniel, G. and Thygesen, A. (2016) ‘‘Effect of pectin and hemicellulose removal from hemp fibres on the mechanical properties of unidirectional hemp / epoxy composites’’, Composites Part A: Applied Science and Manufacturing. Elsevier Ltd, 90, pp. 724–735. doi: 10.1016/j.compositesa.2016.08.037.

[Liu et al., 2017] Liu, M., Baum, A., Odermatt, J., Berger, J., Yu, L., Zeuner, B., Thygesen, A., Holck, J. and Meyer, A. S. (2017) ‘‘Oxidation of lignin in hemp fibres by laccase: Effects on mechanical properties of hemp fibres and unidirectional fibre/epoxy composites’’, Composites Part A: Applied Science and Manufacturing. Elsevier Ltd, 95, pp. 377–387. doi: 10.1016/j.compositesa.2017.01.026.

[Lopez et al., 2011] Lopez, J. P., Méndez, J. A., Mansouri, N. E. E., Mutjé, P. and Vilaseca, F. (2011) ‘‘Mean intrinsic tensile properties of stone groundwood fibers from softwood.’’, BioResources, 6, pp. 5037–5049.

[Lucintel, 2015] Lucintel (2015) ‘‘Growth Opportunities in the Global Natural Fiber Composites Market’’, Lucintel Insights that Matter, pp. 1–170.

[Mahboob et al., 2018] Mahboob, Z. and Bougherara, H. (2018) ‘‘Fatigue of flax-epoxy and other plant fibre composites: Critical review and analysis’’, Composites Part A: Applied Science and Manufacturing. Elsevier, 109(January), pp. 440–462. doi: 10.1016/j.compositesa.2018.03.034.

[Manders et al., 1981] Manders, P. W. and Bader, M. G. (1981) ‘‘The strength of hybrid glass/carbon fibre composites Part 1 Failure strain enhancement and failure mode’’, Journal of Materials Science, 16, pp. 2233–2245.

[Marais et al., 2005] Marais, S., Gouanvé, F., Bonnesoeur, A., Grenet, J., Poncin-Epaillard, F., Morvan, C. and Métayer, M. (2005) ‘‘Unsaturated polyester composites reinforced with flax fibers: Effect of cold plasma and autoclave treatments on mechanical and permeation properties’’, Composites Part A: Applied Science and Manufacturing, 36(7), pp. 975–986. doi: 10.1016/j.compositesa.2004.11.008.

[Maslinda et al., 2017] Maslinda, A. B., Majid, M. S. A., Ridzuan, M. J. M., Afendi, M. and Gibson, A. G. (2017) ‘‘Effect of water absorption on the mechanical properties of hybrid interwoven cellulosiccellulosic fibre reinforced epoxy composites’’, Composite Structures, 167, pp. 227–237.

[Mazian et al., 2018] Mazian, B., Bergeret, A., Benezet, J. and Malhautier, L. (2018) ‘‘Influence of field retting duration on the biochemical, microstructural, thermal and mechanical properties of hemp fibres harvested at the beginning of flowering’’, Industrial Crops & Products, 116, pp. 170–181. doi: 10.1016/j.indcrop.2018.02.062.

[Medina et al., 2016] Medina, C. M., Molina-Aldareguía, J. M., González, C., Melendrez, M. F., Flores, P. and Llorca, J. (2016) ‘‘Comparison of push-in and push-out tests for measuring interfacial

shear strength in nano-reinforced composite materials'', Journal of Composite Materials, 50(12), pp. 1651–1659. doi: 10.1177/0021998315595115.

[Meredith et al., 2013] Meredith, J., Coles, S. R., Powe, R., Collings, E., Cozien-Cazuc, S., Weager, B., Müssig, J. and Kirwan, K. (2013) ''On the static and dynamic properties of flax and Cordenka epoxy composites'', Composites Science and Technology. Elsevier Ltd, 80, pp. 31–38. doi: 10.1016/j.compscitech.2013.03.003.

[Mishra et al., 2001] Mishra, S., Misra, M., Tripathy, S. S., Nayak, S. K. and Mohanty, A. K. (2001) ''Graft Copolymerization of Acrylonitrile on Chemically Modified Sisal Fibers'', Macromolecular Materials and Engineering, 286(2), pp. 107–113.

[Mishra et al., 2003] Mishra, S., Mohanty, A. K., Drzal, L. T., Misra, M., Parija, S., Nayak, S. K. and Tripathy, S. S. (2003) ''Studies on Mechanical Performance of Biofiber/Glass Reinforced Polyester Hybrid Composites.'', Composite Science and Technology, 63, pp. 1377–1385.

[Mochane et al., 2019] Mochane, M. J., Mokhena, T. C., Mokhothu, T. H., Mtibe, A., Sadiku, E. R., Ray, S. S., Ibrahim, I. D. and Daramola, O. O. (2019) ''Recent progress on natural fiber hybrid composites for advanced applications : A review'', Express Polymer Letters, 13(2), pp. 159–198.

[Mohanty et al., 2000] Mohanty, A., Misra, M. and Hinrichsen, G. (2000) ''Biofibres, biodegradable polymers and biocomposites: an overview'', Macromolecular Materials and Engineering, 276/277(1), pp. 1–24.

[Mohanty et al., 2004] Mohanty, S., Nayak, S. K., Verma, S. K. and Tripathy, S. S. (2004) ''Effect of MAPP as Coupling Agent on the Performances of Sisal-PP Composites'', Journal of Reinforced Plastics and Composites, 23(18), pp. 2047–2063. doi: 10.1177/0731684404041711.

[Mukhopadhyay et al., 2009] Mukhopadhyay, S. and Fangueiro, R. (2009) ''Physical modification of natural fibers and thermoplastic films for composites - A review'', Journal of Thermoplastic Composite Materials, 22(2), pp. 135–162. doi: 10.1177/0892705708091860.

[Mwaikambo et al., 2006] Mwaikambo, L. Y. and Ansell, M. P. (2006) ''Mechanical properties of alkali treated plant fibres and their potential as reinforcement materials II. Sisal fibres Mechanical properties of alkali treated plant fibres and their potential as reinforcement materials. I. hemp fibres'', Journal of Materials Science, 41, pp. 2497–2508. doi: 10.1007/s10853-006-5075-4.

[Naidu et al., 2018] Naidu, A. L. and Kona, S. (2018) ''Experimental study of the mechanical properties of banana fiber and groundnut shell ash reinforced epoxy hybrid composite.'', International Journal of Engineering, 31, pp. 659–665.

[Naik et al., 1991] Naik, N. K., Shembekar, P. S. and Hosur, M. V. (1991) ''Failure behavior of woven fabric composites'', Journal of Composites Technology and Research, 13(1), pp. 107–116. doi: 10.1520/ctr10214j.

[Nunna et al., 2016] Nunna, S., Chandra, P. R., Shrivastava, S. and Jalan, A. (2016) ''A review on mechanical behavior of natural fiber based hybrid composites'', Journal of Reinforced Plastics and Composites, 31(11), pp. 759–769. doi: 10.1177/0731684412444325.

[Ohsawa et al., 1978] Ohsawa, T., Nakayama, A., Miwa, M. and Hasegawa, A. (1978) ''Temperature dependence of critical fiber length for glass fiber - reinforced thermosetting resins'', Journal of Applied Polymer Science, 22(11), pp. 3203–3212. doi: 10.1002/app.1978.070221115.

[Padaki et al., 2008] Padaki, N. V., Alagirusamy, R., Deopura, B. L., Sugun, B. S. and Fangueiro, R. (2008) ‘‘Low velocity impact behaviour of textile reinforced composites’’, Indian Journal of Fibre and Textile Research, 33(2), pp. 189–202.

[Padma Priya et al., 2006] Padma Priya, S. and Rai, S. (2006) ‘‘Mechanical performance of bio-fiber/glass-reinforced epoxy hybrid composites.’’, Journal of Industrial Textiles, 35(3), pp. 217–226.

[Pandita et al., 2001] Pandita, S. D., Huysmans, G., Wevers, M. and Verpoest, I. (2001) ‘‘Tensile fatigue behaviour of glass plain-weave fabric composites in on- and off-axis directions’’, Composites - Part A: Applied Science and Manufacturing, 32(10), pp. 1533–1539. doi: 10.1016/S1359-835X(01)00053-7.

[Panigrahi et al., 2009] Panigrahi, X. L. S. and Tabil, L. G. (2009) ‘‘A study on flax fiber-reinforced polyethylene biocomposites’’, Applied Engineering in Agriculture, 25(4), pp. 525–531. doi: 10.13031/2013.27454.

[Panthapulakkal et al., 2007] Panthapulakkal, S. and Sain, M. (2007) ‘‘Studies on the water absorption properties of short hemp-glass fiber hybrid polypropylene composites.’’, Journal of Composite Materials, 41, pp. 1871–83.

[Papa et al., 2018] Papa, I., Ricciardi, M. R., Antonucci, V., Pagliarulo, V. and Lopresto, V. (2018) ‘‘Impact behaviour of hybrid basalt/flax twill laminates’’, Composites Part B: Engineering. Elsevier, 153(April), pp. 17–25. doi: 10.1016/j.compositesb.2018.07.025.

[Park et al., 2006] Park, J. M., Quang, S. T., Hwang, B. S. and DeVries, K. L. (2006) ‘‘Interfacial evaluation of modified Jute and Hemp fibers/polypropylene (PP)-maleic anhydride polypropylene copolymers (PP-MAPP) composites using micromechanical technique and nondestructive acoustic emission’’, Composites Science and Technology, 66(15), pp. 2686–2699. doi: 10.1016/j.compscitech.2006.03.014.

[Paul et al., 2010] Paul, S. A., Joseph, K., Gem Mathew, G. D., Pothen, L. A. and Thomas, S. (2010) ‘‘Influence of polarity parameters on the mechanical properties of composites from polypropylene fiber and short banana fiber’’, Composites Part A: Applied Science and Manufacturing. Elsevier Ltd, 41(10), pp. 1380–1387. doi: 10.1016/j.compositesa.2010.04.015.

[Pegoretti et al., 2004] Pegoretti, A., Fabbri, E., Migliaresi, C. and Pilati, F. (2004) ‘‘Intraply and interply hybrid composites based on E-glass and poly (vinyl alcohol) woven fabrics: tensile and impact properties’’, Polymer International, 53, pp. 1290–1297. doi: 10.1002/pi.1514.

[Perrier et al., 2017] Perrier, A., Touchard, F., Chocinski-Arnault, L. and Mellier, D. (2017) ‘‘Influence of water on damage and mechanical behaviour of single hemp yarn composites’’, Polymer Testing, 57, pp. 17–25. doi: 10.1016/j.polymertesting.2016.10.035.

[Petersen et al., 2013] Petersen, H., Kusano, Y., Brøndsted, P. and Almdal, K. (2013) ‘‘Preliminary Characterization of Glass Fiber Sizing’’, in Proceedings of the 34th Risø International Symposium on Materials Science, Roskilde, Denmark, 2-5 Sep. 2013, pp. 333–340.

[Petrucci et al., 2013] Petrucci, R., Santulli, C., Puglia, D., Sarasini, F., Torre, L. and Kenny, J. (2013) ‘‘Mechanical characterisation of hybrid composite laminates based on basalt fibres in combination with flax, hemp and glass fibres manufactured by vacuum infusion.’’, Materials & Design, 49, pp. 728–735.

[Petrucci et al., 2015] Petrucci, R., Santulli, C., Puglia, D., Nisini, E., Sarasini, F., Tirillò, J. and Al., E. (2015) ‘‘Impact and post-impact damage characterisation of hybrid composite laminates based on

basalt fibres in combination with flax, hemp and glass fibres manufactured by vacuum infusion.'', Composites Part B: Engineering, 69, pp. 507–15.

[Phani et al., 1987] Phani, K. and Bose, N. (1987) ''Hydrothermal aging of juteglass fiber hybrid composites - an acousto-ultrasonic study.'', Journal of Materials Science, 22, pp. 1929–1933.

[Phillips et al., 2013] Phillips, S., Baets, J., Lessard, L., Hubert, P. and Verpoest, I. (2013) ''Characterization of flax/epoxy prepregs before and after cure'', Journal of Reinforced Plastics and Composites, 32(11), pp. 777–785. doi: 10.1177/0731684412473359.

[Pickering et al., 2007] Pickering, K. L., Li, Y., Farrell, R. L. and Lay, M. (2007) ''Interfacial modification of hemp fiber reinforced composites using fungal and alkali treatment'', Journal of Biobased Materials and Bioenergy, 1, pp. 109–117. doi: 10.1166/jbmb.2007.012.

[Pickering et al., 2016] Pickering, K. L., Aruan Efendy, M. G. and Le, T. M. (2016) ''A review of recent developments in natural fibre composites and their mechanical performance'', Composites: Part A, 83, pp. 98–112.

[Pickering, 2006] Pickering, S. J. (2006) ''Recycling technologies for thermoset composite materials-current status'', Composites Part A: Applied Science and Manufacturing, 37(8), pp. 1206–1215. doi: 10.1016/j.compositesa.2005.05.030.

[Pizzi et al., 2009] Pizzi, A., Kueny, R., Lecoanet, F., Massetau, B., Carpentier, D., Krebs, A., Loiseau, F., Molina, S. and Ragoubi, M. (2009) ''High resin content natural matrix-natural fibre biocomposites'', Industrial Crops and Products, 30(2), pp. 235–240. doi: 10.1016/j.indcrop.2009.03.013.

[Pommet et al., 2008] Pommet, M., Juntaro, J., Heng, J. Y. Y., Mantalaris, A., Lee, A. F., Wilson, K., Kalinka, G., Shaffer, M. S. P. and Bismarck, A. (2008) ''Surface modification of natural fibers using bacteria: Depositing bacterial cellulose onto natural fibers to create hierarchical fiber reinforced nanocomposites'', Biomacromolecules, 9(6), pp. 1643–1651. doi: 10.1021/bm800169g.

[Preston et al., 2011] Preston, L. J., Izawa, M. R. M. and Banerjee, N. R. (2011) ''Infrared Spectroscopic Characterization of Organic Matter Associated with Microbial Bioalteration Textures in Basaltic Glass'', Astrobiology, 11(7), pp. 585–599. doi: 10.1089/ast.2010.0604.

[Pucci et al., 2017] Pucci, F. M., Seghini, M. C., Liotier, P.-J., Sarasini, F., Tirillo, J. and Drapier, S. (2017) ''Surface characterisation and wetting properties of single basalt fibres'', Composites Part B: Engineering, 109, pp. 72–81. doi: 10.1016/j.compositesb.2016.09.065.

[Pucci et al., 2017] Pucci, M. F., Liotier, P. and Drapier, S. (2017) ''Tensiometric method to reliably assess wetting properties of single fibers with resins: Validation on cellulosic reinforcements for composites'', Colloids and Surfaces A: Physicochemical and Engineering Aspects. Elsevier B.V., 512, pp. 26–33. doi: 10.1016/j.colsurfa.2016.09.047.

[Pucci et al., 2017] Pucci, M. F., Liotier, P. J., Seveno, D., Fuentes, C., Van Vuure, A. and Drapier, S. (2017) ''Wetting and swelling property modifications of elementary flax fibres and their effects on the Liquid Composite Molding process'', Composites Part A: Applied Science and Manufacturing. Elsevier Ltd, 97, pp. 31–40. doi: 10.1016/j.compositesa.2017.02.028.

[Quaresimin et al., 2010] Quaresimin, M., Susmel, L. and Talreja, R. (2010) ''Fatigue behaviour and life assessment of composite laminates under multiaxial loadings'', International Journal of Fatigue. Elsevier Ltd, 32(1), pp. 2–16. doi: 10.1016/j.ijfatigue.2009.02.012.

[Ragoubi et al., 2010] Ragoubi, M., Bienaimé, D., Molina, S., George, B. and Merlin, A. (2010) ‘‘Impact of corona treated hemp fibres onto mechanical properties of polypropylene composites made thereof’’, Industrial Crops and Products, 31(2), pp. 344–349. doi: 10.1016/j.indcrop.2009.12.004.

[Ramirez et al., 2008] Ramirez, F. A., Carlsson, L. A. and Acha, B. A. (2008) ‘‘Evaluation of water degradation of vinylester and epoxy matrix composites by single fiber and composite tests’’, Journal of Materials Science, 43(15), pp. 5230–5242. doi: 10.1007/s10853-008-2766-z.

[Ravandi et al., 2017] Ravandi, M., Teo, W. S., Tran, L. Q. N., Yong, M. S. and Tay, T. E. (2017) ‘‘Low velocity impact performance of stitched flax/epoxy composite laminates’’, Composites Part B: Engineering. Elsevier Ltd, 117, pp. 89–100. doi: 10.1016/j.compositesb.2017.02.003.

[Reddy et al., 2015] Reddy, K. O., Maheswari, C. U., Reddy, K. R., Shukla, M., Muzenda, E. and Rajulu, A. V. (2015) ‘‘Effect of Chemical Treatment and Fiber Loading on Mechanical Properties of Borassus (Toddy Palm) Fiber/Epoxy Composites’’, International Journal of Polymer Analysis and Characterization, 20(7), pp. 612–626.

[Réquilé et al., 2019] Réquilé, S., Le Duigou, A., Bourmaud, A. and Baley, C. (2019) ‘‘Interfacial properties of hemp fiber/epoxy system measured by microdroplet test: Effect of relative humidity’’, Composites Science and Technology. Elsevier, 181(April), p. 107694. doi: 10.1016/j.compscitech.2019.107694.

[Rulison, 1996] Rulison, C. (1996) ‘Wettability studies for porous solids including powders and fibrous materials, KRÜSS GmbH Technical Note’.

[Saba et al., 2016] Saba, N., Jawaid, M., Alothman, O. Y. and Paridah, M. T. (2016) ‘‘A review on dynamic mechanical properties of natural fibre reinforced polymer composites’’, Construction and Building Materials. Elsevier Ltd, 106, pp. 149–159. doi: 10.1016/j.conbuildmat.2015.12.075.

[Safri et al., 2018] Safri, A., Sultan, M. T. H., Jawaid, M. and Jayakrishna, K. (2018) ‘‘Impact behaviour of hybrid composites for structural applications: A review’’, Composites Part B: Engineering, 133, pp. 112–121. doi: 10.1016/j.compositesb.2017.09.008.

[Sain et al., 2005] Sain, M., Suhara, P., Law, S. and Bouilloux, A. (2005) ‘‘Interface modification and mechanical properties of natural fiber-polyolefin composite products’’, Journal of Reinforced Plastics and Composites, 24, pp. 121–130.

[Saleem et al., 2008] Saleem, Z., Rennebaum, H., Pudel, F. and Grimm, E. (2008) ‘‘Treating bast fibres with pectinase improves mechanical characteristics of reinforced thermoplastic composites’’, Composites Science and Technology, 68(2), pp. 471–476. doi: 10.1016/j.compscitech.2007.06.005.

[Sanjay et al., 2018] Sanjay, M. R., Madhu, P., Jawaid, M., Senthamaraikannan, P., Senthil, S. and Pradeep, S. (2018) ‘‘Characterization and properties of natural fiber polymer composites: A comprehensive review’’, Journal of Cleaner Production. Elsevier Ltd, 172, pp. 566–581. doi: 10.1016/j.jclepro.2017.10.101.

[Santulli et al., 2005] Santulli, C., Janssen, M. and Jeronimidis, G. (2005) ‘‘Partial replacement of E-glass fibers with flax fibers in composites and effect on falling weight impact performance.’’, Journal of Materials Science, 40, pp. 3581–5.

[Santulli, 2019] Santulli, C. (2019) ‘‘Mechanical and Impact Damage Analysis on Carbon / Natural Fibers Hybrid Composites: A Review’’, Materials, 12(517), pp. 1–17. doi: 10.3390/ma12030517.

[Sarasini et al., 2014] Sarasini, F., Tirillò, J., Ferrante, L., Valente, M., Valente, T., Lampani, L., Gaudenzi, P., Cioffi, S., Iannace, S. and Sorrentino, L. (2014) ‘‘Drop-weight impact behaviour of woven hybrid basalt – carbon / epoxy composites’’, Composites Part B: Engineering, 59, pp. 204–220. doi: 10.1016/j.compositesb.2013.12.006.

[Sarasini et al., 2016] Sarasini, F., Tirillò, J., D’Altilia, S., Valente, T., Santulli, C., Touchard, F., Chocinski-Arnault, L., Mellier, D., Lampani, L. and Gaudenzi, P. (2016) ‘‘Damage tolerance of carbon/flax hybrid composites subjected to low velocity impact’’, Composites Part B: Engineering, 91, pp. 144–153. doi: 10.1016/j.compositesb.2016.01.050.

[Sarasini et al., 2017] Sarasini, F., Tirillò, J., Puglia, D., Dominici, F., Santulli, C., Boimau, K., Valente, T. and Torre, L. (2017) ‘‘Biodegradable poly - caprolactone-based composites reinforced with ramie and borassus fibres.’’, Composite Structures, 167, pp. 20–29.

[Sarasini et al., 2018] Sarasini, F., Tirillò, J. and Seghini, M. C. (2018) ‘‘Influence of thermal conditioning on tensile behaviour of single basalt fibres’’, Composites Part B: Engineering, 132, pp. 77–86. doi: 10.1016/j.compositesb.2017.08.014.

[Sarasini et al., 2018] Sarasini, F., Tirillò, J., Sergi, C., Seghini, M. C., Cozzarini, L. and Graupner, N. (no date2018) ‘‘Effect of basalt fibre hybridisation and sizing removal on mechanical and thermal properties of hemp fibre reinforced HDPE composites’’, Composite Structures. Elsevier, pp. 394–406. doi: 10.1016/j.compstruct.2018.01.046.

[Sawpan et al., 2011] Sawpan, M. A., Pickering, K. L. and Fernyhough, A. (2011) ‘‘Effect of various chemical treatments on the fibre structure and tensile properties of industrial hemp fibres’’, Composites Part A: Applied Science and Manufacturing. Elsevier Ltd, 42(8), pp. 888–895. doi: 10.1016/j.compositesa.2011.03.008.

[Scalet et al., 2012] Scalet, B. M., Munoz, M. G. and Queirolo, A. S. (2012) ‘Best Available Techniques (BAT) Reference Document for the Manufacture of Glass’, European Commission. doi: 10.1016/0010-4361(72)90477-6.

[Scalici et al., 2016] Scalici, T., Fiore, V. and Valenza, A. (2016) ‘‘Effect of plasma treatment on the properties of Arundo Donax L. leaf fi bres and its bio-based epoxy composites: A preliminary study’’, Composites Part B: Engineering. Elsevier Ltd, 94, pp. 167–175. doi: 10.1016/j.compositesb.2016.03.053.

[Schirp et al., 2006] Schirp, A., Loge, F., D’Aust, S., Swaner, P., Turner, G. and Wolcolott, M. P. (2006) ‘‘Production and characterization of natural fiber-reinforced thermoplastic composites using wheat straw modified with the fungus Pleurotus ostreatus.’’, Journal of Applied Polymer Science, 102(6), pp. 5191–5201.

[Schutte et al., 1994] Schutte, C. L., Mcdonough, W., Shioya, M., Mcauliffe, M. and Greenwood, M. (1994) ‘‘The use of a single-fibre fragmentation test to study environmental durability of interfaces / interphases between DGEBA / mPDA epoxy and glass fibre: the effect of moisture’’, Composites, 25(7), pp. 617–624.

[Seghini et al., 2018] Seghini M.C., Touchard F., Sarasini F., Chocinski-Arnault L., Mellier D., Tirillò J., (2018) “Interfacial adhesion assessment in flax/epoxy and in flax/vinylester composites by single yarn fragmentation test: correlation with micro-CT analysis”, Composites: Part A, 113, pp. 66-75.

[Seghini et al., 2019] Seghini M.C., Touchard F., Sarasini F., Cech V., Chocinski-Arnault L., Mellier D., Tirillò J., Bracciale M.P., Zvonek M., (2019), "Engineering the interfacial adhesion in basalt/epoxy composites by plasma polymerization", Composites: Part A, 122, pp. 67-76.

[Seghini et al., 2019] Seghini, M.C., Touchard, F., Sarasini F., Chocinski-Arnault L., Tirillo J. Bracciale M.P., Zvonek M., Cech V., (2019), "Effects of oxygen and tetravinylsilane plasma treatments on mechanical and interfacial properties of flax yarns in thermoset matrix composites", Cellulose, pp. 1-20.

[Seki et al., 2010] Seki, Y., Sarikanat, M., Sever, K., Erden, S. and Gulec, H. A. (2010) ''Effect of the low and radio frequency oxygen plasma treatment of jute fiber on mechanical properties of jute fiber/polyester composite'', Fibers and Polymers, 11(8), pp. 1159–1164.

[Senthil Kumar et al., 2016] Senthil Kumar, K., Siva, I., Rajini, N., Winowlin Jappes, J. and Amico, S. (2016) ''Layering pattern effects on vibrational behavior of coconut sheath/banana fiber hybrid composites.'', Materials & Design, 90, pp. 795–803.

[Sergi et al., 2019] Sergi, C., Tirillo, J., Seghini, M. C., Sarasini, F., Fiore, V. and Scalici, T. (2019) ''Durability of Basalt / Hemp Hybrid Thermoplastic Composites'', Polymers, 11, pp. 1–17.

[Sevenois et al., 2015] Sevenois, R. D. B. and Van Paepegem, W. (2015) ''Fatigue Damage Modeling Techniques for Textile Composites: Review and Comparison With Unidirectional Composite Modeling Techniques'', Applied Mechanics Reviews, 67(2), p. 020802.

[Shah et al., 2013] Shah, D. U., Schubel, P. J., Clifford, M. J. and Licence, P. (2013) ''Fatigue life evaluation of aligned plant fibre composites through S-N curves and constant-life diagrams'', Composites Science and Technology, 74, pp. 139–149. doi: 10.1016/j.compscitech.2012.10.015.

[Shahzad, 2011] Shahzad, A. (2011) ''Impact and fatigue properties of hemp-glass fiber hybrid biocomposites'', Journal of Reinforced Plastics and Composites, 30, pp. 1389–98.

[Shokoohi et al., 2008] Shokoohi, S., Arefazar, A. and Khosrokhavar, R. (2008) ''Silane coupling agents in polymer-based reinforced composites: A review'', Journal of Reinforced Plastics and Composites, 27(5), pp. 473–485. doi: 10.1177/0731684407081391.

[Silva et al., 2011] Silva, C. G., Benaducci, D. and Frollini, E. (2011) ''Lyocell and cotton fibers as reinforcements for a thermoset polymer'', Bioresources, 7(1), pp. 78–98. doi: 10.15376/biores.7.1.0078-0098.

[Spinacé et al., 2009] Spinacé, M. A. S., Lambert, C. S., Fermoselli, K. K. G. and De Paoli, M. (2009) ''Characterization of lignocellulosic curaua fibres'', Carbohydrate Polymers. Elsevier Ltd, 77(1), pp. 47–53. doi: 10.1016/j.carbpol.2008.12.005.

[Sreekala et al., 2000] Sreekala, M. S., Kumaran, M. G., Seena, J., Maya, J. and Sabu, T. (2000) ''Oil Palm Fibre Reinforced Phenol Formaldehyde Composites: Influence of Fibre Surface Modifications on the Mechanical Performance'', Applied Composite Materials, 7(5–6), pp. 295–329.

[Sreekala et al., 2002] Sreekala, M. S., Kumaran, M. G. and Thomas, S. (2002) ''Water sorption in oil palm fiber reinforced phenol formaldehyde composites'', Composites - Part A: Applied Science and Manufacturing, 33(6), pp. 763–777.

[Stuart et al., 2006] Stuart, T., Liu, Q., Hughes, M., McCall, R. D., Sharma, H. S. S. and Norton, A. (2006) ''Structural biocomposites from flax - Part I: Effect of bio-technical fibre modification on

composite properties'', Composites Part A: Applied Science and Manufacturing, 37(3), pp. 393–404. doi: 10.1016/j.compositesa.2005.06.002.

[Sun et al., 2006] Sun, D. and Stylios, G. K. (2006) ''Fabric surface properties affected by low temperature plasma treatment'', Journal of Materials Processing Technology, 173(2), pp. 172–177. doi: 10.1016/j.jmatprotec.2005.11.022.

[Sun, 2016] Sun, D. (2016) ''Surface modification of natural fibers using plasma treatment'', in Biodegradable Green Composites, John Wiley & Sons, pp. 19–35.

[Sun et al., 2019] Sun, Z. and Mingming, W. (2019) ''Effects of sol-gel modification on the interfacial and mechanical properties of sisal fiber reinforced polypropylene composites'', Industrial Crops and Products, 137(May), pp. 89–97. doi: 10.1016/j.indcrop.2019.05.021.

[Suresh Kumar et al., 2015] Suresh Kumar, C., Arumugam, V., Dhakal, H. N. and John, R. (2015) ''Effect of temperature and hybridisation on the low velocity impact behavior of hemp-basalt / epoxy composites'', Composite Structures. Elsevier Ltd, 125, pp. 407–416. doi: 10.1016/j.compstruct.2015.01.037.

[Swolfs et al., 2014] Swolfs, Y., Gorbatikh, L. and Verpoest, I. (2014) ''Fibre hybridisation in polymer composites: A review'', Composites: Part A, 67, pp. 181–200.

[Thomason, 1995] Thomason, J. L. (1995) ''The interface region in glass fibre-reinforced epoxy resin composites: 3. Characterization of fibre surface coatings and the interphase'', Composites, 26(7), pp. 487–498. doi: 10.1016/0010-4361(95)96806-H.

[Thomason et al., 1999] Thomason, J. L. and Dwight, D. W. (1999) ''Use of XPS for characterization of glass fibre coatings'', Composites Part A: Applied Science and Manufacturing, 30(12), pp. 1401–1413. doi: 10.1016/S1359-835X(99)00042-1.

[Thomason et al., 2018] Thomason, J. L., Yang, L. and Minty, R. F. (2018) ''Are silanes the primary driver of interface strength in glass fibre composites ? : exploring the relationship of the chemical and physical parameters which control composite interfacial strength'', in Proceedings of the ECCM18 - 18th European Conference on Composite Materials Athens, Greece, 24-28th June 2018, pp. 1–8.

[Thwe et al., 2003] Thwe, M. and Liao, K. (2003) ''Environmental effects on bamboo/glass polypropylene hybrid composites.'', Journal of Materials Science, 38, pp. 363–376.

[Titok et al., 2010] Titok, V., Leontiev, V., Yurenkova, S., Nikitinskaya, T., Barannikova, T. and Khotyleva, L. (2010) ''Infrared Spectroscopy of Fiber Flax'', Journal of Natural Fibers, 7(1), pp. 61–69.

[Torres et al., 2005] Torres, F. G. and Cubillas, M. L. (2005) ''Study of the interfacial properties of natural fibre reinforced polyethylene'', Polymer Testing, 24(6), pp. 694–698. doi: 10.1016/j.polymertesting.2005.05.004.

[Tripathi et al., 1998] Tripathi, D. and Jones, F. R. (1998) ''Review Single fibre fragmentation test for assessing adhesion in fibre reinforced composites'', Journal of materials science, 33, pp. 1–16.

[Van de Weyenberg et al., 2003] Van de Weyenberg, I., Ivens, J., De Coster, A., Kino, B., Baetens, E. and Verpoest, I. (2003) ''Influence of processing and chemical treatment of flax fibres on their composites'', Composites Science and Technology, 63(9), pp. 1241–1246. doi: 10.1016/S0266-3538(03)00093-9.

[Vander Wielen et al., 2004] Vander Wielen, L. C. and Ragauskas, A. J. (2004) ‘‘Grafting of acrylamide onto cellulosic fibers via dielectric-barrier discharge’’, European Polymer Journal, 40, pp. 477–482. doi: 10.1016/j.eurpolymj.2003.10.026.

[Vega et al., 2007] Vega, M., Gouttiere, C., Seveno, D., Blake, T., Voué, M. and De Coninck, J. (2007) ‘‘Experimental investigation of the link between static and dynamic wetting by forced wetting of nylon filament.’’, Langmuir, 23(21), pp. 10628–34.

[Velde et al., 2001] Velde, K. Van De and Baetens, E. (2001) ‘‘Thermal and Mechanical Properties of Flax Fibres as Potential Composite Reinforcement’’, Macromol. Mater. Eng., 286, pp. 342–349.

[Venkatesh, 2015] Venkatesh, Rp. (2015) ‘‘Study on physical and mechanical properties of NFRP hybrid composites.’’, Indian Journal of Pure & Applied Physics (IJPAP), 53(3), pp. 175–80.

[Vijayenthiran, 2015] Vijayenthiran, V. (2015) ‘Jaguar land rover previews future tech including new electric car concepts’, Motor Authority. Available at: https://www.motorauthority.com/news/1099944_jaguar-land-rover-previews-future-tech-including-new-electric-car-concepts.

[Wang et al., 2003] Wang, B., Panigrahi, S., Tabil, L., Crerar, W., Sokansanj, S. and Braun, L. (2003) ‘‘Modification of flax fibres by chemical treatment’’, in CSAE/SCGR 2003 Meeting Montréal, Québec, July 6 - 9, 2003. Montréal: The Canadian society for engineering in agricultural, food, and biological systems, pp. 6–9.

[Wang et al., 2008] Wang, B., Tabil, L. and Panigrahi, S. (2008) ‘‘Effects of chemical treatments on mechanical and physical properties of flax fiber-reinforced composites’’, Science and Engineering of Composite Materials, 15, pp. 43–57. doi: 10.1515/SECM.2008.15.1.43.

[Wang et al., 2010] Wang, X., Zhang, B., Du, S., Wu, Y. and Sun, X. (2010) ‘‘Numerical simulation of the fiber fragmentation process in single-fiber composites’’, Materials and Design. Elsevier Ltd, 31(5), pp. 2464–2470. doi: 10.1016/j.matdes.2009.11.050.

[Wang et al., 2016] Wang, W., Chouw, N. and Jayaraman, K. (2016) ‘‘Effect of thickness on the impact resistance of flax fibre-reinforced polymer’’, Journal of Reinforced Plastics and Composites, 35(17), pp. 1277–1289. doi: 10.1177/0731684416648780.

[Wenzel, 1949] Wenzel, R. N. (1949) ‘‘Surface Roughness and Contact Angle’’, The Journal of Physical and Colloid Chemistry, 53(9), pp. 1466–1467. doi:10.1021/j150474a015.

[Witten et al., 2018] Witten, E., Mathes, V., Sauer, M. and Kühnel, M. (2018) “Composites Market Report 2018 - Market developments, trends, outlooks and challenges”. Available at: https://www.avk-tv.de/files/20190118_avk_ccev__marktbericht_2018_final_2.pdf.

[Xia et al., 1991] Xia, Y. and Ruiz, C. (1991) ‘‘Analysis of damage in stress wave loaded unidirectional composites’’, Computers & Structures, 38(3), pp. 251–8.

[Xing, 1981] Xing, J. (1981) ‘‘A dynamic explanation of the hybrid effect’’, Journal of Composite Materials, 15, pp. 443–461.

[Yang et al., 2013] Yang, L. and Thomason, J. L. (2013) ‘‘Effect of silane coupling agent on mechanical performance of glass fibre’’, Journal of Materials Science, 48(5), pp. 1947–1954. doi: 10.1007/s10853-012-6960-7.

[Yao et al., 2017] Yao, T. T., Wu, G. P. and Song, C. (2017) ‘‘Interfacial adhesion properties of carbon fiber/polycarbonate composites by using a single-filament fragmentation test’’, Composites Science and Technology. Elsevier Ltd, 149, pp. 108–115. doi: 10.1016/j.compscitech.2017.06.017.

[Yu et al., 2010] Yu, T., Ren, J., Li, S., Yuan, H. and Li, Y. (2010) ‘‘Effect of fiber surface treatments on the properties of poly(lactic acid)/ramie composites.’’, Composites Part A: Applied Science and Manufacturing, 41, pp. 499–505.

[Yuan et al., 2013] Yuan, Y. and Lee, R. (2013) ‘‘Contact Angle and Wetting Properties’’, in Surface Science Techniques, pp. 1–34. doi: 10.1007/978-3-642-34243-1.

[Zafeiropoulos et al., 2002] Zafeiropoulos, N. E., Williams, D. R., Baillie, C. A. and Matthews, F. L. (2002) ‘‘Engineering and characterization of the interface in flax fibre-polypropylene composite materials - Part I. Development and investigation of surface treatment’’, Composites: Part A, 33, pp. 1083–1093. doi: http://dx.doi.org/10.1016/S1359-835X(02)00082-9.

[Zafeiropoulos et al., 2002] Zafeiropoulos, N. E., Baillie, C. A. and Hodgkinson, J. M. (2002) ‘‘Engineering and characterisation of the interface in flax fibre / polypropylene composite materials. Part II. The effect of surface treatments on the interface’’, Composites Part A: Applied Science and Manufacturing, 33, pp. 1185–1190.

[Zafeiropoulos et al., 2003] Zafeiropoulos, N. E., Vickers, P. E., Baillie, C. A. and Watts, J. F. (2003) ‘‘An experimental investigation of modified and unmodified flax fibres with XPS, ToF-SIMS and ATR-FTIR’’, Journal of Materials Science, 38(19), pp. 3903–3914. doi: 10.1023/A:1026133826672.

[Zafeiropoulos et al., 2007] Zafeiropoulos, N. E., Dijon, G. G. and Baillie, C. A. (2007) ‘‘A study of the effect of surface treatments on the tensile strength of flax fibres: Part I. Application of Gaussian statistics’’, Composites Part A: Applied Science and Manufacturing, 38, pp. 621–628. doi: 10.1016/j.compositesa.2006.02.004.

[Zafeiropoulos et al., 2007] Zafeiropoulos, N. E. and Baillie, C. A. (2007) ‘‘A study of the effect of surface treatments on the tensile strength of flax fibres: Part II. Application of Weibull statistics’’, Composites Part A: Applied Science and Manufacturing, 38, pp. 629–638. doi: 10.1016/j.compositesa.2006.02.005.

[Zafeiropoulos, 2007] Zafeiropoulos, N. E. (2007) ‘‘On the use of single fibre composites testing to characterise the interface in natural fibre composites’’, Composites Interfaces, 14, pp. 807–820. doi: 10.1163/156855407782106438.

[Zahran et al., 2005] Zahran, M. K., Rehan, M. F. and El-Rafie, M. H. (2005) ‘‘Single Bath Full Bleaching of Flax Fibers Using an Activated Sodium Chlorite/Hexamethylene Tetramine System’’, Journal of Natural Fibers, 2, pp. 49–67. doi: 10.1300/J395v02n02.

[Zamri et al., 2012] Zamri, M., Akil, H., Bakar, A. and Al., E. (2012) ‘‘Effect of water absorption on pultruded jute/glass fiber-reinforced unsaturated polyester hybrid composites’’, Journal of Composite Materials, 46(1), pp. 51–61.

[Zhang et al., 2013] Zhang, Y., Li, Y., Ma, H. and Yu, T. (2013) ‘‘Tensile and interfacial properties of unidirectional flax/glass fiber reinforced hybrid composites.’’, Composites Science and Technology, 88, pp. 172–7.

[Zhang et al., 2015] Zhang, H., Ming, R., Yang, G., Li, Y., Li, Q. and Shao, H. (2015) ‘‘Influence of Alkali Treatment on Flax Fiber for Use as Reinforcements in Polylactide Stereocomplex Composites Huihui’’, Polymer Engineering & Science, 55(11), pp. 2553–2558. doi: 10.1002/pen.

[Zhang et al., 2018] Zhang, J., Zheng, H. and Zheng, L. (2018) ‘‘Effect of treatment temperature on structures and properties of flax rove in supercritical carbon dioxide’’, Textile Research Journal, 88(2), pp. 155–166.

[Zinck et al., 1999] Zinck, P., Pays, M. F., Rezakhanlou, R. and Gerard, J. F. (1999) ‘‘Mechanical characterisation of glass fibres as an indirect analysis of the effect of surface treatment’’, Journal of Materials Science, 34, pp. 2121–2133. doi: 10.1023/A:1004572112470.

[Zivkovic et al., 2017] Zivkovic, I., Fragassa, C., Pavlovi, A. and Brugo, T. (2017) ‘‘Influence of moisture absorption on the impact properties of flax, basalt and hybrid flax / basalt fiber reinforced green composites’’, Composites Part B: Engineering, 111, pp. 148–164. doi: 10.1016/j.compositesb.2016.12.018.

[Zvonek et al., 2019] Zvonek, M., Sirjovova, V., Branecky, M., Plichta, T., Skacel, J. and Cech, V. (2019) ‘‘Plasma Nanocoatings Developed to Control the Shear Strength of Polymer Composites’’, Polymers, 11, pp. 1–16.

[Zweben, 1977] Zweben, C. (1977) ‘‘Tensile strength of hybrid composites’’, Journal of Materials Science, 12, pp. 1325–1337.